

# Synthetic Molecular Nanodevices for Selective Peptide-Based Therapy



by

**Anthony Fernandes**

Degree of Doctor of Philosophy

Department of Chemistry

University of Edinburgh

and

Laboratoire de Chimie des Substances Naturelles, UMR 6514

Université de Poitiers

- April 2009 -

# Table of Contents

|   |     |
|---|-----|
| Declaration   | ii  |
| Acknowledgements  | iii |
| General Remarks on Experimental Data  | v   |
| Layout of this Thesis   | vi  |
| <br>  |     |
| <b>Chapter 1:</b> Strategies for Peptide-Based Chemotherapy   | 1   |
| <b>Chapter 2:</b> Towards a Model Rotaxane-Based Peptide Prodrug  | 41  |
| <b>Chapter 3:</b> Rotaxane-Based Delivery Systems: Protection and Enzymatic Release of a Bioactive Pentapeptide | 108 |
| <b>Chapter 4:</b> Towards a Synthetic Molecular Peptide Synthesiser   | 138 |
| <b>Conclusion</b>   | 160 |

## **Declaration**

The scientific work described in this Thesis was carried out in the Laboratoire de Chimie des Substances Naturelles (UMR 6514) at the Université de Poitiers and in the Department of Chemistry at the University of Edinburgh between November 2005 and September 2008. Unless otherwise stated, it is the work of the author and has not been submitted in whole or in support of an application for another degree or qualification

## **Acknowledgements**

I would like to thank my supervisors Prof. David Leigh and Prof. Jean-Pierre Gesson for giving me the opportunity to do this PhD. These three years, shared between France and Scotland, have been absolutely rewarding both professionally and personally.

I would particularly like to thank my french “supervisor” Dr. Sébastien Papot, who helped me all over this PhD, even when I was in Poitiers or in Edinburgh. The discussions we had guided me all along this work. I also thank him for his efforts in proof reading my thesis.

I would also thank Dr. Vincent Aucagne who is the chemist behind such an innovative project.

I would like to thank Anne-Céline for her support and advices, even if she is not always right...she is just never wrong...

I also acknowledge Aurélien Viterisi who was involved with me in this fabulous project and carried out all the HPLC purifications and monitoring of our molecular devices.

I would also like to thank Paul McGonigal, a.k.a. “blondie”, who carefully corrected my English...and for the long but even too short hours playing guitar together.

I would also like to thank Dr. Dominik Heckmann, another member of the Saturday Guitar Band, for his advices with the peptide synthesiser project.

I would also thank Dr. Stephen Goldulp for his help and advices.

I would like to thank Isabelle Opalinski, Brigitte Renoux, Claudine Dumiot, Jean-Marie Coustard, Martine Mondon, André Amblès, Bruno Violeau and all the researchers I worked with in Poitiers. I particularly thank my colleagues and friends from France: Nicolas “KCo”, Cédric Charrier, Sébastien Picard, Mickaël Thomas, Julien Célérier, Dorothee Moine, Emilie Vardelle and Sophie Vuong.

Thanks to Kevin, Edzard (the “man down under”), Satoshi, Vicky, Amaya, Nathalie, Euan, Brian, Daniel, Michael, Mark, Roy, Tao, Max from the Leigh group.

I would also thank all the people that dealt with all the administrative struggles associated with this first Franco-Scottish PhD, particularly Amanda Ewing and Annette Burgess.

Finally I gratefully thank the Royal Society of Edinburgh for financing this PhD.

## General Remarks on Experimental Data

All the melting points (m.p.) were determined using a Sanyo Gallenkamp apparatus and are uncorrected.  $^1\text{H}$  and  $^{13}\text{C}$  NMR spectra were recorded at 400 MHz on a Bruker AV 400 instrument at 298K unless otherwise stated. Chemical shifts ( $\delta$ ) are reported in parts per million from low to high field and referenced to residual solvent. Coupling constants ( $J$ ) are reported in hertz (Hz). Standard abbreviations indicating multiplicity are used as follows: b = broad, s = singlet, d = doublet, dd = doublet of doublet, t = triplet, q = quartet, m = multiplet,  $J$  = coupling constant). Flash column chromatography was carried out using Kiesegel C60 (Fisher Scientific) as the stationary phase. Analytical TLC was performed on aluminium-backed sheets pre-coated with silica 60 F254 adsorbent (0.25 mm thick, Merck, Germany) and visualized under UV light. Mass spectrometry was carried out by the mass spectrometry services at the University of Edinburgh and at the EPSRC National Centre, Swansea. Size exclusion chromatography was performed using Toyopearl HW-405 (Tosoh, Japan) with methanol/chloroform in a 1:1 v/v ratio as the eluent. Unless otherwise stated, all reactions were run under an atmosphere of  $\text{N}_2$ . Prior to use, isophthaloyl dichloride was purified by recrystallization from hexane; *p*-xylylenediamine was purified by distillation under reduced pressure. Analytical RP-HPLC was carried out on a Gilson instrument composed of 306 pumps, 811C dynamic mixer (100  $\mu\text{L}$ ), 806 manometric module and an Applied Biosciences 759A UV detector with a Phenomenex C18 (2) Luna column (2 x 250 mm, 5  $\mu\text{m}$ , 100A). Preparative RP-HPLC was carried out on a Gilson instrument composed of 306 pumps, 811C dynamic mixer (1.5 ml), 806 manometric module and a 118 UV detector with a Spherisorb ODS2 column (21.2 x 250 mm, 5  $\mu\text{m}$ , 100A). LCMS was carried out on a Finnigan Mat system composed of an LCQ mass spectrometer, P4000 pumps, and a UV2000 UV detector with a Phenomenex C18 (2) Luna column (2 x 250 mm, 5 $\mu$ , 100A). Chromatograms were recorded at 220 nm unless stated otherwise.

## Layout of this Thesis

During this thesis we tried to design, synthesise and analyse some novel devices for the selective delivery of peptides. These systems are based on the enzyme-activated anticancer prodrugs developed by Prof. Gesson in Poitiers and the peptide rotaxanes developed by Prof. Leigh in Edinburgh. The innovative rotaxanes we constructed are devised to protect and selectively release a peptide in response to an enzyme-specific stimulus for the targeted therapy of cancer. In **Chapter 1** we tried to expose the main synthetic strategies aimed at improving the stability and permeation features of biologically active peptides. We examined some prodrug approaches and particularly the tumour-activated prodrugs (TAPs), largely investigated for use in anticancer chemotherapy. TAPs are generally three-part molecules composed of trigger, spacer and effector units. We also presented the original methodology developed by Prof. Leigh, namely the hydrogen bond-directed assembly of peptide rotaxanes, to protect a peptide thread from external environment. Finally we presented our project which consists of a combination of the peptide prodrug and rotaxane approaches. Therefore, based on the knowledge of both research groups we tried in **Chapter 2** to develop some model systems in order to study the influence of the rotaxane architecture upon prodrug molecules. The first step towards such rotaxane-based peptide prodrugs relied on the efficient design of a spacer which has to be bulky enough to work as a stopper for the macrocycle. Much of the work presented in this chapter is based on the design and synthesis of such self-immolative units. We then explored the response of our model rotaxanes under the action of the activating enzyme. After this detailed study, in **Chapter 3** we applied our concept to the biologically active peptide Met-enkephalin. In this chapter we presented a comparison between a rotaxane prodrug of Met-enkephalin and its non-interlocked derivative. Thus both compounds were successfully synthesised and evaluated to release the free peptide after enzymatic activation. The protective effect of encapsulating the peptide within a rotaxane assembly was also studied in human plasma and with different proteases. Finally, in **Chapter 4**, we introduced the construction of a rotaxane-based molecular machine programmed to synthesise a short peptide unit from the amino acids carried on its thread. We synthesised with success a one-station model rotaxane to study the catalyst effect of the macrocycle. Unfortunately this model machine proved not to work and current research is still ongoing to achieve such a synthetic device.

*A mes parents*

# CHAPT. 1 | STRATEGIES FOR PEPTIDE-BASED CHEMOTHERAPY

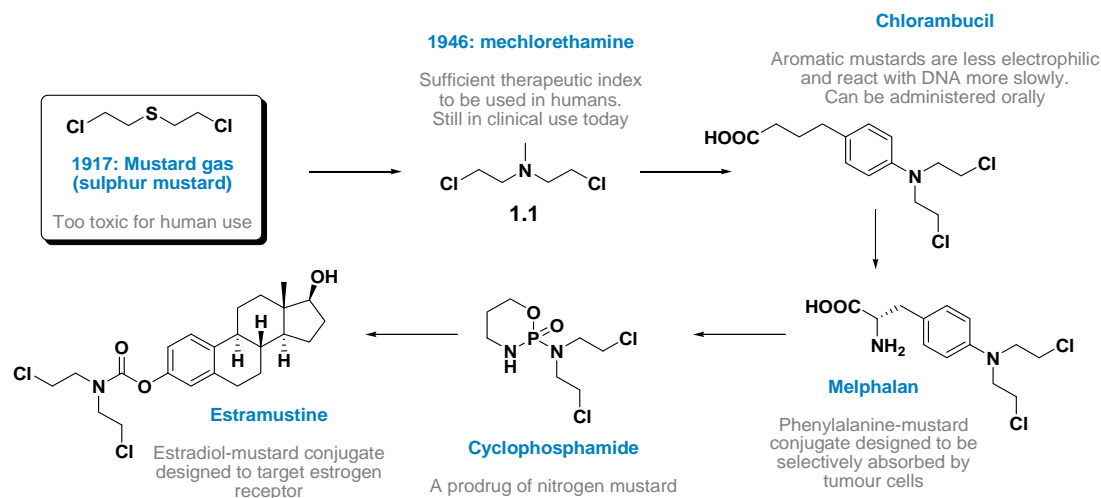
|  |           |
|--|-----------|
| <b>I. Strategies to enhance peptide delivery</b> .....                     | <b>7</b>  |
| I.1. Peptidomimetics.....  | 8         |
| I.1.1. Backbone modification.....  | 8         |
| I.1.2. Secondary structure mimetics.....                                   | 10        |
| I.1.3. Functional and topographical peptidomimetics.....                   | 11        |
| I.2. Cyclic peptides.....  | 13        |
| I.3. The prodrug approach.....   | 15        |
| I.3.1. Prodrugs to improve bioavailability.....                            | 16        |
| I.3.2. Bioreversible cyclic peptides.....                                  | 19        |
| <b>II. Tumour-activated prodrugs</b> .....                                 | <b>21</b> |
| II.1. Prodrug monotherapy (PMT).....                                       | 22        |
| II.1.1. Glucuronylated prodrugs.....                                       | 23        |
| II.1.2. HMR 1826.....  | 24        |
| II.2. Antibody-Directed Enzyme Prodrug Therapy (ADEPT).....                | 26        |
| II.3. Targeted delivery of peptides.....                                   | 29        |
| <b>III. Rotaxane-based peptide prodrugs</b> .....                          | <b>30</b> |
| III.1. Rotaxanes and other interlocked molecules.....                      | 30        |
| III.2. Hydrogen bond directed assembly of synthetic peptide rotaxanes..... | 32        |
| III.3. Rotaxane-based peptide prodrugs.....                                | 37        |

Over the past few decades peptides and proteins have received considerable attention not only in terms of their chemistry but also for their roles in various biological processes and their potential use as tools to explore new prospects in chemotherapy. It is now possible that in the close future peptides and their derivatives will play a significant role in the field of medicinal chemistry. Nevertheless to reach this point, extended bioavailability strategies and site-selective delivery methods constitute a fundamental prerequisite. Indeed, while a few are already approved for medical use, peptide drugs have been applied in a very limited extent since they are highly unstable *via* oral administration and are mainly unable to cross the cell layers. As a result most of these therapeutics are currently administered by the parenteral route (intravenous or subcutaneous), which represents obvious drawbacks considering patient acceptability and compliance in the course of long-term treatments. Moreover parenteral formulations are still not efficient enough to assure the peptide a prolonged time of action. Therefore the design of oral delivery strategies represents a major challenge for peptide-based therapy. Modern techniques using special formulation, encapsulation, conjugation and other delivery devices offer promising outlooks but are still at a development stage. The incorporation of unnatural amino acids, the introduction of totally modified subunits, the derivatisation into cyclic structures and other chemical alterations of the original bioactive peptide represent some of the most advanced synthetic techniques towards the improvement of peptide pharmacological applications. Thus this peptidomimetic approach currently appears as one of the most encouraging strategies but requires a significant knowledge to rationally manipulate the peptide architecture without losing its unique activity corresponding to a unique conformation. Alternatively, another ongoing approach that does not alter the peptide structure is to temporarily derivatise it into a biologically inactive prodrug, which after a selective activation would release the parent peptide.

In this chapter we will try to review some of the different chemical strategies aimed at improving peptide delivery focusing mainly on the area of anticancer chemotherapy and targeted therapy. We will also introduce the concept of rotaxane-based peptide prodrugs.

Conventional cancer chemotherapy has historically been developed by delivering small molecules to target and damage malignant DNA replication. Until the twentieth century and the beginning of modern science and medicine, most therapeutics was provided by plants and minerals. The use of natural products to fight disease and particularly cancer, which is far from being a modern age disease, has a rich ancient history.<sup>1</sup> However the rise of modern organic chemistry and the still-increasing knowledge of malignant growth enabled the first efforts towards the design and synthesis of new highly potent anticancer drugs.<sup>2</sup> In fact, most of the current pharmaceuticals are directly inspired from naturally occurring structures, nature serving as a template lead for novel drug design.<sup>3,4,5</sup>

The modern era of cancer chemotherapy started serendipitously by the discovery of the potential antitumour effects of mustard gas, a chemical warfare used during World War I. The successive endeavour to design more active compounds led to the development of the “first” anticancer chemicals: mustine **1.1** (a.k.a. mechlorethamine) and other nitrogen mustard derivatives (**Scheme 1.1**).<sup>6</sup> This marked the beginning of contemporary chemotherapy and paved the way to drug development.



**Scheme 1.1** | Nitrogen mustards: drug design and targeted strategy. (Adapted from ref. 2)

<sup>1</sup> Heller, J. R. *Bull. N. Y. Acad. Med.* **1962**, *38*, 348-359.

<sup>2</sup> Neidle, S.; Thurston, D. E. *Nature Rev. Cancer* **2005**, *5*, 285-296.

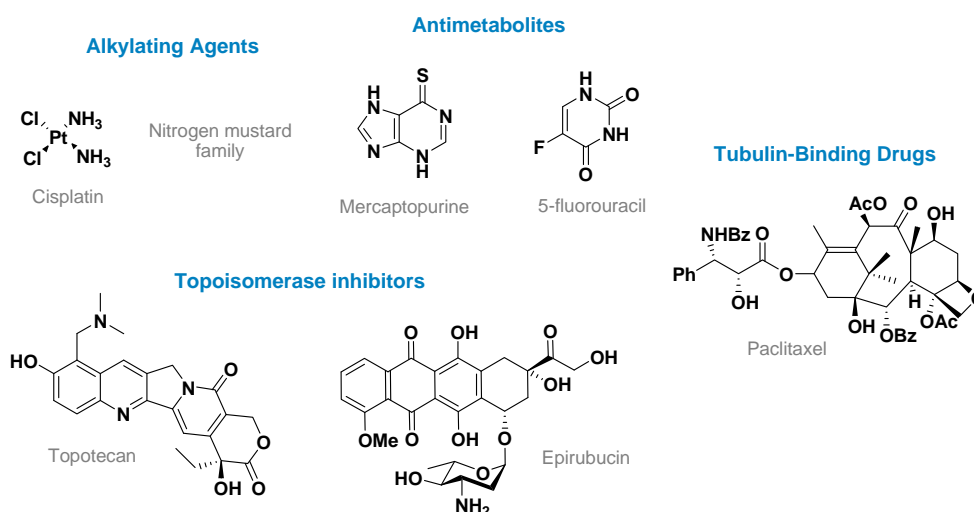
<sup>3</sup> Clardy, J.; Walsh, C. *Nature* **2004**, *432*, 829-837.

<sup>4</sup> Mann, J. *Nature Rev. Cancer* **2002**, *2*, 143-148.

<sup>5</sup> Itokawa, H.; Morris-Natschke, S. L.; Akiyama, T.; Lee, K.-H. *J. Nat. Med.* **2008**, *62*, 263-280.

<sup>6</sup> Gilman, A.; Philips, F. S. *Science* **1946**, *103*, 409-436.

To date DNA alkylating agents, antimetabolites, tubulin-binding drugs and topoisomerase inhibitors are the most common chemical weapons clinically used to kill tumour cells (**Figure 1.1**).<sup>7</sup>



**Figure 1.1** | Examples of current anticancer drugs

Despite the great advances achieved during the last decades and the wide chemical arsenal available for the treatment of cancer, the main drawback still remains the lack of selectivity of anticancer chemotherapy. Indeed, being incapable of differentiating rapidly dividing healthy cells from tumour cells, most of the current antiproliferative drugs frequently induce side effects. As a result, the amount of drug that can be administered is usually insufficient to deliver a lethal concentration at the tumour site and hence, in most of the cases, only allows the prevention of its growth. Another dramatic consequence is the emergence of cancer resistance to chemotherapy.<sup>8</sup> Combination of anticancer agents without overlapping toxicity is currently used to overcome and bias such behaviour. An understanding of the biochemistry of resistance is warranted in order to develop new strategies to assure a long-term control of cancers.<sup>9</sup>

<sup>7</sup> Médicaments antitumoraux et perspective dans le traitement des cancers, in *Traité de chimie thérapeutique*, Volume 6, Edition TEC and DOC, Edition Médicales Internationales, **2003**.

<sup>8</sup> Kruh, G. D. *Oncogene* **2003**, 22, 7262-7264.

<sup>9</sup> Fojo, T.; Bates, S. *Oncogene* **2003**, 22, 7512-7523.

In the early twentieth century the revolutionary “magic bullet” concept introduced by the pioneering work of Ehrlich, the father of chemotherapy, highlighted the potential of targeted toxicity which would allow the lethal delivery of cytotoxic agents within malignant cells.<sup>10</sup> Since then, the design of drugs and prodrugs directed towards specific toxicity expanded by progressively understanding the unique features of cancer cells (*e.g.* tumour hypoxia, tumour vasculature, angiogenesis, tumour-specific membrane transporters/receptors, antigens, enzymes...).<sup>11</sup>

Molecularly targeted therapy, the new generation of anticancer drugs designed to interact with tumour specific hallmarks, offers the prospect of differentiating healthy cells from malignant cells and therefore to conquer cancer.<sup>12</sup> Even though new biological targets are still being discovered (*e.g.* mutant kinases, the tumour micro-environment, cancer stem cells, telomerases, HDACs)<sup>13</sup> there is still a need to identify/create smart drugs acting only at tumour sites and to develop effective tumour-activated prodrugs, making the visionary “magic bullet” concept quite topical.<sup>14</sup>

Cancer development is clearly associated with genetic alterations and instability: proto-oncogenes, tumour suppressor and DNA damage repair genes have all been associated with most human malignancies. The resulting mutated genes induce continuous proliferation, usually considered as a kind of cellular immortality. Furthermore, regulatory proteins are also affected, thus being incapable of restoring or killing the expressed malignant proteins. Cancer is consequently a strongly developed and complex disease involving defensive as well as aggressive biological tools to overcome cellular processes and death (*e.g.* autoemission of growth signals, induction of angiogenesis, extended proliferation, resistance to inhibiting signals, development of drug efflux pumps, enhanced DNA repair, hypoxia resistance and apoptosis evasion...).<sup>15</sup>

---

<sup>10</sup> Stern, F. *Angew. Chem. Int. Ed.* **2004**, *43*, 4254-4261.

<sup>11</sup> Denny, W. A. *Eur. J. Med. Chem.* **2001**, *36*, 577-595.

<sup>12</sup> Vamus, H. *Science* **2006**, *312*, 1162-1165.

<sup>13</sup> Sawyers, C. *Nature* **2004**, *432*, 294-297.

<sup>14</sup> Strebhardt, K.; Ullrich, A. *Nature Rev. Cancer* **2008**, *8*, 473-480.

<sup>15</sup> Hanahan, D.; Weinberg, R. A. *Cell* **2000**, *100*, 57-70.

As a result mutated proteins represent serious targets for peptide-based therapy.<sup>16</sup> Further determination of the critical interacting region may allow the development of effective small peptidic fragments to specifically restore the disrupted protein functions, offering the possibility to jam the mechanism of cancer survival without any DNA-based methods.<sup>17</sup> Indeed reconstitution, replacement or inhibition of dysregulated proteins might be accomplished by specific transduction, thus delivering peptides to tumours may allow cell biology modulation at the protein level.

By comparison with “small” molecules, peptide therapeutics have shown extremely limited clinical development because of their associated physiological drawbacks. Following even oral or parenteral administration, peptides have to overcome diverse physical and biochemical barriers. Typically, peptide oral bioavailability ranges from 1 to 2 % with *in vivo* half-lives inferior to 30 minutes.<sup>18</sup> The main reasons for the low bioavailability of peptide drugs are their rapid enzymatic degradation and poor penetration of the biological membranes.<sup>19</sup>

However peptides have the great potential to be highly selective powerful drugs, thereby considerably decreasing the risks of systemic toxicity.<sup>20</sup> Peptides with anticancer use or potential have recently been reviewed and classified according to their biological mechanism of action: enzyme inhibitors, protein-protein interaction inhibitors, receptor-interacting peptides and nucleic acid-interacting peptides.<sup>21</sup> The wide diversity of peptides presented in this review clearly illustrates the promising future of peptide drugs in the chemotherapy of various diseases.<sup>22, 23</sup>

---

<sup>16</sup> Borghouts, C.; Kunz, C.; Groner, B. *J. Peptide Sci.* **2005**, *11*, 713-726.

<sup>17</sup> Wadia, J. S.; Dowdy, S. F. *Adv. Drug Deliv. Rev.* **2005**, *57*, 579-596.

<sup>18</sup> Lee, V. H. L.; Yamamoto, A. *Adv. Drug Deliv. Rev.* **1990**, *4*, 171-207.

<sup>19</sup> Gangwar, S.; Pauletti, G. M.; Wang, B.; Siahaan, T.; Stella, V. J.; Borchardt, R. T. *Drug Discovery Today* **1997**, *2*, 148-155.

<sup>20</sup> Mendoza, F. J.; Espino, P. S.; Cann, K. L.; Bristow, N.; McCrea, K.; Los, M. *Arch. Immunol. Ther. Exp.* **2005**, *53*, 47-60.

<sup>21</sup> Janin, Y. L. *Amino Acids* **2003**, *25*, 1-40.

<sup>22</sup> Kieber-Emmons, T.; Murali, R.; Greene, M. *Curr. Opin. Biotech.* **1997**, *8*, 435-441.

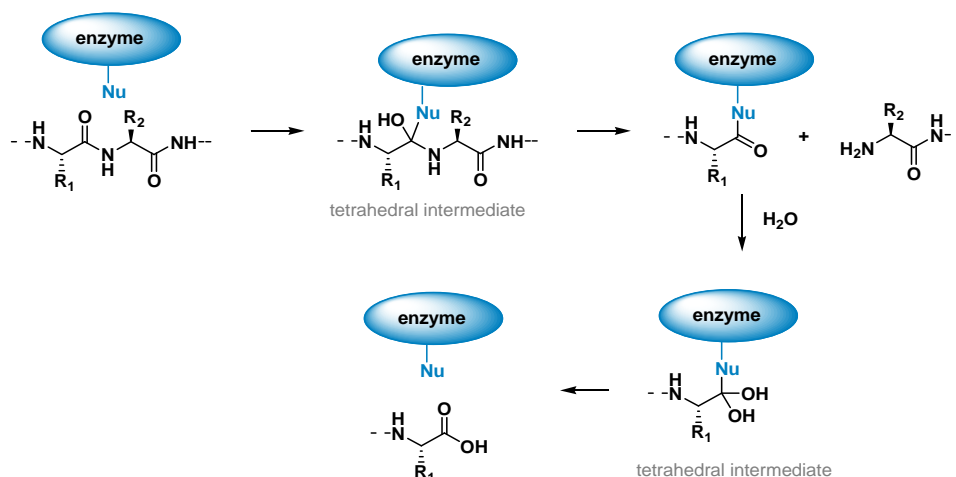
<sup>23</sup> Meloen, R.; Timmerman, P.; Langedijk, H. *Molecular Diversity* **2004**, *0*, 1-3.

## I. Strategies to enhance peptide delivery

*“the less peptide character in a drug candidate, the more stable it is likely to be towards protease cleavage”* [Borchardt, R. T. *et al. Adv. Drug Deliv. Rev.* **1997**, 27, 235-256.]

As briefly mentioned, peptide drugs need to overcome several barriers before properly reaching their target. Rapid degradation by proteases and low membrane permeability are essentially the main drawbacks restricting the direct pharmacological use of native peptides. Considering the extraordinary potential of this class of natural molecules, a great amount of research has been developed in order to enhance peptide stability and permeation. The knowledge acquired over the years now allows the design of new peptide-like candidates and other delivery systems to be constructed to overcome the challenge of peptide oral bioavailability. These strategies can be classified into three general categories: peptidomimetics, cyclic peptides and prodrugs.

The purpose of these strategies is to protect the peptidic bond from enzymatic cleavage in order to enhance its biological stability. From a mechanistic point of view, the enzymatic hydrolysis of peptides can be roughly represented as shown in **Scheme 1.2**.



**Scheme 1.2** | Schematic protease catalytic mechanism

Manifold modified peptides have been prepared in order to access enhanced biostability, preventing the protease recognition process. Structural alterations are also well recognised to

generate the fundamental changes in peptide conformation responsible for improved penetration and stability.<sup>24</sup> Amongst the best examples are cyclic peptides which exhibit uncommon permeation and stability characteristics.

### I.1. Peptidomimetics

Nowadays, the conception and synthesis of peptidomimetics have attracted major attention and the term “peptidomimetics” itself is often associated with confusion since extensive works has been carried out in this subject area. Peptidomimetics are “nonpeptidic” compounds designed to translate the functional and topographical information carried by bioactive peptides into small biologically stable organic molecules. A scheme has even been published classifying peptidomimetics in three different categories: peptide backbone mimetics (type I), functional mimetics (type II) and topographical mimetics (type III).<sup>25</sup> Curiously, type I peptidomimetics are slightly modified peptide derivatives while for mimetics of type II and III, the peptide structure is hardly recognisable.

Globally, the successful design of all three types of peptidomimetics closely depends on the careful appreciation of the essential requirements needed to maintain the biological activity of the parent peptide. Furthermore the structural knowledge of the peptide target (*i.e.* a receptor or an enzyme) is also of fundamental importance. As a consequence, modern techniques such as Structure-Activity Relationship (SAR), combinatorial chemistry, NMR, X-Ray crystallography and computational modelling are commonly used to rationally assist the conception of peptidomimetics.<sup>26</sup> Accordingly, the artificial peptide should present a superior biological index, demonstrating either agonist or antagonist activity.

#### I.1.1. Backbone modification

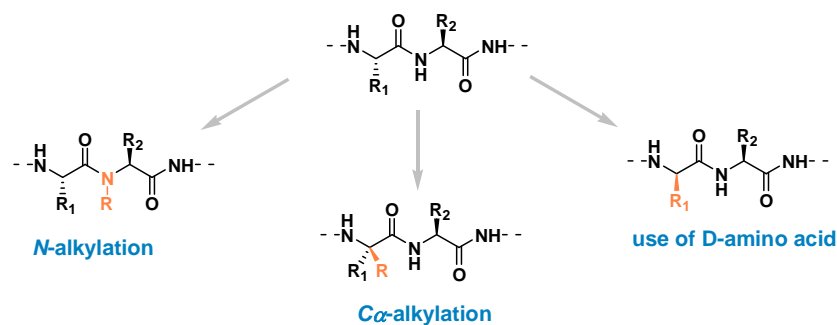
From the straightforward protease mechanism depicted in **Scheme 1.2**, it can be expected that chemical modifications of the amide linkage or near to the peptidic bond such as  $C_{\alpha}$ -alkylation,  $N$ -alkylation (peptoids), or use of D-amino acids may hinder enzymatic hydrolysis (**Scheme 1.3**).

---

<sup>24</sup> Pauletti, G. M.; Gangwar, S.; Siahaan, T. J.; Aubé, J.; Borchardt, R. T. *Adv. Drug Deliv. Rev.* **1997**, *27*, 235-256.

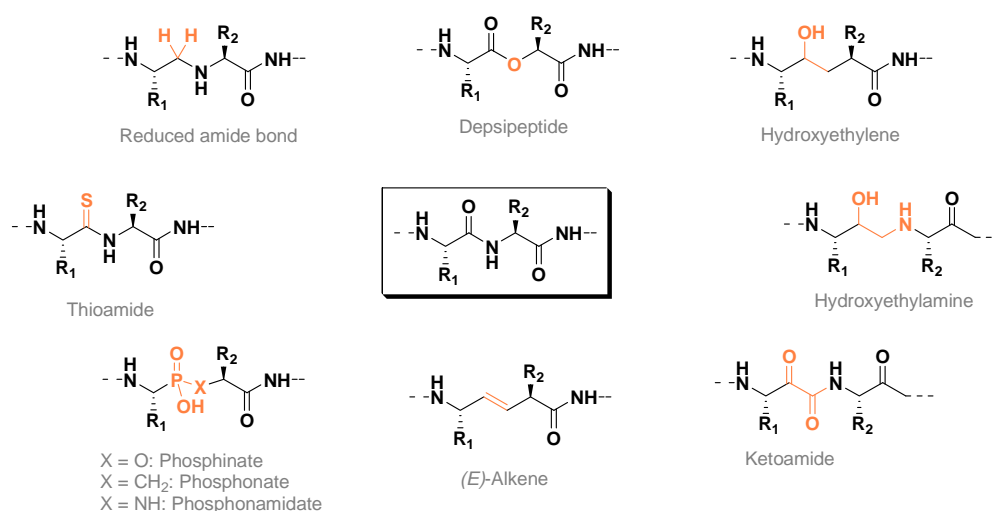
<sup>25</sup> Ripka, A. S.; Rich, D. H. *Curr. Opin. Chem. Biol.* **1998**, *2*, 441-452.

<sup>26</sup> Gante, J. *Angew. Chem. Int. Ed.* **1994**, *33*, 1699-1720.



**Scheme 1.3** | Examples of investigated chemical peptide backbone modifications

Modification of the amide bond has been extensively studied and a large number of surrogates are now reported: reduced amide bond, depsipeptide (ester linkage), hydroxyethylene, phosphinate, (*E*)-alkene, hydroxyethylamine...and many other (**Figure 1.2**).<sup>27</sup>



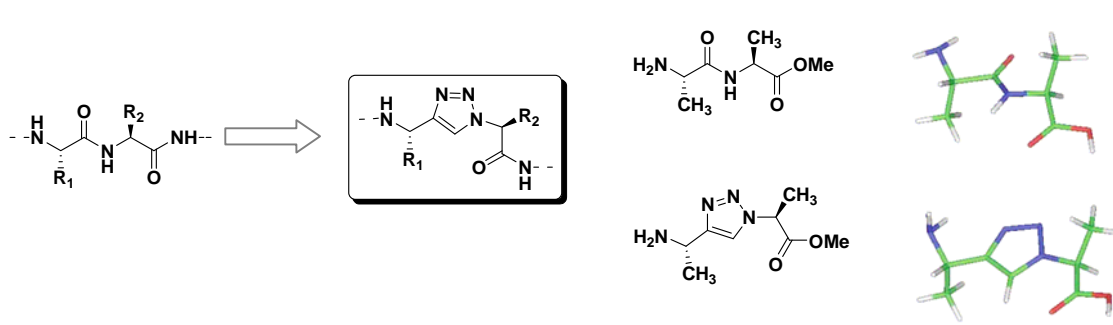
**Figure 1.2** | Examples of investigated peptide bond surrogates

For instance one of the most current and significantly studied alternatives is the use of 1,4-substituted 1,2,3-triazoles as peptide bond mimetics. Indeed, these kinds of motifs are readily accessible *via* the powerful Copper-Catalyzed Azide-Alkyne Cycloadditions (CuCAAC), a.k.a. the Huisgen 1,3-dipolar cycloaddition updated by Meldal and Sharpless.<sup>28,29</sup> 1,2,3-Triazoles are quite appealing for peptide chemists since their stereoelectronic similarity with amide bonds is quite remarkable (**Scheme 1.4**).

<sup>27</sup> Gautier, A.; Pitrat, D.; Hasserodt, J. *Bioorg. Med. Chem.* **2006**, *14*, 3835-3847.

<sup>28</sup> Tornøe, C. W.; Christensen, C.; Meldal, M. *J. Org. Chem.*, **2002**, *67*, 3057-3064.

<sup>29</sup> Rostovtsev, V. V.; Green, L. G.; Fokin, V. V.; Sharpless, K. B. *Angew. Chem. Int. Ed.* **2002**, *41*, 2596-2599.



**Scheme 1.4** | Peptidotriazoles as peptidomimetics (*X-ray from ref. 30*)

As depicted in the excellent review by Angell and Burgess the reaction has been widely used not only to join peptide fragments together, thus forming acyclic or cyclic triazole-based peptidomimetics, but also to access peptido-conjugates (ligation with carbohydrates, labeling agents, polymers, dendrimers).<sup>30</sup>

### I.1.2. Secondary structure mimetics

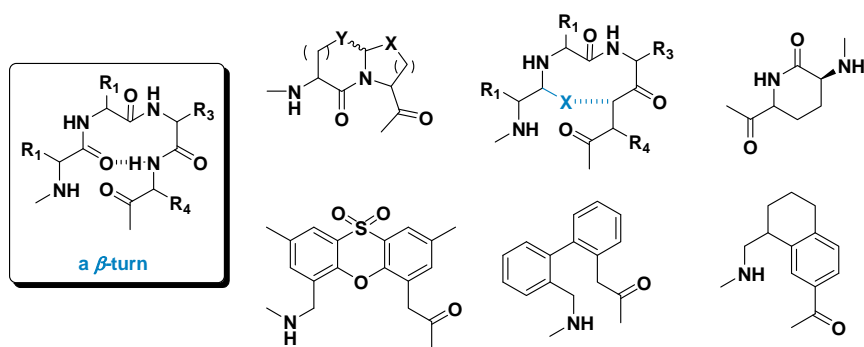
Particular efforts have been undertaken to prevent the protease recognition process by controlling peptide conformation.<sup>31</sup> Restricting peptides in one particular conformation might be more efficient than locally replacing a functional group, though this is not so simple since even modifying a single functional group may also result in a dramatic modification in regards to the peptide conformation. However the idea here is to closely imitate a desired conformation by introducing a synthetic module to achieve considerably reduced protease affinity as well as enhanced membrane permeation of a parent peptide. The incorporation of such modules (also called scaffolds or foldamers), special building blocks locally restricting peptide conformational freedom, has largely been explored however the list is too exhaustive to be discussed here.<sup>32</sup> Not only do foldamers improve bioavailability by inducing significant changes in the peptide three-dimensional structure, they have also contributed to understanding and enhancing peptide selective binding to biological receptors. In this case the peptidomimetic is designed to retain the biologically-active conformation of a natural ligand or peptide inhibitor.

<sup>30</sup> Angell, Y. L.; Burgess, K. *Chem. Soc. Rev.* **2007**, *36*, 1674-1689.

<sup>31</sup> Stigers, K. D.; Soth, M. J.; Nowick, J. S. *Curr. Opin. Chem. Biol.* **1999**, *3*, 714-723.

<sup>32</sup> Hanessian, S.; McNaughton-Smith, G.; Lombart, H.-G.; Lubell, W. D. *Tetrahedron* **1997**, *53*, 12789-12854.

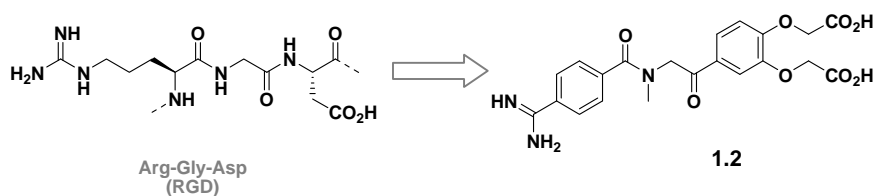
Among the various conformational features displayed by peptides and proteins,  $\beta$ -turns are certainly one of the most biologically-relevant structural motifs found in these therapeutic derivatives. Consequently the development of  $\beta$ -turn rigid scaffolds has been widely investigated and many of the secondary structure mimetics are designed to incorporate this feature (**Figure 1.3**).<sup>33</sup>



**Figure 1.3** | Examples of  $\beta$ -turn mimetics

### I.1.3. Functional and topographical peptidomimetics

Type II peptidomimetics are rationally designed to precisely adjust the essential peptide side chains responsible for biological activity into a rigid scaffold. These unnatural frameworks present interesting oral bioavailabilities since most of the original peptide bonds are depleted in the final architecture. For instance the RGD motif has been converted into the peptidomimetic equivalent **1.2** that has demonstrated potent fibrinogen antagonist activity (**Scheme 1.5**).<sup>34</sup>



**Scheme 1.5** | A RGD peptidomimetic

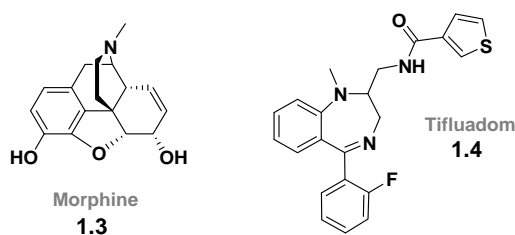
<sup>33</sup> Sewald, N.; Jakubke, H.-D. *Peptides: Chemistry and Biology*, Wiley-VCH, 2002.

<sup>34</sup> Alig, L.; Edenhofer, A.; Hadvary, P.; Huerzeler, M.; Knopp, D.; Mueller, M.; Steiner, B.; Trzeciak, A.; Weller, T. *J. Med. Chem.* **1992**, 35, 4393-4407.

The use of a rigid backbone is generally warranted to prevent the hydrophobic collapse effect. This effect refers to the conformational change observed when organic molecules containing hydrophobic groups enter an aqueous environment. In fact, within unrestricted molecular structures those functionalities tend to associate due to intramolecular hydrophobic interaction and finally form biologically inactive conformations.

Topographical mimetics can be regarded as the perfect peptidomimetics. These compounds have clearly no obvious relationship with the corresponding natural peptide ligand and are rationally designed (or the result of large screening methods) to perfectly fit a target protein binding domain. The term limetics (a contraction of ligand mimetic)<sup>35</sup> was also coined to characterise this type of molecules as the only common thing they share with the parent peptide is their common target. As a result topographical peptidomimetics possess the necessary pharmacophoric elements flanked in a rigid backbone that perfectly directs the orientation of these biologically relevant elements.

Morphine **1.3** is, unknowingly, a famous type III peptidomimetic (**Figure 1.4**). Indeed this non-peptidic molecule was found to agonise the effect of the endogenous  $\beta$ -endorphin peptide on opioid receptors. Tifluadom **1.4** is also a selective agonist of opioid receptor which demonstrated no addictive effects in animal experiments.

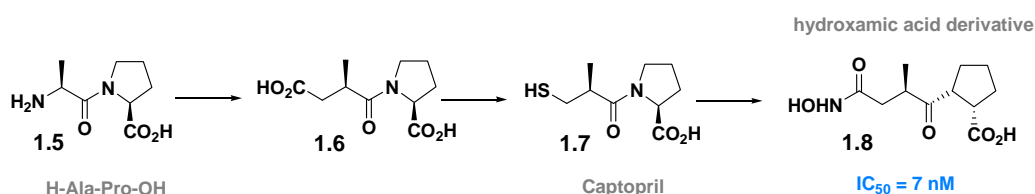


**Figure 1.4** | Non-peptide mimetics

This approach has been used, for instance, to prepare mimetics of inhibitors of the angiotensin converting enzyme (ACE), a zinc metalloprotease (**Scheme 1.6**). Starting from the nonapeptide teprotide, a natural inhibitor of ACE isolated from snake venoms, it was first observed that the C-terminal fragment Ala-Pro **1.5** already inhibited ACE, albeit weakly.

<sup>35</sup> Veber, D. F. In *Peptides: Chemistry and Biology, Proceedings of the Twelfth American Peptide Symposium*; Smith, J. A.; Rivier, J. E., Eds.; Escom: Leiden, **1992**, 3-14.

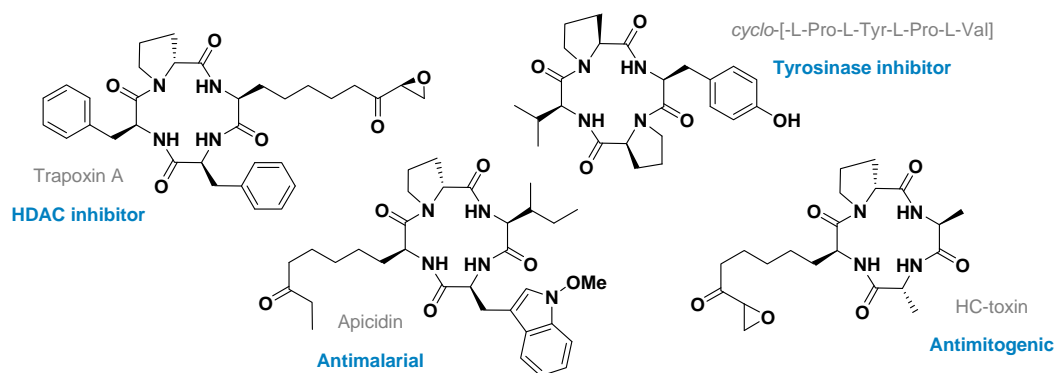
This dipeptide was then transformed to  $\alpha$ -methylsuccinylproline **1.6**, the carboxyl group being expected to coordinate the Zn ion. Satisfied in that reasoning, the carboxyl group was finally replaced by the more effective Zn-ligating thiol function to lead the first rationally developed inhibitor of ACE, captopril **1.7**, currently used to treat hypertension.<sup>36</sup> This was further optimised to afford the more active hydroxamic acid peptidomimetic **1.8**.<sup>37</sup>



**Scheme 1.6** | Development of ACE inhibitors

## I.2. Cyclic peptides

Cyclic peptides are covalently constrained peptides. Demonstrating increased stability, enhanced bioavailability and receptor selectivity, cyclopeptides have become increasingly important towards the development of peptide-based drugs. This growing interest is further explained by the high potential exhibited by a large variety of cyclic peptides. For instance, cyclic tetrapeptides have demonstrated significant activity against various pathologies (**Figure 1.5**).<sup>38</sup>



**Figure 1.5** | Examples of biologically relevant cyclic tetrapeptides

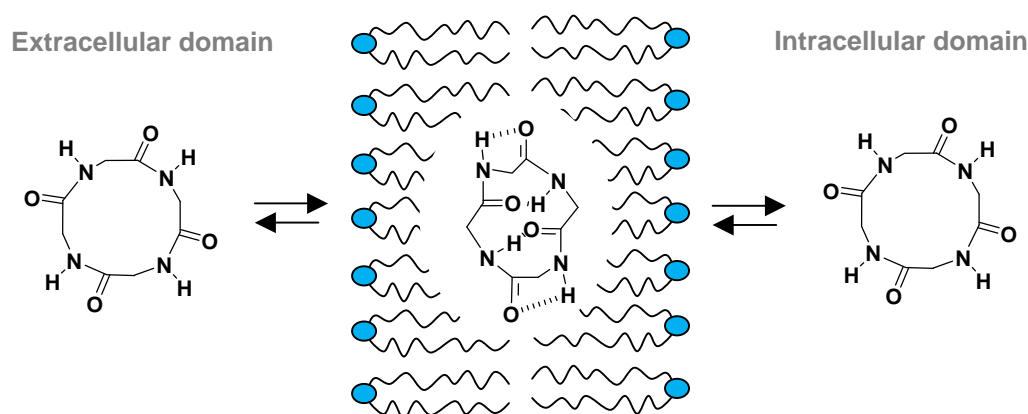
<sup>36</sup> Ondetti, M. A.; Rubín, B.; Cushman, D. W. *Science* **1977**, *196*, 441-444.

<sup>37</sup> Turbanti, L.; Cerbai, G.; Di Bugno, C.; Giorgi, R.; Garzelli, G.; Criscuoli, M.; Renzetti, A. R.; Subissi, A.; Bramante, G.; DePriest, S. A. *J. Med. Chem.* **1993**, *36*, 699-707.

<sup>38</sup> Katsara, M.; Tselios, T.; Deraos, G.; Matsoukas, M.-T.; Lazoura, E.; Matsoukas, J.; Apostolopoulos, V. *Curr. Med. Chem.* **2006**, *13*, 2221-2232.

Strained peptides and particularly cyclic analogues have been shown to present enhanced bioavailability due to a reduced hydrophilic nature, hence being more easily absorbed *via* the transcellular pathway. In agreement with the fact that the cell membrane consists of a complex lipid bilayer matrix, hydrophobicity has been traditionally accepted as the most important requirement for peptide absorption. However, it has been demonstrated that a compromise needs to be found for optimal transcellular internalization. Schematically in the transcellular route, peptides have to pass from an aqueous media to a hydrophobic environment, the energetic barrier to this diffusion process being the desolvation energy. Cyclic peptides have a decreased hydrogen bonding capacity as a result of intramolecular hydrogen bond formation, therefore energy transfer is less expensive and internalisation favoured.

Nevertheless cyclic peptides are not totally conformationally locked but take the best structure to accord with their surroundings, and the notion of “membrane-induced conformational changes” is here clearly understood (**Scheme 1.7**).<sup>39</sup>

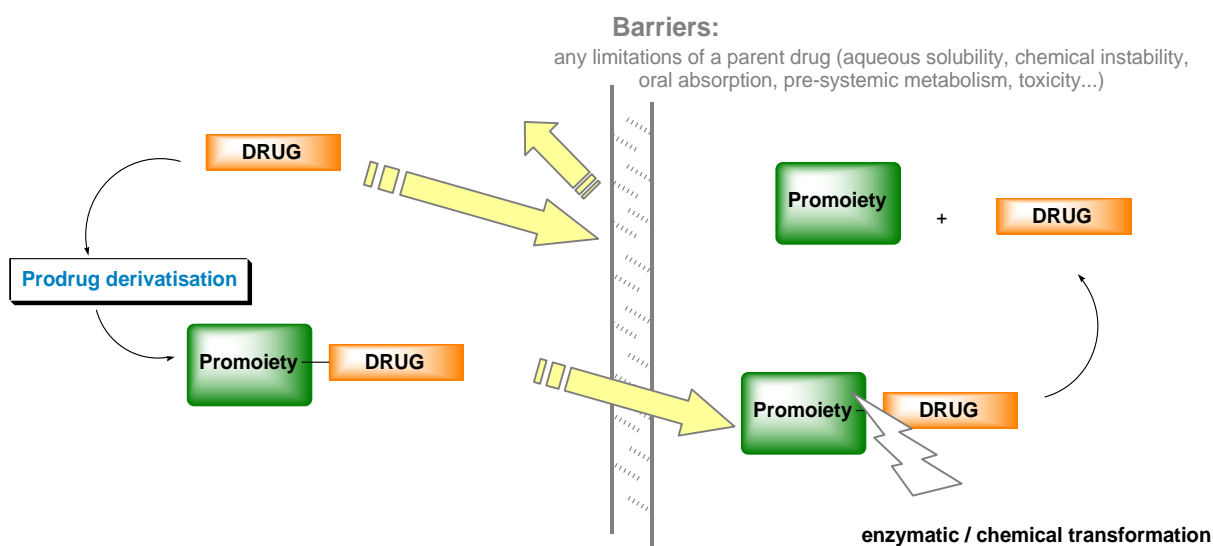


**Scheme 1.7** | Schematic representation of conformational basis of membrane permeability in cyclic peptides (*adapted from ref. 39*)

<sup>39</sup> Rezai, T.; Yu, B.; Millhauser, G. L.; Jacobson, M. P.; Lokey, R. S. *J. Am. Chem. Soc.* **2006**, *128*, 2510-2511.

### I.3. The prodrug approach

As first defined by Albert in 1958, prodrugs are therapeutic agents which are inactive *per se* but are transformed into one or more active metabolites *in vivo*.<sup>40</sup> As outlined here, the aim of a prodrug strategy is to modify drugs into inactive derivatives showing enhanced pharmaceutical and pharmacokinetic (the ADME profile: Absorption, Distribution, Metabolism, Elimination) releasing the active parent species after enzymatic or chemical activation.<sup>41</sup> Thus prodrug derivatisation provides a solution to the many drawbacks associated with drug formulation and delivery (*e.g.* poor aqueous solubility, chemical instability, oral absorption, pre-systemic metabolism, toxicity...) but one of the most appealing aspects of prodrugs is that they could make the ultimate targeted delivery possible, delivering a lethal dose of anticancerous agents at the tumour sites (**Scheme 1.8**).<sup>42</sup>



**Scheme 1.8** | Illustration of the prodrug concept

Indeed, with regards to anticancer chemotherapy, prodrugs have been widely investigated to overcome these barriers and to target therapy, leading to the so-called Tumour-Activated Prodrugs (TAPs) (*see Chapter II*).

<sup>40</sup> Albert, A. *Nature* **1958**, *182*, 421-423.

<sup>41</sup> Testa, B. *Biochem. Pharma.* **2004**, *68*, 2097-2106.

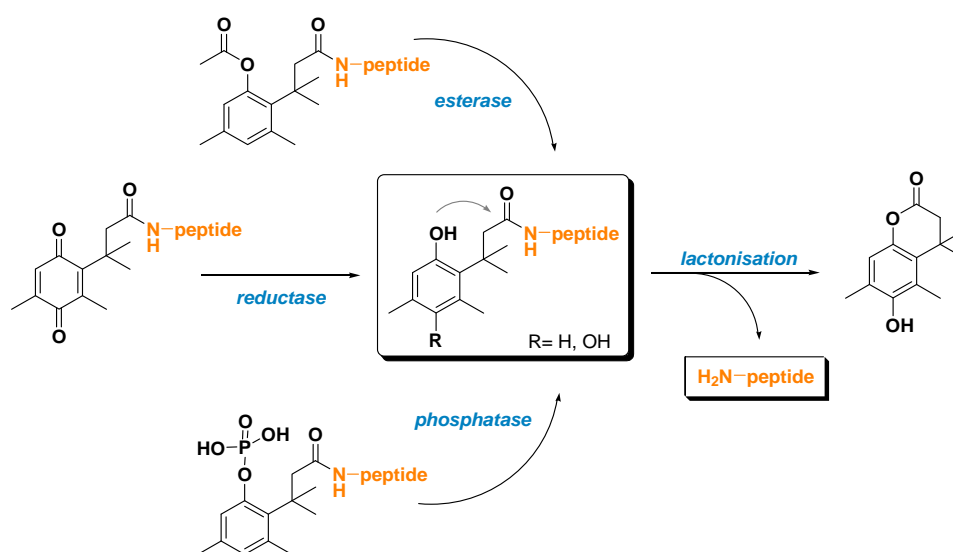
<sup>42</sup> Rautio, J.; Kumpulainen, H.; Heimbach, T.; Oliyai, R.; Oh, D.; Jarvinen, T.; Savolainen, J. *Nature Rev. Drug Disc.* **2008**, *7*, 255-270.

The field of prodrugs in chemotherapy is quite vast so we will discuss only the appropriate area of prodrugs of peptides.

### I.3.1. Prodrugs to improve bioavailability

With regards to peptide therapeutics, various prodrug approaches have been considered to improve formulation and delivery.<sup>43</sup> Masking *N*-positive and/or *C*-negative terminal charges of peptide backbone is for instance commonly explored to reduce susceptibility to exopeptidases and improve permeability properties.

Indeed Borchardt *et al.* investigated aminopeptidase resistant peptides using bioreversible linkages: *N*-termini were attached to an auto-immolable spacer moiety which can be activated through enzymatic reduction, ester or phosphate hydrolysis (**Scheme 1.9**).<sup>44,45,46</sup>



**Scheme 1.9** | Biocleavable aminopeptidase resistant peptides

Following the initial enzymatic activation, the fast hydroxy amide lactonisation primed by the unmasked phenol allow the release of the parent amine. It is worth mentioning that this cyclisation step is facilitated by the presence of a conformational “trimethyl lock”.

<sup>43</sup> Oliyai, R. *Adv. Drug Deliv. Rev.* **1996**, *19*, 275-286.

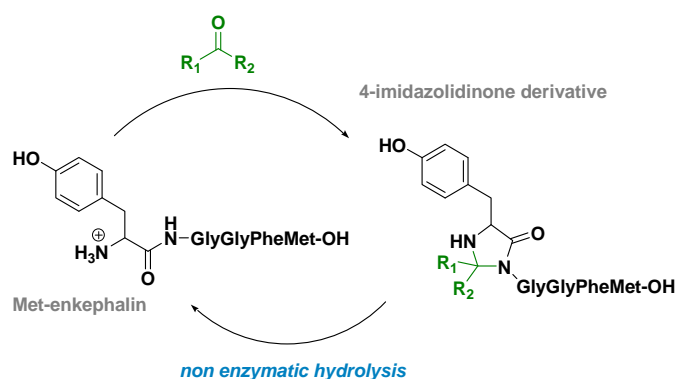
<sup>44</sup> Amsberry, K. L.; Borchardt, R. T. *Pharm. Res.* **1991**, *8*, 323-330.

<sup>45</sup> Amsberry, K. L.; Gerstenberger, E.; Borchardt, R. T. *Pharm. Res.* **1991**, *8*, 455-461.

<sup>46</sup> Nicolaou, M. G.; Yuan, C.-S.; Borchardt, R. T. *J. Org. Chem.* **1996**, *61*, 8636-8641.

Later on, this two-step process has successfully been used to prepare a prodrug of the pentapeptide Leu-enkephalin (H-Tyr-Gly-Gly-Phe-Leu-OH). The self-immolative prodrug system was able to release the peptide in presence of Pig Liver Esterase, however permeation across Caco 2 cells was not improved and the prodrug was shown to have as poor stability as Leu-enkephalin itself in cell culture models. An enhanced susceptibility to endopeptidase activity was invoked to explain this limited bioavailability.

Bundgaard and Rasmussen also constructed aminopeptidase resistant enkephalin prodrugs by condensing their *N*-terminal part with aldehydes and ketones, leading to a series of 4-imidazolidinones (**Scheme 1.10**). This derivatisation was effective in improving the metabolic stability of enkephalins. Furthermore the kinetics of the non-enzymatic hydrolysis, while being slow, could be controlled by tuning the carbonyl substituents  $R_1$  and  $R_2$  to favour peptide release *versus* systemic clearance.<sup>47</sup>

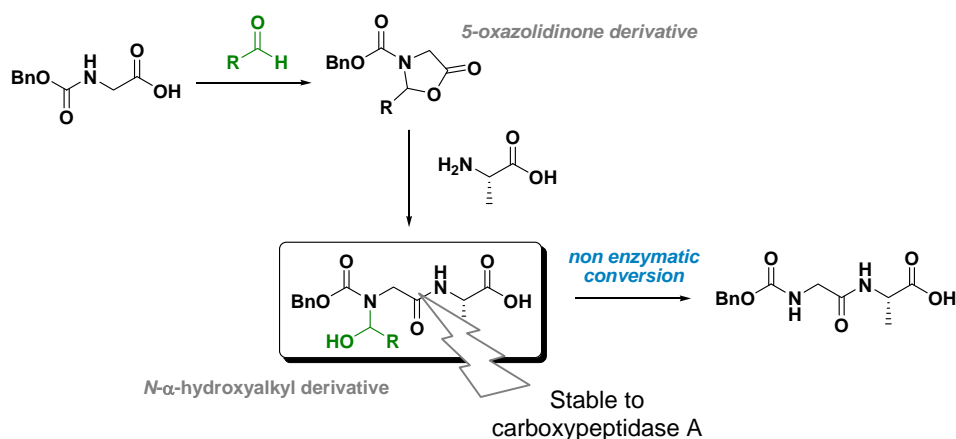


**Scheme 1.10** | 4-imidazolidinone masked Met-enkephalin

In the same way, Bundgaard and Rasmussen also reported the synthesis and evaluation of carboxypeptidase resistant peptides by forming *N*- $\alpha$ -hydroxyalkyl prodrug derivatives (**Scheme 1.11**).<sup>48</sup> Prepared by hydrolysis or aminolysis of *N*-acyl-5-oxazolidinones, the prodrug was demonstrated to display a greater stability than the parent peptide against carboxypeptidase A, an enzyme hydrolysing the *C*-terminal amide of peptides.

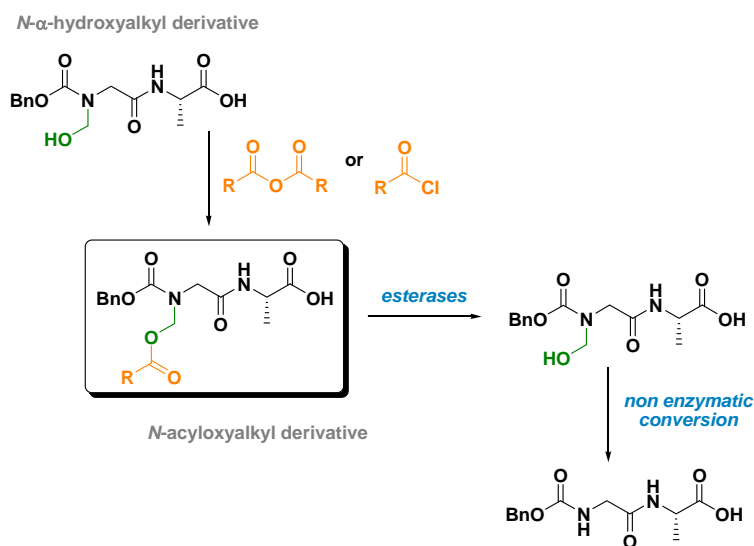
<sup>47</sup> Rasmussen, G. J.; Bundgaard, H. *Int. J. Pharm.* **1991**, 76, 113-122.

<sup>48</sup> Bundgaard, H.; Rasmussen, G. J. *Pharm. Res.* **1991**, 8, 313-322.



**Scheme 1.11** | *N*- $\alpha$ -hydroxyalkyl peptide prodrugs

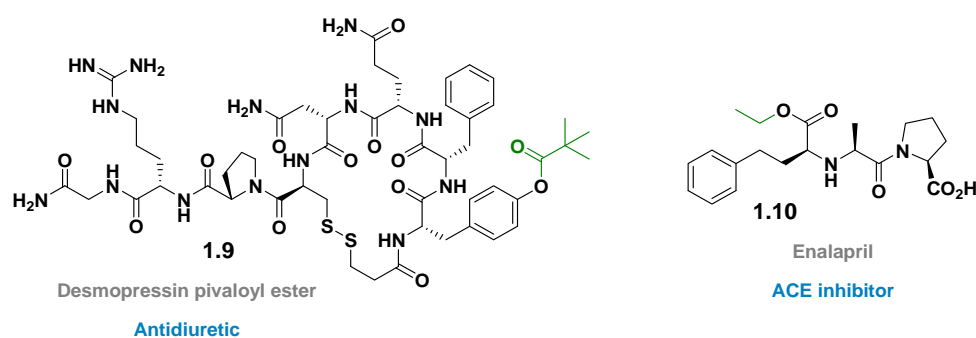
The same strategy is applicable for the synthesis of endopeptidase (*e.g.* trypsin, chymotrypsin) resistant peptides by reversibly alkylating the susceptible endo peptide bond. However the poor stability of such derivatives led to the development of the more stable *N*-acyloxyalkyl derivative (**Scheme 1.12**).<sup>49</sup> Unfortunately, this attempt was proved to be unfruitful as the stability of both prodrug types was shown to be surprisingly comparable.



**Scheme 1.12** | *N*-acyloxyalkyl peptide prodrugs

<sup>49</sup> Bundgaard, H.; Rasmussen, G. J. *Pharm. Res.* **1991**, *8*, 1238-1242.

Formation of ester derivatives (the most common prodrug approach) from residual peptide carboxylic acids, alcohols or phenols was also shown to benefit bioavailability due to increased lipophilicity, rapidly releasing the parent drug after enzymatic ester bond hydrolysis.<sup>50</sup> For instance the pivaloyl ester of desmopressin **1.9**, a synthetic analogue of vasopressin, demonstrated higher stability and transport across Caco-2 cells.<sup>51</sup> Similarly, the Angiotensin Converting Enzyme inhibitor enalapril **1.10** is a commercially available prodrug derivative of enalaprilate used for the treatment of hypertension (**Figure 1.6**).



**Figure 1.6** | Ester prodrugs of peptides

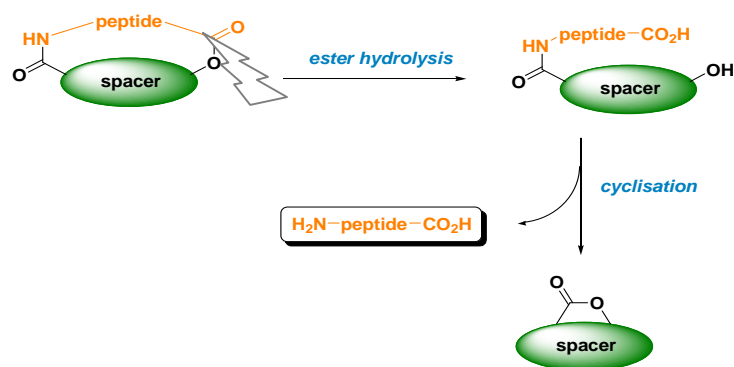
### I.3.2. Bioreversible cyclic peptides

Reversible modifications of the peptide backbone are unambiguously one of the most interesting alternatives for improved peptide delivery. The more promising “bioreversible cyclic peptides” have harnessed considerable attention. As mentioned previously, cyclic peptides are good candidates for enhanced peptide delivery strategies and a prodrug approach restricting temporarily a bioactive peptide into a cyclic conformation is obviously attractive.

Within this framework Borchardt *et al.* developed an esterase-sensitive cyclic prodrug by linking both C- and N-terminal of the peptide to a spacer unit (**Scheme 1.13**). With this design the authors anticipated that enzymatic cleavage of the ester functional group followed by fast intramolecular cyclization should lead to the release of the parent peptide.

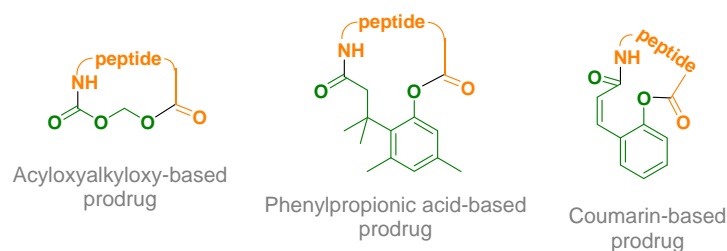
<sup>50</sup> Etmayer, P.; Amidon, G. L.; Clement, B.; Testa, B. *J. Med. Chem.* **2004**, *47*, 2393-2404.

<sup>51</sup> Kahns, A. H.; Buur, A.; Bundgaard, H. *Pharm. Res.* **1993**, *10*, 68-74.



**Scheme 1.13** | Bioreversible cyclic peptides

Therefore Borchardt and co-workers constructed various types of esterase-sensitive spacers to study the cyclisation and release of linear bioactive peptides (**Figure 1.7**). As expected the prodrugs were found to be resistant to both amino- and carboxypeptidases. Furthermore, the cyclic structure conferred the peptide an enhanced hydrophobicity as a consequence of favoured intramolecular hydrogen bonding, pointing to increased permeation.



**Figure 1.7** | Examples of bioreversible cyclic peptides

For instance, the phenylpropionic acid-based cyclic prodrug of the H-TrpAlaGlyGlyAspAla-OH model peptide displayed an enhanced profile and *in vitro* studies demonstrated the great potential of such derivatisation. Indeed, transport experiments revealed that the cyclic prodrug is permeable across Caco-2 cells while the linear peptide is rapidly metabolised at the apical side of the membrane. Furthermore the cyclic prodrug was shown to release the parent peptide in human plasma.<sup>52</sup>

<sup>52</sup> Wang, B.; Gangwar, S.; Pauletti, G. M.; Siahaan, T. J.; Borchardt, R. T. *J. Org. Chem.* **1997**, *62*, 1363-1367.

In the same manner a cyclic prodrug of the opioid peptide DADLE was constructed using a coumarinic spacer.<sup>53</sup> Indeed the *cis* double bond of the coumarinic derivative also affords a favourable conformation lock for the lactonisation release mechanism.

The concept of bioreversible cyclic peptides reinforces the idea that restricting peptide conformational freedom decreases the susceptibility to proteolytic degradation and more importantly increases the permeation potential due to reduced hydrogen bonding capacity to the aqueous solvent and a more compacted and rigidified structure.<sup>54</sup>

## II. Tumour-activated prodrugs

The concept behind such an approach is to selectively activate a non-toxic prodrug within the tumour, resulting in the site-controlled release of the parent drug and therefore limited systemic toxicity. Activation of those prodrugs can be achieved in multiple ways considering cancer hallmarks (*e.g.* pH differences, tumour hypoxia, selective enzyme expression, tumour-specific antigens).<sup>55</sup> Therefore achieving an appropriate prodrug approach may allow the tumour-directed delivery of most anticancer drugs and consequently overcome systemic toxicity due to non-selective interactions. Accordingly, design of efficient selective drug delivery systems has an important initial requirement: the knowledge of the biochemical cancer hallmarks that can allow differentiation between malignant and healthy cells and in this way carry out the desired toxicity-selectivity. Thus the prodrug monotherapy (PMT) approach aims at selectively activating prodrugs of anticancer agents using the features particular to the tumours. Alternative strategies are the two-steps targeting approaches (the so-called DEPT: Directed-Enzyme Prodrug Therapy) which involve the preliminary targeting of an enzyme to the tumour cells (*see II.2.*).

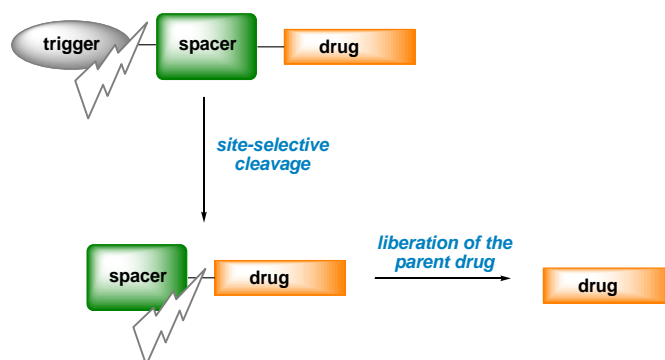
Although the design of Tumour-Activated Prodrugs (TAPs) is slightly different from the classic prodrug molecules described previously, it schematically remains simple: the TAP is usually a three-part modular molecule comprising trigger, spacer and effector units (**Scheme 1.14**).

---

<sup>53</sup> Wang, B.; Wang, W.; Zhang, H.; Shan, D.; Smith, T. D. *Bioorg. Med. Chem. Lett.* **1996**, *6*, 2823-2826.

<sup>54</sup> Gangwar, S.; Jois, S. D. S.; Siahaan, T. J.; Vander Velde, D. G.; Stella, V. J.; Borchardt, R. T. *Pharm. Res.* **1996**, *13*, 1657-1662.

<sup>55</sup> Murray, J. C.; Carmichael, J. *Adv. Drug Deliv. Rev.* **1995**, *17*, 117-127.



**Scheme 1.14** | General scheme for targeted prodrug design

The trigger is designed to target cancer cells and to cause the prodrug activation. The drug is generally linked to the trigger through a spacer unit. In some cases TAPs can be simply two part trigger-drug conjugates however the size of the drug often restrict the recognition of the trigger motif. Accordingly a self-immolative spacer is introduced to simultaneously enhance trigger accessibility and reduce drug toxicity. Therefore the liberated spacer-drug intermediate undergoes further spontaneous degradation ideally liberating the parent drug at the initial site of activation. The choice of the self-immolative spacer is of fundamental importance and considerable research is pursued in this direction.<sup>56</sup>

## II.1. Prodrug monotherapy (PMT)

As already mentioned PMT aims at designing anticancer prodrugs that are directly recognised by means of tumour-associated factors, such as hypoxia, tumour associated enzymes and receptors.<sup>57</sup>

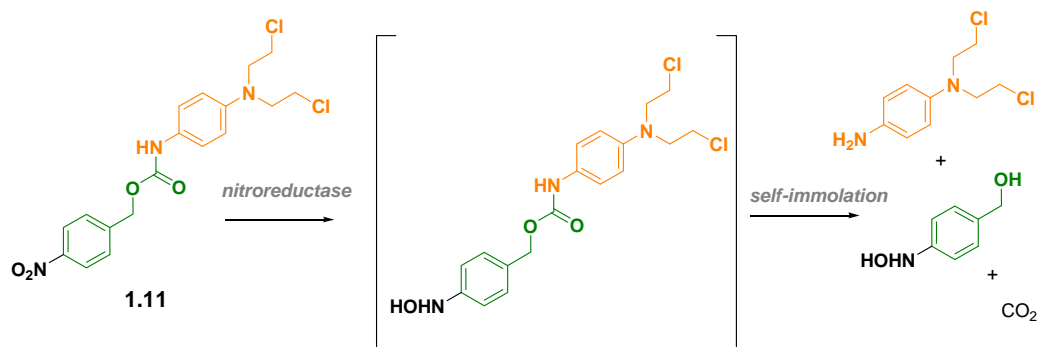
Hypoxia is a unique physiological phenomenon observed in solid tumours due to their imperfect neovascularisation. Thus oxygen deficiency in solid tumours results in the enhanced activity of reducing enzymes, such as nitroreductase, which can be used for the selective activation of anticancer prodrugs.<sup>58</sup> Nitroaromatics are generally the most representative examples of bioreductive prodrugs. For instance the nitrogen mustard prodrug **1.11** was shown to rapidly release the parent drug after action of nitroreductase (**Scheme 1.15**).<sup>59</sup>

<sup>56</sup> Papot, S.; Tranoy, I.; Tillequin, F.; Florent, J.-C.; Gesson, J.-P. *Curr. Med. Chem.: Anticancer Agents* **2002**, *2*, 155-185.

<sup>57</sup> de Groot, F.M.; Damen, E. W.; Scheeren, H. W. *Curr. Med. Chem.* **2001**, *8*, 1093-1122.

<sup>58</sup> Denny, W. A. *Aust. J. Chem.* **2004**, *57*, 821-828.

<sup>59</sup> Mauger, A. B.; Burke, P. J.; Somani, H. H.; Friedlos, F.; Knox, R. J. *J. Med. Chem.* **1994**, *37*, 3452-3458.



Scheme 1.15 | Nitroreductase-activated prodrug

Moreover the selective expression of receptors at the tumour surface also constitutes a way to selectively deliver antitumour agents. Once identified, the ligand to these receptors can be attached to a cytotoxic agent to form a conjugate that would be targeted to the tumour.

Finally some enzymes, such as  $\beta$ -glucuronidase, were found to be present in elevated level in and around tumour tissues.

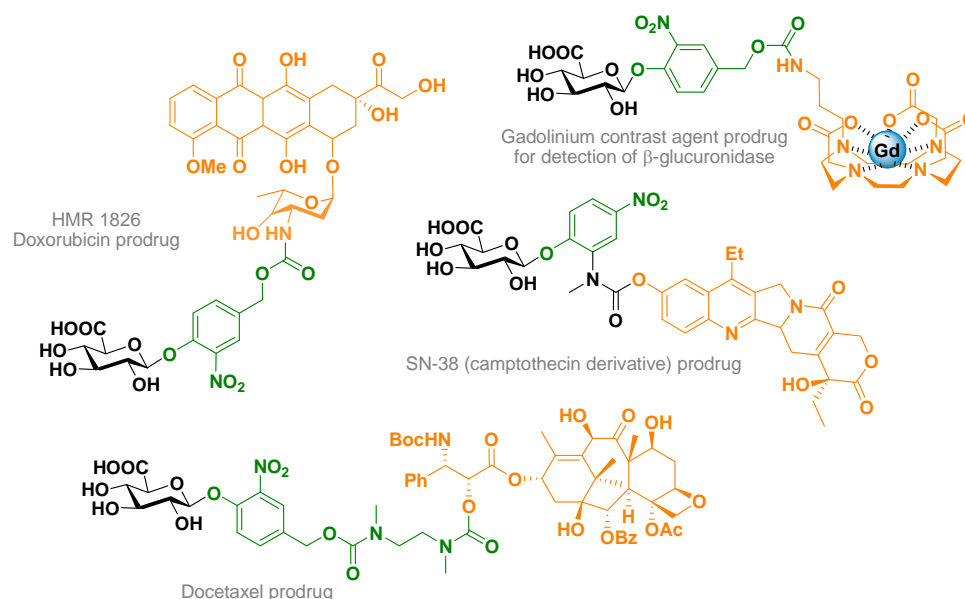
### II.1.1. Glucuronylated prodrugs

Since the last ten years glucuronylated prodrugs have been widely investigated for the selective chemotherapy of cancer. In fact Gesson *et al.* demonstrated that active  $\beta$ -glucuronidase, an endogenous enzyme hydrolysing  $\beta$ -glucuronides, is liberated in necrotic areas surrounding tumours.<sup>60</sup> On the other hand, in normal tissues this enzyme is exclusively located in lysosomes.

Therefore the elevated tumour  $\beta$ -glucuronidase extracellular activity allowed its development in the PMT strategy. In this approach  $\beta$ -glucuronidase activates the glucuronylated prodrug into highly toxic agent specifically at the tumour site. More interestingly in normal tissues, the intracellular location of  $\beta$ -glucuronidase limits the risk of non-selective drug release since the highly hydrophilic nature of glucuronylated prodrugs reduces their ability to penetrate cells.

<sup>60</sup> Bosslet, K.; Straub, R.; Blumrich, M.; Czech, J.; Gerken, M.; Sperker, B.; Kroemer, H. K.; Gesson, J.-P.; Koch, M.; Monneret, C. *Cancer Res.* **1998**, 58, 1195-1201.

To date numerous glucuronylated prodrugs have been constructed and evaluated to demonstrate promising efficacy (**Figure 1.8**).<sup>61</sup>



**Figure 1.8** | Examples of glucuronylated prodrug for detection and treatment of cancer<sup>62,63,64</sup>

Among the various glucuronylated prodrugs developed over the years, HMR 1826 is probably one of the most representative examples and has been the subject of extensive studies.<sup>65</sup>

### II.1.2. HMR 1826

HMR 1826, a prodrug of doxorubicin developed within Gesson group, is based on the self-immolative benzyloxycarbonyl linker attached to the carbohydrate moiety. Following the action of  $\beta$ -glucuronidase the released nitrophenol undergoes a spontaneous 1,6-elimination to liberate a carbamic acid which spontaneously decarboxylate to yield the parent amine drug (**Scheme 1.16**).

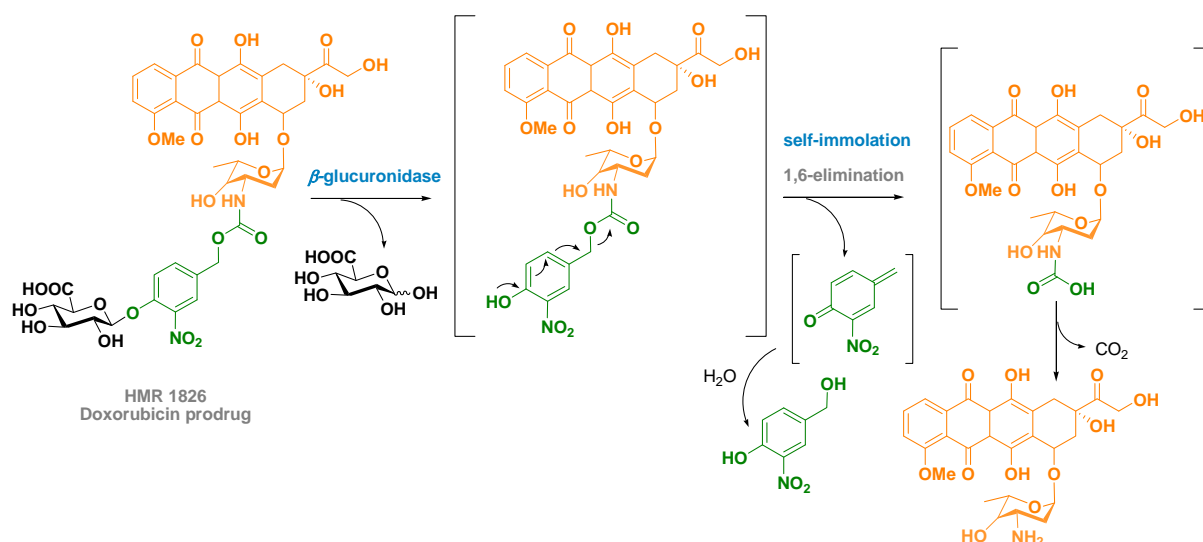
<sup>61</sup> Chen, Xi, Wu, B.; Wang, P. G. *Curr. Med. Chem.- Anti-Cancer Agents* **2003**, *3*, 139-150.

<sup>62</sup> Angenault, S.; Thirot, S.; Schmidt, F.; Monneret, C.; Pfeiffer, B.; Renard, P. *Bioorg. Med. Chem. Lett.* **2003**, *13*, 947-950.

<sup>63</sup> Bouvier, E.; Thirot, F.; Schmidt, F.; Monneret, C. *Bioorg. Med. Chem.* **2004**, *12*, 969-977.

<sup>64</sup> Duimstra, J. A.; Femia, F. J.; Meade, T. J. *J. Am. Chem. Soc.* **2005**, *127*, 12847-12855.

<sup>65</sup> Bosslet, K.; Czech, J.; Hoffmann, D. *Tumor Targeting* **1995**, *1*, 45-50.



**Scheme 1.16** | HMR 1826, a glucuronylated prodrug of doxorubicin

Due to its attractive self-immolative properties this elimination-based spacer is still widely used for the development of enzyme-responsive prodrugs. Indeed it was demonstrated for HMR 1826 that the quinone methide rearrangement of the *o*-nitrophenol intermediate is extremely fast (< 5 min.). A correlation was further established between the phenol's pKa and the kinetics of liberation of the drug. While *o*-nitrophenol (pKa = 7.2) released the drug almost instantaneously the non-nitrated phenol (pKa = 10.0) analogue never released doxorubicin.<sup>66</sup>

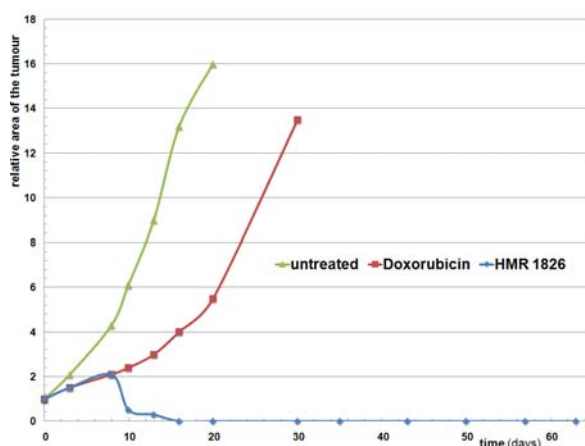
*In vitro* experiments established the excellent stability of HMR 1826 in various plasma (mice, rat and human) showing a maximum 20% degradation after 50 hours incubation at 37°C.<sup>67</sup> *In vivo* studies demonstrated that the relatively non-toxic prodrug HMR 1826 is selectively activated in tumour necrotic areas due to the liberation of  $\beta$ -glucuronidase in disintegrating tumour tissues. Moreover, the excellent tolerance of HMR 1826 allows overcoming the problem of dose-limiting cardiac toxicity associated with doxorubicin. In fact *in vivo* studies in nude mice revealed that the prodrug is 100-fold less toxic than doxorubicin itself.<sup>68</sup>

<sup>66</sup> Florent, J.-C.; Dong, X.; Gaudel, G.; Mitaku, S.; Monneret, C.; Gesson, J.-P.; Jacquesy, J.-C.; Mondon, M.; Renoux, B.; Andrianomenjanahary, S.; Michel, S.; Koch, M.; Tillequin, F.; Gerken, M.; Czech, J.; Straub, R.; Bosslet, K. *J. Med. Chem.* **1998**, *41*, 3572-3581.

<sup>67</sup> Bosslet, K.; Czech, J.; Hoffmann, D. *Cancer Res.* **1994**, *54*, 2151-2159.

<sup>68</sup> Platel, D.; Bonoron-Adèle, S.; Dix, R. K.; Robert, J. *Br. J. Cancer* **1999**, *81*, 24-27.

Comparison between doxorubicin and HMR 1826 in human lung tumours indicated the superior potential of the glucuronylated prodrug approach.<sup>69</sup> Indeed after perfusion with HMR 1826 the level of doxorubicin in tumour tissue was about 7-fold higher than after perfusion with doxorubicin alone. Moreover doxorubicin showed poor uptake difference between normal and tumour lung while co-administration of a specific  $\beta$ -glucuronidase inhibitor (D-saccharolactone) with HMR 1826 resulted in no drug release. Further *in vivo* studies revealed the noteworthy effect of HMR 1826 in breast tumour xenografts in nude mice (**Figure 1.9**).



**Figure 1.9** | Comparison of Doxorubicin and HMR 1826 in MX1 breast tumour xenografts

These results were attributed to the increased drug deposition and retention in the tumour connected with reduced concentration of the anticancer agent in normal tissues, considerably lowering the destruction of normal cells.

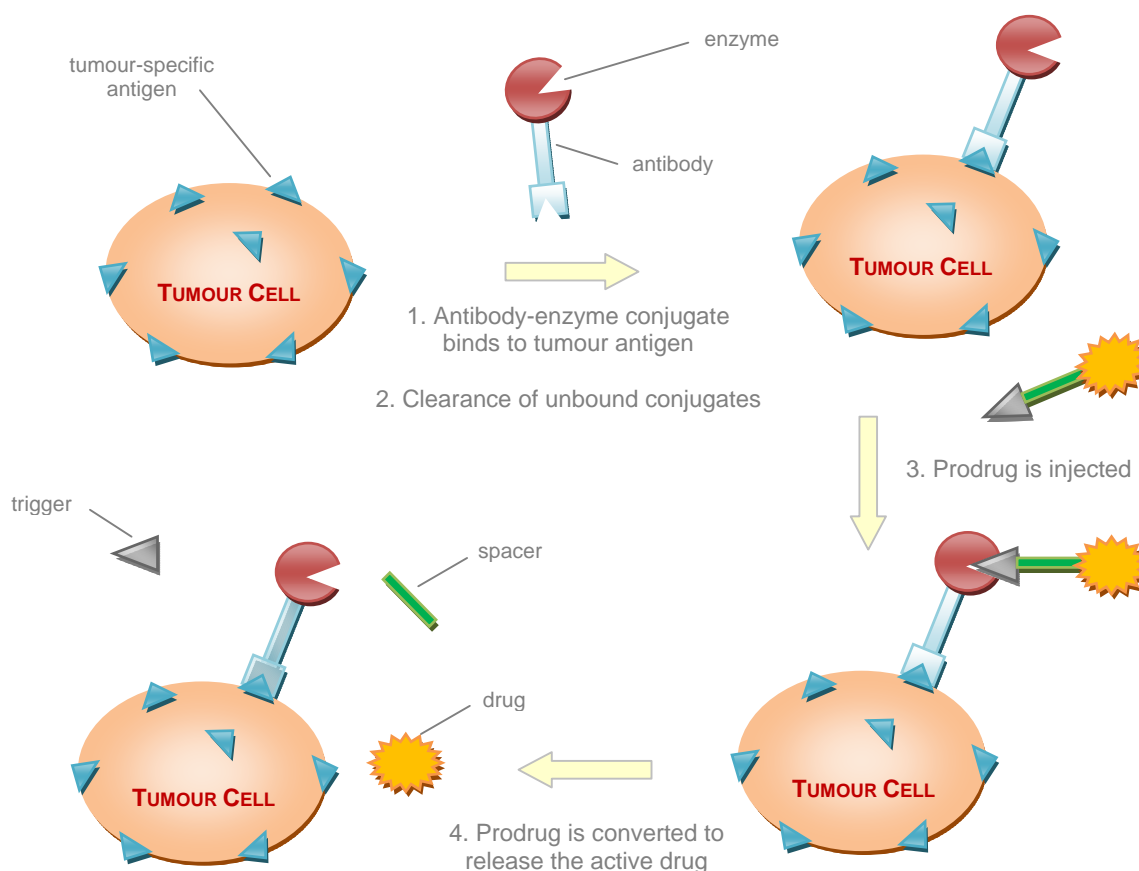
## II.2. Antibody-Directed Enzyme Prodrug Therapy (ADEPT)

ADEPT is another alternative approach to the differentiation between healthy and neoplastic cells.<sup>70</sup> This two-step drug delivery strategy consists of locating an enzyme at the tumour surface that would then activate a related prodrug. First of all an antibody-enzyme conjugate targeted against a specific cancer antigen is administered. After a period of time, once the level of discrimination is sufficiently significant and the unbound immunoconjugate

<sup>69</sup> Mürdter, T. E.; Sperker, B.; Kivistö, K. T.; McClellan, M.; Fritz, P.; Friedel, G.; Linder, A.; Bosslet, K.; Toomes, H.; Dierkesmann, R.; Kroemer, H. K. *Cancer Res.* **1997**, *57*, 2440-2445.

<sup>70</sup> Bagshawe, K. D. *Expert Rev. Anticancer Ther.* **2006**, *6*, 1421-1431.

removed from the blood circulation, the prodrug is injected and converted by the targeted enzyme (Scheme 1.17).



**Scheme 1.17** | Schematic representation of ADEPT

Proposed by Bagshawe in 1987,<sup>71</sup> the strategy has known many improvements coming about with the advances in antibody technology. In the early stages, ADEPT demonstrated extraordinary experimental results, however the immune response generated by the murine antibody and the bacterial enzyme only allowed a single cycle of therapy.<sup>72</sup> Progress in the preparation of humanised antibodies by recombinant DNA technology now allows the preparation of various fusion protein's that do not present risks due to immune response, preserving the protein's activity (*i.e.* binding and enzymatic activity). Since these significant efforts a multitude of antibody-enzyme/prodrug combination has demonstrated encouraging results in preclinical models of human cancers.<sup>73</sup>

<sup>71</sup> Bagshawe, K. D. *Br. J. Cancer* **1987**, *56*, 531-532.

<sup>72</sup> Knox, R. J.; Connors, T. A. *Pathology Oncology Res.* **1997**, *3*, 309-324.

<sup>73</sup> Senter, P. D.; Springer, C. J. *Adv. Drug Deliv. Rev.* **2001**, *53*, 247-264.

For instance, the use of an mAb- $\beta$ -glucuronidase fusion protein in combination with HMR 1826 was the first example of the use of a human enzyme in ADEPT.<sup>74,75</sup> *In vivo* experiments were conducted in nude mice with subcutaneous human colorectal carcinoma xenografts. HMR 1826 was injected one week after the administration of the glucuronidase immunoconjugate. Pharmacokinetic investigations revealed that the doxorubicin was distributed preferentially in intratumoral tissues than in normal tissues, this being a serious improvement in comparison with non-targeted doxorubicin.

More recently, Kamal *et al.* prepared two galactosylated prodrugs of anticancer agents which were evaluated in the course of ADEPT and PMT model protocols.<sup>76</sup> Indeed endogenous  $\beta$ -galactosidase was demonstrated to be overexpressed in hepatocellular carcinoma cell line (Hep G2) thus allowing its use in PMT. Following *in vitro* studies, the prodrugs were found to be good substrates for *E. coli*  $\beta$ -galactosidase and significantly less toxic than the parent drugs. Indeed, the ADEPT and PMT type studies conducted on A375 cell line (presenting no  $\beta$ -galactosidase activity) and the Hep G2 cell line revealed an excellent activation factor QIC<sub>50</sub> (IC<sub>50</sub>[prodrug]/IC<sub>50</sub>[prodrug+enzyme]) of the galactosylated prodrugs. Detailed *in vivo* investigations are ongoing.

GDEPT (Gene-Directed Enzyme Prodrug Therapy), also called suicide gene therapy, is another valuable alternative to ADEPT.<sup>77</sup> The only difference in this strategy is the way of localising non-endogenous enzymes to tumours. In GDEPT a gene is transfected specifically to tumour cells to express the expected enzyme inside the cell, contrary to ADEPT where the enzyme is extracellularly located. The difficulty of this approach results in the effective intracellular delivery of the gene. Many vectors are currently studied such as virus, bacteria, liposomes... which are also being investigated for the genetic therapy of cancer.<sup>78</sup> The use of viruses as transfecting agents led to the Virus-Directed Enzyme Prodrug Therapy (VDEPT). In this case, a genetically modified virus (composed of a tissue-specific transcriptional regulatory sequence linked to a protein coding domain) is used to express a prodrug-converting enzyme in infected cells.

---

<sup>74</sup> Bosslet, K.; Czech, J.; Lorenz, P.; Sedlacek, H.; Schuermann, M.; Seemann, G. *Br. J. Cancer* **1992**, *65*, 234-238.

<sup>75</sup> Bosslet, K.; Czech, J.; Hoffmann, D. *Cancer Res.* **1994**, *54*, 2151-2159.

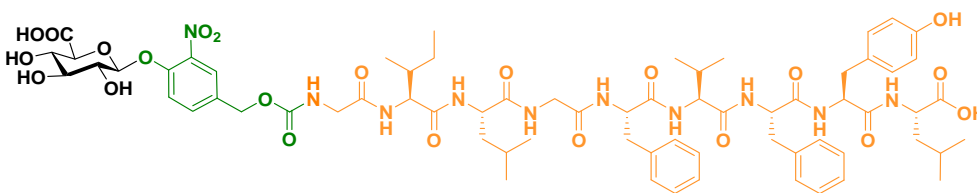
<sup>76</sup> Kamal, A.; Tekumalla, V.; Krishnan, A.; Pal-Bhadra, M.; Bhadra, U. *Chem. Med. Chem.* **2008**, *3*, 794-802.

<sup>77</sup> Denny, W. A. *J. Biomed. Biotech.* **2003**, *1*, 48-70.

<sup>78</sup> Scholl, S. M.; Michaelis, S.; McDermott, R. *J. Biomed. Biotech.* **2003**, *1*, 35-47.

### II.3. Targeted delivery of peptides

To the best of our knowledge only two enigmatic examples of such an approach have been reported concerning peptides, based on the well-known glucuronylated prodrugs. Considering this promising approach, Zemlicka and co-workers developed in 2002 a glucuronylated prodrug of the Class I Major HistoCompatibility (MHC) peptide GILGFVFTL (**Figure 1.10**).<sup>79</sup> Although the synthesis turned out to be more complicated than expected, the prodrug was successfully synthesised and evaluated *in vitro*.



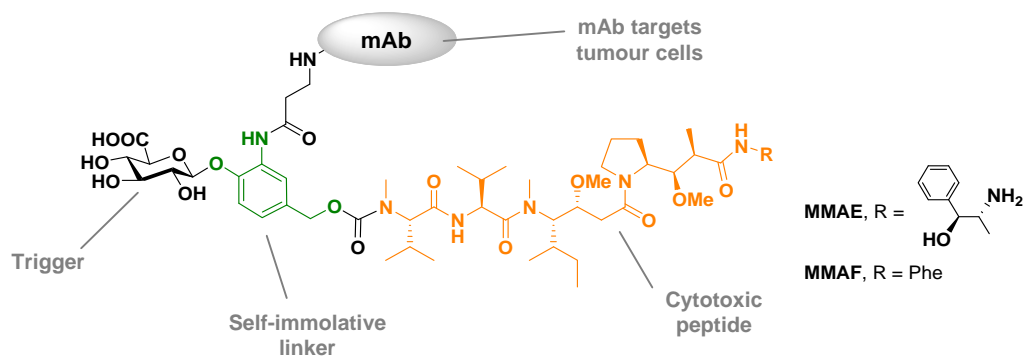
**Figure 1.10** | The first glucuronylated peptide prodrug

Biological studies demonstrated that on the one hand the prodrug has no binding activity on T2 human cells defective in MHC I-associated peptide processing (inactivated T cells). On the other hand the addition of a large excess of  $\beta$ -glucuronidase resulted in an increased level of HLA-A2.1, demonstrating the release of the antigenic peptide and subsequent binding with HLA-A2.1 antigen. This example illustrated the validity of the prodrug approach which in this case is essential. Indeed systemic delivery of such antigenic peptides to mark tumour cells is absolutely inconceivable since such chemotherapy is not able to differentiate cancerous cells and would immediately alert the immune system resulting in severe anarchical cellular destruction.

A few years later, Jeffrey *et al.* accomplished a further step forward by using such glucuronide-based linkers to construct antibody-drug conjugates.<sup>80</sup> The cytotoxic peptides monomethyl auristatin E and F (MMAE and MMAF) were linked to the self-immolative system and a supplementary mAb was attached to target antigen positive tumour cells (**Figure 1.11**).

<sup>79</sup> Rawale, S.; Hrihorczuk, L. M.; Wei, W.-Z.; Zemlicka, J. *J. Med. Chem.* **2002**, *45*, 937-943.

<sup>80</sup> Jeffrey, S. C.; Andreyka, J. B.; Bernhardt, S. X.; Kissler, K. M.; Kline, T.; Lenox, J. S.; Moser, R. F.; Nguyen, M. T.; Okeley, N. M.; Stone, I. J.; Zhang, X.; Senter, P. D. *Bioconjugate Chem.* **2006**, *17*, 831-840.



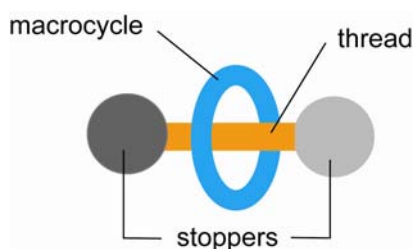
**Figure 1.11** | An antibody targeted peptide prodrug

Such devices were designed here to exploit lysosomal  $\beta$ -glucuronidase as a release mechanism within antibody-targeted cancer cells. Biological studies revealed that such systems are able to specifically release the active drug to the target antigen-positive cells. *In vivo* evaluations in nude mice demonstrated the efficacy of such conjugates as all implanted tumours were cured. A non binding antibody prodrug conjugate was also injected to demonstrate the specificity of the prodrug system. Indeed, this conjugate displayed no antitumour activity as it was not activated in the course of the therapy.

### III. Rotaxane-based peptide prodrugs

#### III.1. Rotaxanes and other interlocked molecules

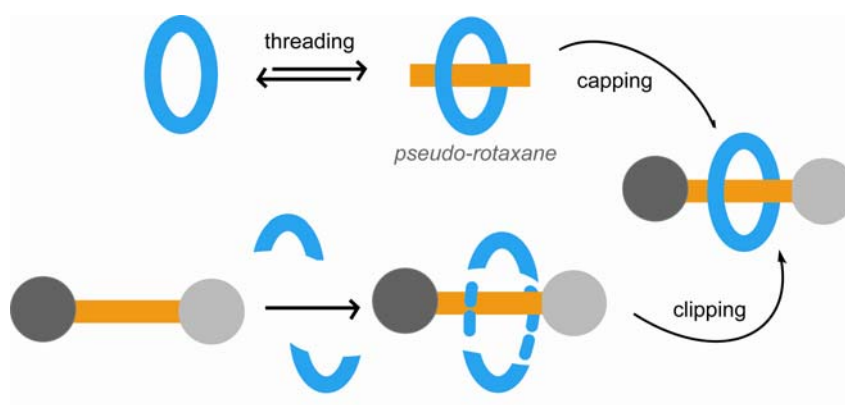
Rotaxanes constitute a class of mechanically-interlocked molecular architectures consisting of one or more rings trapped around a thread presenting final bulky stoppers (Figure 1.12). Although the two components are not covalently connected, rotaxanes are still considered as a single molecule since a covalent bond needs to be disrupted to separate the two intimate components.



**Figure 1.12** | Representation of a rotaxane

Rotaxanes and other mechanically-interlocked molecules such as catenanes (two or more interlocked macrocycles), display a great interest and potential in the construction of synthetic molecular machines, as they constitute the central elements of such machinery. However before reaching this point much of the research has focused in the straightforward and efficient accessibility of such molecules.

Concerning the preparation of rotaxanes, two main synthetic strategies have been commonly developed (**Scheme 1.18**).



**Scheme 1.18** | The two main synthetic strategies for the preparation of rotaxanes

In the capping approach, the previously formed pseudo-rotaxane is trapped by capping the thread ends with two bulky stoppers. In the clipping strategy the macrocycle components wrap around the stoppered thread and the final “clipping” ring closing reaction leads to the rotaxane.

After the first trivial statistical low-yielding approaches,<sup>81, 82</sup> molecular templation brought a dramatic improvement in the assembly of interlocked molecules and it is today the way of excellence for their preparation. Thus using a variety of non-covalent intermolecular interactions (ranging from metal-ligand coordination, hydrogen bonding,  $\pi$ - $\pi$  stacking, hydrophobic and electrostatic interactions)<sup>83</sup> allows the preorganisation of the various components of the interlocked target so that the desired final mechanical linking is greatly

<sup>81</sup> Wasserman, E. *J. Am. Chem. Soc.* **1960**, *82*, 4433-4434.

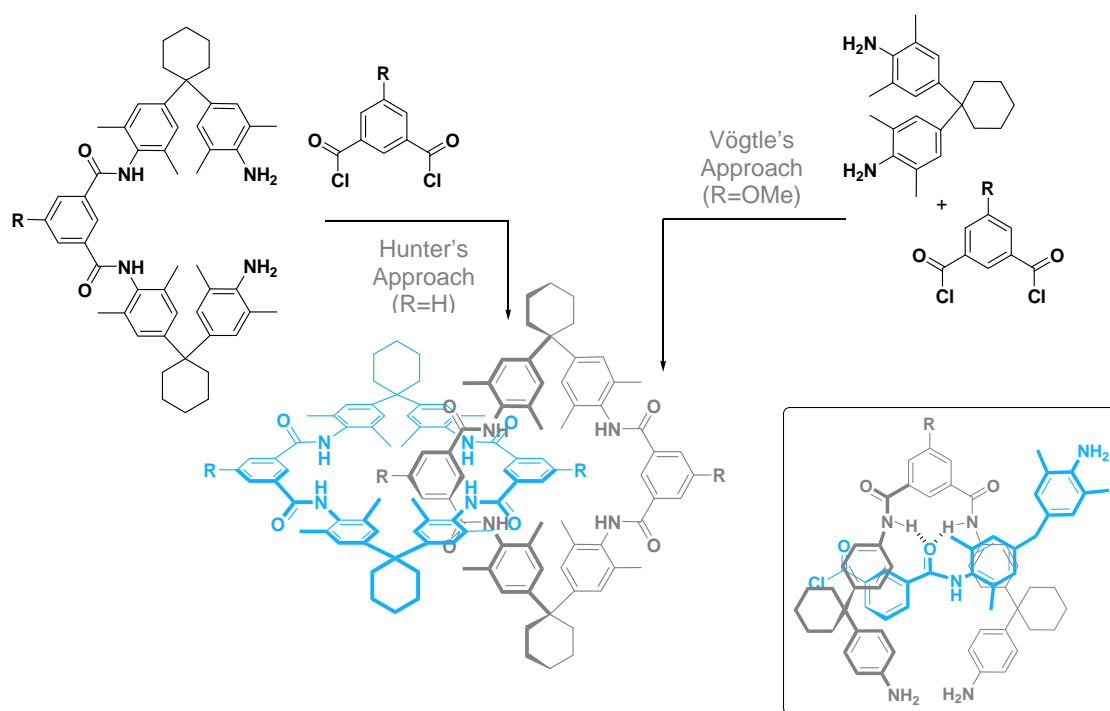
<sup>82</sup> Harrison, I. T.; Harrison, S. J. *J. Am. Chem. Soc.* **1967**, *89*, 5723-5725.

<sup>83</sup> Schill, G. *Catenanes, Rotaxanes and Knots* **1971**, Academic Press, New York.

facilitated. However we will only focus here on the hydrogen bond directed assembly of rotaxanes.

### III.2. Hydrogen bond directed assembly of synthetic peptide rotaxanes

Hunter,<sup>84</sup> closely followed by Vögtle,<sup>85</sup> was one of the firsts to access interlocked molecules using a hydrogen bond template approach (**Scheme 1.19**).



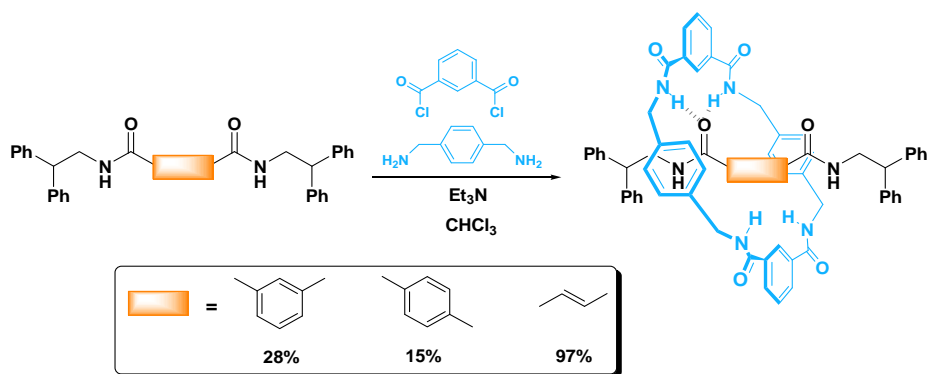
**Scheme 1.19** | The first hydrogen bond-directed amide-based catenanes

Generally to offset the weakness of hydrogen bonds, multiple interaction sites are used to maintain the two components together, finally obtaining a high degree of preorganisation between the two interlocking parts. Indeed in the examples published by Hunter and Vögtle, the templated formation of [2]-catenanes is directed by hydrogen-bonding interactions between the carbonyl groups of isophthaloyl units and the NH groups of amides. Supplementary  $\pi$ - $\pi$  interactions between phenyl rings also assist the formation of these amide-based catenanes.

<sup>84</sup> Hunter, C. A. *J. Am. Chem. Soc.* **1992**, *114*, 5303-5311.

<sup>85</sup> Vögtle, F.; Meier, S.; Hoss, R. *Angew. Chem. Int. Ed.* **1992**, *31*, 1619-1622.

A few years later, Leigh and co-workers reported the synthesis of a [2]-catenane from the reaction of isophthaloyl chloride and *p*-xylylenediamine at high dilution.<sup>86</sup> Taking the mechanism of this reaction into consideration, the methodology was extended to the preparation of [2]-rotaxanes using suitably stoppered diamide threads.<sup>87</sup> Using a fumaric template led to an incredible 97% yield, this success being explained by the quasi-ideal preorganisation of the intercomponents (**Scheme 1.20**).<sup>88</sup>



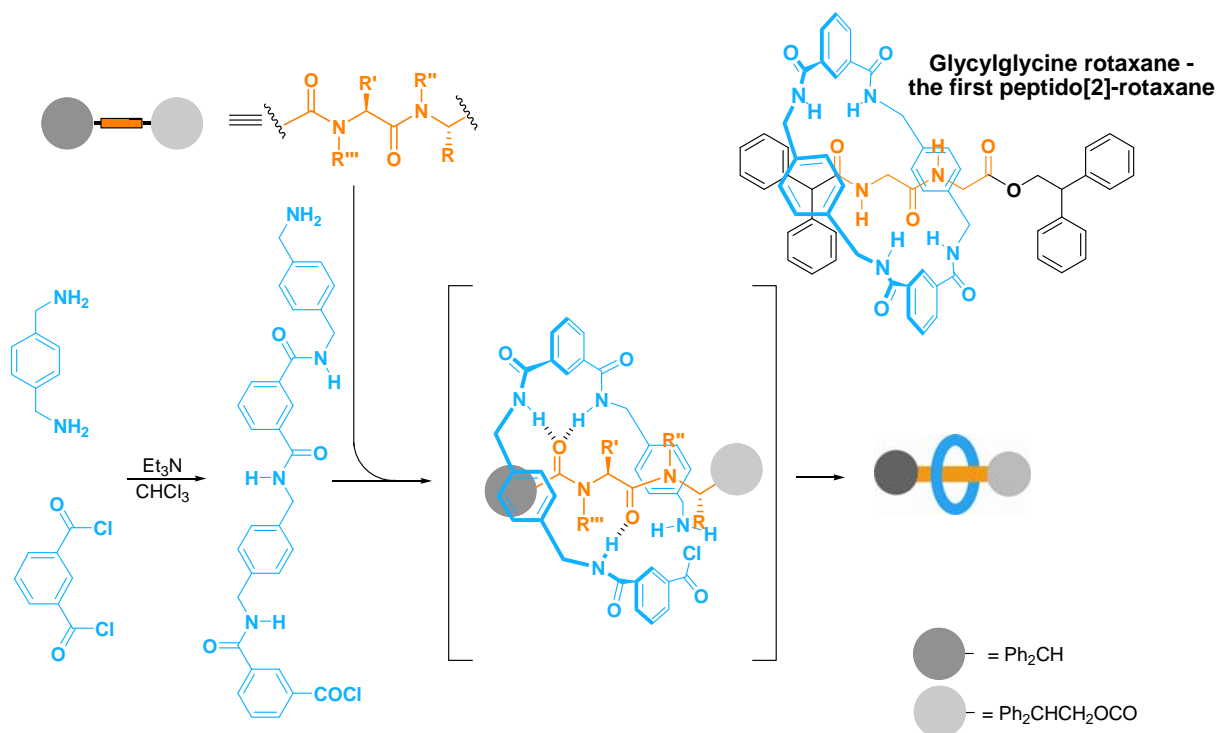
**Scheme 1.20** | Leigh's synthesis of diamide rotaxane by the clipping strategy

Subsequently, Leigh *et al.* also found that simple peptides could be used as a template for the formation of amide-based rotaxanes. In fact the mechanism for the formation of such interlocked products relies primarily on the templated assembly of the benzylic amide macrocycle around two transoid amide groups. Amides in similar spatial arrangements can indeed be found in simple peptides, so peptides may consequently be able to template the cyclisation of benzylic amide macrocycles around them to give peptide rotaxanes (**Scheme 1.21**).

<sup>86</sup> Johnston, A. G.; Leigh, D. A.; Nezhat, L.; Smart, J. P.; Deegan, M. D. *Angew. Chem. Int. Ed.* **1995**, *34*, 1212-1216.

<sup>87</sup> Johnston, A. G.; Leigh, D. A.; Murphy, A.; Smart, J. P.; Deegan, M. D. *J. Am. Chem. Soc.* **1996**, *118*, 10662-10663.

<sup>88</sup> Gatti, F. G.; Leigh, D. A.; Nepogodiev, S. A.; Slawin, A. M. Z.; Teat, S. J.; Wong, J. K. Y. *J. Am. Chem. Soc.* **2001**, *123*, 5983-5989.



**Scheme 1.21** | Mechanism of formation of peptide rotaxane

A glycylglycine rotaxane was the first peptide rotaxane to be synthesised using this clipping strategy, in 62% yield, leading to the conclusion that such rotaxane encapsulation could be used to enhance the pharmacological features of peptide drugs.<sup>89</sup>

*“If the hydrogen bond directed synthesis described here can be extrapolated to more complex peptides, then temporary housing within a rotaxane superstructure could simultaneously provide protection from hostile environments, improved stability, and engineered lipophilicity/solubility characteristics.”*

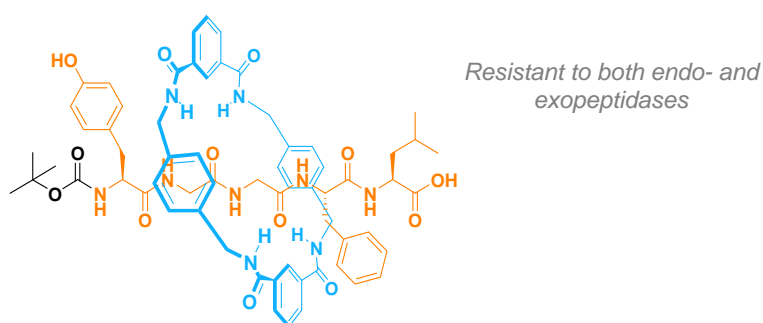
Following this first success several dipeptide rotaxanes were constructed varying the amino acid residues in order to determine the essential structural requirements for a suitable hydrogen-bonding template between appropriately stoppered peptide threads and benzylic amide macrocycles.<sup>90, 91</sup> It briefly appears, because of the evident steric restrictions, that one glycine residue is absolutely necessary to efficiently access dipeptide rotaxanes.

<sup>89</sup> Leigh, D. A.; Murphy, A.; Smart, J. P.; Slawin, A. M. Z. *Angew. Chem. Int. Ed.* **1997**, *36*, 728-732.

<sup>90</sup> Asakawa, M.; Brancato, G.; Fanti, M.; Leigh, D. A.; Shimizu, T.; Slawin, A. M. Z.; Wong, J. K. Y. *J. Am. Chem. Soc.* **2002**, *124*, 2939-2950.

The synthesis of longer peptide rotaxanes proved more difficult since, in apolar solvent (necessary for using hydrogen-bond template), the peptide thread tends to autosatisfy itself in term of hydrogen bonding (folding) preventing good preorganisation with the macrocycle precursors. The supplementary lack of solubility also contributes to dramatically decreased yields. However, it appears that a single internal template site (*i.e.* a glycine residue) is able to satisfy those structural requirements in longer peptide threads.

A Boc-Leu-enkephalin (Boc-Tyr-Gly-Gly-Phe-Leu-OH) rotaxane was prepared (**Figure 1.13**), albeit in 1% yield, and its properties evaluated. It appeared that, contrary to the instantaneous degradation of Boc-Leu-enkephalin, the peptide rotaxane was completely resistant to proteolytic degradations by several exo- and endopeptidases. Preliminary studies at *GlaxoSmithKline* confirmed that the rotaxane-encapsulated form of Leu-enkephalin does not bind to opioid receptors, but that the released peptide does.<sup>92</sup>



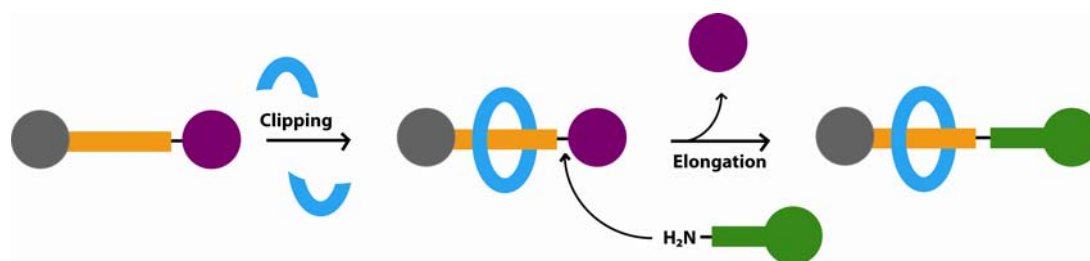
**Figure 1.13** | Boc-Leu-enkephalin rotaxane

From that point, the concept of using rotaxanes as peptide delivery agents became extremely attractive. Indeed on top of providing a protective shield to the peptide, encapsulation within a rotaxane superstructure would allow the modulation of the hydrophilic character of the peptidic thread, thus engineering its membrane permeation ability. Indeed Leigh *et al.* also investigated the influence of attaching substituents to the macrocycle unit and proved that this could efficiently modulate lipophilicity.<sup>92</sup>

<sup>91</sup> Brancato, G.; Coutrot, F.; Leigh, D. A.; Murphy, A.; Wong, J. K. Y.; Zerbetto, F. *Proc. Natl. Acad. Sci. USA* **2002**, *99*, 4967-4971.

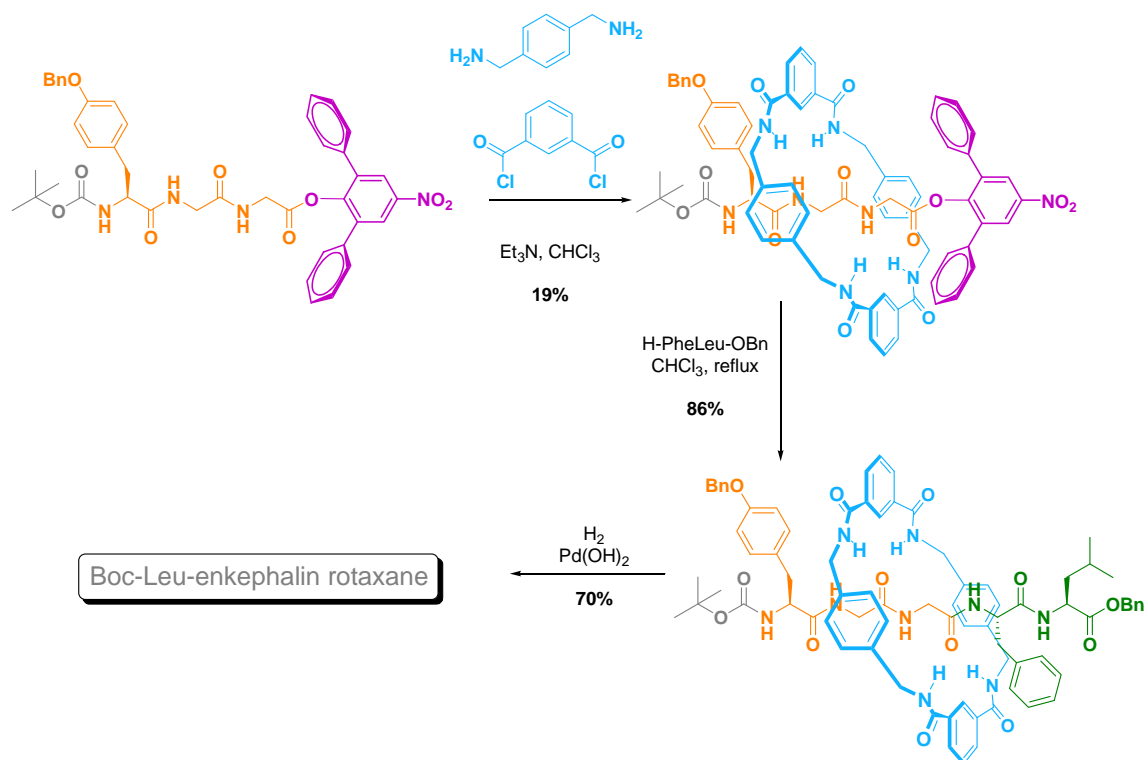
<sup>92</sup> Potok, S. *PhD Thesis*, University of Edinburgh, **2004**.

Those great results therefore pointed out the difficulty in accessing long peptide rotaxanes. A straightforward sequence needs to be developed to magnify the potential of such delivery devices, and a convergent approach using preformed rotaxane building blocks seems to be appropriate in this case. To remedy this disadvantage, an efficient and versatile methodology was developed in the Leigh group to elongate previously-formed peptide rotaxane building blocks. The strategy relied on the assembly of a peptide rotaxane bearing a temporary stopper which can be easily displaced by another stoppered *N*-free peptide sequence (**Scheme 1.22**).<sup>92</sup>



**Scheme 1.22** | Elongation of peptide rotaxane building blocks

The temporary stopper needs to be carefully designed: it should be bulky enough to lock the macrocycle and reactive enough to nucleophilic attack without being displaced by *p*-xylylenediamine during the rotaxane formation process. The ideal stopper to fulfil these requirements was found to be the 2,6-diphenyl-4-nitrophenyl ester. Accordingly, various rotaxanes bearing this activated ester stopper were prepared and successfully elongated with a range of *C*-stoppered peptides.<sup>92</sup> The encouraging results obtained prompted Leigh *et al.* to explore those conditions in the novel synthesis of the Boc-Leu-enkephalin rotaxane (**Scheme 1.23**).

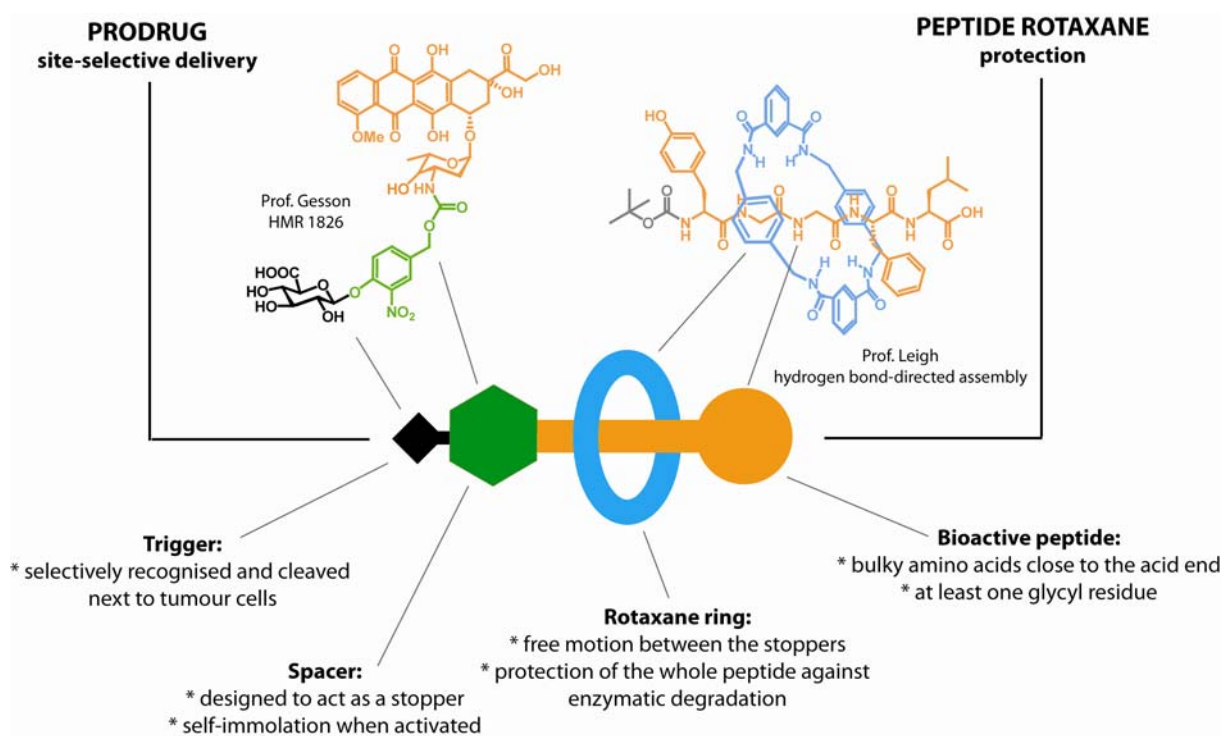


**Scheme 1.23** | Synthesis of Boc-Leu-enkephalin rotaxane *via* the elongation strategy

The synthesis of Boc-Leu-enkephalin was readily improved, bringing an admirable advancement in the preparation of therapeutic mechanically-interlocked nanodevices. However, for these devices to be considered as prodrugs, the encapsulated compound needs to be released at some point. These kinds of rotaxane-based prodrugs could however be devised by using a stimuli-responsive stopper that, once activated and cleaved, would release the active thread following the mechanical disassembly of the rotaxane architecture. More interestingly, incorporating a trigger unit at the stopper would be ideal for the development of rotaxane-based peptide prodrugs selectively targeting tumour cells.

### III.3. Rotaxane-based peptide prodrugs

Our concept consists in associating the targeted delivery system elaborated by Prof. Gesson in Poitiers (*e.g.* HMR 1826) and the supramolecular assembly process developed in Edinburgh by Prof. Leigh (*e.g.* Boc-Leu-enkephalin rotaxane) in order to derivatise bioactive peptides into rotaxane-based prodrugs. As a result such anticancer devices would be selectively activated at tumour sites (**Scheme 1.24**).

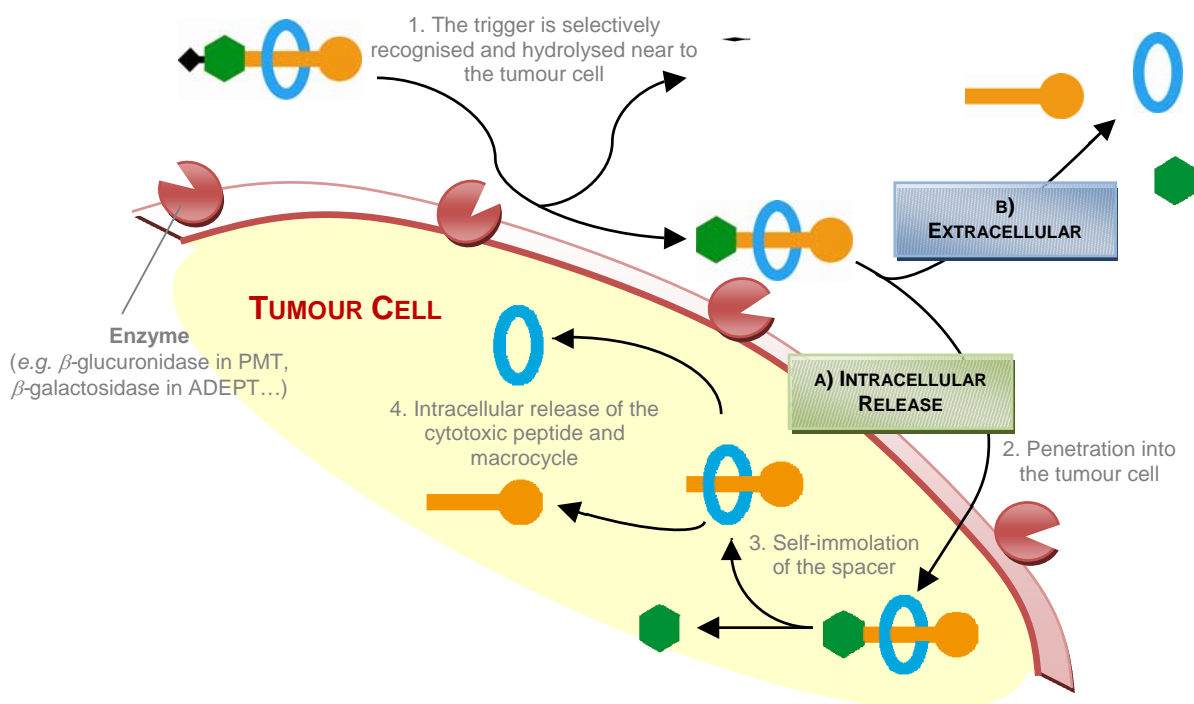


**Scheme 1.24** | Designing novel nanodevices for the selective delivery of cytotoxic peptides

The rotaxane-based peptide prodrugs strictly follow the design of TAPs. The trigger, spacer and peptide drug constitute the heart of the molecule. Encapsulation by a well-suited macrocycle would afford a protective shield to that heart. Furthermore, the synthetic derivatisation of classical prodrug constructions is essential to reach a prodrug thread presenting bulky stoppers which would permanently lock the macrocycle around the peptide template.

First of all, the trigger moiety is selectively recognised and hydrolysed around tumour cells (**Scheme 1.25**). Such activation may occur even in the course of a PMT protocol (*e.g.* with  $\beta$ -glucuronidase as the activating enzyme) or ADEPT strategy (*e.g.*  $\beta$ -galactosidase as the directed enzyme). The subsequent removal of the polar trigger (*e.g.* glucuronic acid or galactose) should mediate the penetration of the peptide rotaxane across cancer membranes (case A). Self-immolation of the activated spacer should result in the release of the bioactive peptide and complementarily in the liberation of the macrocycle.

The extracellular release of the peptide is also conceivable (case B). This possibility is quite interesting in the case of membrane receptor-interacting peptides since the level of the peptide ligand would be highly increased in the tumour area.



**Scheme 1.25** | Mechanism of rotaxane-based peptide prodrugs

Our machine should present limited toxicity regarding healthy cells however, once activated, the consecutive release of the parent anticancer peptide should selectively kill tumour cells. Consequently this innovative delivery device is designed to overcome the two main drawbacks associated with peptide therapy: their rapid degradation by proteases and their poor absorption. Furthermore, this rotaxane-based molecular machine also addresses the challenge of obtaining more selectivity in anticancer chemotherapy. Indeed being constructed upon a prodrug design, the machine should not present any side-effects due to systemic toxicity and should only be targeted and activated around cancerous tissues.

Based on the knowledge acquired by the two universities over the years we decided to construct a model rotaxane-based peptide prodrug to test the validity of such a concept. We focused on spacer moieties already developed within Gesson group to prepare simple peptide prodrugs. The successful encapsulation of the resulting prodrug using the rotaxane forming reaction developed within Leigh group would afford the first peptide rotaxane prodrugs.

Accordingly a careful study of the peptide prodrug and its corresponding rotaxane is warranted to comprehend the influence of encapsulating peptides upon their physiological and therapeutic properties. The targeted activation of our machine should liberate the fully-functional peptide at tumour sites, accompanied with the tetraamide macrocycle, for which toxicity should also be evaluated.

# CHAPT. 2 | TOWARDS A MODEL ROTAXANE-BASED PEPTIDE PRODRUG

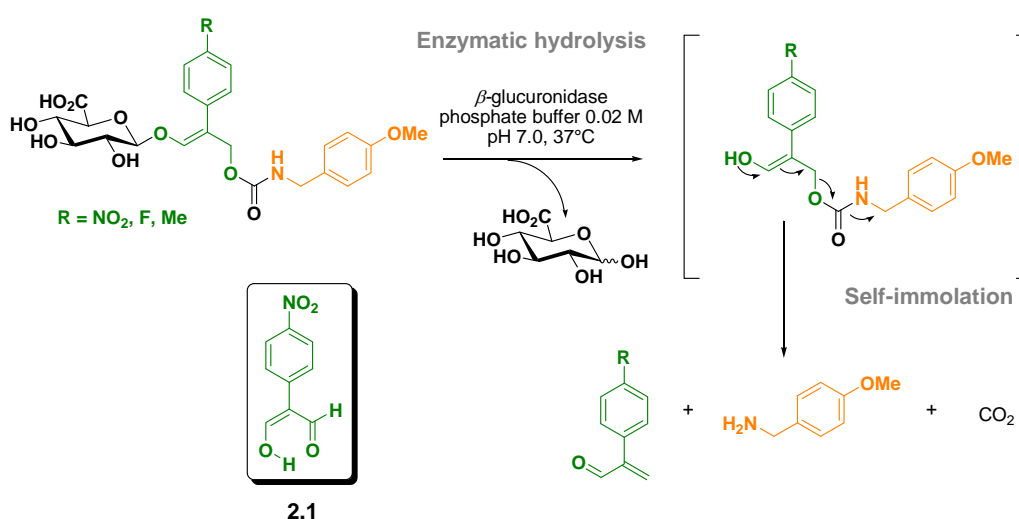
The work presented in this chapter was done in collaboration with Aurélien Viterisi who prepared model peptides **2.2** and **2.33**, synthesised macrocycles **2.53** and **2.54** and carried out the HPLC purifications of the final prodrugs. He also monitored the enzymatic hydrolysis of our prodrug molecules along with the measurement of their water solubility.

|  |           |
|--|-----------|
| <b>I. Arylmalonaldehyde-based delivery system .....</b>                                | <b>42</b> |
| I.1. Introduction.....   | 42        |
| I.2. The acid-catalysed dimerisation of arylmalonaldehydes.....                        | 43        |
| I.3. Arylmalonaldehyde-based rotaxane prodrug.....                                     | 49        |
| <b>II. “Allyl-based” delivery system .....</b>   | <b>51</b> |
| II.1. Synthesis and preliminary enzymatic evaluation of the new “allyl spacer”.....    | 51        |
| II.2. Synthesis of “allyl-based” model prodrugs .....                                  | 54        |
| II.3. Enzymatic hydrolysis .....   | 56        |
| II.4. Synthesis of the tunable “allyl-based” rotaxane model prodrugs.....              | 58        |
| II.5. Synthesis of the functionalised macrocycles .....                                | 61        |
| II.6. Water solubility and enzymatic hydrolysis of PEG-grafted rotaxane prodrugs ..... | 62        |
| II.6.1 Water solubility .....  | 62        |
| II.6.2 Enzymatic hydrolysis .....  | 63        |
| II.7. Observations .....   | 64        |
| <b>III. <i>bis</i>-Galactosyl-based delivery system.....</b>                           | <b>65</b> |
| III.1. Introduction .....  | 65        |
| III.2. Synthesis.....  | 67        |
| III.3. Enzymatic hydrolysis .....  | 70        |
| <b>IV. Conclusion .....</b>  | <b>72</b> |
| <b>V. Supporting information .....</b>   | <b>73</b> |
| V.1. The acid-catalysed dimerisation of arylmalonaldehydes .....                       | 73        |
| V.2. “Allyl-based” delivery system.....  | 75        |
| V.3. <i>bis</i> -Galactosyl-based delivery system .....                                | 102       |

## I. Arylmalonaldehyde-based delivery system

### I.1. Introduction

Our first attempts to prepare a model rotaxane-based peptide prodrug focused on the arylmalonaldehyde spacer which was previously developed within the Gesson group to target doxorubicin.<sup>93</sup> A preliminary enzymatic study conducted with three glucuronylated model prodrugs bearing the variously substituted arylmalonaldehydes (NO<sub>2</sub>, F and Me) revealed that the nitro derivative **2.1** represents a good spacer candidate for prodrug development (**Scheme 2.1**).<sup>94</sup>



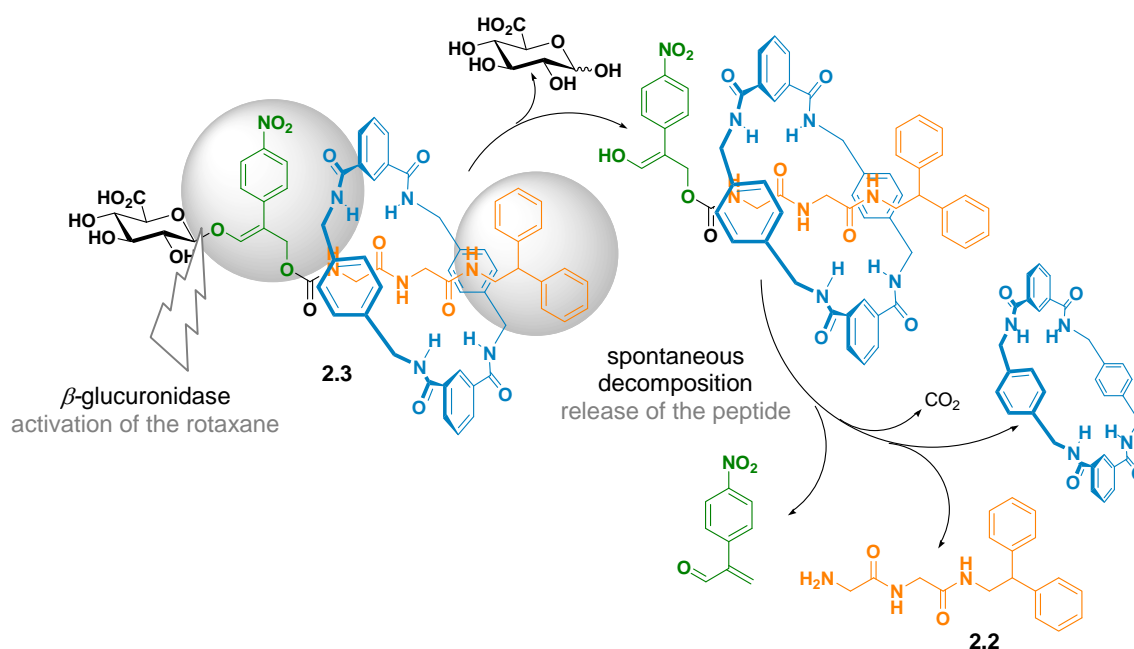
**Scheme 2.1** | Arylmalonaldehyde-based glucuronylated prodrugs

CPK models confirmed that nitro-arylmalonaldehyde linker **2.1** is bulky enough to act as a stopper and therefore could be used for the investigation of our concept. For a model peptide we decided to use the stoppered glycylglycine dipeptide **2.2** (which has been widely applied as a template for peptide rotaxane formation),<sup>95</sup> and to synthesise its rotaxane derivative **2.3**. The enzymatic hydrolysis of the glucuronide moiety should activate our drug delivery device, releasing the model peptide after self-immolation of the arylmalonaldehyde unit (**Scheme 2.2**).

<sup>93</sup> Papot, S.; Combaud, D.; Gesson, J.-P. *Bioorg. Med. Chem. Lett.* **1998**, *8*, 2545-2548.

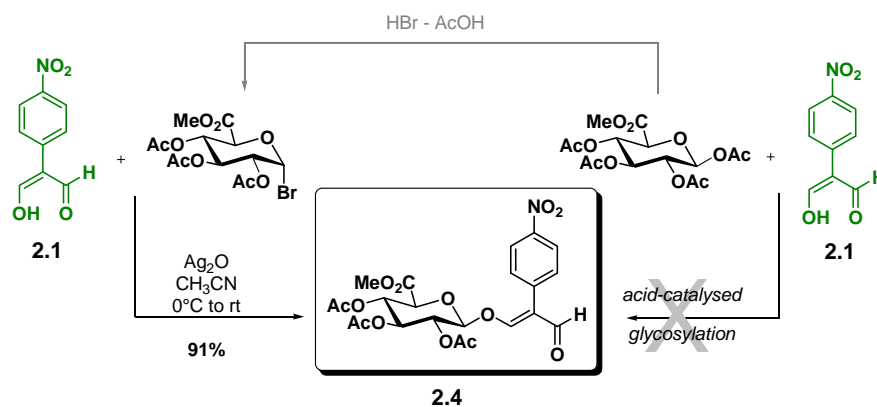
<sup>94</sup> Rivault, F.; Tranoy-Opalinski, I.; Gesson J.-P. *Bioorg. Med. Chem.* **2004**, *12*, 675-682.

<sup>95</sup> Leigh, D. A.; Murphy, A.; Smart, J. P.; Slawin, A. M. Z. *Angew. Chem. Int. Ed.* **1997**, *36*, 728-732.



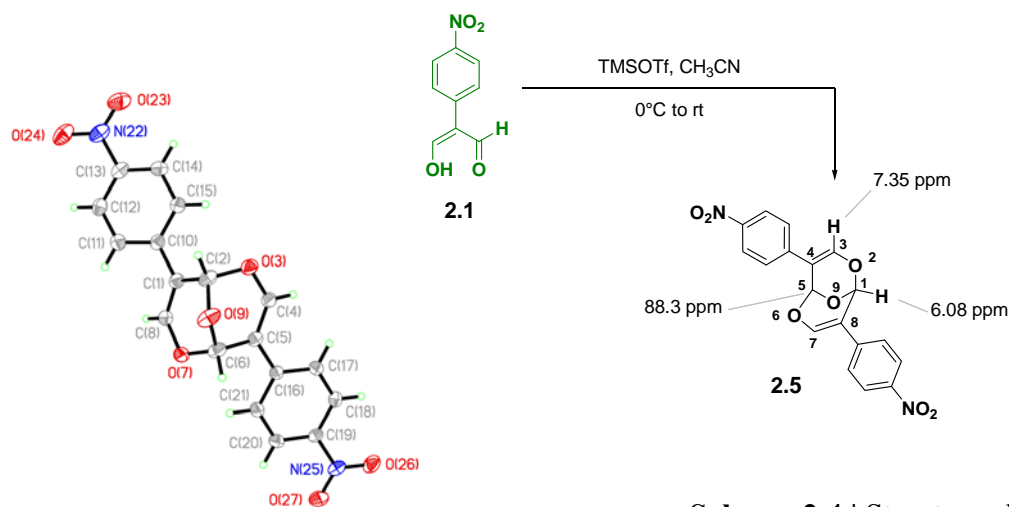
## I.2. The acid-catalysed dimerisation of arylmalonaldehydes

In the synthesis described by Gesson *et al.*, glycosylation of 2-(4-nitrophenyl) malondialdehyde **2.1** was conducted in the presence of the protected glucuronyl bromide using the classical Koenigs-Knorr reaction. With the aim to reduce the number of steps to access compound **2.4** we investigated the acid-catalysed glycosylation of **2.1** directly from the fully protected glucuronide. Surprisingly glycosylation of **2.1** in the presence of various Lewis acids was not successful while **2.4** was synthesised with excellent yields, selectively in the form of the  $\beta$ -anomer, using the reported procedure (**Scheme 2.3**).



However, an intriguing main product was isolated from the acid-catalysed glycosylation mixture. The straightforward  $^1\text{H}$  NMR spectrum prompted us to envisage the formation of a highly symmetric compound, presenting no sugar signals. Accordingly, we decided to study the behaviour of arylmalonaldehyde **2.1** under acid conditions (TMSOTf,  $\text{CH}_3\text{CN}$ ) and could rapidly observe the formation of a single apolar product, revealing NMR profiles identical to the unknown isolated product. Beside the signals corresponding to aromatic protons, the  $^1\text{H}$  NMR spectrum displayed only two singlets at  $\delta$  6.08 and 7.35 ppm with a 1:1 intensity which indicated the symmetry of the molecule, along with the absence of any aldehyde functionality. The  $^{13}\text{C}$  NMR spectrum revealed no signal downfield from 147 ppm, confirming the absence of any carbonyl group. More importantly, the signal at  $\delta$  88.3 ppm suggested the presence of an acetalic carbon.

Therefore based on those experimental observations, structure **2.5** was proposed, which would result from the acid-catalysed dimerisation of arylmalonaldehyde **2.1** (Scheme 2.4). Mass spectrometry and X-ray crystallography further confirmed the molecular structure of **2.5**.

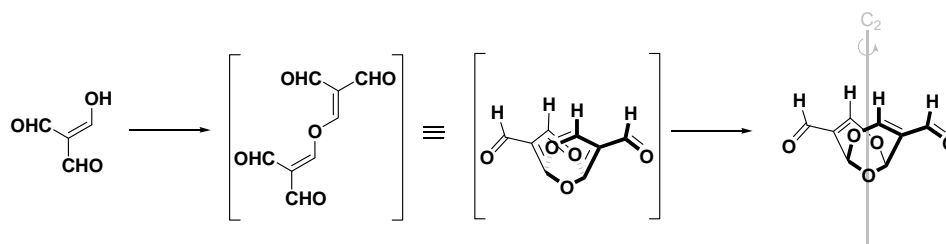


Scheme 2.4 | Structure elucidation

Historically this kind of motif, namely 2,6,9-trioxabicyclo[3.3.1]nona-3,7-diene (also called bridged *bis*-dioxines), was prepared in 1965 *via* a platinum (II)-promoted condensation of acetylacetone.<sup>96</sup> To the best of our knowledge only two synthetic methods leading to this diene system have been reported. Arnold and Budesinsky observed in 1988 the formation of the 4,8-dicarbaldehyde as the dimer product of triformylmethane (Scheme 2.5).<sup>97</sup>

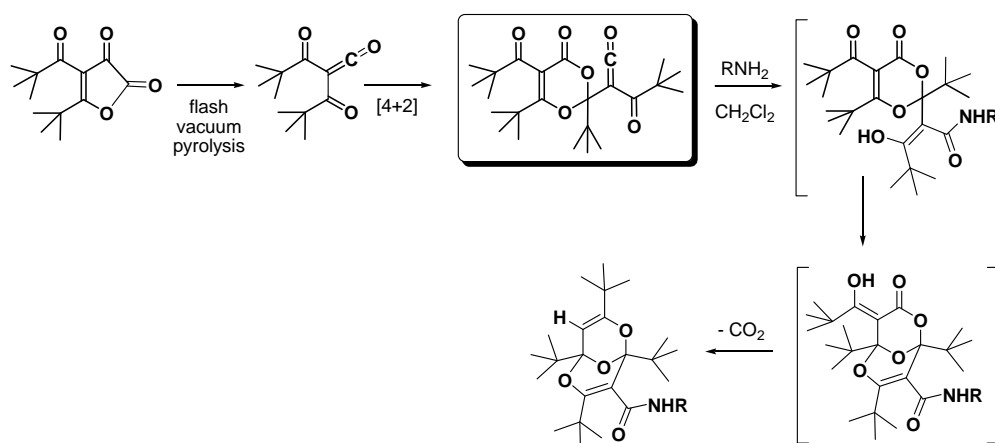
<sup>96</sup> Gibson, D.; Oldham, C.; Lewis, J.; Lawton, D.; Mason, R.; Robertson, G. B. *Nature* **1965**, *208*, 580-581.

<sup>97</sup> Arnold, Z.; Budesinsky, M. *J. Org. Chem.* **1988**, *53*, 5352-5353.


**Scheme 2.5** | Dimerisation of triformaldehyde

NMR studies with a chiral shift reagent demonstrated the chirality of such bicyclic structure possessing a 2-fold rotational axis as the only element of symmetry.

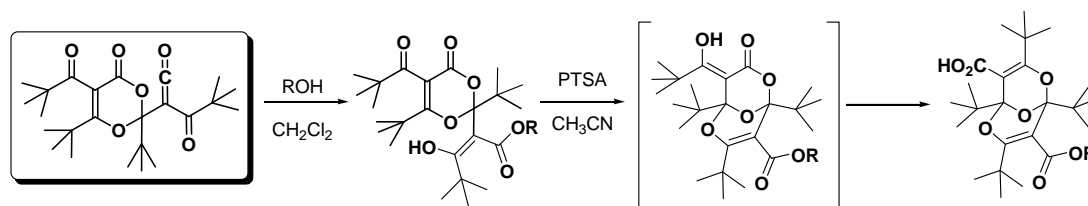
Later on, Kollenz *et al.* proposed the unique general synthetic method to access substituted trioxabicyclononadienes.<sup>98</sup> Addition of various aromatic amines to a stable  $\alpha$ -oxoketene yielded the corresponding bridged *bis*-dioxines (**Scheme 2.6**).


**Scheme 2.6** | The Kollenz method, amine nucleophiles

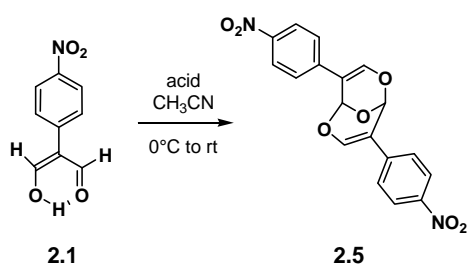
Kollenz *et al.* also reported the synthesis of bifunctionalised *bis*-dioxines using hydroxyl nucleophiles.<sup>99</sup> Indeed, addition of such nucleophiles to the stable  $\alpha$ -oxoketene resulted in the formation of a stable 1:1 adduct which was further cyclised under acidic conditions to afford the difunctional derivative (**Scheme 2.7**).

<sup>98</sup> Kappe, C. O.; Farber, G.; Wentrup, C.; Kollenz, G. *Tetrahedron Lett.* **1992**, 33, 4553-4556.

<sup>99</sup> Kappe, C. O.; Kollenz, G.; Fabian, W. M. F.; Wentrup C.; Färber, G. *J. Org. Chem.* **1993**, 58, 3361-3367.


**Scheme 2.7** | The Kollenz method, hydroxyl nucleophiles

Thus considering the few methodologies described to reach such bicyclic core, we envisaged to develop a novel and convenient strategy for the preparation of substituted 2,6,9-trioxabicyclo[3.3.1]-nona-3,7-diene starting from arylmalonaldehydes. Therefore we started exploring the behaviour of nitroarylmalonaldehyde **2.1** under various acidic conditions (**Scheme 2.8**).

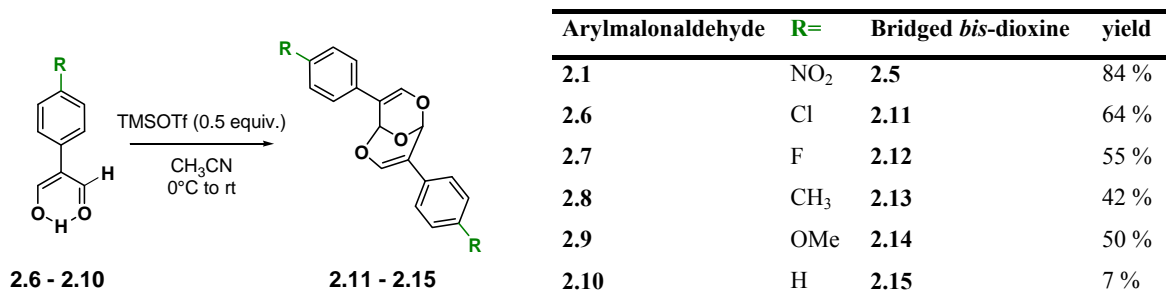


| entry    | acid (equiv.)                            | yield       |
|----------|--|-------------|
| 1        | TFA (0.5)                                | -           |
| 2        | H <sub>2</sub> SO <sub>4</sub> (0.25)    | -           |
| 3        | BF <sub>3</sub> .Et <sub>2</sub> O (0.5) | 28 %        |
| 4        | TiCl <sub>4</sub> (0.5)                  | -           |
| 5        | SnCl <sub>2</sub> (0.5)                  | -           |
| 6        | ZnCl <sub>2</sub> (0.5)                  | traces      |
| 7        | CF <sub>3</sub> SO <sub>3</sub> H (0.5)  | 65 %        |
| <b>8</b> | <b>TMSOTf (0.5)</b>                      | <b>84 %</b> |
| 9        | TMSOTf (1)                               | 55 %        |
| 10       | TMSOTf (0.3)                             | 61 %        |
| 11       | TMSOTf (<0.3)                            | -           |

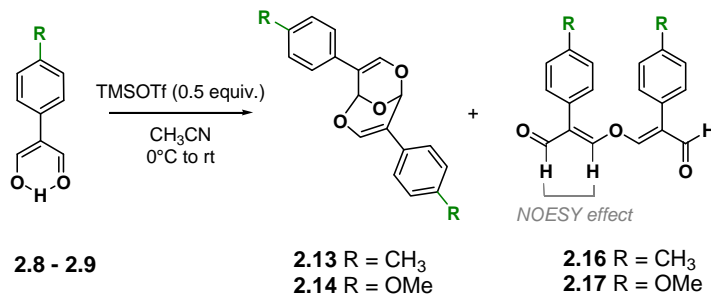
**Scheme 2.8** | Investigating conditions

Formation of **2.5** was observed using 0.5 equiv. of BF<sub>3</sub>.Et<sub>2</sub>O, ZnCl<sub>2</sub>, CF<sub>3</sub>SO<sub>3</sub>H or TMSOTf. The best result obtained with TMSOTf (84% yield) prompted us to investigate the acid stoichiometry. However every further attempt to optimise the yield of this reaction failed employing either more or less equivalent of the acid catalyst. In the light of these first results, those optimal conditions were applied to the variously substituted arylmalonaldehydes **2.6**, **2.7**, **2.8**, **2.9** and **2.10** (**Scheme 2.9**).<sup>100</sup>

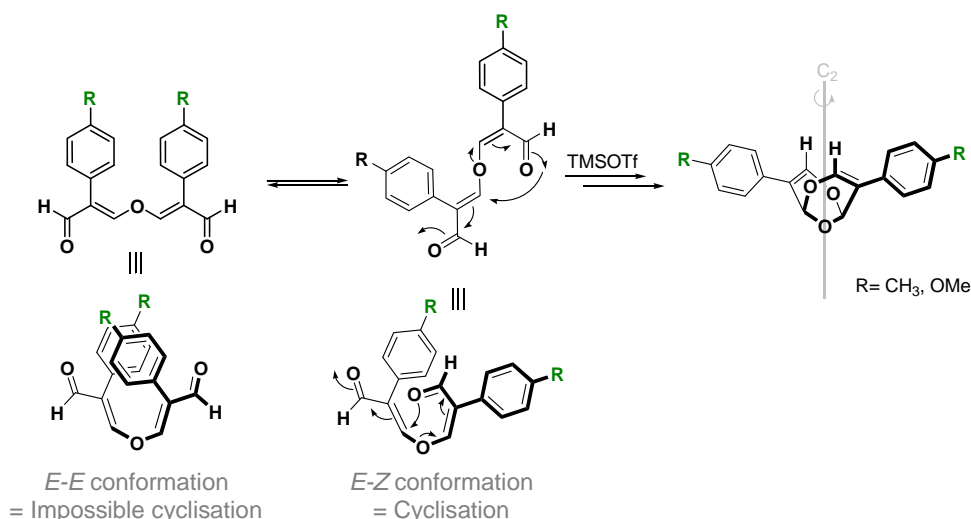
<sup>100</sup> The starting arylmalondialdehydes **2.1**, **2.6**, **2.7**, **2.8**, **2.9** and **2.10** were either commercially available (**2.6** and **2.8**) or prepared in two steps from the corresponding arylacetic acid (**2.2**, **2.7**, **2.9** and **2.10**) according to the method of Arnold: Arnold, *Z. Collect. Czech. Chem. Commun.* **1961**, 26, 3051.


**Scheme 2.9** | Extending scope

Except for the bridged *bis*-dioxine **2.15** (R= H), all the expected bicyclic products were isolated in moderate to good yields after purification by flash column chromatography (42–84%). Moreover, in the course of the studies conducted with arylmalondialdehydes bearing an electron-donating group (**2.8** and **2.9**, R= CH<sub>3</sub> and R= OMe), we were able to isolate compounds **2.16** and **2.17** respectively (**Scheme 2.10**). The <sup>1</sup>H and <sup>13</sup>C NMR analysis of both compounds demonstrated the symmetry of these molecules and further NOESY experiments allowed the determination of the *E* configuration of both double bonds.

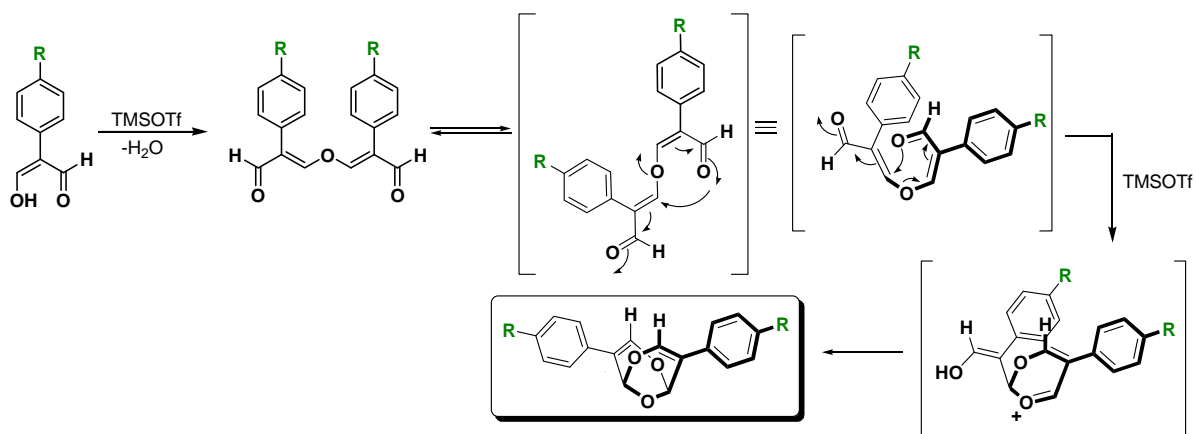

**Scheme 2.10** | Arylmalonaldehydes **2.8** and **2.9** under acid catalysis

Accordingly **2.16** and **2.17** were supposed to be reactive intermediates in the formation of bridged *bis*-dioxines (they are quite similar to the intermediate compound proposed by Arnold and Budesinsky). Indeed, treatment of **2.16** and **2.17** in the presence of catalytic amount of TMSOTf led to the formation of the corresponding trioxabicyclononadienes **2.13** and **2.14** (**Scheme 2.11**).



**Scheme 2.11** | Isomerisation and acid-catalysed cyclisation of **2.16** and **2.17**

Such demonstration reasonably allowed the proposal of a general mechanism for the acid catalysed dimerisation-cyclisation of arylmalonaldehydes (**Scheme 2.12**). In the primary step, TMSOTf catalyses the dimerisation of the starting arylmalonaldehyde. Subsequent *Z-E* isomerisation of at least one double bond facilitates acid-catalysed intramolecular cyclisation to the oxonium intermediate, which finally generates bridged *bis*-dioxines.



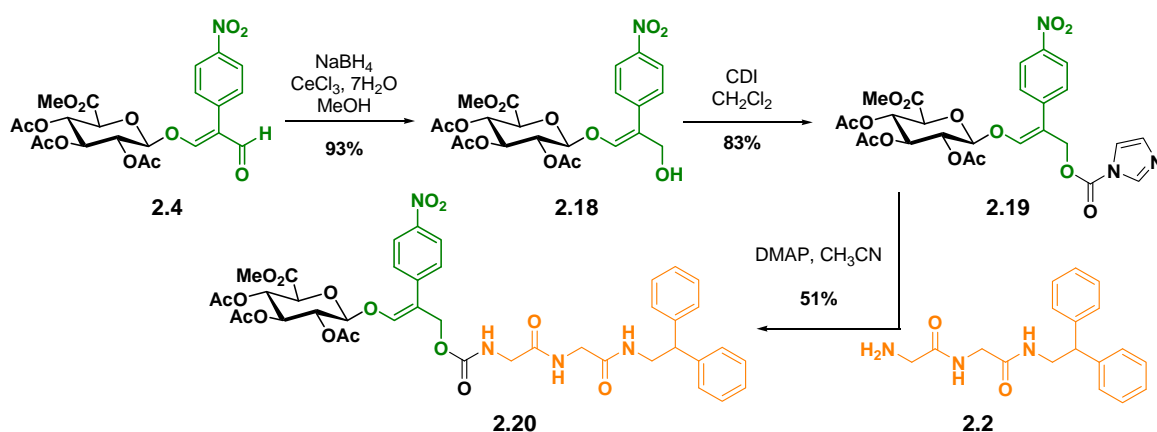
**Scheme 2.12** | Postulated mechanism for the formation of bridged *bis*-dioxines

Since none of these intermediates have been detected with arylmalondialdehydes **2.1**, **2.6** and **2.7** ( $R = \text{NO}_2, \text{Cl}$  and  $\text{F}$ ) it may be postulated that the presence of electron-withdrawing *para*-substituents on the aromatic ring favours the double bond isomerisation and consequently increases the rate of formation of the corresponding cyclic dimers.

In conclusion, this study allowed the description of new “bridged *bis*-dioxines” obtained in moderate to good yields by dimerization of arylmalondialdehydes in the presence of a catalytic amount of TMSOTf. This constitutes a new unexpected methodology for the preparation of the uncommon 2,6,9-trioxabicyclo[3.3.1]-nona-3,7-diene motif.<sup>101</sup>

### I.3. Arylmalonaldehyde-based rotaxane prodrug

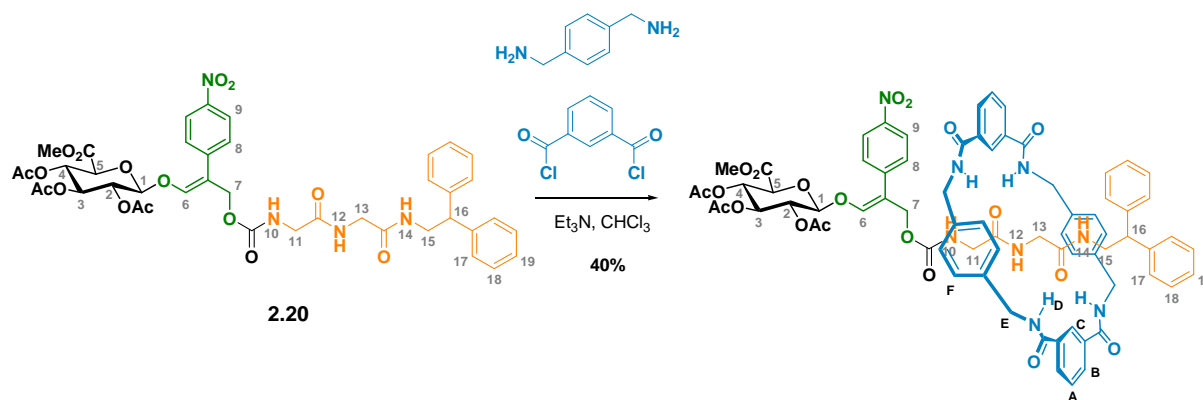
Accordingly, using the original synthesis reported by Gesson *et al.* we prepared intermediate **2.19**. The regioselective reduction of  $\alpha,\beta$ -unsaturated aldehyde **2.4** was performed using Luche reagent ( $\text{NaBH}_4\text{-CeCl}_3$ ) (93%) and the resulting allylic alcohol **2.18** was activated with carbonyl diimidazole (83%). **2.19** was finally coupled with glycylglycine derivative **2.2** to obtain the model protected prodrug thread **2.20** in a moderate 51% yield (**Scheme 2.13**).



**Scheme 2.13** | Preparation of the arylmalonaldehyde-based thread

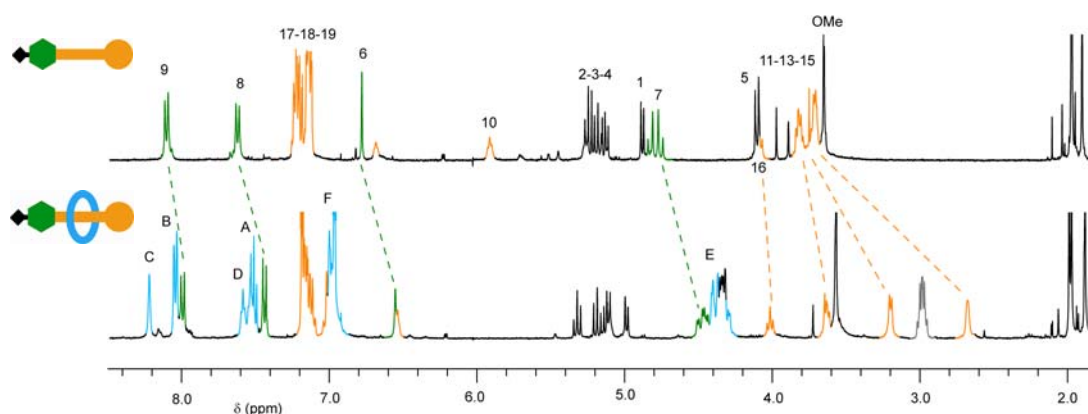
Thread **2.20** was then submitted to the classical rotaxane-forming reaction conditions. Thus **2.20** was reacted with *p*-xylylene diamine (16 equiv.) and isophthaloyl chloride (16 equiv.) in chloroform in presence of triethylamine (32 equiv.) at high dilution (**Scheme 2.14**).

<sup>101</sup> Fernandes, A.; Marrot, J.; Gesson, J.-P.; Papot, S. *Tetrahedron Lett.* **2006**, *47*, 5961-5964.



**Scheme 2.14** | Preparation of the arylmalonaldehyde-based rotaxane **2.21**

After many efforts the interlocked structure was finally separated from the starting thread and could be observed by  $^1\text{H}$  NMR (**Figure 2.1**). The large shielding effect experienced by the glycine protons ( $\text{H}_{11}$ ,  $\text{H}_{13}$  and  $\text{H}_{15}$ ) along with the additional macrocyclic protons ( $\text{H}_A$ ,  $\text{H}_B$ ,  $\text{H}_C$ ,  $\text{H}_D$ ,  $\text{H}_E$  and  $\text{H}_F$ ) confirmed the formation of the rotaxane.

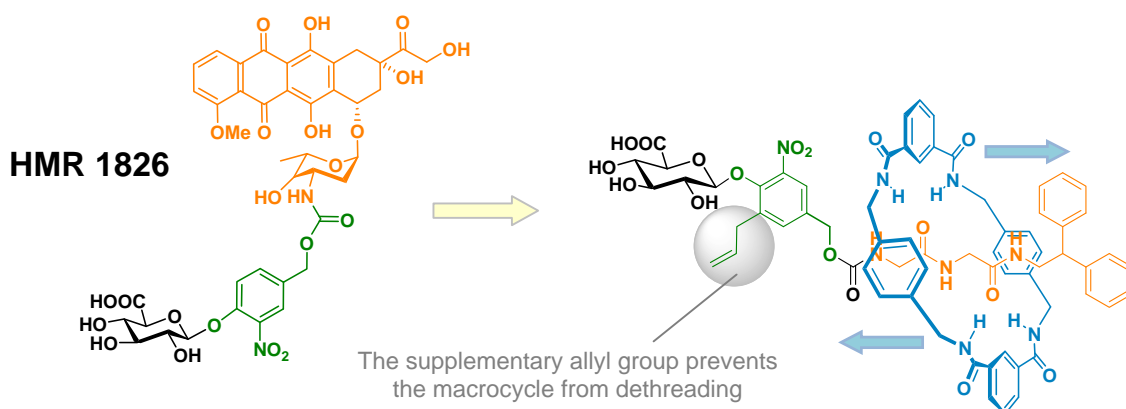


**Figure 2.1** |  $^1\text{H}$  NMR spectra of thread **2.20** and rotaxane **2.21**, (400 MHz, 298 K,  $\text{CDCl}_3$ )

Nevertheless, the rotaxane proved to be rapidly degraded and could not be used for further experiments. This prompted us to envisage the construction of a new system enabling the enzyme-mediated activation of peptide rotaxane prodrugs. One of the crucial points of our machines is the design of the spacer unit which must be bulky enough to stop the macrocycle, allow a good recognition of the trigger component by the enzyme and lead efficiently to the release of the encapsulated peptide after trigger activation.

## II. “Allyl-based” delivery system

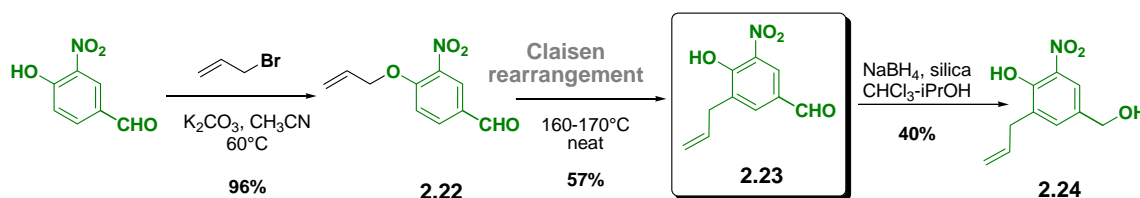
After several unfruitful attempts we managed to design a spacer which seems to fulfil our main requirements. This novel unit is directly derived from the HMR 1826 spacer which is probably one of the most efficient self-immolative linkers used in prodrug systems to date.<sup>102,103</sup> Therefore the straightforward derivatisation of the 4-hydroxy-3-nitrobenzylalcohol (*i.e.* HMR 1826 spacer) depicted in **Scheme 2.15** afforded a valuable solution for the construction of our delivery devices.



**Scheme 2.15** | Design of a new model rotaxane prodrug based on HMR 1826 spacer

### II.1. Synthesis and preliminary enzymatic evaluation of the new “allyl spacer”

“Allyl spacer” **2.23** is quite appealing since it is easily obtained from commercially available 4-hydroxy-3-nitrobenzaldehyde *via* a Claisen rearrangement (**Scheme 2.16**).



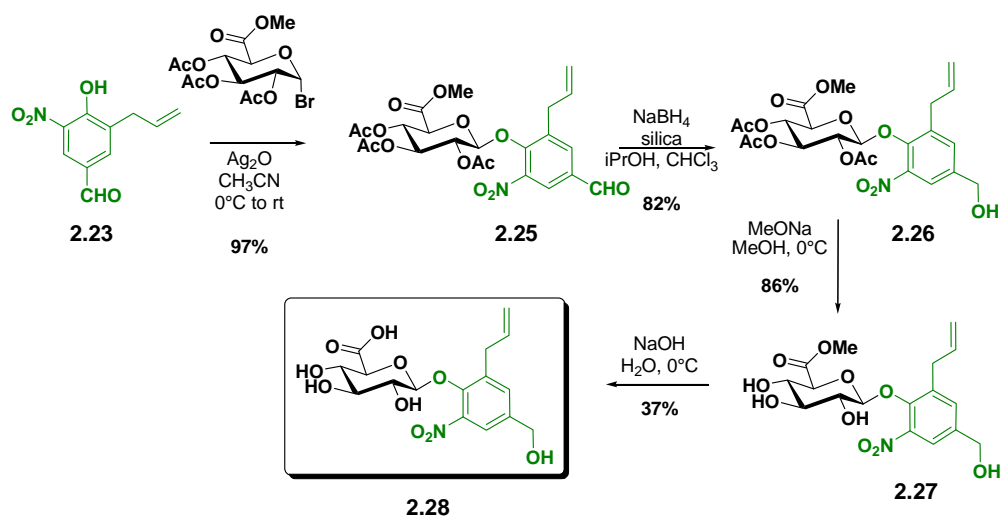
**Scheme 2.16** | Preparation of the new “allyl spacer”

<sup>102</sup> Papot, S.; Tranoy, I.; Tillequin, F.; Florent, J.-C.; Gesson, J. P. *Curr. Med. Chem. Anti-Cancer Agents* **2002**, 2, 155-185.

<sup>103</sup> Tranoy-Opalinski, I.; Fernandes, A.; Thomas, M.; Gesson, J.-P.; Papot, S. *Anti-Cancer Agents Med. Chem.* **2008**, 8, 618-637.

Allylation of 4-hydroxy-3-nitrobenzaldehyde under the classical Williamson procedure afforded allyl ether **2.22** (96%) which was then submitted to various Claisen conditions. The best results were obtained heating **2.22** at 160-170°C neat leading to 57% of the expected spacer along with the remaining starting allylated phenol. Compound **2.24** was prepared by reduction of **2.23** (40%) to serve as a reference for the enzymatic studies.

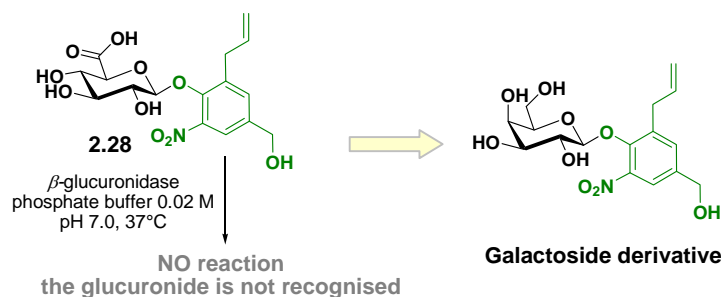
However before going in depth in the study, a preliminary test had to be carried out: the enzymatic recognition of the *bis-ortho*-substituted phenol glucuronide had to be demonstrated. Accordingly the simple glucuronide derivative **2.28** was prepared and evaluated with  $\beta$ -glucuronidase (Scheme 2.17).



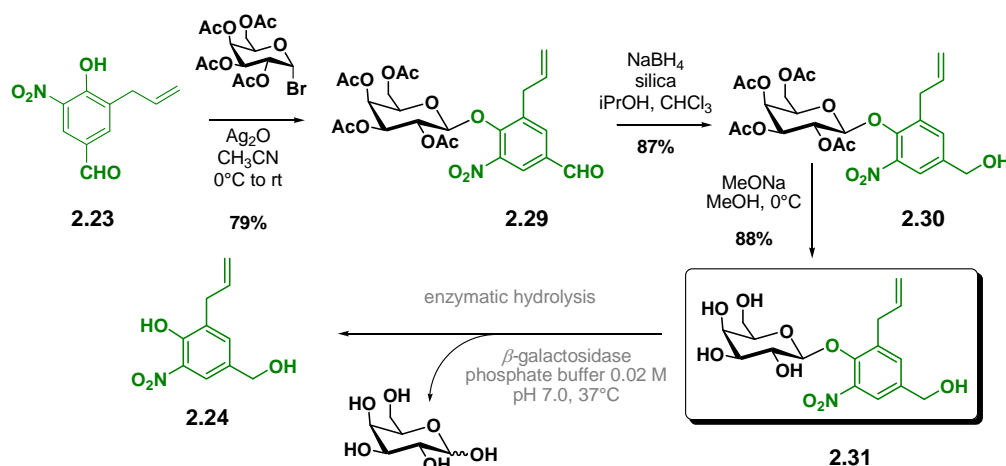
Scheme 2.17 | Synthesis of model glucuronide **2.28**

The newly-built spacer **2.23** was glycosylated using Koenigs-Knorr conditions (97%) and then reduced to its benzylic alcohol derivative **2.26** (82%). Transesterification of the acetate protecting groups (86%) followed by saponification of the methyl ester furnished model glucuronide **2.28** (37%).

Glucuronide **2.28** (490  $\mu\text{g}$ ) was incubated with bovine liver  $\beta$ -glucuronidase (100 U) in phosphate buffer (0.02 M, pH 7.0, 1 mL) at  $37^\circ\text{C}$ . HPLC monitoring showed no reaction at all suggesting that the supplementary allyl group prevents the glucuronide from being recognised and hydrolysed (Scheme 2.18).


**Scheme 2.18** | Enzymatic hydrolysis of model glucuronide **2.28**

Disposing of a promising rapidly-accessed spacer, we decided to focus our efforts in preparing a galactoside derivative of **2.23**. Indeed, galactosylated prodrugs can be used in ADEPT protocols.<sup>104,105,106</sup> Furthermore, literature demonstrated that highly substituted phenolic  $\beta$ -galactosides are substrates for  $\beta$ -galactosidase.<sup>107</sup> Thus treatment of **2.23** with *per*-acetylated galactosyl bromide in the presence of silver (I) oxide afforded  $\beta$ -galactosyl **2.29** (79%). Reduction of the aldehyde function (87%) and subsequent deprotection of the acetyl protecting groups (88%) afforded the desired model **2.31**. Incubation of **2.31** (510  $\mu$ g) with *Escherichia coli*  $\beta$ -galactosidase (40 U) in phosphate buffer (0.02 M, pH 7.0, 1 mL) at 37°C was followed by HPLC. The later revealed the total disappearance of starting galactoside **2.31** along with the release of spacer **2.24** in approximately 30 minutes (**Scheme 2.19**).


**Scheme 2.19** | Synthesis and enzymatic hydrolysis of model galactoside **2.31**

<sup>104</sup> Cheng, H.; Cao, X.; Xian, M.; Fang, L.; Cai, T. B.; Ji, J. J.; Tunac, J. B.; Sun, D.; Wang, P. G. *J. Med. Chem.* **2005**, *48*, 645-652.

<sup>105</sup> Tietze, L. F.; Major, F.; Schubert, I. *Angew. Chem. Int. Ed.* **2006**, *45*, 6574-6577.

<sup>106</sup> Kamal, A.; Tekumalla, V.; Krishnan, A.; Pal-Bhadra, M.; Bhadra, U. *Chem. Med. Chem.* **2008**, *3*, 794-802.

<sup>107</sup> Yu, J.; Mason, R. P. *J. Med. Chem.* **2006**, *49*, 1991-1999.

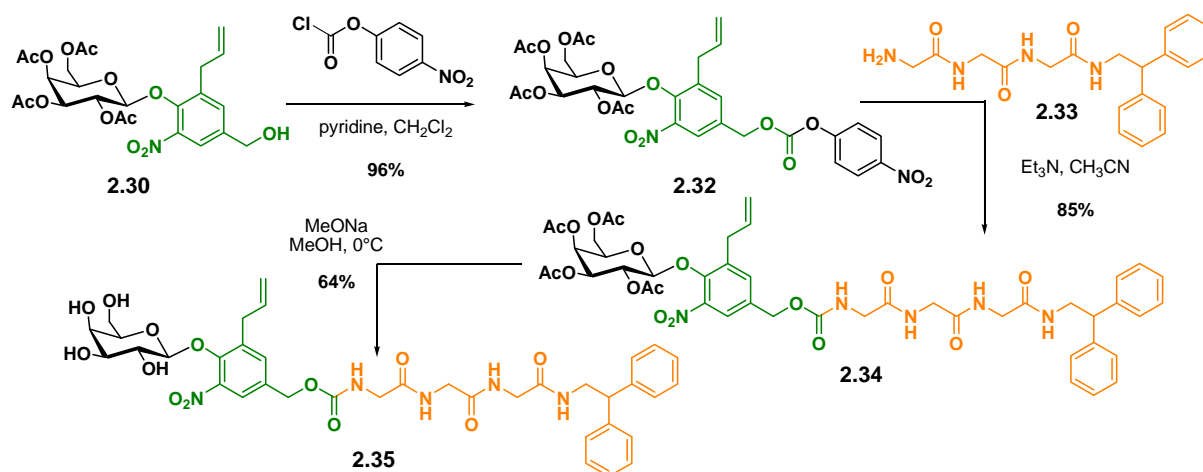
However these results also depicted the poor affinity of our model galactoside **2.31** for  $\beta$ -galactosidase. Indeed 1 unit of *E.coli*  $\beta$ -galactosidase is known to hydrolyse 1  $\mu\text{mol}$  of the *o*-nitrophenyl  $\beta$ -D-galactoside model substrate per minute at 37°C. In our case (1.37  $\mu\text{mol}$  of **2.31** and 40 U of *E.coli*  $\beta$ -galactosidase) the extremely slow kinetics of the enzymatic hydrolysis (30 minutes) demonstrated the dramatic effect of blocking the two *o*-phenolic positions.

Since the nitro function is essential for rapid 1,6-eliminations, modification of *meta* positions of the aromatic ring or functionalisation of the benzylic position obviously appears as alternative solutions to introduce a stopper part to the HMR 1826 spacer without altering its self-immolative properties.

Nevertheless, considering the many parameters to reach an efficient rotaxane-based delivery device we decided to pursue with this spacer in the galactose series even if the preliminary enzymatic studies, although demonstrating the complete hydrolysis of the model galactoside, were not really encouraging in term of kinetics. In addition, galactoside prodrugs can be used in ADEPT protocols and are easier to prepare and to handle in comparison with the glucuronylated prodrugs used in the PMT approach. Thus with this model system we can study the effect of the macrocycle upon the release of the model peptide along with the influence of the stopper on the self-immolative spacer.

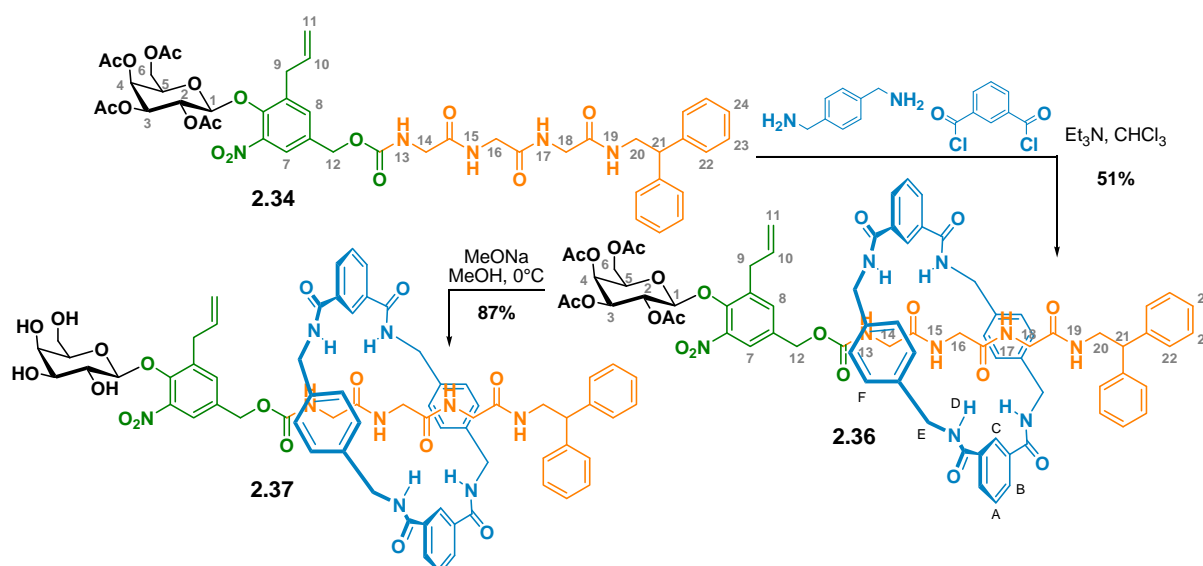
## II.2. Synthesis of “allyl-based” model prodrugs

Thus to pursue our investigations we prepared the Gly-Gly-Gly model prodrug thread **2.35** (Scheme 2.20). Activation of benzylic alcohol **2.30** with *p*-nitrophenylchloroformate (96%) and coupling with the model stoppered tripeptide **2.33** afforded intermediate **2.34** (85%). Final deprotection of the carbohydrate moiety yielded prodrug **2.35** (64%).



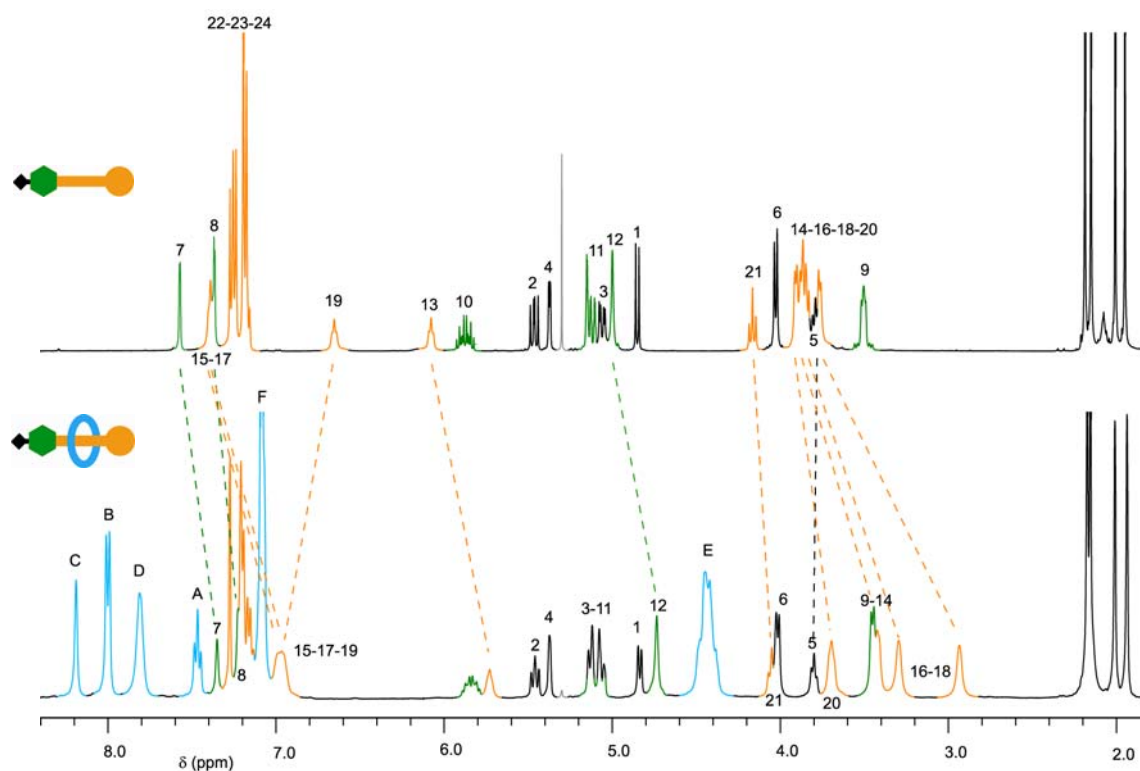
**Scheme 2.20** | Synthesis of model galactoside prodrug thread **2.35**

Rotaxane **2.36** was prepared using the classical hydrogen bond-directed assembly with a satisfying 51% yield (confirming that our spacer is an efficient stopper), isolated after classical chromatography on silica gel and subsequent size exclusion chromatography. Sugar deprotection gave prodrug rotaxane **2.37** in 87% yield (**Scheme 2.21**).



**Scheme 2.21** | Synthesis of model galactoside prodrug rotaxane **2.37**

Comparison of the  $^1\text{H}$  NMR spectra of **2.34** and **2.36** evidenced the formation of the interlocked architecture (**Figure 2.2**).

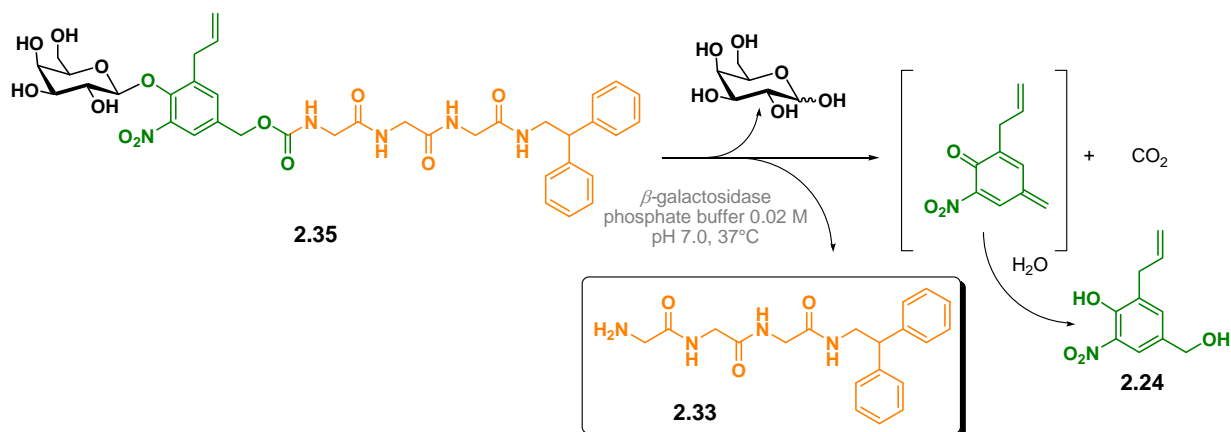


**Figure 2.2** |  $^1\text{H}$  NMR spectra of thread **2.34** and rotaxane **2.36**, (400 MHz, 298 K,  $\text{CDCl}_3$ )

Indeed, besides the supplementary protons corresponding to the macrocycle ( $\text{H}_\text{A}$ ,  $\text{H}_\text{B}$ ,  $\text{H}_\text{C}$ ,  $\text{H}_\text{D}$ ,  $\text{H}_\text{E}$  and  $\text{H}_\text{F}$ ), most of the resonances of the stoppered tripeptide ( $\text{H}_{14}$ ,  $\text{H}_{16}$ ,  $\text{H}_{18}$ ,  $\text{H}_{20}$  and  $\text{H}_{21}$ ) are significantly shifted to higher field in the rotaxane due to the shielding effect of the aromatic rings of the macrocycle. The major shifts of the glycine protons  $\text{H}_{14}$ ,  $\text{H}_{16}$  and  $\text{H}_{18}$  indicate that the glycine residues are directly located in the cavity of the macrocycle in the predominant structure of **2.36** in  $\text{CDCl}_3$ . Higher field shifts of the spacer protons  $\text{H}_7$ ,  $\text{H}_8$  and  $\text{H}_{12}$  are also observed while no modifications are noticed for the galactose trigger ( $\text{H}_1$ ,  $\text{H}_2$ ,  $\text{H}_3$ ,  $\text{H}_4$ ,  $\text{H}_5$  and  $\text{H}_6$ ). This information suggests that the macrocycle is able to shuttle up to the spacer unit and then blocked by the nitro- and allyl- substituents, as demonstrated by the CPK models of rotaxane **2.36**.

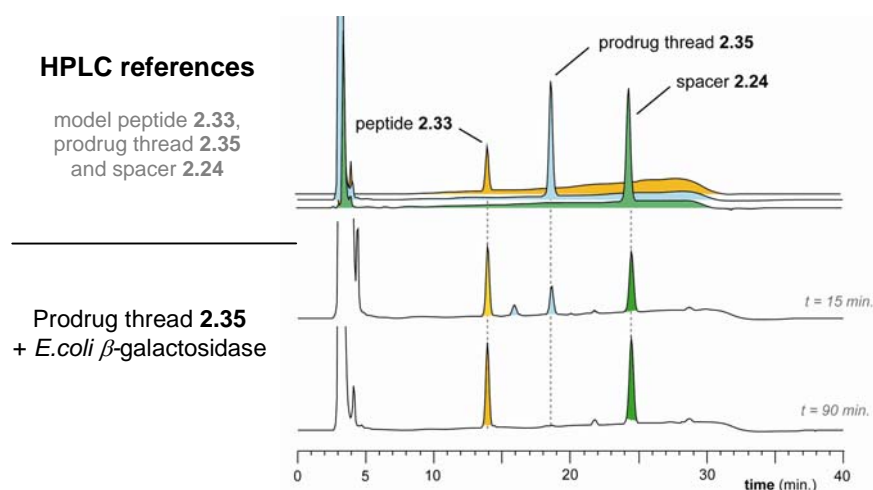
### II.3. Enzymatic hydrolysis

Enzymatic hydrolysis of prodrug thread **2.35** (0.1  $\mu\text{mol}$ ) was conducted with *E. coli*  $\beta$ -galactosidase (10 U) in phosphate buffer (0.02 M, pH 7.0, 500  $\mu\text{L}$ , 5% DMSO) at 37  $^\circ\text{C}$  (Scheme 2.22).



**Scheme 2.22** | Enzymatic release of the model peptide from prodrug thread **2.35**

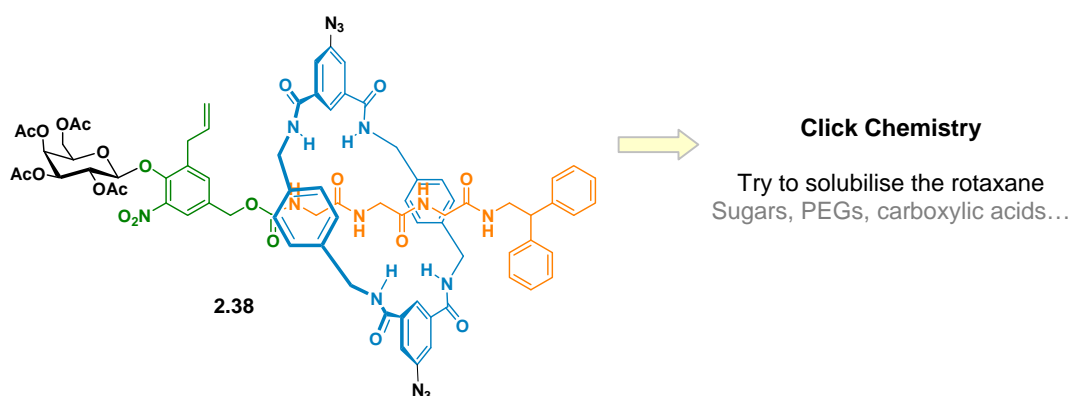
The enzymatic reaction was monitored by HPLC and revealed the release of model peptide **2.33** in approximately 90 minutes. Thereby HPLC chromatograms displayed the appearance of the model tripeptide along with spacer **2.24** and disappearance of **2.35** (Figure 2.3).



**Figure 2.3** | Enzymatic hydrolysis of prodrug thread **2.35**

These results confirmed that our galactosides are definitively not good substrates for *E.coli*  $\beta$ -galactosidase. However, even if the enzymatic hydrolysis occurred over prolonged reaction time, we could observe the total release of the peptide, meaning that this simple and easy-accessed system is a good model to study our concept.

Unfortunately galactoside rotaxane **2.37** proved to be totally insoluble in phosphate buffer (0.02 M, pH 7.0). Even the addition of up to 50% DMSO was not sufficient to solubilise the rotaxane. To overcome this drawback, the functionalisation of the macrocycle unit seems to be a good recourse to tune the hydrophilic character of our rotaxane. Indeed *Leigh et al.* recently developed an efficient method for the functionalisation of rotaxanes using the Copper-Catalysed Azide Alkyne Cycloaddition (CuCAAC).<sup>108</sup> Therefore we decided to construct the *bis*-azide rotaxane **2.38** (Scheme 2.23).

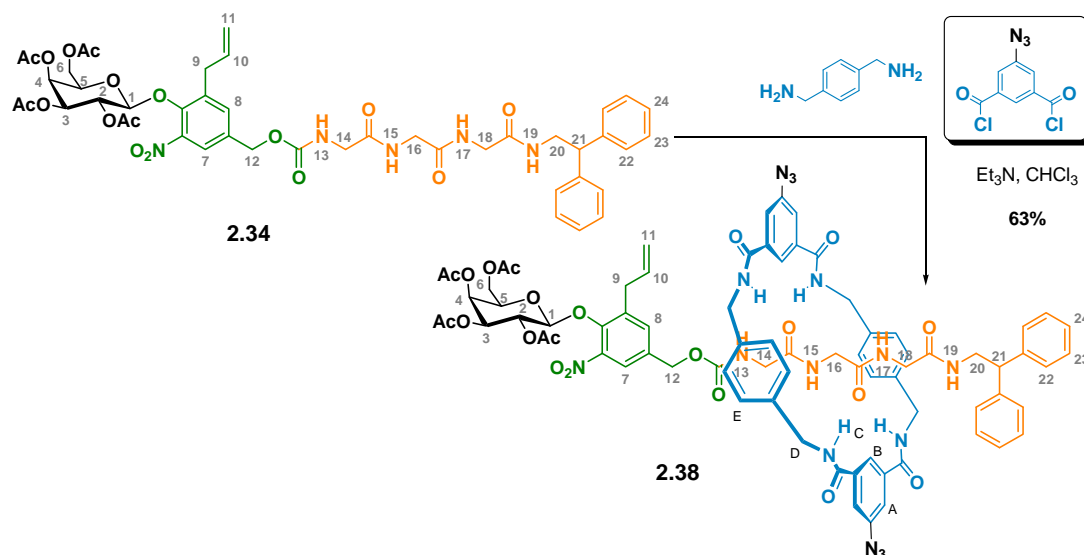


Scheme 2.23 | The “tunable” model rotaxane prodrug

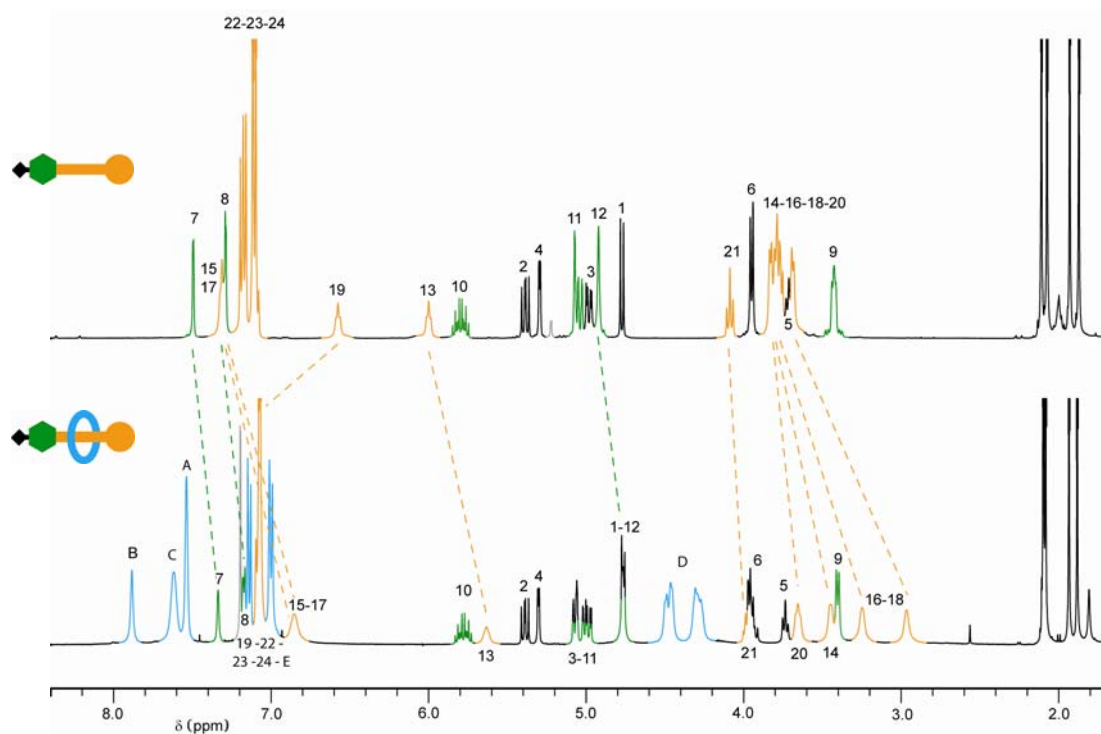
#### II.4. Synthesis of the tunable “allyl-based” rotaxane model prodrugs

Rotaxane **2.38** was easily synthesised from thread **2.34** using the classical hydrogen bond directed assembly with the isophthaloyl dichloride azido derivative and isolated with a 63% yield (Scheme 2.24).

<sup>108</sup> Gonzalez Cabrera, D.; Koivisto, B.; Leigh, D. A. *Chem. Commun.* **2007**, 41, 4218-4220.

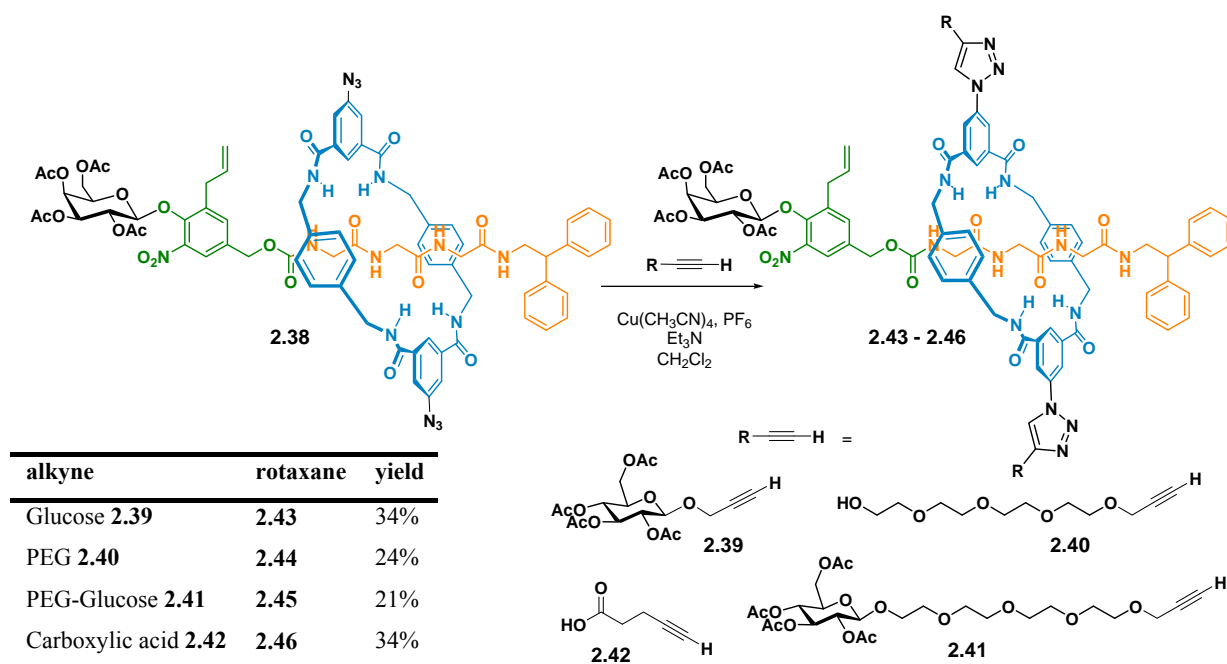


The  $^1\text{H}$  NMR spectra of **2.34** and **2.38** also illustrated the formation of the rotaxane (**Figure 2.4**). Indeed, apart from the signals corresponding to the sugar, most of the resonances experience shifts in the rotaxane architecture and particularly the glycyl protons  $\text{H}_{14}$ ,  $\text{H}_{16}$  and  $\text{H}_{18}$ .



**Figure 2.4** |  $^1\text{H}$  NMR spectra of thread **2.34** and rotaxane **2.38**, (400 MHz, 298 K,  $\text{CDCl}_3$ )

Thus rotaxane **2.38** was functionalised *via* CuCAAC with different alkyne derivatives (**2.39** to **2.42**, prepared by Aurélien Viterisi) to afford a small library of protected rotaxane-based prodrugs (Scheme 2.25).

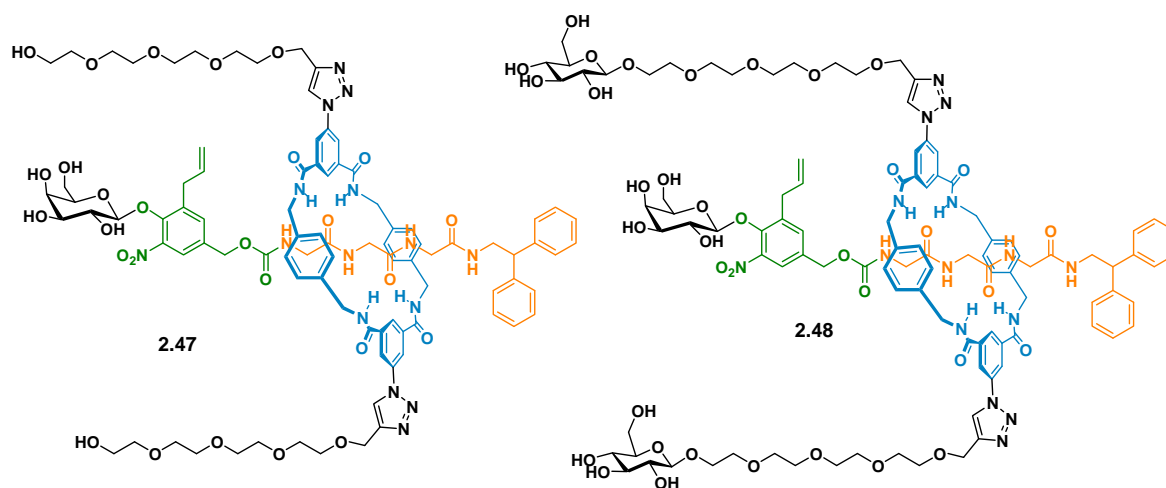


Scheme 2.25 | “Tuning” model rotaxane **2.38**

Rotaxanes **2.43** to **2.46** were isolated in moderate yield (21 to 34%) which is quite unusual for this kind of reaction. Even the use of TBTA (tris-(benzyltriazolylmethyl)amine), which is known to effectively enhance the copper-catalysed cycloaddition, did not afford significant improvement.<sup>109</sup>

To study our concept we initially focused on rotaxanes **2.44** and **2.45**, bearing respectively PEG and PEG-glucose chains. Removal of the acetyl protecting groups (MeONa, MeOH, 0°C) of both rotaxane **2.44** and **2.45** afforded the final model rotaxane prodrugs **2.47** and **2.48** which were further purified by preparative HPLC (Figure 2.5).

<sup>109</sup> Chan, T. R. ; Hilgraf, R.; Sharpless, K. B.; Fokin, V. V. *Org. Lett.* **2004**, *6*, 2853-2855.



**Figure 2.5** | The PEG-grafted rotaxane prodrugs

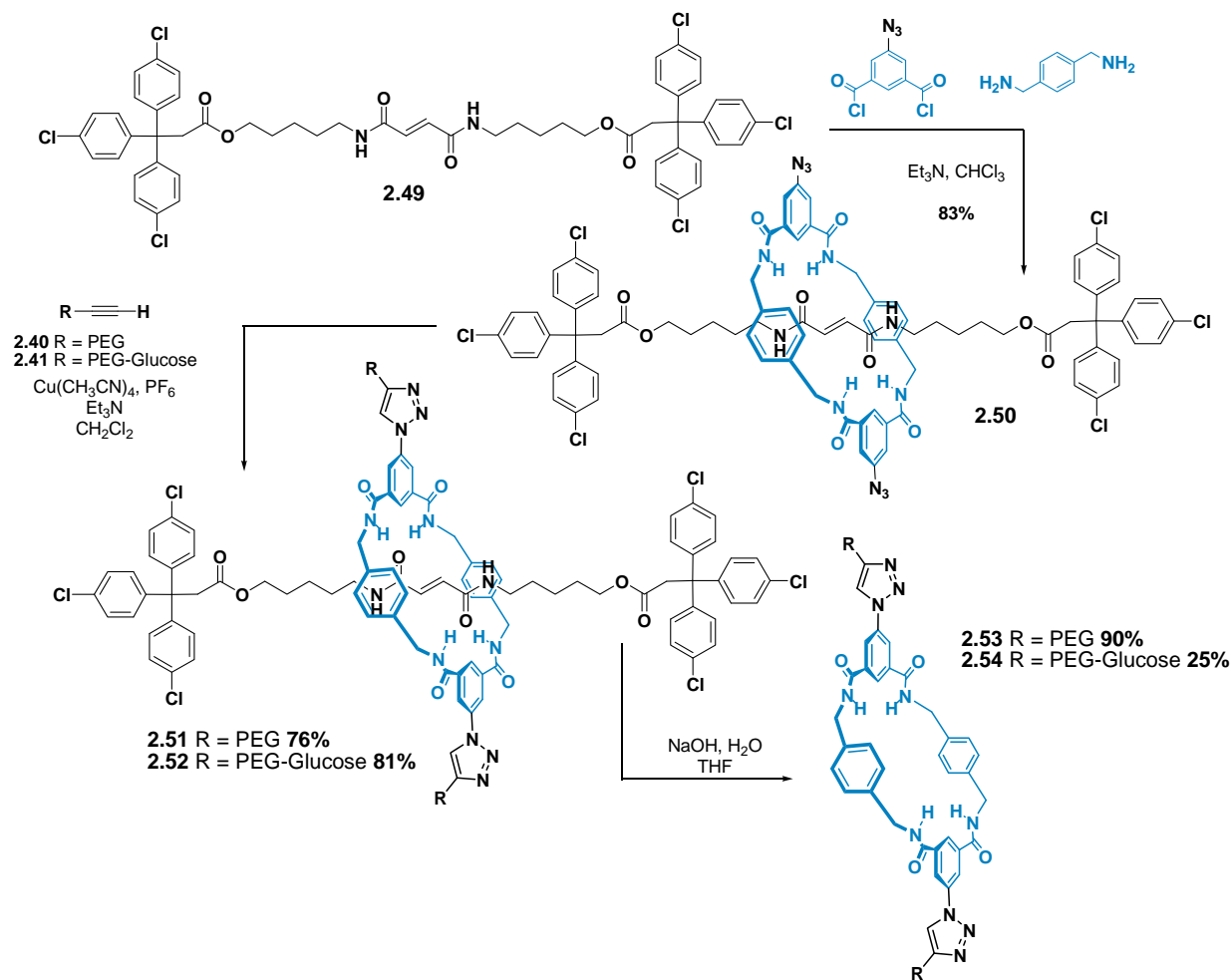
## II.5. Synthesis of the functionalised macrocycles

For both rotaxanes **2.47** and **2.48** described above, the corresponding macrocycles were prepared and isolated by Aurélien Viterisi. These macrocycles would serve as HPLC references in the enzymatic hydrolysis studies and also for the eventuality of biological tests.

Accordingly, as the synthesis of such macrocycles is extremely difficult, we opted for a rotaxane-derived strategy. Therefore an ester-bearing thread was prepared and interlocked with the amide-based macrocycles. The *bis*-azide rotaxanes were then functionalised and finally hydrolysed to release the free macrocycles (**Scheme 2.26**).

Thus rotaxane **2.50** was prepared by the classical hydrogen bond-directed assembly using fumaramide thread **2.49**. The fumaramide unit is to date one of the most effective templates for the formation of rotaxanes by a clipping reaction.<sup>110</sup> Therefore *bis*-azide rotaxane **2.50** was isolated in 83% yield and further reacted with alkynes **2.40** and **2.41** *via* the Copper-Catalysed Azide-Alkyne Cycloaddition (CuCAAC) (76% and 81% respectively). Saponification of stoppers from rotaxanes **2.51** and **2.52** led to the mechanical disassembly of the interlocked architectures to afford the desired PEG and PEG-glucose macrocycle **2.53** and **2.54**.

<sup>110</sup> Gatti, F. G.; Leigh, D. A.; Negogodiev, S. A.; Slawin, A. M. Z.; Teat, S. J.; Wong, J. K. Y. *J. Am. Chem. Soc.* **2001**, *123*, 5983-5989.



**Scheme 2.26** | Synthetic route for the preparation of the functionalised macrocycles

## II.6. Water solubility and enzymatic hydrolysis of PEG-grafted rotaxane prodrugs

### II.6.1 Water solubility

Water solubility was determined by HPLC for both thread and rotaxane prodrugs (**Table 2.1**). In a typical procedure, a sample of known concentration was injected in HPLC and its corresponding peak integrated on the chromatogram. Then a saturated solution of the compound was prepared, filtered and injected on HPLC and its signal integrated, giving thus a relative solubility limit.

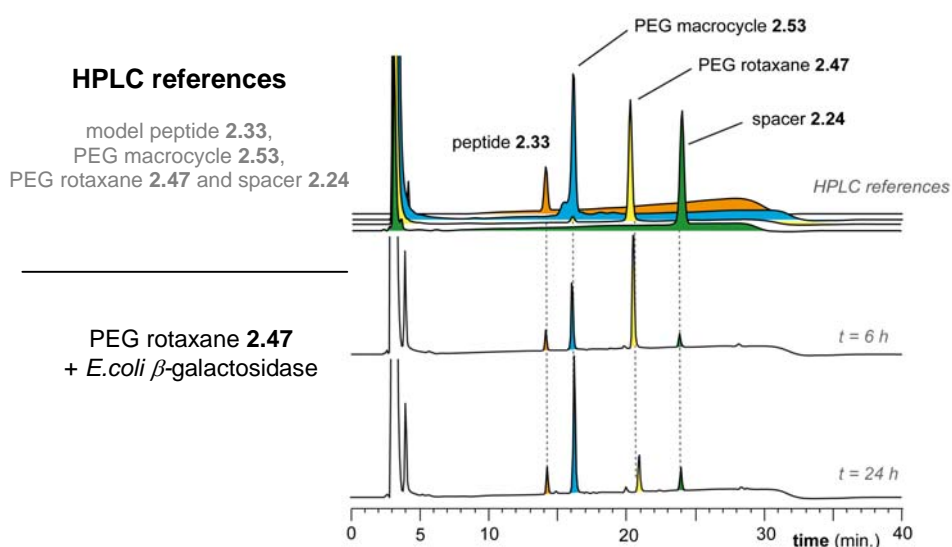
| Compound                           | Solubility in water (at 20°C)   |
|------------------------------------|---------------------------------|
| Allyl thread <b>2.35</b>           | 870.0 $\mu\text{mol.L}^{-1}$    |
| Allyl rotaxane <b>2.37</b>         | < 0.4 $\mu\text{mol.L}^{-1}$    |
| PEG rotaxane <b>2.47</b>           | 6.0 $\mu\text{mol.L}^{-1}$      |
| PEG-glucose rotaxane <b>2.48</b>   | 22 590.0 $\mu\text{mol.L}^{-1}$ |
| PEG macrocycle <b>2.53</b>         | 17.0 $\mu\text{mol.L}^{-1}$     |
| PEG-glucose macrocycle <b>2.54</b> | 170.0 $\mu\text{mol.L}^{-1}$    |

**Table 2.1** | Water solubility of the “allyl-based” prodrugs and grafted macrocycles

The data revealed that both PEG-grafted rotaxanes **2.47** and **2.48** were more soluble than the simple rotaxane prodrug **2.37**. We could also notice that rotaxane **2.48** ( $22\,590.0\ \mu\text{mol.L}^{-1}$ ) is much more soluble than **2.47** ( $6.0\ \mu\text{mol.L}^{-1}$ ) in water. The solubility of  $22\,590.0\ \mu\text{mol.L}^{-1}$  is strange in comparison with the other systems. Interestingly **2.48** is even more soluble than the non-interlocked prodrug **2.35** ( $870.0\ \mu\text{mol.L}^{-1}$ ). Macrocycles **2.53** and **2.54** displayed moderate solubility (the simple amide-based macrocycle is almost totally insoluble in water).

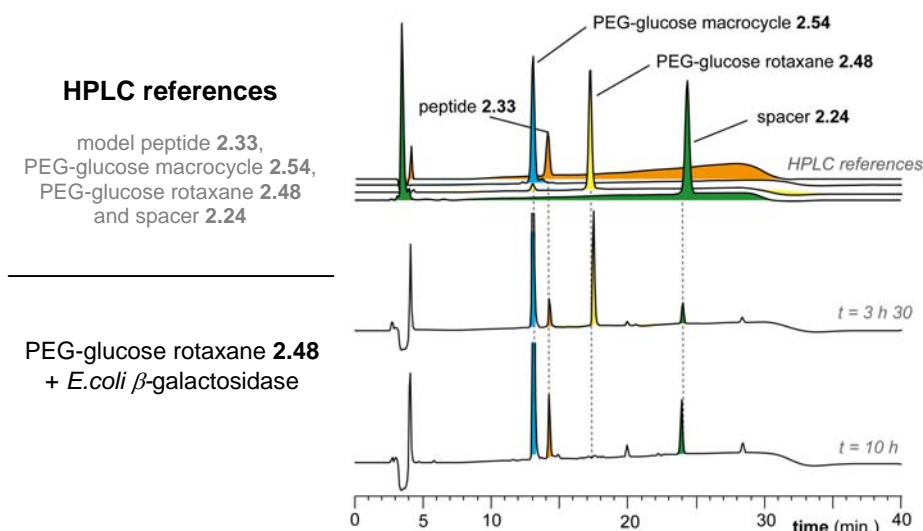
## II.6.2 Enzymatic hydrolysis

PEG-rotaxane **2.47** ( $0.1\ \mu\text{mol}$ ) was incubated with *E. coli*  $\beta$ -galactosidase (100 U) in phosphate buffer (0.02 M, pH 7.0, 500  $\mu\text{L}$ , 10% DMSO) at 37 °C. HPLC monitoring revealed slow and incomplete release of the model peptide (**Figure 2.6**).



**Figure 2.6** | Enzymatic hydrolysis of PEG rotaxane **2.47**

The same conditions were applied for the PEG-glucose grafted rotaxane. Therefore enzymatic hydrolysis of **2.48** (0.1  $\mu\text{mol}$ ) was conducted in the presence of *E. coli*  $\beta$ -galactosidase (100 U) in phosphate buffer (0.02 M, pH 7.0, 500  $\mu\text{L}$ ) at 37°C. Conversion of **2.48** was monitored by HPLC and indicated the complete release of model peptide **2.33** along with the functionalised macrocycle **2.54** and spacer **2.24** after a period of approximately 10 hours (Figure 2.7).



**Figure 2.7** | Enzymatic hydrolysis of PEG-glucose rotaxane **2.48**

## II.7. Observations

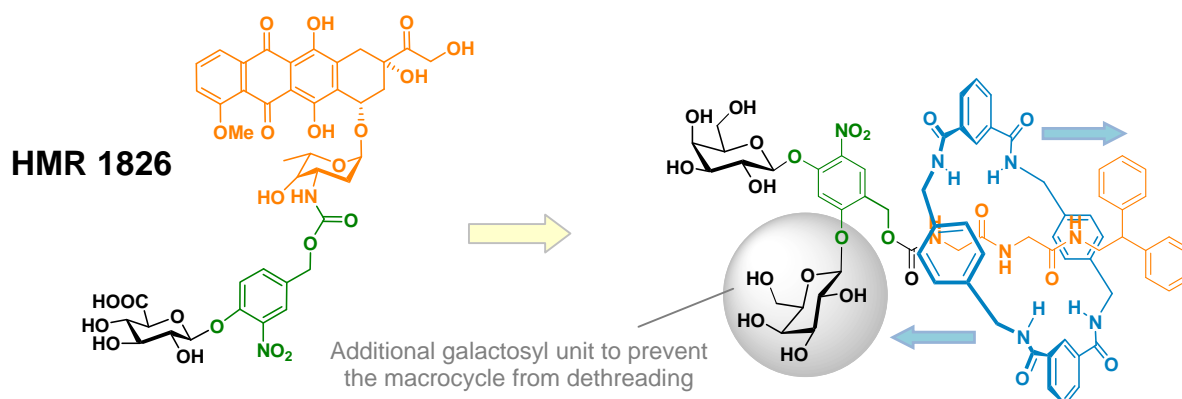
Enzymatic hydrolysis of our “allyl-based” model prodrugs reveals several important features. First the prodrug thread **2.35** is effectively activated by *E. coli*  $\beta$ -galactosidase to form spacer **2.24** and free peptide **2.33**. Nevertheless the enzymatic studies conducted for both interlocked and non-interlocked prodrugs unambiguously revealed that our “allyl-based” prodrugs are not good substrates for  $\beta$ -galactosidase, resulting in prolonged reaction times to release the parent peptide. Thereby while the non-interlocked prodrug **2.35** liberates the peptide in approximately 90 minutes, the release of the peptide from PEG-glucose rotaxane **2.48** was approximately 7 times slower (and even incomplete from PEG rotaxane **2.47** after one day).

Although we succeeded in solubilising our prodrug rotaxanes, it appears that the macrocycle considerably decreases the kinetics of release of the peptide. The close proximity of the macrocycle and the trigger moiety may account for this behaviour. Moreover the additional large chains grafted on the macrocycle may also participate in this decrease in activity. At this point it appears that, on one hand, the macrocycle has to be moved away from the trigger and on the other hand its functionalisation might be accomplished by “clicking” small polar molecules able to drive its hydrophilic properties. From that point of view, the carboxylic acid-grafted rotaxane **2.46** should be a good candidate that we will need to investigate to test the hypothesis of the proximity between macrocycle and trigger.

### III. *bis*-Galactosyl-based delivery system

#### III.1. Introduction

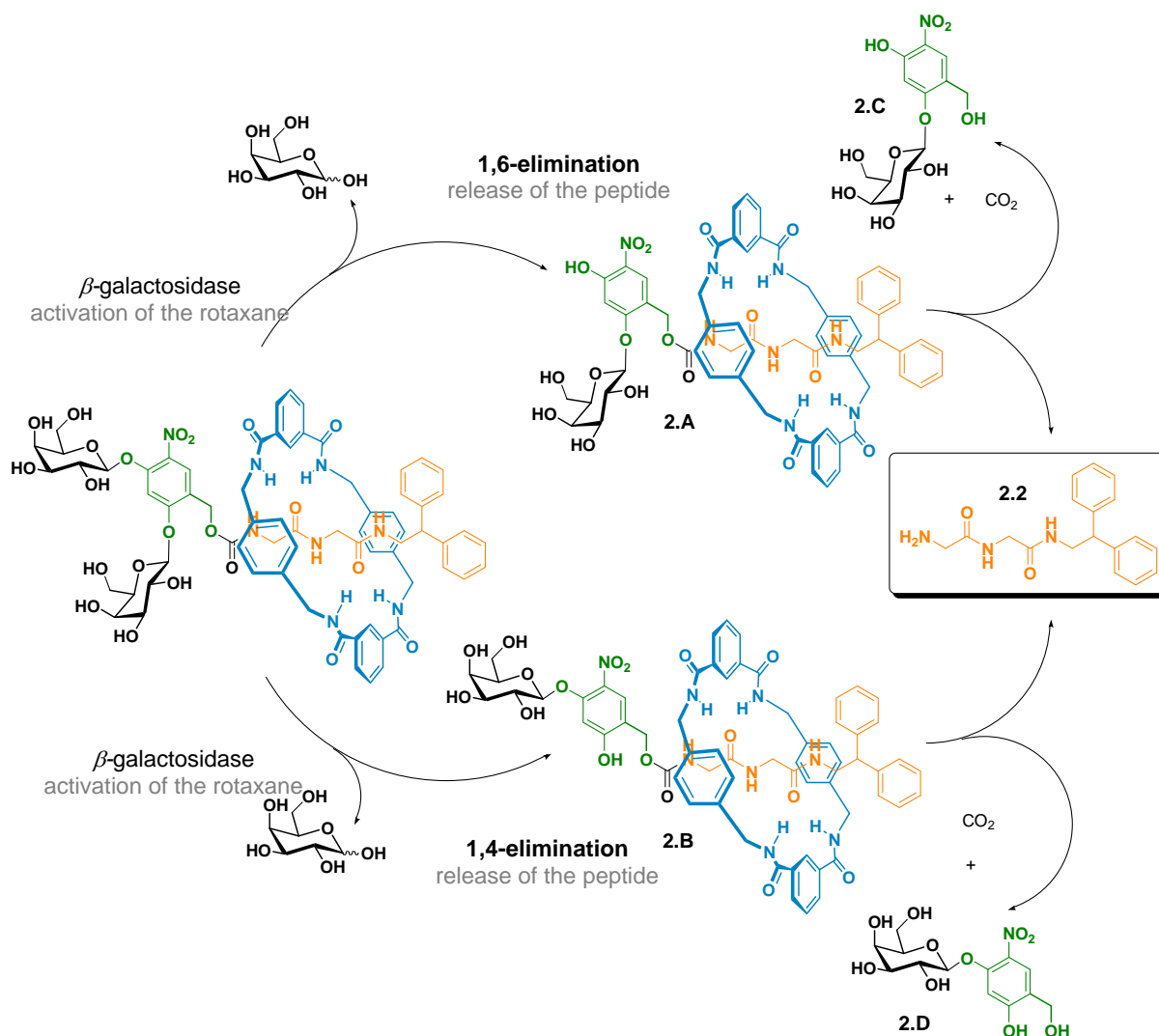
In the light of the results described previously we envisaged the design of a new rotaxane prodrug system. Indeed, the studies conducted with the “allyl-based” models demonstrated that additional modification of HMR 1826 spacer has to be moved away from the carbohydrate trigger unit to promote an efficient enzymatic recognition. Thus the confinement of the macrocycle unit around the peptide template should make the trigger-spacer conjugate more accessible for enzymatic activation. Moreover the evidence that water solubility constitutes a serious drawback of our delivery device is now clearly obvious. From this point of view the *bis*-galactosylated rotaxane derivative depicted in **Scheme 2.27** appears quite interesting.



**Scheme 2.27** | Design of a new model rotaxane prodrug based on HMR 1826 spacer

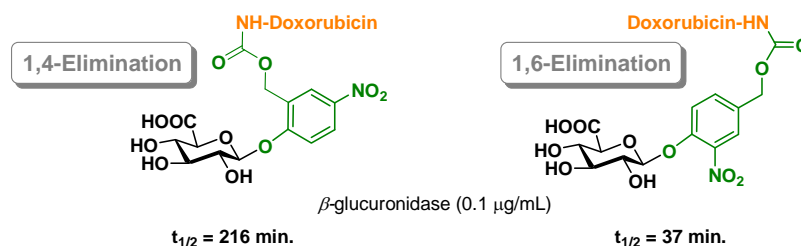
CPK models demonstrated that the additional sugar appropriately positioned on the spacer unit allows containment of the macrocycle away from the *o*-nitro-galactose trigger. Furthermore the presence of two carbohydrate units on the rotaxane should assure good water-solubility of the whole device.

In the present case, two possible mechanisms can be invoked for the liberation of the encapsulated peptide. Indeed the presence of two galactose triggers on the novel prodrug rotaxane allows two potential enzymatic activations. On one hand, hydrolysis of the *o*-nitro galactoside should mediate the release by the classical 1,6-elimination; alternative hydrolysis of the other site promotes a 1,4-elimination mechanism for the release of the model peptide (Scheme 2.28).



Scheme 2.28 | Mechanism of enzymatic release

Self-immolative spacers involving 1,4-quinone methide rearrangement have already been investigated for application in prodrug systems. For instance Shabat and co-workers recently reported the assembly of first-generation bioactivable dendritic prodrugs able to achieve multidrug release following successive 1,4-eliminations.<sup>111</sup> However Gesson and co-workers demonstrated that the 1,6-elimination is considerably faster than the corresponding 1,4 mechanism (Scheme 2.29).<sup>112</sup>



Scheme 2.29 | 1,4- versus 1,6-elimination

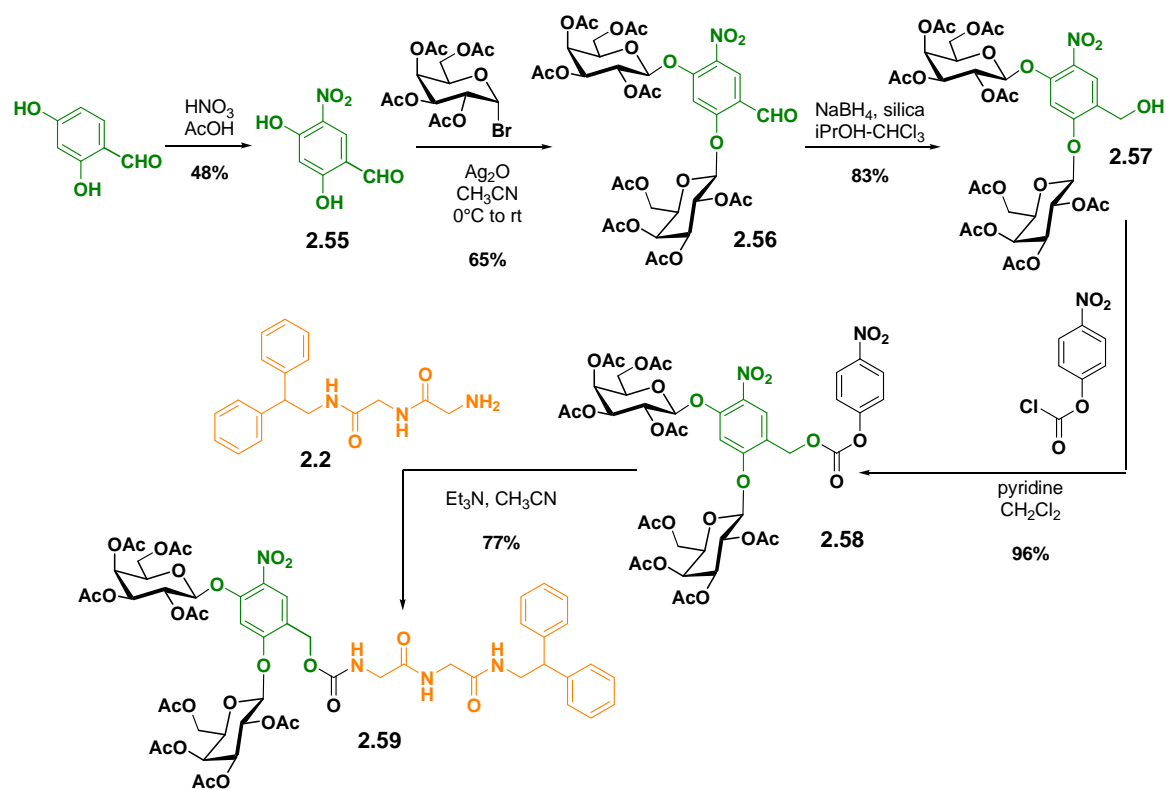
In our case the *p*-nitro galactoside seems to be less prone to enzymatic hydrolysis. The close presence of the benzylic amide macrocycle should indeed hinder the  $\beta$ -galactosidase approach from this side of the rotaxane, consequently favouring the 1,6-elimination mechanism. Furthermore the kinetic difference between 1,4- and 1,6-eliminations should also benefit the 1,6-elimination even if the *p*-nitro galactoside is hydrolysed first.

### III.2. Synthesis

Regioselective nitration of 3,4-dihydroxybenzaldehyde gave spacer **2.55** (48%) which was then *bis*-galactosylated using Koenigs-Knorr conditions (65%). Reduction of aldehyde **2.56** (83%), activation of the resulting benzylic alcohol **2.57** with *p*-nitrophenylchloroformate (96%) and coupling with the model stoppered peptide **2.2** (77%) finally afforded thread **2.59** (Scheme 2.30).

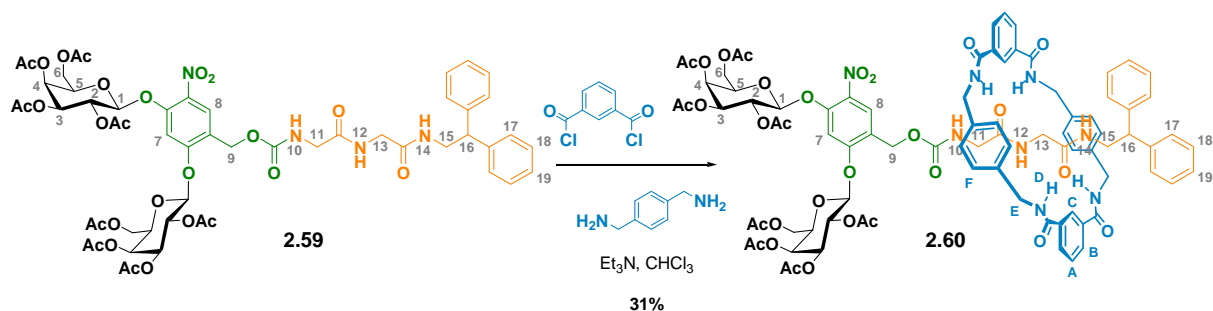
<sup>111</sup> Shamis, M.; Lode, H. N.; Shabat, D. *J. Am. Chem. Soc.* **2004**, *126*, 1726-1731.

<sup>112</sup> Florent, J.-C.; Dong, X.; Gaudel, G.; Mitaku, S.; Monneret, C.; Gesson, J.-P.; Jacquesy, J.-C.; Mondon, M.; Renoux, B.; Andrianomenjanahary, S.; Michel, S.; Koch, M.; Tillequin, F.; Gerken, M.; Czech, J.; Straub, R.; Bosslet, K. *J. Med. Chem.* **1998**, *41*, 3572-3581.



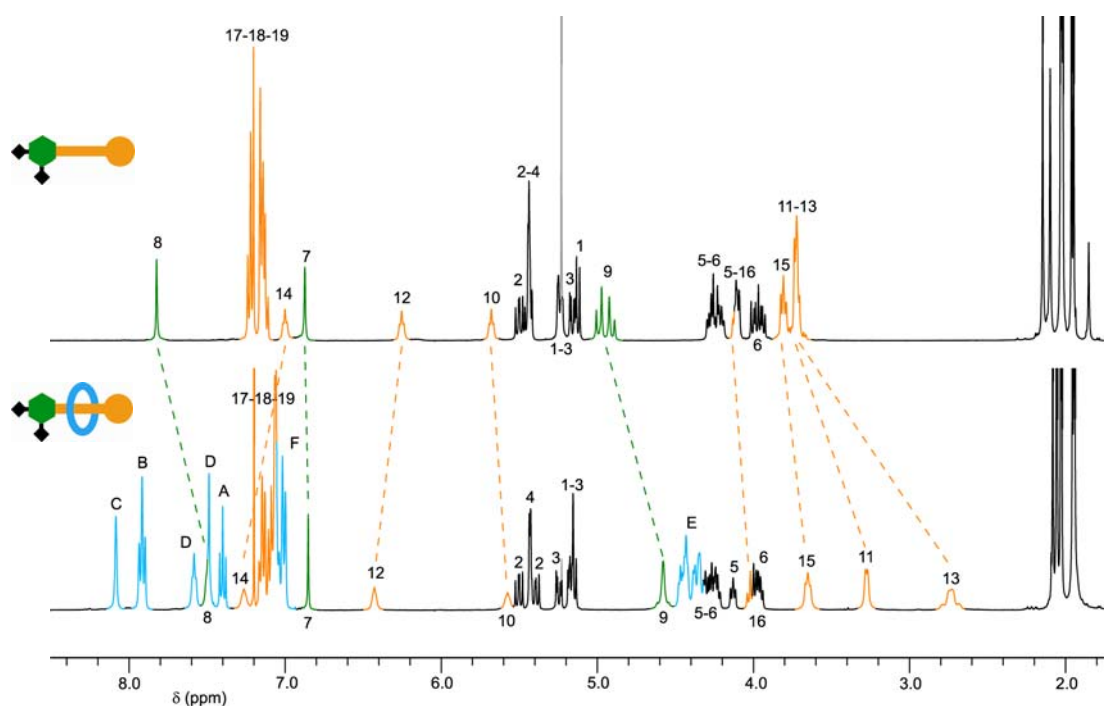
**Scheme 2.30** | Preparation of the *bis*-galactosylated thread

Thread **2.59** was then subjected to rotaxane forming conditions and the desired rotaxane **2.60** isolated in 31% yield (**Scheme 2.31**).



**Scheme 2.31** | Preparation of the *bis*-galactosylated rotaxane **2.60**

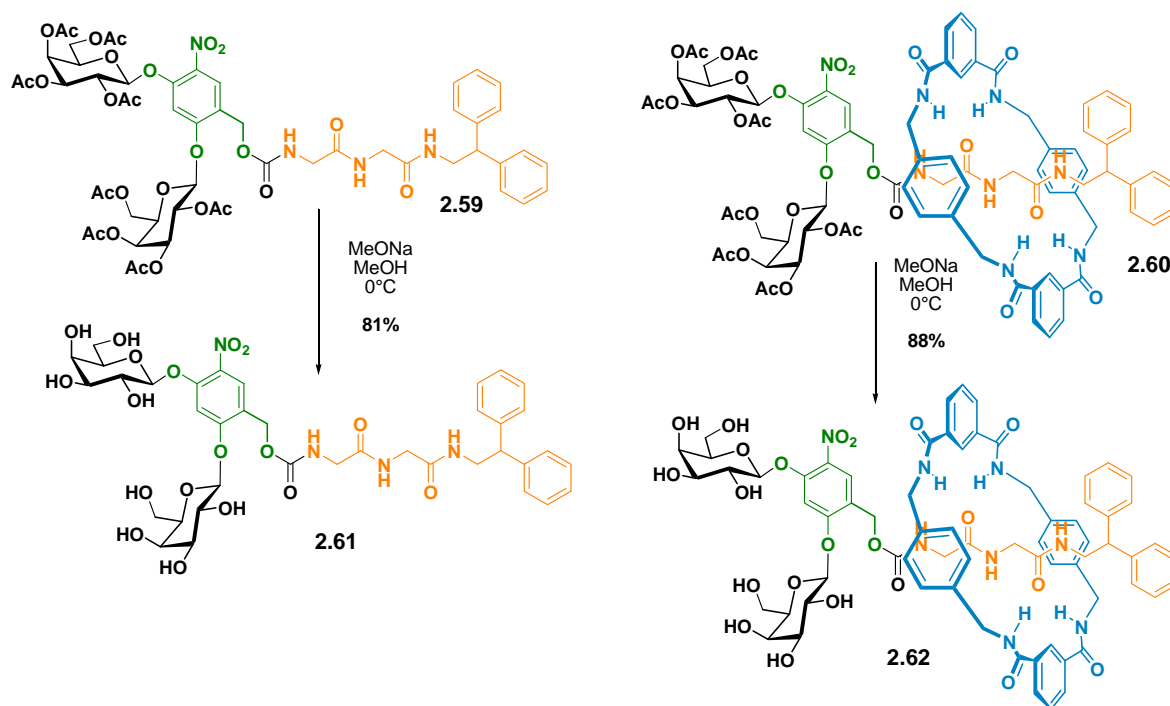
Comparison of the  $^1\text{H}$  NMR spectra between thread and rotaxane clearly illustrates the formation of the interlocked architecture (**Figure 2.8**).



**Figure 2.8** |  $^1\text{H}$  NMR spectra of thread **2.59** and rotaxane **2.60**, (400 MHz, 298 K,  $\text{CDCl}_3$ )

Indeed, apart from amide protons (*i.e.*  $\text{H}_{12}$  and  $\text{H}_{14}$ ), most of the resonances of the stoppered peptide ( $\text{H}_{11}$ ,  $\text{H}_{13}$ ,  $\text{H}_{15}$  and  $\text{H}_{16}$ ) are predominantly shifted to higher field. The downfield shift observed for amide protons  $\text{H}_{12}$  and  $\text{H}_{14}$  is due to intermolecular hydrogen bonding to the tetraamide macrocycle. Spacer protons  $\text{H}_8$  and  $\text{H}_9$  also experience the shielding effect of the macrocycle, which is not the case for spacer proton  $\text{H}_7$ . These observations indicate that the macrocycle is stoppered by the additional galactose unit and the nitro group, thus favouring the enzyme accessibility to the *o*-nitro trigger.

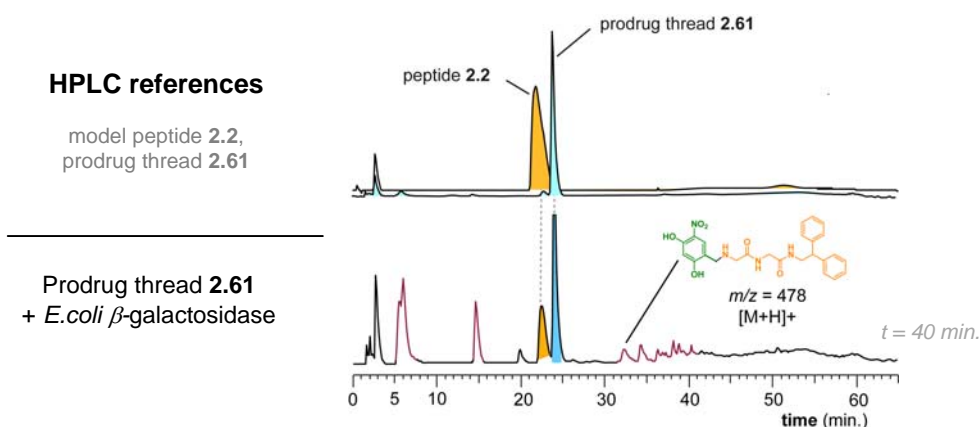
Finally, both thread **2.59** and corresponding rotaxane **2.60** were deprotected to obtain the active prodrug systems **2.61** and **2.62** in 81% and 88% respectively (**Scheme 2.32**).



**Scheme 2.32** | Preparation of the *bis*-galactosylated prodrug thread **2.61** and rotaxane **2.62**

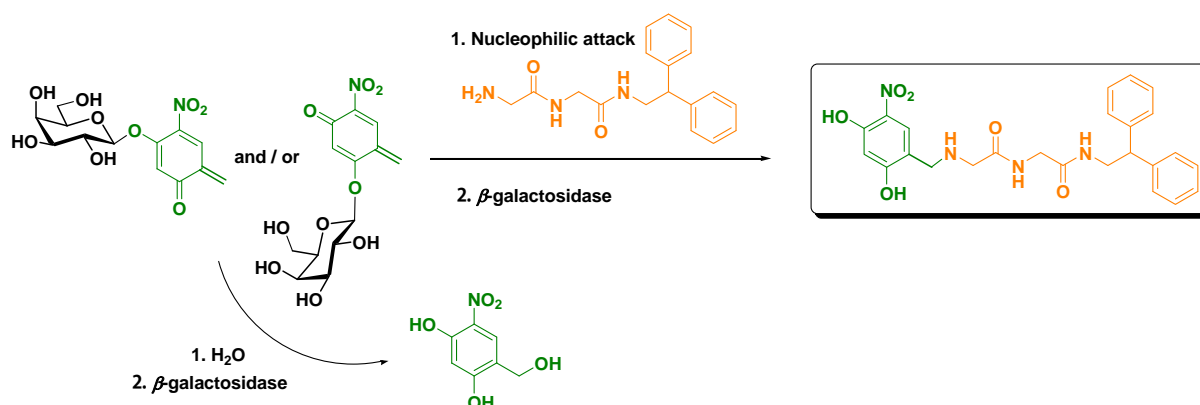
### III.3. Enzymatic hydrolysis

HPLC analysis of the enzymatic hydrolysis of prodrug thread **2.61** (0.5  $\mu\text{mol}$ ) in the presence of *E. coli*  $\beta$ -galactosidase (40 U) in phosphate buffer (0.02M, pH 7.0, 1mL) at 37  $^{\circ}\text{C}$  demonstrated the slow and incomplete release of the model peptide (**Figure 2.9**).



**Figure 2.9** | Enzymatic hydrolysis *bis*-Gal prodrug thread **2.61**

We could also observe many additional peaks on the chromatogram. Unfortunately LCMS analysis allowed the identification of only one compound which corresponds to the nucleophilic attack of the released peptide on the quinone methide intermediate, which could result from either 1,6- or 1,4-eliminations (**Scheme 2.33**).



**Scheme 2.33** | Nucleophilic attack of the released peptide

Generally with this class of elimination spacer, the highly reactive quinone methide intermediate is rapidly trapped by water to obtain a benzylic alcohol. In our case, it seems like the quinone methides are stabilised by the extra galactose units and thus react first with the amine nucleophile. This kind of behaviour has already been observed with other quinone methides and was recently used to detect enzyme activity.<sup>113</sup>

Unfortunately rotaxane prodrug **2.62** is totally insoluble in the phosphate buffer and therefore no enzymatic activation can occur. Considering the complex release observed with this model system we did not explore the use of our “clickable” macrocycles to try solubilising rotaxane **2.62**.

<sup>113</sup> Komatsu, T.; Kikuchi, K.; Takakusa, H.; Hanaoka, K.; Ueno, T.; Kamiya, M.; Urano, Y.; Nagano, T. *J. Am. Chem. Soc.* **2006**, *128*, 15946-15947.

## IV. Conclusion

The model study investigated here revealed that various fundamental features have to be considered before achieving efficient rotaxane-based peptide delivery devices. First of all, while one of the main drawbacks associated with peptide drugs is their high hydrophilicity, the considerably decreased hydrophilic character encountered with peptide rotaxanes represents a serious issue. Consequently the poor or even non-existent water-solubility of enzyme-activable rotaxane prodrugs prevent such machines from working.

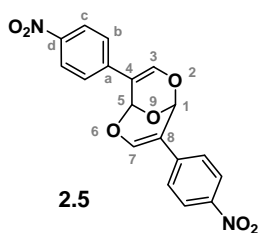
Accordingly, after dealing with the unstable glucuronylated arylmalonaldehyde model rotaxane, we based our efforts on derivatising one of the most successful anticancer prodrugs, HMR 1826, comprising a benzyloxycarbonyl based 1,6-elimination spacer. Thus the first attempt was based on an “allyl-modified” HMR 1826 spacer. Nevertheless such chemical modification proved to totally inhibit the recognition of the glucuronide motif (PMT) and encouraged us to investigate a galactose trigger, which can be used in an ADEPT protocol. The resulting glycoside appeared to be recognised by *E. coli*  $\beta$ -galactosidase while the rotaxane derivative displayed limited water-solubility. As a consequence, variation of the macrocycle unit seems, to date, the ultimate measure to finely tune the physical properties of our rotaxane-based peptide prodrugs. Such an advance was achieved by constructing a rotaxane bearing a “clickable” macrocycle. Nevertheless the “allyl spacer” system has one limitation: the supplementary allyl group (along with the large macrocycles) significantly hinders the glycosidic bond and therefore the enzymatic activation of our delivery device, resulting in slow kinetics of peptide release.

Consequently we developed the *bis*-galactosylated spacer. Introduction of a supplementary trigger unit to the self-immolative spacer results in the appropriate blockade of the amide-based macrocycle. However such modification resulted in a complex enzymatic release with the prodrug thread and even two carbohydrates units are not enough to solubilise the rotaxane in water. Moreover, the possibility of using glucuronic acid triggers has to be considered since the *o*-nitro glycosidic bond does not seem to be so hindered in this case. The *bis*-glucuronylated rotaxane should also present largely increased water-solubility.

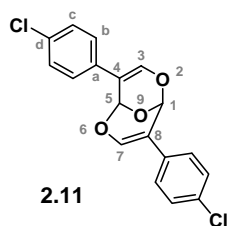
## V. Supporting information

### V.1. The acid-catalysed dimerisation of arylmalonaldehydes

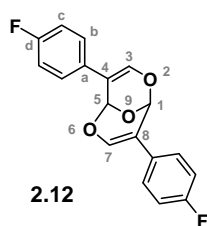
In a typical procedure, the arylmalonaldehyde (100 mg) was placed in CH<sub>3</sub>CN (0.2 mmol/mL) and the slurry cooled to 0°C. TMSOTf (0.5 equiv.) was then added dropwise and the stirred mixture was slowly allowed to reach room temperature. Stirring was continued at room temperature for 17 hours. The reaction was quenched with a saturated aqueous solution of NaHCO<sub>3</sub> and the aqueous layer was extracted 3 times with ethyl acetate. The combined organic extracts were dried (MgSO<sub>4</sub>), evaporated and concentrated *in vacuo*. Purification by flash column chromatography (petroleum ether/ethyl acetate: 6/4) afforded the corresponding substituted 2,6,9-Trioxabicyclo[3.3.1]-nona-3,7-diene.



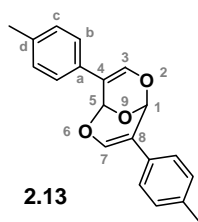
**Yield 84%** <sup>1</sup>H NMR (300 MHz, CDCl<sub>3</sub>): δ 8.14 (d, 4H, *J* = 9.3 Hz, H<sub>c</sub>), 7.45 (d, 4H, *J* = 9.3 Hz, H<sub>b</sub>), 7.35 (s, 2H, H<sub>3+7</sub>), 6.08 (s, 2H, H<sub>1+5</sub>) <sup>13</sup>C NMR (75 MHz, CDCl<sub>3</sub>): δ 146.6, 143.1, 140.5, 124.6, 124.4, 111.8, 88.3 **HRMS (EI):** calcd. for C<sub>18</sub>H<sub>12</sub>N<sub>2</sub>O<sub>7</sub> (M<sup>+</sup>) 368.0645, found 368.0646



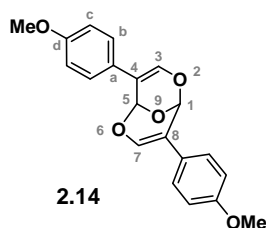
**Yield 64%** <sup>1</sup>H NMR (300 MHz, CDCl<sub>3</sub>): δ 7.24 to 7.18 (m, 8H, H<sub>b+c</sub>), 7.00 (s, 2H, H<sub>3+7</sub>), 5.93 (s, 2H, H<sub>1+5</sub>) <sup>13</sup>C NMR (75 MHz, CDCl<sub>3</sub>): δ 140.6, 133.8, 133.0, 129.4, 126.0, 112.5, 88.6 **HRMS (EI):** calcd. for C<sub>18</sub>H<sub>12</sub>O<sub>3</sub>Cl<sub>2</sub> (M<sup>+</sup>) 346.0163, found 346.0159



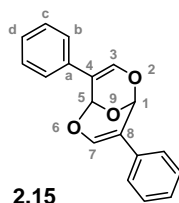
**Yield 55%** <sup>1</sup>H NMR (300 MHz, CDCl<sub>3</sub>): δ 7.06 to 7.00 (m, 10H, H<sub>3+7+b+c</sub>), 5.99 (s, 2H, H<sub>1+5</sub>) <sup>13</sup>C NMR (75 MHz, CDCl<sub>3</sub>): δ 160.1, 139.7, 130.1, 126.4, 114.4, 112.3, 88.4 **HRMS (EI):** calcd. for C<sub>18</sub>H<sub>12</sub>O<sub>3</sub>F<sub>2</sub> (M<sup>+</sup>) 314.0755, found 314.0755



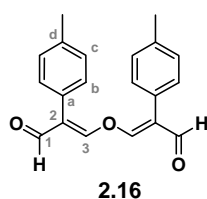
**Yield 42%**  $^1\text{H NMR}$  (300 MHz,  $\text{CDCl}_3$ ):  $\delta$  7.17 (d, 2H,  $J = 8.3$  Hz,  $\text{H}_b$ ), 7.07 (d, 2H,  $J = 8.3$  Hz,  $\text{H}_c$ ), 6.97 (s, 2H,  $\text{H}_{3+7}$ ), 5.97 (s, 2H,  $\text{H}_{1+5}$ ), 2.26 (s, 6H,  $\text{CH}_3$ )  $^{13}\text{C NMR}$  (75 MHz,  $\text{CDCl}_3$ ):  $\delta$  139.8, 137.0, 131.7, 129.7, 124.8, 113.3, 88.8, 21.2



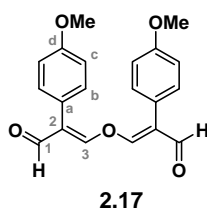
**Yield 50%**  $^1\text{H NMR}$  (300 MHz,  $\text{CDCl}_3$ ):  $\delta$  7.21 (d, 2H,  $J = 8.4$  Hz,  $\text{H}_b$ ), 6.91 (s, 2H,  $\text{H}_{3+7}$ ), 6.81 (d, 4H,  $J = 8.4$  Hz,  $\text{H}_c$ ), 5.94 (s, 2H,  $\text{H}_{1+5}$ ), 3.73 (s, 6H, OMe)  $^{13}\text{C NMR}$  (75 MHz,  $\text{CDCl}_3$ ):  $\delta$  158.9, 139.1, 127.1, 126.2, 114.4, 113.1, 88.9, 55.5 **HRMS (EI)**: calcd. for  $\text{C}_{20}\text{H}_{18}\text{O}_5$  ( $\text{M}^{+\bullet}$ ) 338.1154, found 338.1149



**Yield 7%**  $^1\text{H NMR}$  (300 MHz,  $\text{CDCl}_3$ ):  $\delta$  7.29 (bs, 8H,  $\text{H}_{b+c}$ ), 7.18 (bs, 2H,  $\text{H}_d$ ), 7.03 (s, 2H,  $\text{H}_{3+7}$ ), 6.01 (s, 2H,  $\text{H}_{1+5}$ )  $^{13}\text{C NMR}$  (75 MHz,  $\text{CDCl}_3$ ):  $\delta$  140.3, 134.5, 129.3, 129.0, 128.2, 127.4, 124.9, 113.3, 88.8

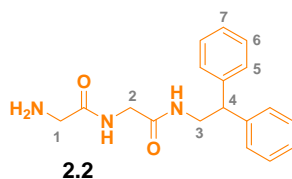


**Yield 4%**  $^1\text{H NMR}$  (300 MHz,  $\text{CDCl}_3$ ):  $\delta$  9.61 (s, 2H, CHO), 7.44 (s, 2H,  $\text{H}_3$ ), 7.33 (d, 4H,  $J = 8.2$  Hz,  $\text{H}_b$ ), 7.17 (d, 4H,  $J = 8.2$  Hz,  $\text{H}_c$ ), 2.40 (s, 6H,  $\text{CH}_3$ )  $^{13}\text{C NMR}$  (75 MHz,  $\text{CDCl}_3$ ):  $\delta$  190.2, 160.6, 138.7, 129.4, 129.0, 126.7, 125.6, 21.5



**Yield 11%**  $^1\text{H NMR}$  (300 MHz,  $\text{CDCl}_3$ ):  $\delta$  9.49 (s, 2H, CHO), 7.32 to 7.30 (m, 6H,  $\text{H}_{3+b}$ ), 6.80 (d, 4H,  $J = 7.9$  Hz,  $\text{H}_c$ ), 3.75 (s, 6H, OMe)  $^{13}\text{C NMR}$  (75 MHz,  $\text{CDCl}_3$ ):  $\delta$  190.1, 160.4, 159.6, 130.0, 126.1, 120.6, 113.5, 55.2

## V.2. “Allyl-based” delivery system



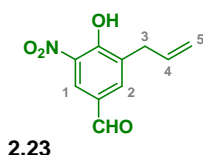
To a solution of Boc-glycylglycine (2.63 g, 9.10 mmol), EDC.HCl (2.09 g, 1.2 equiv.) and DMAP (1.32 g, 1.2 equiv.) in CH<sub>2</sub>Cl<sub>2</sub> (100 mL) at room temperature, was added 2,2-diphenylethanamine (1.70 g, 0.95 equiv.) and the reaction mixture was stirred overnight. An aqueous solution of HCl (1M) (150 mL) was added. The layers were separated and the aqueous layer was extracted with CH<sub>2</sub>Cl<sub>2</sub> (3 × 50 mL). The combined organic fractions were washed with H<sub>2</sub>O (50 mL), dried (MgSO<sub>4</sub>) and concentrated under reduced pressure. The crude solid was dissolved in CH<sub>2</sub>Cl<sub>2</sub> (10 mL) and Et<sub>2</sub>O (150 mL) was added. The resulting white precipitate was sonicated for 5 minutes and filtered by gravity to give **2.2** as a white solid (3.59 g, 8.70 mmol, 96%). The product (133 mg, 0.43 mmol) was dissolved in a 15% (v/v) solution of TFA in CH<sub>2</sub>Cl<sub>2</sub> (15 mL) and the mixture was stirred overnight at room temperature. Solvents were evaporated under reduced pressure. To the crude oil was added Et<sub>2</sub>O (30 mL) and the resulting white precipitate was sonicated for 10 minutes and filtered by gravity. The solid was re-dissolved in CH<sub>2</sub>Cl<sub>2</sub> (50 mL), an aqueous saturated solution of NaHCO<sub>3</sub> (20 mL) was added, the layers were separated and the aqueous layer was extracted with CH<sub>2</sub>Cl<sub>2</sub> (5 × 50 mL). The combined organic fractions were dried (MgSO<sub>4</sub>) and concentrated under reduced pressure to afford pure **2.2** as a light yellow oil (**48%**).

**<sup>1</sup>H NMR (400 MHz, CDCl<sub>3</sub>/CD<sub>3</sub>OD: 3/1):** δ 7.31-7.12 (m, 10H, H<sub>5+6+7</sub>), 4.26-4.12 (m, 3H, H<sub>3</sub> and H<sub>1</sub> or H<sub>2</sub>), 3.83 (d, 2H, *J* = 8.0 Hz, H<sub>4</sub>), 3.72 (s, 2H, H<sub>1</sub> or H<sub>2</sub>) **<sup>13</sup>C NMR (100 MHz, CDCl<sub>3</sub>/CD<sub>3</sub>OD: 3/1):** δ 173.4, 169.8, 142.1, 128.8, 128.2, 127.0, 50.6, 44.1 (×2), 42.6 **LRESI-MS: *m/z*** 312 [M+H]<sup>+</sup> **HRESI-MS: *m/z*** 312.1705 (calcd. for C<sub>18</sub>H<sub>22</sub>O<sub>2</sub>N<sub>3</sub> 312.1707 [M+H]<sup>+</sup>)



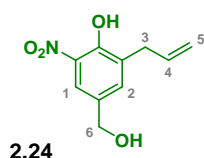
To a solution of 4-hydroxy-3-nitrobenzaldehyde (5.00 g, 29.94 mmol) in CH<sub>3</sub>CN (200 mL) were added allyl bromide (10.40 mL, 4.0 equiv.) and K<sub>2</sub>CO<sub>3</sub> (12.40 g, 3.0 equiv.). After being stirred at 60°C for 72 hours, the mixture was diluted with EtOAc and washed with water and brine. The combined organic layers were dried (MgSO<sub>4</sub>), filtered and concentrated *in vacuo*. Purification by column chromatography over silica gel (petroleum ether/ethyl acetate: 7/3 then 6/4) afforded **2.22** (5.70 g, 27.54 mmol, **92%**) as a white yellow powder. The compound showed identical spectroscopic data to that reported in Ando, H.; Manabe, S.; Nakahara, Y.; Ito, Y. *J. Am. Chem. Soc.*, **2001**, *123*, 3848-9.

<sup>1</sup>H NMR (400 MHz, CDCl<sub>3</sub>): δ 9.91 (s, 1H, CHO), 8.32 (d, 1H, *J* = 2.0 Hz, H<sub>1</sub>), 8.04 (dd, 1H, *J* = 8.8 Hz, *J* = 2.0 Hz, H<sub>2</sub>), 7.21 (d, 1H, *J* = 8.8 Hz, H<sub>3</sub>), 6.07 to 5.98 (m, 1H, H<sub>5</sub>), 5.50 (dd, 1H, *J* = 17.6 Hz, *J* = 1.2 Hz, H<sub>6</sub>), 5.37 (dd, 1H, *J* = 7.8 Hz, *J* = 1.2 Hz, H<sub>6</sub>), 4.78 (dt, 2H, *J* = 4.8 Hz, *J* = 1.6 Hz, H<sub>4</sub>)



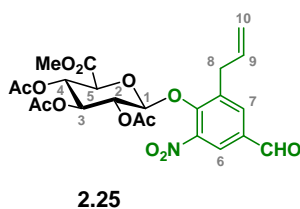
3-Nitro-4-(2-propenyloxy)benzaldehyde **2.22** (5.60 g, 27.05 mmol) was added in a 10 mL round-bottom flask equipped with a condenser and then heated at 160-165°C over a period of 17 hours. After allowing the dark brown mixture to reach room temperature, it was poured into 1M HCl and extracted with dichloromethane. The combined organic layers were dried with MgSO<sub>4</sub>, filtered and concentrated *in vacuo*. Purification by column chromatography over silica gel (petroleum ether/ethyl acetate: 8/2 to 6/4) afforded **2.23** (3.20 g, 15.46 mmol, **57%**) as a yellow powder and the remaining starting material **2.22**. The latter was put in a second run in the same conditions described before to afford 680 mg of **2.23** (3.29 mmol, **12%**) resulting in a total yield of **69%**.

**<sup>1</sup>H NMR (400 MHz, CDCl<sub>3</sub>):**  $\delta$  11.41 (bs, 1H, OH), 9.91 (s, 1H, CHO), 8.51 (d, 1H,  $J = 2.0$  Hz, H<sub>1</sub>), 8.01 (d, 1H,  $J = 2.0$  Hz, H<sub>2</sub>), 6.03 to 5.93 (m, 1H, H<sub>4</sub>), 5.20 to 5.18 (m, 1H, H<sub>5</sub>), 5.16 (dq, 1H,  $J = 11.2$  Hz,  $J = 1.6$  Hz, H<sub>5</sub>), 3.53 (d, 2H,  $J = 6.8$  Hz, H<sub>3</sub>) **<sup>13</sup>C NMR (100 MHz, CDCl<sub>3</sub>):**  $\delta$  189.0, 157.7, 135.8, 134.1, 133.5, 133.3, 128.4, 126.9, 118.0, 33.7 **LRFAB-MS (3-NOBA matrix):**  $m/z$  208 [M+H]<sup>+</sup> **m.p.** 82-84°C



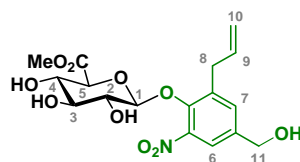
To a solution of **2.23** (100 mg, 0.48 mmol) in CHCl<sub>3</sub>/*i*PrOH (2.40 mL/1.60 mL) was added silica (90 mg). The mixture was cooled in an ice-water bath and NaBH<sub>4</sub> (320 mg, 12.0 equiv.) was added portion wise. After 1 hour at 0°C, the solution was allowed to reach room temperature and filtered on Celite<sup>®</sup>, the pad being washed with CH<sub>2</sub>Cl<sub>2</sub>. Evaporation and purification by column chromatography over silica gel (petroleum ether/ethyl acetate: 9/1 to 8/2) afforded **2.24** as a yellow solid (40 mg, 0.19 mmol, 40%).

**<sup>1</sup>H NMR (400 MHz, CDCl<sub>3</sub>):**  $\delta$  10.92 (bs, 1H, OH), 7.98 (d, 1H,  $J = 2.0$  Hz, H<sub>1</sub>), 7.48 (d, 1H,  $J = 2.0$  Hz, H<sub>2</sub>), 6.03 to 5.93 (m, 1H, H<sub>4</sub>), 5.15 (t, 1H,  $J = 1.2$  Hz, H<sub>5</sub>), 5.12 (dq, 1H,  $J = 6.4$  Hz,  $J = 1.2$  Hz, H<sub>5</sub>), 4.65 (s, 2H, H<sub>6</sub>), 3.48 (d, 2H,  $J = 6.4$  Hz, H<sub>3</sub>), 1.91 (bs, 1H, CH<sub>2</sub>-OH) **<sup>13</sup>C NMR (100 MHz, CDCl<sub>3</sub>):**  $\delta$  152.8, 136.4, 135.1, 133.3, 132.5, 131.9, 121.2, 117.2, 64.0, 33.9 **LRESI-MS (negative):**  $m/z$  208 [M-H]<sup>-</sup> **m.p.** 40-42°C



To a solution of **2.23** (370 mg, 1.79 mmol, 1.1 equiv.) in CH<sub>3</sub>CN (20 mL) cooled in an ice-water bath was added glucuronide (645 mg, 1.62 mmol) and Ag<sub>2</sub>O (565 mg, 1.5 equiv.). After overnight stirring at room temperature, the solution was filtered through silica, eluted with ethyl acetate and concentrated under reduced pressure. Purification by column

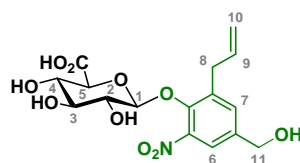




2.27

To a solution of **2.26** (328 mg, 0.62 mmol) in MeOH (20 mL) cooled in an ice-water bath was added dropwise at 0°C solution of MeONa (68 mg, 2.0 equiv.) in MeOH (5 mL). Stirring was continued for 2 hours at 0°C and the solution was neutralised with Amberlite IR-120 and filtered. MeOH was then evaporated and the resulting mixture was purified by column chromatography over silica gel (CH<sub>2</sub>Cl<sub>2</sub>/MeOH: 1 to 10% MeOH) to afford **2.27** (242 mg, 0.61 mmol, **98%**) as a white yellow powder.

**<sup>1</sup>H NMR (400 MHz, CD<sub>3</sub>OD):** δ 7.56 (d, 1H, *J* = 2.0 Hz, H<sub>6</sub>), 7.46 (d, 1H, *J* = 2.0 Hz, H<sub>7</sub>), 6.02 to 5.92 (m, 1H, H<sub>9</sub>), 5.14 to 5.09 (m, 2H, H<sub>10</sub>), 4.61 to 4.58 (m, 3H, H<sub>1+11</sub>), 3.73 (s, 3H, COOMe), 3.67 to 3.29 (m, 6H, H<sub>2+3+4+5+8</sub>) **<sup>13</sup>C NMR (100 MHz, CD<sub>3</sub>OD):** δ 170.1, 147.7, 145.9, 140.8, 138.0, 137.6, 133.5, 121.8, 117.4, 106.2, 76.9 (x2), 74.9, 72.6, 63.6, 52.8, 34.5 **LRESI-MS: *m/z*** 423 [M+Na]<sup>+</sup> **HRESI-MS: *m/z*** 417.1504 (calcd. for C<sub>17</sub>H<sub>25</sub>N<sub>2</sub>O<sub>10</sub> 417.1504 [M+NH<sub>4</sub>]<sup>+</sup>) **m.p.** 65-67°C

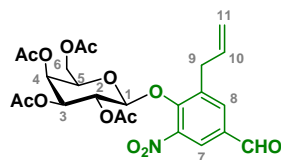


2.28

To a solution of **2.27** (133 mg, 0.34 mmol) in H<sub>2</sub>O (10 mL) cooled in an ice-water bath was added dropwise at 0°C solution of 1M NaOH (2 mL). Stirring was continued for 30 minutes at 0°C and the solution was neutralised with Amberlite IR-120, filtered and washed with MeOH. The crude was then evaporated to afford **2.28** (242 mg, 0.61 mmol, **98%**) as a white yellow powder.

**<sup>1</sup>H NMR (400 MHz, CD<sub>3</sub>OD):** δ 7.55 (d, 1H, *J* = 2.0 Hz, H<sub>6</sub>), 7.42 (d, 1H, *J* = 2.0 Hz, H<sub>7</sub>), 6.01 to 5.91 (m, 1H, H<sub>9</sub>), 5.10 to 5.05 (m, 2H, H<sub>10</sub>), 4.61 (d, 1H, *J* = 7.6 Hz, H<sub>1</sub>), 4.55 (s, 2H, H<sub>11</sub>), 3.60 (d, 1H, *J* = 6.8 Hz, H<sub>5</sub>), 3.54 to 3.25 (m, 5H, H<sub>2+3+4+8</sub>) **<sup>13</sup>C NMR (100 MHz,**

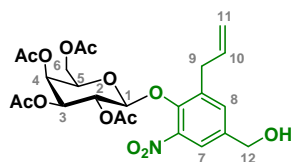
**CD<sub>3</sub>OD):**  $\delta$  171.5, 147.3, 146.0, 140.6, 138.2, 137.6, 133.5, 121.8, 117.3, 106.2, 77.1, 77.0, 74.9, 72.8, 63.6, 34.6 **LRESI-MS (negative mode):**  $m/z$  384 [M-H]<sup>-</sup> **HRESI-MS (negative mode):**  $m/z$  384.0930 (calcd. for C<sub>16</sub>H<sub>18</sub>NO<sub>10</sub> 384.0925 [M-H]<sup>-</sup>) **m.p.** 74-76°C



2.29

To a solution of **2.23** (570 mg, 2.75 mmol, 1.1 equiv.) in CH<sub>3</sub>CN (30 mL) cooled in an ice-water bath was added  $\alpha$ -D-galactopyranosyl bromide-2,3,4,6-tetraacetate (1.03 g, 2.51 mmol) and Ag<sub>2</sub>O (872 mg, 1.5 equiv.). After overnight stirring at room temperature, the solution was filtered through silica, eluted with ethyl acetate and concentrated under reduced pressure. Purification by column chromatography over silica gel (petroleum ether/ethyl acetate: 85/15 then 6/4) afforded **2.29** as a white yellow powder (1.16 g, 2.16 mmol, **79%**).

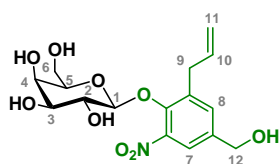
**<sup>1</sup>H NMR (400 MHz, CDCl<sub>3</sub>):**  $\delta$  9.97 (s, 1H, CHO), 8.11 (d, 1H,  $J = 2.0$  Hz, H<sub>7</sub>), 7.96 (d, 1H,  $J = 2.0$  Hz, H<sub>8</sub>), 5.96 to 5.86 (m, 1H, H<sub>10</sub>), 5.48 (dd, 1H,  $J = 10.4$  Hz,  $J = 7.6$  Hz, H<sub>2</sub>), 5.37 (d, 1H,  $J = 2.8$  Hz, H<sub>4</sub>), 5.22 to 5.14 (m, 2H, H<sub>11</sub>), 5.05 (dd, 1H,  $J = 10.4$  Hz,  $J = 3.2$ , H<sub>3</sub>), 4.95 (d, 1H,  $J = 8.0$  Hz, H<sub>1</sub>), 4.02 (d, 2H,  $J = 6.8$  Hz, H<sub>6</sub>), 3.81 (dt, 1H,  $J = 6.8$  Hz,  $J = 0.8$  Hz, H<sub>5</sub>), 3.58 (dd, 2H,  $J = 6.4$  Hz,  $J = 1.2$  Hz, H<sub>9</sub>), 2.18 (s, 3H, H-Ac), 2.16 (s, 3H, H-Ac), 1.99 (s, 3H, H-Ac), 1.96 (s, 3H, H-Ac) **<sup>13</sup>C NMR (100 MHz, CDCl<sub>3</sub>):**  $\delta$  189.1, 170.3, 170.2, 170.1, 169.6, 149.6, 145.5, 139.2, 134.7, 134.6, 133.1, 124.1, 118.3, 102.3, 71.5, 70.6, 68.7, 66.6, 60.8, 34.1, 20.9, 20.8, 20.7, 20.6 **LRFAB-MS (3-NOBA matrix):**  $m/z$  538 [M+H]<sup>+</sup>, 560 [M+Na]<sup>+</sup> **HRFAB-MS (3-NOBA matrix):**  $m/z$  538.1552 (calcd. for C<sub>24</sub>H<sub>28</sub>NO<sub>13</sub> 538.1561 [M+H]<sup>+</sup>) **m.p.** 78-80°C



2.30

To a solution of **2.29** (700 mg, 1.30 mmol) in  $\text{CHCl}_3/i\text{PrOH}$  (20 mL/14 mL) was added silica (1.0 g). The mixture was cooled in an ice-water bath and  $\text{NaBH}_4$  (594 mg, 12.0 equiv.) was added portion-wise. After 2 hours at  $0^\circ\text{C}$ , the solution was allowed to reach room temperature and filtered on Celite<sup>®</sup>, the pad being washed with  $\text{CH}_2\text{Cl}_2$ . Evaporation and purification by column chromatography over silica gel (petroleum ether/ethyl acetate: 6/4 to 3/7) afforded **2.30** as a white yellow powder (608 mg, 1.13 mmol, **87%**).

**<sup>1</sup>H NMR (400 MHz,  $\text{CDCl}_3$ ):**  $\delta$  7.60 (d, 1H,  $J = 2.0$  Hz, H<sub>9</sub>), 7.40 (d, 1H,  $J = 1.6$  Hz, H<sub>11</sub>), 5.93 to 5.83 (m, 1H, H<sub>14</sub>), 5.45 (dd, 1H,  $J = 10.4$  Hz,  $J = 8.0$  Hz, H<sub>2</sub>), 5.35 (d, 1H,  $J = 2.8$  Hz, H<sub>4</sub>), 5.14 (bs, 1H, H<sub>15</sub>), 5.11 (dd, 1H,  $J = 7.2$  Hz,  $J = 1.2$  Hz, H<sub>15</sub>), 5.02 (dd, 1H,  $J = 10.4$  Hz,  $J = 3.6$  Hz, H<sub>3</sub>), 4.82 (d, 1H,  $J = 8.0$  Hz, H<sub>1</sub>), 4.69 (bs, 2H, H<sub>16</sub>), 4.03 (dd, 2H,  $J = 6.8$  Hz,  $J = 3.6$  Hz, H<sub>6</sub>), 3.77 (t, 1H,  $J = 6.4$  Hz, H<sub>5</sub>), 3.50 (t, 2H,  $J = 4.8$  Hz, H<sub>13</sub>), 2.37 (bs, 1H,  $\text{CH}_2\text{-OH}$ ), 2.18 (s, 3H, *H*-Ac), 2.15 (s, 3H, *H*-Ac), 1.98 (s, 3H, *H*-Ac), 1.96 (s, 3H, *H*-Ac) **<sup>13</sup>C NMR (100 MHz,  $\text{CDCl}_3$ ):**  $\delta$  170.5, 170.4, 170.2, 169.7, 145.3, 144.4, 139.0, 137.5, 135.6, 132.2, 121.0, 117.4, 102.7, 71.2, 70.7, 68.7, 66.7, 63.5, 60.8, 34.1, 21.1, 20.9, 20.7, 20.6 **LRFAB-MS (3-NOBA matrix):**  $m/z$  538  $[\text{M}+\text{H}]^+$ , 562  $[\text{M}+\text{Na}]^+$  **HRFAB-MS (3-NOBA matrix):**  $m/z$  562.1528 (calcd. for  $\text{C}_{24}\text{H}_{29}\text{NO}_{13}\text{Na}$  562.1537  $[\text{M}+\text{Na}]^+$ ) **m.p.** 110-112 $^\circ\text{C}$

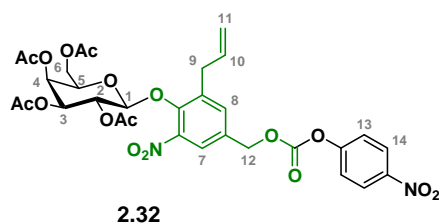


2.31

To a solution of **2.30** (90 mg, 0.17 mmol) in MeOH (10 mL) cooled in an ice-water bath was added dropwise at  $0^\circ\text{C}$  solution of MeONa (90 mg, 10.0 equiv.) in MeOH (5 mL). Stirring was continued for one hour at  $0^\circ\text{C}$  and the solution was neutralised with Amberlite IRC-50 and filtered. MeOH was then evaporated and the resulting mixture was purified by column

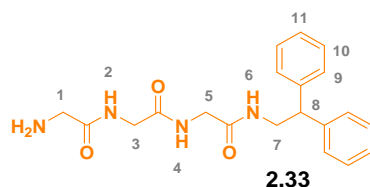
chromatography over silica gel (CH<sub>2</sub>Cl<sub>2</sub>/MeOH: 10 to 15% MeOH) to afford **2.31** (55 mg, 0.15 mmol, **88%**) as a white brown powder.

**<sup>1</sup>H NMR (400 MHz, CD<sub>3</sub>OD):**  $\delta$  7.57 (d, 1H,  $J$  = 2.0 Hz, H<sub>7</sub>), 7.48 (d, 1H,  $J$  = 2.0 Hz, H<sub>8</sub>), 6.06 to 5.96 (m, 1H, H<sub>10</sub>), 5.17 to 5.10 (m, 2H, H<sub>11</sub>), 4.60 (bs, 2H, H<sub>12</sub>), 4.50 (d, 1H,  $J$  = 7.6 Hz, H<sub>1</sub>), 3.84 (d, 1H,  $J$  = 2.8 Hz, H<sub>4</sub>), 3.78 (dd, 1H,  $J$  = 10.0 Hz,  $J$  = 8.0 Hz, H<sub>2</sub>), 3.72 to 3.55 (m, 4H, H<sub>6+9</sub>), 3.48 (dd, 1H,  $J$  = 9.6 Hz,  $J$  = 3.2 Hz, H<sub>3</sub>), 3.35 (t, 1H,  $J$  = 6.4 Hz, H<sub>5</sub>) **<sup>13</sup>C NMR (100 MHz, CD<sub>3</sub>OD):**  $\delta$  147.9, 146.3, 140.5, 138.1, 137.7, 133.4, 121.5, 117.3, 107.1, 77.0, 74.7, 72.5, 69.7, 63.7, 61.6, 34.5 **LRFAB-MS (3-NOBA matrix):**  $m/z$  394 [M+Na]<sup>+</sup> **HRFAB-MS (3-NOBA matrix):**  $m/z$  394.1124 (calcd. for C<sub>16</sub>H<sub>21</sub>NO<sub>9</sub>Na 394.1114 [M+Na]<sup>+</sup>) **m.p.** 140-142°C



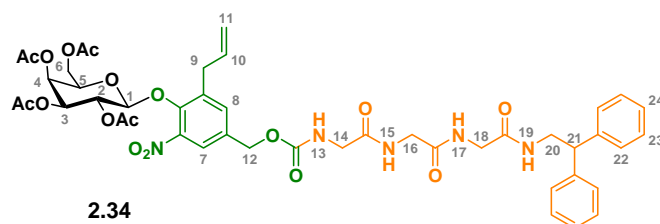
To a solution of **5** (433 mg, 0.80 mmol) in CH<sub>2</sub>Cl<sub>2</sub> (15 mL) was added *para*-nitrophenyl chloroformate (356 mg, 2.2 equiv.) and pyridine (160  $\mu$ L, 2.5 equiv.). After one day at room temperature, the solution was diluted with water and extracted with CH<sub>2</sub>Cl<sub>2</sub>. The combined organic layers were washed with water, dried over MgSO<sub>4</sub> and concentrated *in vacuo*. Purification by column chromatography over silica gel (petroleum ether/ethyl acetate: 6/4) afforded **7** (540 mg, 0.77 mmol, **96%**) as a white powder.

**<sup>1</sup>H NMR (400 MHz, CDCl<sub>3</sub>):**  $\delta$  8.29 (d, 2H,  $J$  = 9.2 Hz, H<sub>14</sub>), 7.71 (d, 1H,  $J$  = 2.0 Hz, H<sub>7</sub>), 7.50 (d, 1H,  $J$  = 2.0 Hz, H<sub>8</sub>), 7.39 (d, 2H,  $J$  = 9.2 Hz, H<sub>13</sub>), 5.96 to 5.85 (m, 1H, H<sub>10</sub>), 5.48 (dd, 1H,  $J$  = 10.8 Hz,  $J$  = 8.0 Hz, H<sub>2</sub>), 5.38 (d, 1H,  $J$  = 2.4 Hz, H<sub>4</sub>), 5.27 (bs, 2H, H<sub>12</sub>), 5.20 to 5.14 (m, 2H, H<sub>11</sub>), 5.05 (dd, 1H,  $J$  = 10.8 Hz,  $J$  = 3.6 Hz, H<sub>3</sub>), 4.88 (d, 1H,  $J$  = 8.0 Hz, H<sub>1</sub>), 4.06 (t, 2H,  $J$  = 6.8 Hz, H<sub>6</sub>), 3.80 (t, 1H,  $J$  = 7.6 Hz, H<sub>5</sub>), 3.56 (t, 2H,  $J$  = 6.0 Hz, H<sub>9</sub>), 2.20 (s, 3H, *H*-Ac), 2.17 (s, 3H, *H*-Ac), 2.01 (s, 3H, *H*-Ac), 1.97 (s, 3H, *H*-Ac) **<sup>13</sup>C NMR (100 MHz, CDCl<sub>3</sub>):**  $\delta$  170.4, 170.3, 170.2, 169.7, 155.4, 152.4, 145.7, 145.4, 138.5, 135.3, 134.1, 132.1, 125.5, 122.9, 121.8, 118.0, 102.7, 71.3, 70.7, 69.1, 68.7, 66.7, 60.8, 34.1, 20.9, 20.8, 20.7, 20.6 **LRFAB-MS (3-NOBA matrix):**  $m/z$  705 [M+H]<sup>+</sup>, 727 [M+Na]<sup>+</sup> **m.p.** 66-68°C



A solution of the Cbz-protected peptide (2.65 g, 5.27 mmol) in a 3:4:13 mixture H<sub>2</sub>O/MeOH/THF (500 mL) was heated up to 50°C until it had fully dissolved (5 min). The solution was then allowed to cool to room temperature and palladium (10%) on carbon (561 mg) was added in one portion. The reaction vessel was purged with H<sub>2</sub> by means of three vacuum/H<sub>2</sub> cycles and the mixture stirred at room temperature for 15 hours. The solid was filtered off with Celite<sup>®</sup>, MeOH and THF were evaporated under reduced pressure and the remaining aqueous layer was extracted with CH<sub>2</sub>Cl<sub>2</sub>/iPrOH (3/1) (3×50 mL). The combined organic fractions were dried (MgSO<sub>4</sub>) and concentrated under reduced pressure. The resulting yellow oil was re-dissolved in CH<sub>2</sub>Cl<sub>2</sub> (10 mL) and Et<sub>2</sub>O (50 mL) was added. The resulting white precipitate was sonicated for 5 minutes and filtered by gravity to afford **2.33** as a white solid (1.30 g, 3.52 mmol, **67%**).

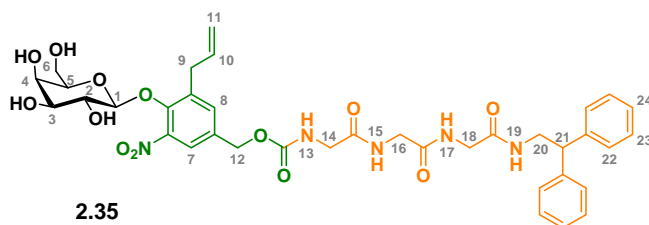
**<sup>1</sup>H NMR (400 MHz, CDCl<sub>3</sub>):** δ 8.07-7.81 (m, 1H, H<sub>6</sub>), 7.42-7.25, 6.75-6.58 (2m, 2H, H<sub>2+4</sub>), 7.25-6.95 (m, 10H, H<sub>9+10+11</sub>), 4.10 (t, 1H, *J* = 7.8 Hz, H<sub>8</sub>), 3.75-3.67 (m, 4H, H<sub>6+11</sub>), 3.75, 3.64, 3.28 (3s, 4H, H<sub>3+5+7</sub>) **<sup>13</sup>C NMR (100 MHz, CDCl<sub>3</sub>):** δ 169.7 (×2), 169.0, 141.7, 128.6, 128.0, 126.7, 50.2, 43.8 (×2), 42.8, 42.6 **LRESI-MS:** *m/z* 391 [M+Na]<sup>+</sup> **HRESI-MS:** *m/z* 369.1924 (calcd. for C<sub>20</sub>H<sub>25</sub>O<sub>3</sub>N<sub>4</sub> 369.1921 [M+H]<sup>+</sup>) **m.p.** 50-52°C



To a solution of **2.30** (529 mg, 0.75 mmol) in CH<sub>3</sub>CN (35 mL) was added the peptide **2.33** (332 mg, 1.2 equiv.) and Et<sub>3</sub>N (260 μL, 2.5 equiv.). Stirring was continued at room temperature during one day and the solution was diluted with water and extracted with ethyl acetate. The combined extracts were washed with water, dried over MgSO<sub>4</sub> and concentrated. Purification by column chromatography over silica gel (petroleum ether/ethyl acetate: 4/6 to

2/8 then CH<sub>2</sub>Cl<sub>2</sub>/MeOH: 9/1) yielded **2.34** as a white brown powder (599 mg, 0.64 mmol, **85%**).

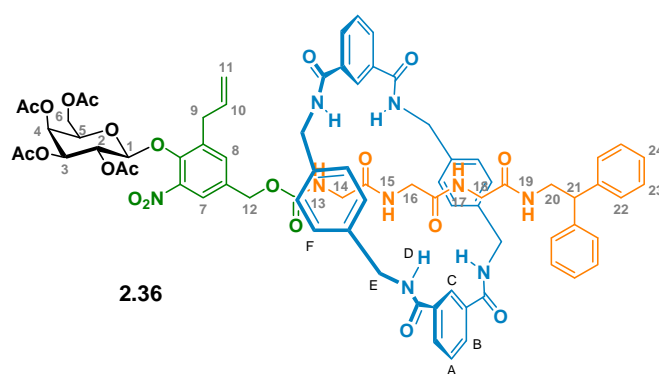
**<sup>1</sup>H NMR (400 MHz, CDCl<sub>3</sub>):** δ 7.57 (d, 1H, *J* = 2.0 Hz, H<sub>7</sub>), 7.39 (m, 2H, NH<sub>15+17</sub>), 7.37 (d, 1H, *J* = 2.0 Hz, H<sub>8</sub>), 7.27 to 7.16 (m, 10H, H<sub>22+23+24</sub>), 6.65 (t, 1H, *J* = 5.2 Hz, NH<sub>19</sub>), 6.08 (t, 1H, *J* = 4.8 Hz, NH<sub>13</sub>), 5.93 to 5.82 (m, 1H, H<sub>10</sub>), 5.46 (dd, 1H, *J* = 10.8 Hz, *J* = 8.0 Hz, H<sub>2</sub>), 5.37 (d, 1H, *J* = 2.8 Hz, H<sub>4</sub>), 5.15 (d, 1H, *J* = 1.2 Hz, H<sub>11</sub>), 5.12 (dd, 1H, *J* = 9.2 Hz, *J* = 1.2 Hz, H<sub>11</sub>), 5.06 (dd, 1H, *J* = 10.4 Hz, *J* = 3.6 Hz, H<sub>3</sub>), 5.00 (s, 2H, H<sub>12</sub>), 4.85 (d, 1H, *J* = 8.0 Hz, H<sub>1</sub>), 4.17 (t, 1H, *J* = 8.0 Hz, H<sub>21</sub>), 4.03 (d, 2H, *J* = 6.4 Hz, H<sub>6</sub>), 3.91 to 3.76 (m, 9H, H<sub>5+14+16+18+20</sub>), 3.50 (m, 2H, H<sub>9</sub>), 2.19 (s, 3H, *H*-Ac), 2.15 (s, 3H, *H*-Ac), 2.00 (s, 3H, *H*-Ac), 1.95 (s, 3H, *H*-Ac) **<sup>13</sup>C NMR (100 MHz, CDCl<sub>3</sub>):** δ 170.5, 170.4, 170.2, 169.8, 169.7, 169.3, 168.9, 156.4, 145.4, 145.0, 141.9, 137.9, 135.4, 134.4, 133.5, 128.8, 128.1, 126.9, 122.2, 117.7, 102.7, 71.1, 70.7, 68.8, 66.7, 65.3, 60.7, 50.5, 44.4, 44.0, 43.1, 42.9, 34.0, 29.8, 20.9, 20.8, 20.7, 20.6 **LRESI-MS: *m/z*** 957 [M+Na]<sup>+</sup> **LRFAB-MS (3-NOBA matrix): *m/z*** 935 [M+H]<sup>+</sup> **HRFAB-MS (3-NOBA matrix): *m/z*** 934.3384 (calcd. for C<sub>45</sub>H<sub>52</sub>N<sub>5</sub>O<sub>17</sub> 934.3359 [M+H]<sup>+</sup>) **m.p.** 126-128°C



To a solution of **2.34** (100 mg, 0.11 mmol) in MeOH (10 mL) cooled in an ice-water bath was added dropwise at 0°C solution of MeONa (58 mg, 10.0 equiv.) in MeOH (5 mL). Stirring was continued for one hour at 0°C and the solution was neutralised with Amberlite IRC-50 and filtered. MeOH was then evaporated and the resulting mixture was purified by column chromatography over silica gel (CH<sub>2</sub>Cl<sub>2</sub>/MeOH: 5 to 20% MeOH) to afford **2.35** (57 mg, 0.07 mmol, **64%**) as a white brown powder.

**<sup>1</sup>H NMR (400 MHz, CD<sub>3</sub>OD):** δ 7.57 (d, 1H, *J* = 2.0 Hz, H<sub>7</sub>), 7.45 (d, 1H, *J* = 2.0 Hz, H<sub>8</sub>), 7.24 to 7.19 (m, 8H, H<sub>22+23</sub>), 7.14 to 7.10 (m, 2H, H<sub>24</sub>), 5.99 to 5.89 (m, 1H, H<sub>10</sub>), 5.11 to 5.04 (m, 4H, H<sub>11+12</sub>), 4.47 (d, 1H, *J* = 8.0 Hz, H<sub>1</sub>), 4.24 (t, 1H, *J* = 8.0 Hz, H<sub>21</sub>), 3.80 to 3.73 (m, 8H, H<sub>14+16+18+20</sub>), 3.70 (m, 2H, H<sub>4+5</sub>), 3.66 to 3.54 (m, 4H, H<sub>6+9</sub>), 3.44 (dd, 1H, *J* = 10.0 Hz, *J*

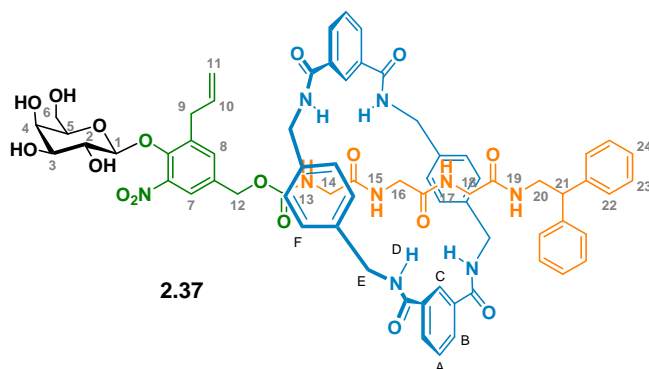
= 3.6 Hz, H<sub>3</sub>) **<sup>13</sup>C NMR (100 MHz, CD<sub>3</sub>OD):**  $\delta$  173.1, 172.1, 171.5, 159.0, 147.9, 147.0, 143.8, 138.5, 137.5, 135.5, 134.7, 129.6, 129.2, 127.7, 122.8, 117.4, 107.1, 77.1, 74.7, 72.5, 69.7, 66.5, 61.6, 51.6, 49.9, 45.1, 43.8, 43.3, 34.5 **LRES<sup>+</sup>-MS:**  $m/z$  766 [M+H]<sup>+</sup>, 788-789-790 [M+Na]<sup>+</sup> **LRFAB-MS (3-NOBA matrix):**  $m/z$  766 [M+H]<sup>+</sup> **HRFAB-MS (3-NOBA matrix):**  $m/z$  766.2928 (calcd. for C<sub>37</sub>H<sub>44</sub>N<sub>5</sub>O<sub>13</sub> 766.2936 [M+H]<sup>+</sup>) **m.p.** 145-147°C



Thread **2.34** (200 mg, 0.21 mmol) and Et<sub>3</sub>N (1.0 mL, 35.0 equiv.) were dissolved in anhydrous chloroform (40 mL) and stirred vigorously whilst solutions of *p*-xylylene diamine (466 mg, 16.0 equiv.) in anhydrous chloroform (40 mL) and isophthaloyl dichloride (696 mg, 16.0 equiv.) in anhydrous chloroform (40 mL) were simultaneously added over a period of 3 hours using motor-driven syringe pumps. After overnight stirring, 1 mL of MeOH was added and the resulting suspension filtered through Celite<sup>®</sup>. The pad was washed with CHCl<sub>3</sub>/MeOH 2% (3 x 100 mL) and the combined filtrates were concentrated under reduced pressure. The residue was purified by column chromatography on silica gel using CH<sub>2</sub>Cl<sub>2</sub>/MeOH (1 to 15% MeOH) as eluent to give a mixture of thread **2.34** and rotaxane **2.36**. This mixture was resolved by running a size exclusion chromatography using CHCl<sub>3</sub>/MeOH (50/50) as eluent to give rotaxane **2.36** as a white brown powder (161 mg, 0.11 mmol, **51%**).

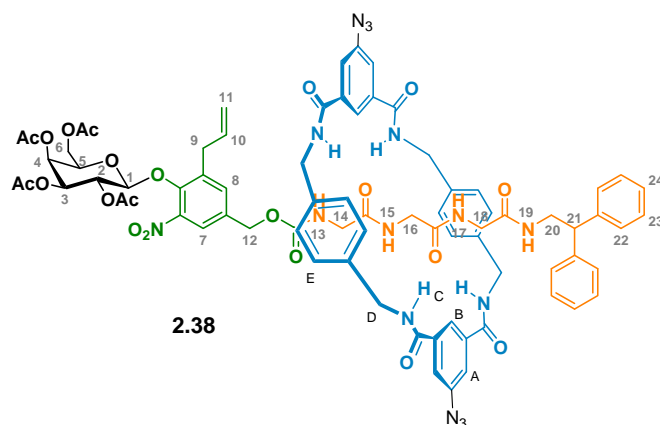
**<sup>1</sup>H NMR (400 MHz, CDCl<sub>3</sub>):**  $\delta$  8.19 (s, 2H, H<sub>C</sub>), 8.00 (d, 4H,  $J$  = 7.2 Hz, H<sub>B</sub>), 7.81 (bs, 4H, H<sub>D</sub>), 7.47 (t, 2H,  $J$  = 7.6 Hz, H<sub>A</sub>), 7.35 (s, 1H, H<sub>7</sub>), 7.23 (s, 1H, H<sub>8</sub>), 7.21 to 7.09 (m, 18H, H<sub>22+23+24+F</sub>), 6.98 (bs, 3H, NH<sub>15+17+19</sub>), 5.89 to 5.79 (m, 1H, H<sub>10</sub>), 5.73 (bs, 1H, NH<sub>13</sub>), 5.46 (t, 1H,  $J$  = 8.8 Hz, H<sub>2</sub>), 5.37 (bs, 1H, H<sub>4</sub>), 5.14 to 5.05 (m, 3H, H<sub>3+11</sub>), 4.84 (d, 1H,  $J$  = 7.6 Hz, H<sub>1</sub>), 4.74 (bs, 2H, H<sub>12</sub>), 4.48 to 4.39 (m, 8H, H<sub>E</sub>), 4.05 (t, 1H,  $J$  = 8.0 Hz, H<sub>21</sub>), 4.02 (d, 2H,  $J$  = 6.8 Hz, H<sub>6</sub>), 3.80 (t, 1H,  $J$  = 6.0 Hz, H<sub>5</sub>), 3.70 (bs, 2H, H<sub>20</sub>), 3.46 to 3.42 (m, 4H, H<sub>9+14</sub>), 3.30 (bs, 2H, H<sub>18</sub>), 2.93 (bs, 2H, H<sub>16</sub>), 2.17 (s, 3H, *H*-Ac), 2.16 (s, 3H, *H*-Ac), 2.01 (s, 3H, *H*-

Ac), 1.94 (s, 3H, *H*-Ac)  $^{13}\text{C}$  NMR (100 MHz,  $\text{CDCl}_3$ ):  $\delta$  170.5, 170.3, 170.2, 170.1, 169.7, 169.2, 168.2, 167.2, 156.3, 145.3, 145.0, 141.7, 137.7, 137.4, 135.3, 134.3, 133.9, 133.7, 131.0, 129.1, 129.0, 128.8, 128.0, 127.0, 125.4, 122.2, 117.7, 102.6, 71.1, 70.7, 68.8, 66.7, 65.3, 60.7, 50.5, 44.5, 44.2, 42.7, 42.1, 33.9, 20.9, 20.8, 20.7, 20.6 LRFAB-MS (3-NOBA matrix):  $m/z$  1467  $[\text{M}+\text{H}]^+$  HRFAB-MS (3-NOBA matrix):  $m/z$  1466.5485 (calcd. for  $\text{C}_{77}\text{H}_{80}\text{N}_9\text{O}_{21}$  1466.5469  $[\text{M}+\text{H}]^+$ ) m.p. 160-162°C



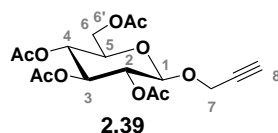
To a solution of **2.36** (98 mg, 0.067 mmol) in MeOH (10 mL) cooled in an ice-water bath was added dropwise at 0°C solution of MeONa (36 mg, 10.0 equiv.) in MeOH (5 mL). Stirring was continued for one hour at 0°C and the solution was neutralised with Amberlite IRC-50 resin and filtered. MeOH was then evaporated and the resulting mixture was purified by column chromatography over silica gel ( $\text{CH}_2\text{Cl}_2/\text{MeOH}$ : 2 to 10% MeOH) to afford **2.37** (75 mg, 0.058 mmol, **87%**) as a white brown powder.

$^1\text{H}$  NMR (400 MHz,  $\text{CD}_3\text{OD}$ ):  $\delta$  8.34 (bs, 2H,  $\text{H}_\text{C}$ ), 8.05 to 8.03 (m, 4H,  $\text{H}_\text{B}$ ), 7.59 (t, 2H,  $J = 7.6$  Hz,  $\text{H}_\text{A}$ ), 7.23 to 7.01 (m, 18H,  $\text{H}_{22+23+24+\text{F}}$ ), 5.97 to 5.87 (m, 1H,  $\text{H}_{10}$ ), 5.09 (dd, 1H,  $J = 8.8$  Hz,  $J = 1.6$  Hz,  $\text{H}_{11}$ ), 5.05 (bs, 1H,  $\text{H}_{11}$ ), 4.57 (bs, 2H,  $\text{H}_{12}$ ), 4.48 to 4.39 (m, 9H), 3.93 (t, 1H,  $J = 8.0$  Hz,  $\text{H}_{21}$ ), 3.82 (t, 1H,  $J = 3.2$  Hz), 3.76 (dd, 1H,  $J = 9.6$  Hz,  $J = 7.6$  Hz), 3.65 (dd, 1H,  $J = 11.2$  Hz,  $J = 6.8$  Hz), 3.57 to 3.44 (m, 10H,  $\text{H}_{14+16+18+20}$ )  $^{13}\text{C}$  NMR (100 MHz,  $\text{CD}_3\text{OD}$ ):  $\delta$  172.4, 171.2, 170.5, 169.0, 158.1, 147.7, 147.0, 143.6, 138.8, 138.3, 137.5, 135.7, 134.9, 134.7, 131.7, 130.1, 130.0, 129.9, 129.8, 129.6, 129.4, 129.0, 127.8, 127.7, 122.8, 117.4, 107.1, 77.1, 74.7, 72.5, 69.7, 66.2, 61.7, 51.7, 49.9, 45.2, 45.0, 44.9, 43.2, 42.6, 34.4 LRFAB-MS (3-NOBA matrix):  $m/z$  1299  $[\text{M}+\text{H}]^+$  HRFAB-MS (3-NOBA matrix):  $m/z$  1299.5104 (calcd. for  $\text{C}_{69}\text{H}_{73}\text{N}_9\text{O}_{17}$  calcd. 1299.5124  $[\text{M}+\text{H}]^+$ ) m.p. 178-180°C



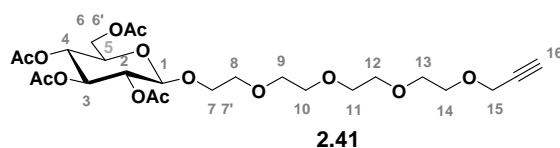
Thread **2.34** (400 mg, 0.43 mmol) and Et<sub>3</sub>N (2.1 mL, 35.0 equiv.) were dissolved in anhydrous chloroform (80 mL) and stirred vigorously whilst solutions of *p*-xylylene diamine (933 mg, 16.0 equiv.) in anhydrous chloroform (60 mL) and 5-azidoisophthaloyl dichloride (1.67 g, 16.0 equiv.) in anhydrous chloroform (60 mL) were simultaneously added over a period of 5 hours using motor-driven syringe pumps. After overnight stirring, 2 mL of MeOH were added and the resulting suspension filtered through Celite<sup>®</sup>. The pad was washed with CHCl<sub>3</sub>/MeOH 2% (2 x 200 mL) and the combined filtrates were concentrated under reduced pressure. The residue was purified by column chromatography on silica gel using CHCl<sub>3</sub>/acetone (10 to 60% acetone) as eluent to give rotaxane **2.38** as a white yellow powder (421 mg, 0.27 mmol, **63%**).

**<sup>1</sup>H NMR (400 MHz, CDCl<sub>3</sub>):**  $\delta$  7.88 (bs, 2H, H<sub>B</sub>), 7.62 (bs, 4H, H<sub>C</sub>), 7.54 (bs, 4H, H<sub>A</sub>), 7.34 (s, 1H, H<sub>7</sub>), 7.18 to 7.17 (m, 1H, NH), 7.14 (d, 4H,  $J = 7.6$  Hz, H<sub>E</sub>), 7.10 (s, 1H, H<sub>8</sub>), 7.07 (bs, 10H, H<sub>22+23+24</sub>), 7.01 (d, 4H,  $J = 7.2$  Hz, H<sub>E</sub>), 6.86 (bs, 2H, NH), 5.83 to 5.73 (m, 1H, H<sub>10</sub>), 5.63 (bs, 1H, NH<sub>13</sub>), 5.39 (dd, 1H,  $J = 10.4$  Hz,  $J = 8.0$  Hz, H<sub>2</sub>), 5.30 (d, 1H,  $J = 3.6$  Hz, H<sub>4</sub>), 5.08 to 4.97 (m, 3H, H<sub>3+11</sub>), 4.77 to 4.76 (m, 3H, H<sub>1+12</sub>), 4.50 to 4.46 (m, 4H, H<sub>D</sub>), 4.31 to 4.27 (m, 4H, H<sub>D</sub>), 4.00 to 3.91 (m, 3H, H<sub>6+21</sub>), 3.74 (t, 1H,  $J = 7.2$  Hz, H<sub>5</sub>), 3.66 (bs, 2H, H<sub>20</sub>), 3.45 (bs, 2H, H<sub>14</sub>), 3.41 (d, 2H,  $J = 6.4$  Hz, H<sub>9</sub>), 3.25 (bs, 2H, H<sub>16/18</sub>), 2.97 (bs, 2H, H<sub>16/18</sub>), 2.10 (s, 3H, *H*-Ac), 2.08 (s, 3H, *H*-Ac), 1.93 (s, 3H, *H*-Ac), 1.88 (s, 3H, *H*-Ac) **<sup>13</sup>C NMR (100 MHz, CDCl<sub>3</sub>):**  $\delta$  170.6, 170.4, 170.2, 169.7, 169.4, 168.1, 166.0, 156.5, 145.3, 145.1, 141.6, 141.5, 137.8, 137.2, 135.7, 135.3, 133.8, 133.5, 129.3, 128.9, 127.9, 127.2, 122.1, 121.6, 121.0, 117.8, 102.7, 71.1, 70.7, 68.7, 66.7, 65.4, 60.7, 53.9, 50.6, 44.5, 44.4, 42.9, 42.4, 34.0, 31.9, 29.4, 21.0, 20.8, 20.7 (x2) **LRESI-MS:**  $m/z$  1550 [M+H]<sup>+</sup> **LRFAB-MS (3-NOBA matrix):**  $m/z$  1551 [M+H]<sup>+</sup> **m.p.** degradation



To a solution of peracetylated  $\beta$ -D-glucose (1.21 g, 3.10 mmol) and propargyl alcohol (0.27 mL, 1.5 equiv.) in anhydrous  $\text{CH}_2\text{Cl}_2$  (8 mL) under  $\text{N}_2$  at  $0^\circ\text{C}$ , was added  $\text{BF}_3\cdot\text{Et}_2\text{O}$  (2 mL, 5.0 equiv.) dropwise. The reaction mixture was allowed to warm up to room temperature and stirred overnight. An aqueous saturated solution of  $\text{NaHCO}_3$  (30 mL) was added, the layers were separated and the aqueous layer was extracted with  $\text{CH}_2\text{Cl}_2$  ( $3\times 25$  mL). The combined organic fractions were dried ( $\text{Na}_2\text{SO}_4$ ) and concentrated under reduced pressure. The resulting brown residue was purified by flash column chromatography on silica gel with  $\text{CH}_2\text{Cl}_2$ -acetone (98/2) as eluent to give pure **2.39** as a white solid (940 mg, 2.43 mmol, **79%**). The compound showed identical spectroscopic data to that reported in Hoheisel, T. N.; Frauenrath, H. *Org. Lett.* **2008**, *10*, 4525-4528.

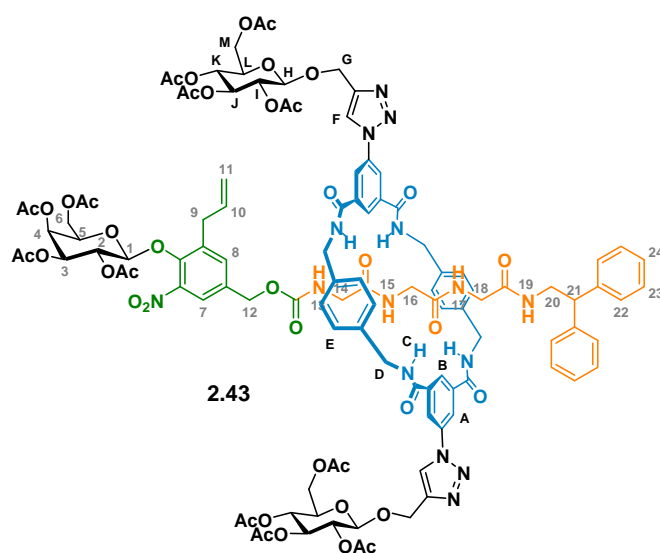
**$^1\text{H}$  NMR (400 MHz,  $\text{CDCl}_3$ ):**  $\delta$  5.22 (t, 1H,  $J = 9.5$  Hz,  $\text{H}_3$ ), 5.08 (t, 1H,  $J = 9.5$  Hz,  $\text{H}_4$ ), 4.99 (t, 1H,  $J = 9.5$  Hz,  $\text{H}_2$ ), 4.76 (d, 1H,  $J = 7.9$  Hz,  $\text{H}_1$ ), 4.35 (d, 2H,  $J = 2.4$  Hz,  $\text{H}_7$ ), 4.26 (dd, 1H,  $J = 4.6$  Hz,  $J = 12.3$  Hz,  $\text{H}_6$ ), 4.13 (dd, 1H,  $J = 2.2$  Hz,  $J = 12.3$  Hz,  $\text{H}_{6'}$ ), 3.71 (ddd, 1H,  $J = 2.4$  Hz,  $J = 4.5$  Hz,  $J = 10.0$  Hz,  $\text{H}_5$ ), 2.46 (t, 1H,  $J = 2.4$  Hz,  $\text{H}_8$ ), 2.07, 2.04, 2.10, 1.99 (4s, 12H,  $\text{H-Ac}$ )  **$^{13}\text{C}$  NMR (100 MHz,  $\text{CDCl}_3$ ):**  $\delta$  170.6, 170.2, 169.3, 169.2, 98.0, 78.0, 75.4, 72.6, 71.8, 70.8, 68.2, 61.6, 55.8, 20.7, 20.6, 20.5, 20.4 **LRESI-MS:**  $m/z$  409  $[\text{M}+\text{Na}]^+$  **HRESI-MS:**  $m/z$  404.1552 (calcd. for  $\text{C}_{17}\text{H}_{26}\text{O}_{10}\text{N}$  404.1551  $[\text{M}+\text{H}]^+$ ) **m.p.** 100-102 $^\circ\text{C}$  (litt. 116-117 $^\circ\text{C}$ )



To a solution of peracetylated  $\beta$ -D-glucose (317 mg, 0.81 mmol) and alcohol (283 mg, 1.5 equiv.) in anhydrous  $\text{CH}_2\text{Cl}_2$  (2 mL) under  $\text{N}_2$  at  $0^\circ\text{C}$ , was added  $\text{BF}_3\cdot\text{Et}_2\text{O}$  (0.52 mL, 5.0 equiv.) dropwise. The reaction mixture was allowed to warm up to room temperature and stirred overnight. An aqueous saturated solution of  $\text{NaHCO}_3$  (10 mL) was added, the layers were separated and the aqueous layer was extracted with  $\text{CH}_2\text{Cl}_2$  ( $3\times 15$  mL). The combined organic fractions were dried ( $\text{Na}_2\text{SO}_4$ ) and concentrated under reduced pressure. The resulting

brown residue was purified by flash column chromatography on silica gel with CH<sub>2</sub>Cl<sub>2</sub>/acetone (93/7) as eluent to give pure **2.41** as a colorless oil (378 mg, 0.67 mmol, **83%**).

**<sup>1</sup>H NMR (400 MHz, CDCl<sub>3</sub>):**  $\delta$  5.13 (t, 1H,  $J = 9.5$  Hz, H<sub>3</sub>), 5.01 (t, 1H,  $J = 9.6$  Hz, H<sub>4</sub>), 4.91 (dd, 1H,  $J = 8.0$  Hz,  $J = 9.5$  Hz, H<sub>2</sub>), 4.55 (d, 1H,  $J = 8.0$  Hz, H<sub>1</sub>), 4.19 (dd, 1H,  $J = 4.7$  Hz,  $J = 12.3$  Hz, H<sub>6</sub>), 4.14 (d, 2H,  $J = 2.4$  Hz, H<sub>15</sub>), 4.06 (dd, 1H,  $J = 2.3$  Hz,  $J = 12.3$  Hz, H<sub>6'</sub>), 3.87 (dt, 1H,  $J = 4.0$  Hz,  $J = 11.0$  Hz, H<sub>7</sub>), 3.71 to 3.52 (m, 16H, H<sub>5+7'+8+9+10+11+12+13+14</sub>), 2.40 (t, 1H,  $J = 2.3$  Hz, H<sub>16</sub>), 2.01, 1.97, 1.95, 1.93 (4s, 12H, *H*-Ac) **<sup>13</sup>C NMR (100 MHz, CDCl<sub>3</sub>):**  $\delta$  170.4, 170.0, 169.2, 169.1, 100.6, 79.5, 74.4, 72.6, 71.5, 71.0, 70.5, 70.4 ( $\times 2$ ), 70.3, 70.1, 70.0, 68.8 ( $\times 2$ ), 68.2, 61.7, 58.1, 20.6, 20.5, 20.4, 20.3 **LRESI-MS:**  $m/z$  585 [M+Na]<sup>+</sup> **HRESI-MS:**  $m/z$  580.2600 (calcd. for C<sub>25</sub>H<sub>42</sub>O<sub>14</sub>N 580.2600 [M+NH<sub>4</sub>]<sup>+</sup>)

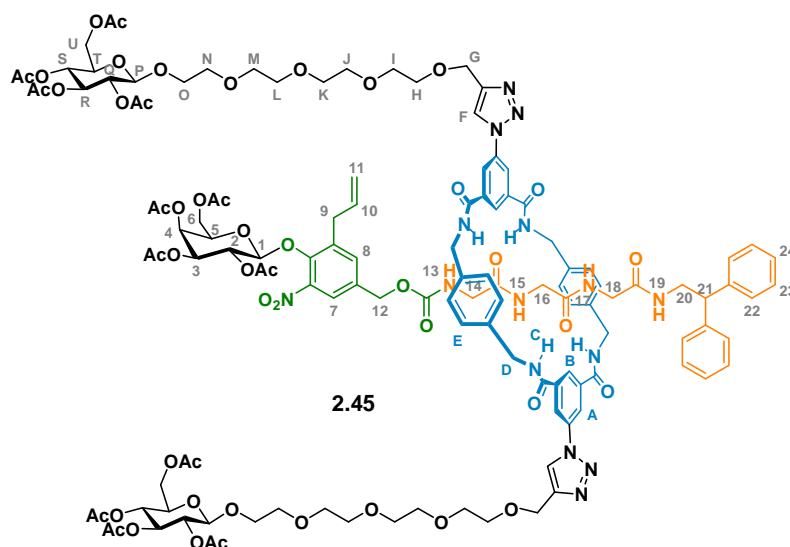


To a solution of rotaxane **2.38** (61 mg, 39.40  $\mu$ mol) and alkyne **2.39** (30 mg, 2.0 equiv.) in CH<sub>2</sub>Cl<sub>2</sub> (7 mL) was added Cu(CH<sub>3</sub>CN)<sub>4</sub>PF<sub>6</sub> (7 mg, 0.5 equiv.) and Et<sub>3</sub>N (12  $\mu$ L, 2.2 equiv.) and the solution stirred overnight at room temperature. A saturated NH<sub>4</sub>Cl solution was then added to the reaction mixture and air was bubbled for 30 min. The organic layer was separated and washed with 1M EDTA, dried over MgSO<sub>4</sub>, filtrated and concentrated under reduced pressure. The resulting solid was purified by column chromatography on silica gel using CHCl<sub>3</sub>/acetone (30 to 55% acetone) to give rotaxane **2.43** as a white yellow powder (31 mg, 13.40  $\mu$ mol, **34%**).



using  $\text{CHCl}_3/\text{acetone}$  (30 to 55% acetone) to give rotaxane **2.44** as a white yellow powder (31 mg, 13.40  $\mu\text{mol}$ , **24%**).

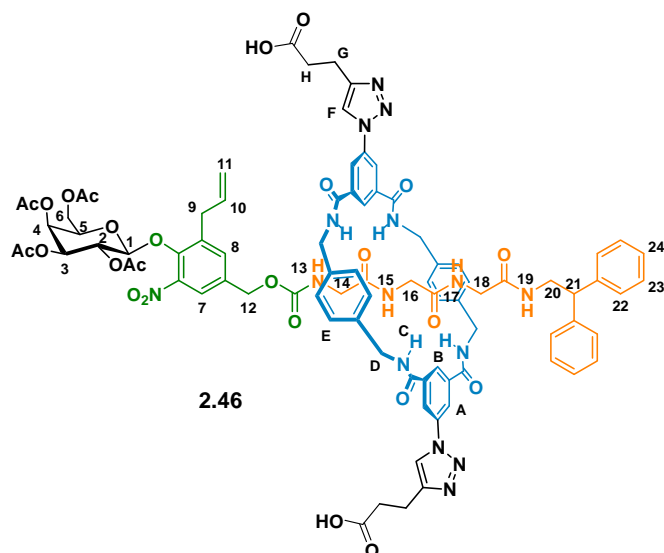
**$^1\text{H}$  NMR (400 MHz,  $\text{CDCl}_3$ ):**  $\delta$  8.31 (bs, 6H,  $\text{H}_{\text{A}+\text{F}}$ ), 8.22 (bs, 2H,  $\text{H}_{\text{B}}$ ), 8.18 (bs, 4H,  $\text{H}_{\text{C}}$ ), 7.35 (s, 1H,  $\text{H}_7$ ), 7.18 (s, 1H,  $\text{H}_8$ ), 7.09 to 6.99 (m, 21H,  $\text{H}_{\text{E}+22+23+24+15+17+19}$ ), 5.96 (bs, 1H,  $\text{H}_{13}$ ), 5.79 to 5.69 (m, 1H,  $\text{H}_{10}$ ), 5.36 (dd, 1H,  $J = 10.4$  Hz,  $J = 8.0$  Hz,  $\text{H}_2$ ), 5.30 (d, 1H,  $J = 3.2$  Hz,  $\text{H}_4$ ), 5.03 to 4.98 (m, 3H,  $\text{H}_{3+11}$ ), 4.77 to 4.74 (m, 3H,  $\text{H}_{1+12}$ ), 4.68 (bs, 4H,  $\text{H}_{\text{G}}$ ), 4.39 to 4.35 (m, 8H,  $\text{H}_{\text{D}}$ ), 3.97 to 3.94 (m, 3H,  $\text{H}_{6+21}$ ), 3.77 (t, 1H,  $J = 6.8$  Hz,  $\text{H}_5$ ), 3.69 to 3.47 (m, 34H,  $\text{H}_{20+\text{H}+\text{I}+\text{J}+\text{K}+\text{L}+\text{M}+\text{N}+\text{O}$ ), 3.37 to 3.35 (m, 2H,  $\text{H}_9$ ), 2.96 to 2.79 (m, 7H,  $\text{H}_{14+16+18}$ ), 2.11 (s, 3H,  $\text{H-Ac}$ ), 2.06 (s, 3H,  $\text{H-Ac}$ ), 1.93 (s, 3H,  $\text{H-Ac}$ ), 1.87 (s, 3H,  $\text{H-Ac}$ )  **$^{13}\text{C}$  NMR (100 MHz,  $\text{CDCl}_3$ ):**  $\delta$  170.6, 170.4, 170.2, 170.1, 170.0, 169.7, 169.2, 168.6, 166.0 (x2), 156.3, 146.2, 145.3, 145.0, 141.9, 137.7, 137.3, 137.2, 136.3, 136.2, 135.4, 134.2, 133.4, 129.1, 128.7, 128.0, 126.9, 126.2, 122.0, 121.4, 117.7, 102.6, 72.7, 71.1, 70.7, 70.5 (x2), 70.2, 70.1, 68.8, 66.7, 65.2, 64.6, 61.5, 60.7, 50.5, 44.7, 44.2, 42.4, 41.8, 34.0, 29.8, 20.9, 20.8, 20.7 (x2) **LRFAB-MS (3-NOBA matrix):**  $m/z$  2014  $[\text{M}+\text{H}]^+$ , 2036  $[\text{M}+\text{Na}]^+$  **HRFAB-MS (3-NOBA matrix):**  $m/z$  2013.8153 (calcd. for  $\text{C}_{98}\text{H}_{118}^{13}\text{CN}_{15}\text{O}_{31}$  2013.8152  $[\text{M}+\text{H}]^+$ )



To a solution of rotaxane **2.38** (70 mg, 45.20  $\mu\text{mol}$ ) and alkyne **2.41** (51 mg, 2.0 equiv.) in  $\text{CH}_2\text{Cl}_2$  (7 mL) was added  $\text{Cu}(\text{CH}_3\text{CN})_4\text{PF}_6$  (8 mg, 0.5 equiv.) and  $\text{Et}_3\text{N}$  (14  $\mu\text{L}$ , 2.2 equiv.) and the solution was stirred overnight at room temperature. A saturated  $\text{NH}_4\text{Cl}$  solution was then added to the reaction mixture and air was bubbled for 30 min. The organic layer was separated and washed with 1M EDTA, dried over  $\text{MgSO}_4$ , filtrated and concentrated under

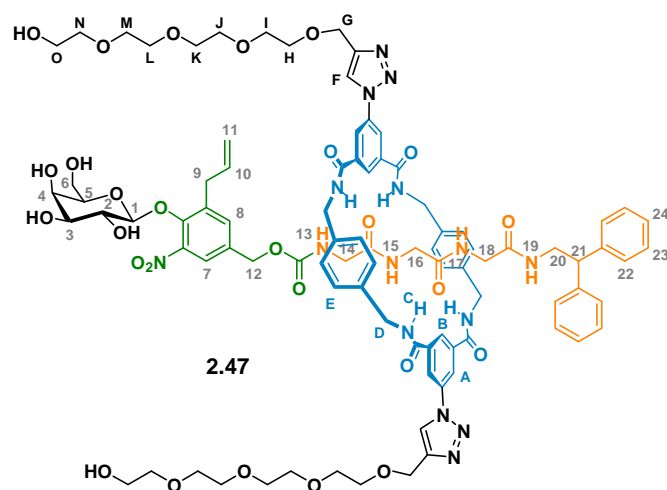
reduced pressure. The resulting solid was purified by column chromatography on silica gel using CHCl<sub>3</sub>/acetone (50 to 80% acetone) to give rotaxane **2.45** as a white yellow powder (26 mg, 9.70 μmol, **21%**).

**<sup>1</sup>H NMR (400 MHz, CDCl<sub>3</sub>):** δ 8.38 (bs, 2H, H<sub>B</sub>), 8.34 (bs, 2H, H<sub>F</sub>), 8.25 to 8.19 (m, 8H, H<sub>A+C</sub>), 7.40 (s, 1H, H<sub>7</sub>), 7.22 (s, 1H, H<sub>8</sub>), 7.18 to 6.95 (m, 21H, H<sub>15+17+19+22+23+24+E</sub>), 5.85 to 5.75 (m, 2H, H<sub>10+13</sub>), 5.43 (dd, 1H, *J* = 10.4 Hz, *J* = 8.0 Hz, H<sub>2</sub>), 5.37 (d, 1H, *J* = 3.6 Hz, H<sub>4</sub>), 5.20 (t, 2H, *J* = 9.6 Hz, H<sub>R</sub>), 5.10 to 5.04 (m, 5H, H<sub>3+11+S</sub>), 5.97 (dd, 2H, *J* = 9.6 Hz, *J* = 8.0 Hz, H<sub>Q</sub>), 4.82 (m, 3H, H<sub>1+12</sub>), 4.76 (bs, 4H, H<sub>G</sub>), 4.58 (d, 2H, *J* = 8.0 Hz, H<sub>P</sub>), 4.55 to 4.43 (m, 8H, H<sub>D</sub>), 4.24 (dd, 2H, *J* = 12.0 Hz, *J* = 4.4 Hz, H<sub>U</sub>), 4.11 (dd, 2H, *J* = 12.0 Hz, *J* = 2.0 Hz, H<sub>U</sub>), 4.07 to 3.98 (m, 3H, H<sub>6+21</sub>), 3.77 to 3.76 (m, 3H, H<sub>5+T</sub>), 3.72 to 3.56 (m, 36H, H<sub>14+20+H+I+J+K+L+M+N+O</sub>), 3.42 (d, 2H, *J* = 6.4 Hz, H<sub>9</sub>), 3.34 to 3.25 (m, 2H, H<sub>18</sub>), 2.84 (bs, 2H, H<sub>16</sub>), 2.17 (s, 3H, *H*-Ac), 2.13 (s, 3H, *H*-Ac), 2.06 (s, 6H, *H*-Ac), 2.03 (s, 6H, *H*-Ac), 2.01 (s, 6H, *H*-Ac), 2.00 (s, 3H, *H*-Ac), 1.99 (s, 6H, *H*-Ac), 1.95 (s, 3H) **<sup>13</sup>C NMR (100 MHz, CDCl<sub>3</sub>):** δ 170.9, 170.4 (x2), 170.2, 169.7, 169.6, 165.8, 146.5, 145.0, 141.8, 137.7, 137.4, 137.3, 136.4, 136.3, 135.3, 134.1, 133.3, 129.9, 129.1, 128.8, 128.0, 126.9, 126.1, 121.9 (x2), 121.2, 117.7, 102.6, 101.0 (x2), 72.9, 71.9, 71.4, 71.0, 70.7, 70.6, 70.3, 70.1, 69.3, 68.8, 68.5, 66.8, 65.2, 64.6, 62.1, 60.7, 50.5, 44.7, 44.3, 44.1, 42.4, 42.3, 41.8, 33.9, 29.8, 29.4, 21.0, 20.9 (x2), 20.8, 20.7 **LRFAB-MS (3-NOBA matrix):** *m/z* 2675 [M+H]<sup>+</sup>, 2699 [M+Na]<sup>+</sup> **HRFAB-MS (3-NOBA matrix):** *m/z* 2695.9802 (calcd. for C<sub>126</sub><sup>13</sup>CH<sub>153</sub>N<sub>15</sub>O<sub>49</sub>Na calcd. 2695.9873 [M+Na]<sup>+</sup>) **m.p.** 133-135°C



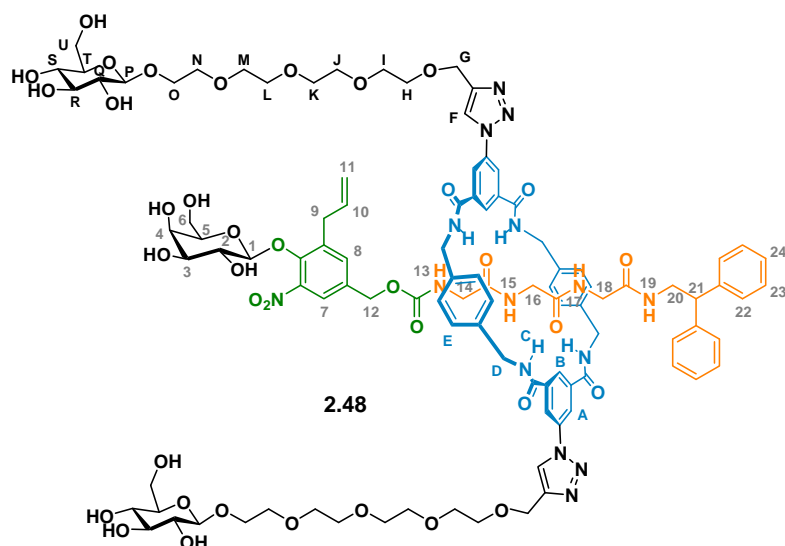
To a solution of rotaxane **2.38** (107 mg, 69.20  $\mu\text{mol}$ ) and alkyne **2.42** (14 mg, 2.0 equiv.) in  $\text{CH}_2\text{Cl}_2$  (10 mL) was added  $\text{Cu}(\text{CH}_3\text{CN})_4\text{PF}_6$  (52 mg, 2.0 equiv.) and the solution stirred overnight at room temperature. The solution was then acidified with 1N HCl and then extracted with  $\text{CHCl}_3/\text{iPrOH}$  (3/1). The organic layer was dried over  $\text{MgSO}_4$ , filtrated and concentrated under reduced pressure. The resulting solid was purified by column chromatography on silica gel using  $\text{CH}_2\text{Cl}_2/\text{MeOH}$  (2 to 9% MeOH) followed by  $\text{CH}_2\text{Cl}_2/\text{MeOH}/\text{AcOH}$  (9% MeOH, 0.25% AcOH) to give rotaxane **2.46** as a white yellow powder (41 mg, 13.40  $\mu\text{mol}$ , 34%).

**$^1\text{H}$  NMR (400 MHz,  $\text{CDCl}_3:\text{CD}_3\text{OD}$  7:3):**  $\delta$  8.40 (bs, 4H,  $\text{H}_A$ ), 8.27 (bs, 2H,  $\text{H}_F$ ), 8.14 (bs, 2H,  $\text{H}_B$ ), 7.20 to 6.84 (m, 20H,  $\text{H}_{7+8+22+23+24+E}$ ), 5.84 to 5.74 (m, 1H,  $\text{H}_{10}$ ), 5.37 (dd, 1H,  $J = 10.4$  Hz,  $J = 8.0$  Hz,  $\text{H}_2$ ), 5.32 (d, 1H,  $J = 3.2$  Hz,  $\text{H}_4$ ), 5.07 to 5.02 (m, 3H,  $\text{H}_{3+11}$ ), 4.79 (d, 1H,  $J = 7.6$  Hz,  $\text{H}_1$ ), 4.75 (bs, 2H,  $\text{H}_{12}$ ), 4.49 to 4.26 (m, 12H,  $\text{H}_{D+G}$ ), 3.99 to 3.95 (m, 4H,  $\text{H}_{6+21}$ ), 3.82 (t, 1H,  $J = 6.8$  Hz,  $\text{H}_5$ ), 3.56 (d, 2H,  $J = 7.6$  Hz,  $\text{H}_H$ ), 3.45 (bs, 2H), 3.39 (d, 2H,  $J = 6.4$  Hz,  $\text{H}_H$ ), 3.27 (m, 2H,  $\text{H}_9$ ), 3.12 to 3.09 (m, 4H,  $\text{H}_{14+18}$ ), 2.76 (bs, 2H,  $\text{H}_{16}$ ), 2.16 (s, 3H,  $\text{H-Ac}$ ), 2.11 (s, 3H,  $\text{H-Ac}$ ), 1.97 (s, 3H,  $\text{H-Ac}$ ), 1.92 (s, 3H,  $\text{H-Ac}$ )  **$^{13}\text{C}$  NMR (100 MHz,  $\text{CDCl}_3:\text{CD}_3\text{OD}$  7:3):**  $\delta$  170.7, 170.6, 170.3, 170.1, 169.9, 169.1, 167.3, 166.1, 156.3, 145.1, 144.6, 141.7, 137.3, 137.2, 136.9, 136.0, 135.9, 135.0, 134.0, 133.2, 128.8, 128.4, 127.6, 126.6, 126.0, 121.8, 121.7, 120.9, 120.1, 117.2, 102.3, 70.8, 70.6, 68.6, 66.6, 64.9, 60.5, 50.2, 44.3, 43.7, 43.6, 43.3, 41.8, 41.2, 33.6, 29.5, 20.7, 20.5, 20.3, 20.2 **LRESI-MS (negative):**  $m/z$  1743  $[\text{M-H}]^-$  **HRFAB-MS (3-NOBA matrix):**  $m/z$  1766.6040 (calcd. for  $\text{C}_{87}\text{H}_{89}\text{N}_{15}\text{O}_{25}\text{Na}$  1766.6052  $[\text{M}+\text{Na}]^+$ )



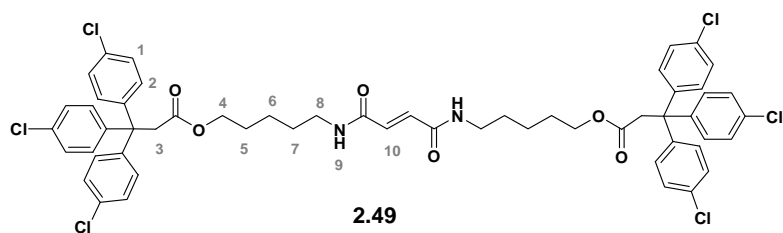
To a solution of **2.44** (27 mg, 13.40  $\mu\text{mol}$ ) in MeOH (4 mL) cooled in an ice-water bath was added dropwise at 0°C solution of MeONa (7 mg, 10.0 equiv.) in MeOH (2 mL). Stirring was continued for one hour at 0°C and the solution was neutralised with Amberlite IR-120 resin and filtered. MeOH was then evaporated and the resulting mixture was purified by preparative RP-HPLC using a linear gradient (37 to 55% in 20 min) of MeCN (containing 6.6 mM of HCOOH) in H<sub>2</sub>O (containing 6.6 mM of HCOOH) at a flow rate of 10 ml/min to give rotaxane **2.47** as a light yellow solid (17 mg, 9.40  $\mu\text{mol}$ , **70%**). Purity (HPLC): >94%.

**<sup>1</sup>H NMR (400 MHz, CD<sub>3</sub>OD):**  $\delta$  8.57 (s, 2H, H<sub>B</sub>), 8.36 (s, 4H, H<sub>A</sub>), 8.29 (s, 2H, H<sub>F</sub>), 7.16 to 6.89 (m, 20H, H<sub>7+8+22+23+24+E</sub>), 5.78 to 5.68 (m, 1H, H<sub>10</sub>), 4.95 to 4.90 (m, 2H, H<sub>11</sub>), 4.45 to 4.34 (m, 12H, H<sub>D+G</sub>), 4.21 (d, 1H,  $J = 8.0$  Hz, H<sub>1</sub>), 3.88 (t, 1H,  $J = 8.0$  Hz, H<sub>21</sub>), 3.69 to 3.28 (m, 52H, H<sub>2+3+4+5+6+9+12+14+16+18+20+H+I+J+K+L+M+N+O</sub>) **<sup>13</sup>C NMR (100 MHz, CD<sub>3</sub>OD):**  $\delta$  171.2, 167.5, 167.4, 158.1, 147.4, 143.6, 138.7 (x2), 137.4, 134.4, 130.0, 129.6, 129.0, 127.8, 127.7, 127.3, 123.5, 123.1, 123.0, 122.6, 117.4, 106.9, 77.1, 74.6, 73.6, 72.4, 71.6, 71.5, 71.4, 71.0, 69.7, 66.1, 65.0, 62.2, 61.8, 51.7, 45.2, 45.0, 43.1, 42.8, 34.3, 30.8 **m.p.** 102-104°C



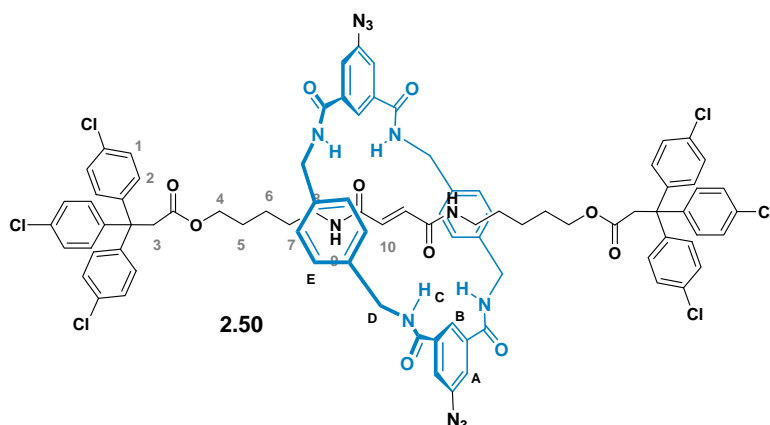
To a solution of **2.45** (24 mg, 9.00  $\mu\text{mol}$ ) in MeOH (4 mL) cooled in an ice-water bath was added dropwise at  $0^\circ\text{C}$  solution of MeONa (16 mg, 30.0 equiv.) in MeOH (3 mL). Stirring was continued for one hour at  $0^\circ\text{C}$  and the solution was neutralised with Amberlite IRC-50 resin and filtered. MeOH was then evaporated and the resulting mixture was purified by preparative RP-HPLC using a linear gradient (33 to 45 % in 15 min) of MeCN (containing 6.6 mM of HCOOH) in  $\text{H}_2\text{O}$  (containing 6.6 mM of HCOOH) at a flow rate of 10 ml/min to give rotaxane **2.48** as a pink solid (12 mg, 5.50  $\mu\text{mol}$ , **61%**). Purity (HPLC):  $>94\%$ .

**$^1\text{H}$  NMR (400 MHz,  $\text{CD}_3\text{OD}$ ):**  $\delta$  8.72 (s, 2H,  $\text{H}_\text{B}$ ), 8.54 to 8.51 (m, 4H,  $\text{H}_\text{A}$ ), 8.43 (s, 2H,  $\text{H}_\text{F}$ ), 7.35 to 6.99 (m, 20H,  $\text{H}_{7+8+22+23+24+\text{E}}$ ), 5.89 to 5.79 (m, 1H,  $\text{H}_{10}$ ), 5.05 to 4.79 (m, 6H,  $\text{H}_{11+\text{G}}$ ), 4.57 to 4.38 (m, 8H,  $\text{H}_\text{D}$ ), 4.32 (d, 1H,  $J = 7.7$  Hz,  $\text{H}_1$ ), 4.29 (d, 2H,  $J = 7.8$  Hz,  $\text{H}_\text{P}$ ), 4.03 to 3.99 (m, 3H,  $\text{H}_{21+\text{O}}$ ), 3.87 to 3.39 (m, 52 H,  $\text{H}_{2+3+4+5+6+9+12+14+16+18+20+\text{H}+\text{I}+\text{J}+\text{K}+\text{L}+\text{M}+\text{N}+\text{O}$ )  **$^{13}\text{C}$  NMR (100 MHz,  $\text{CD}_3\text{OD}$ ):**  $\delta$  168.7, 154.4, 142.0, 137.1, 136.6, 135.9, 128.4, 128.0, 127.4, 126.2, 126.1, 122.1, 121.7, 121.1, 101.9, 76.5, 76.4, 73.3, 70.0, 69.4 (x2), 69.3, 69.0, 68.9, 67.6, 63.2, 60.9, 60.1, 43.6, 43.4, 29.2 **LRFAB-MS (3-NOBA matrix):**  $m/z$  1085  $[\text{M}+2\text{H}]^{2+}$ , isotopic pattern matches that calculated for  $\text{C}_{103}\text{H}_{131}\text{N}_{15}\text{O}_{37}$  **m.p.** 129-131 $^\circ\text{C}$  (decomposition)



To a solution of 3,3,3-tris-(4-chloro-phenyl)-propionic acid (1.53 g, 2.0 equiv.), EDC.HCl (984 mg, 3.0 equiv.) and DMAP (625 mg, 3.0 equiv.) in CH<sub>2</sub>Cl<sub>2</sub> (30 mL) at room temperature, was added fumaramide (490 mg, 1.71 mmol). The reaction mixture was stirred overnight. CH<sub>2</sub>Cl<sub>2</sub> (250 mL) and an aqueous solution (1M) of HCl (50 mL) were added. The layers were separated and the aqueous layer was extracted with CH<sub>2</sub>Cl<sub>2</sub> (2×25 mL). The combined organic fractions were washed with an aqueous saturated solution of NaHCO<sub>3</sub>, dried (MgSO<sub>4</sub>) and concentrated under reduced pressure. Purification by flash column chromatography on silica using CH<sub>2</sub>Cl<sub>2</sub>/MeOH (98/2) as eluent gave **2.49** as a white solid (1.50 g, 1.41 mmol, **84%**).

**<sup>1</sup>H NMR (400 MHz, CDCl<sub>3</sub>/CD<sub>3</sub>OD: 9/1):**  $\delta$  8.01 (t, 2H,  $J = 5.6$  Hz, H<sub>9</sub>), 7.23 to 7.16 (m, 12H, H<sub>1</sub>), 7.12 to 7.04 (m, 12H, H<sub>2</sub>), 6.71 (s, 2H, H<sub>10</sub>), 3.75 (t, 4H,  $J = 6.5$  Hz, H<sub>4</sub>), 3.59 (s, 4H, H<sub>3</sub>), 3.23 to 3.17 (m, 4H, H<sub>8</sub>), 1.51-1.26 (m, 8H, H<sub>5+7</sub>), 1.19 to 1.05 (m, 4H, H<sub>6</sub>) **<sup>13</sup>C NMR (400 MHz, CDCl<sub>3</sub>/CD<sub>3</sub>OD: 9/1):**  $\delta$  170.4, 164.2, 144.2, 133.0, 132.6, 130.3, 128.2, 64.3, 54.6, 46.0, 39.6, 29.0, 28.0, 23.2 **LRFAB-MS:  $m/z$  1061 [M+H]<sup>+</sup> HRFAB-MS (glycerol matrix):  $m/z$  1061.2029 (calcd. for C<sub>56</sub><sup>13</sup>CH<sub>52</sub>D<sup>35</sup>Cl<sub>6</sub>N<sub>2</sub>O<sub>6</sub> 1061.2005 [M+H]<sup>+</sup>) m.p.** 132-136°C



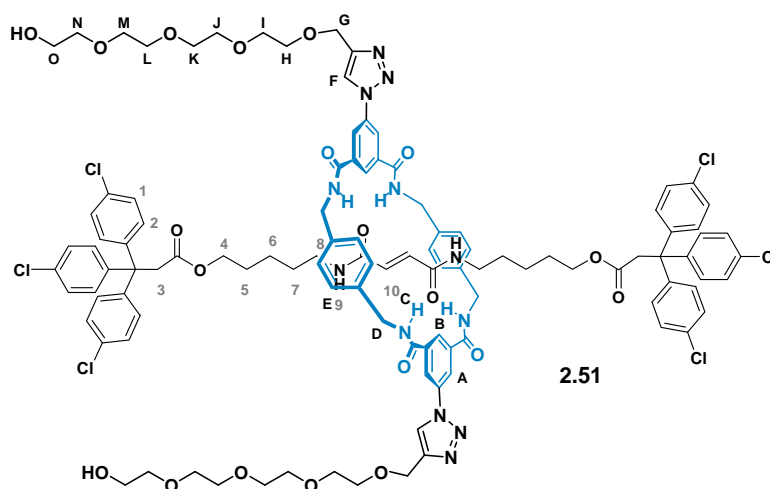
To a vigorously stirred solution of thread **2.49** (525 mg, 4.94 mmol) and Et<sub>3</sub>N (2 ml, 30.0 equiv.) in 1 L of dry CHCl<sub>3</sub> under nitrogen, was simultaneously added a solution of *para*-xylylene diamine (1.00 g, 15.0 equiv.) in CHCl<sub>3</sub> (50 mL) and a solution of isophthaloyl dichloride (1.81 g, 15.0 equiv.) in CHCl<sub>3</sub> (50 mL) over a period of 3 hours using motor-driven syringe pumps. The reaction mixture was stirred for another 2 hours, filtered over a Celite<sup>®</sup> pad and the filtrate was concentrated under reduced pressure. The resulting orange solid was purified by flash column chromatography on silica with acetone/CH<sub>2</sub>Cl<sub>2</sub> (10/90) as eluent to give rotaxane **2.50** (690 mg, 4.12 mmol, **83%**).

**<sup>1</sup>H NMR (400 MHz, CDCl<sub>3</sub>):**  $\delta$  8.03 (m, 2H, H<sub>C</sub>), 7.81-7.67 (m, 6H, H<sub>10+D</sub>), 7.66 (s, 4H, H<sub>B</sub>), 7.21-7.12 (m, 20H, H<sub>1+F</sub>), 7.09-7.01 (m, 12H, H<sub>2</sub>), 5.74 (s, 2H, H<sub>10</sub>), 4.45 (bs, 8H, H<sub>E</sub>), 3.72 (t, 4H,  $J = 6.5$  Hz, H<sub>4</sub>), 3.14 (m, 2H, H<sub>8</sub>), 1.45 (bquint, 4H,  $J = 7.2$  Hz, H<sub>5</sub>), 1.37 to 1.21 (m, 4H, H<sub>7</sub>), 1.17 to 1.05 (m, 4H, H<sub>6</sub>) **<sup>13</sup>C NMR (100 MHz, CDCl<sub>3</sub>):**  $\delta$  170.3, 165.9, 165.4, 143.8, 141.6, 136.6, 135.3, 132.3, 130.0, 129.5, 128.7, 127.9, 121.4, 120.8, 64.0, 54.4, 45.7, 43.8, 39.5, 28.4, 27.7, 23.0 **LRESI-MS:**  $m/z$  1697 [M+Na]<sup>+</sup> **HRESI-MS:**  $m/z$  1694.4408 (calcd. for C<sub>88</sub>H<sub>82</sub>C<sub>16</sub>N<sub>13</sub>O<sub>10</sub> 1694,4439 [M+NH<sub>4</sub>]<sup>+</sup>), isotopic pattern matches that calculated for C<sub>88</sub>H<sub>82</sub>Cl<sub>6</sub>N<sub>13</sub>O<sub>10</sub> **m.p.** 174-176°C (decomposition)

### General method to access functionalised macrocycle **2.53** and **2.54** (click)

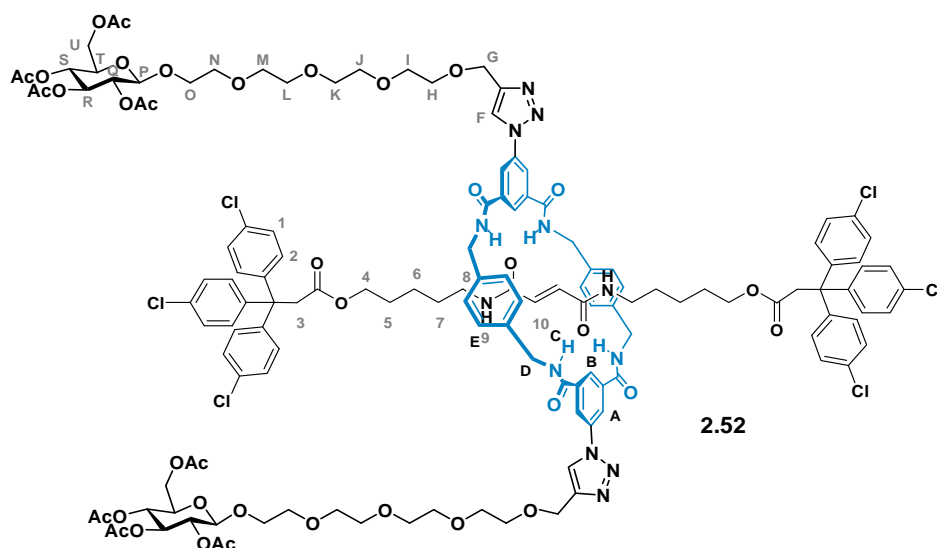
To a solution of rotaxane, alkyne (2.0 equiv.), and Cu(CH<sub>3</sub>CN)<sub>4</sub>PF<sub>6</sub> (0.5 equiv.) in dry CH<sub>2</sub>Cl<sub>2</sub> (5 mL) and under N<sub>2</sub> at room temperature was added Et<sub>3</sub>N (2.2 equiv.) and the mixture was stirred overnight. Air was bubbled through the mixture for 15 minutes then a saturated solution of NH<sub>4</sub>Cl was added (15 ml). The layers were separated and the aqueous layer was extracted with CH<sub>2</sub>Cl<sub>2</sub> (1 × 10 mL). The combined organic fractions were washed with a 1M

solution of EDTA/K<sub>2</sub>CO<sub>3</sub> (2 x 10 mL) and brine (10 mL), then dried (MgSO<sub>4</sub>) and concentrated under reduced pressure.



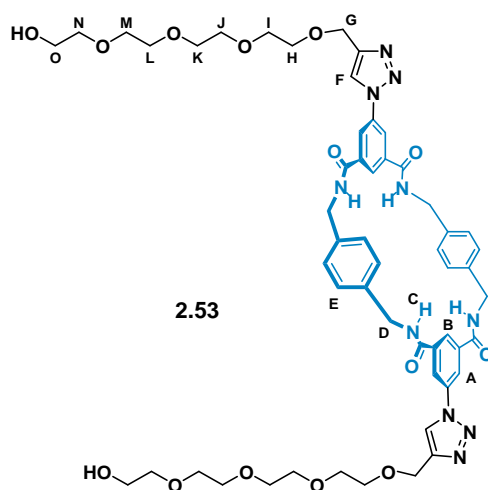
Using the general method, rotaxane **2.50** (97 mg, 0.060 mmol), alkyne **2.40** (27 mg, 2.0 equiv.), Cu(CH<sub>3</sub>CN)<sub>4</sub>(PF<sub>6</sub>) (11 mg, 0.5 equiv.) and Et<sub>3</sub>N (16 μL, 2.2 equiv.) in CH<sub>2</sub>Cl<sub>2</sub> (15 mL) at room temperature overnight gave **2.51** as a light yellow solid (115 mg, 0.054 mmol, **93%**).

**<sup>1</sup>H NMR (400 MHz, CDCl<sub>3</sub>):** δ 8.50 to 8.23 (m, 8H, H<sub>A</sub>, H<sub>B+F</sub>), 8.23 to 8.07 (m, 2H, H<sub>9</sub>), 7.95 to 7.74 (m, 4H, H<sub>C</sub>), 7.21 to 6.92 (m, 32H, H<sub>1</sub>, H<sub>2+E</sub>), 5.86 (s, 2H, H<sub>10</sub>), 4.80 (s, 4H, H<sub>G</sub>), 4.46 to 4.09 (m, 8H, H<sub>D</sub>), 3.84 to 3.43 (m, 40H, H<sub>3+4+H+I+J+K+L+M+N+O</sub>), 3.21 to 3.03 (m, 4H, H<sub>8</sub>), 1.53 to 1.19 (m, 8H, H<sub>5+7</sub>), 1.18 to 1.00 (m, 4H, H<sub>6</sub>) **<sup>13</sup>C NMR (100 MHz, CDCl<sub>3</sub>):** δ 170.2, 165.6, 165.0, 146.1, 144.0, 137.4, 136.6, 135.5, 132.4, 130.2, 129.1 (x 2), 129.0, 128.1, 124.5, 122.2, 121.8, 72.5, 70.5, 70.4, 70.3, 70.0, 69.9, 64.5, 64.1, 61.4, 54.5, 45.8, 44.1, 39.7, 29.6, 27.9, 23.2 **LRMALDI-MS:** *m/z* 2164 [M+Na]<sup>+</sup>, isotopic pattern matches that calculated for C<sub>110</sub>H<sub>118</sub>Cl<sub>6</sub>N<sub>12</sub>O<sub>20</sub>Na **m.p.** 100-102°C



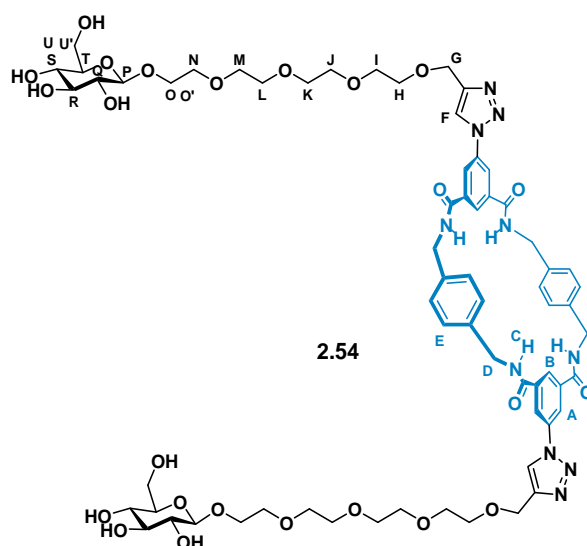
Using the general method, rotaxane **2.50** (250 mg, 0.150 mmol), alkyne **2.41** (168 mg, 2.0 equiv.),  $\text{Cu}(\text{CH}_3\text{CN})_4(\text{PF}_6)$  (28 mg, 0.5 equiv.) and  $\text{Et}_3\text{N}$  (455  $\mu\text{L}$ , 2.2 equiv.) in  $\text{CH}_2\text{Cl}_2$  (15 mL) at room temperature overnight gave **2.52** as a light yellow solid (296 mg, 0.105 mmol, **78%**).

**$^1\text{H}$  NMR (400 MHz,  $\text{CDCl}_3$ ):**  $\delta$  8.41 (s, 2H,  $\text{H}_\text{B}$ ), 8.36 (s, 4H,  $\text{H}_\text{A}$ ), 8.26 (s, 2H,  $\text{H}_\text{F}$ ), 7.98-7.77 (m, 4H,  $\text{H}_\text{C}$ ), 7.74-7.56 (m, 2H,  $\text{H}_\text{G}$ ), 7.22-7.12 (m, 12H,  $\text{H}_\text{I}$ ), 7.12-6.97 (m, 20H,  $\text{H}_\text{2}$  and  $\text{H}_\text{E}$ ), 5.75 (s, 2H,  $\text{H}_{10}$ ) 5.21 (t, 2H,  $J = 9.5$  Hz,  $\text{H}_\text{R}$ ), 5.08 (t, 2H,  $J = 9.6$  Hz,  $\text{H}_\text{S}$ ), 4.98 (t, 2H,  $J = 8.8$  Hz,  $\text{H}_\text{Q}$ ), 4.80 (s, 4H,  $\text{H}_\text{G}$ ), 4.60 (d, 2H,  $J = 7.9$  Hz,  $\text{H}_\text{P}$ ), 4.47-4.30 (m, 8H,  $\text{H}_\text{D}$ ), 4.25 (dd, 2H,  $J = 4.4$  Hz and  $J = 12.2$  Hz,  $\text{H}_\text{U}$ ), 4.13 (d, 2H,  $J = 11.5$  Hz,  $\text{H}_\text{U}$ ), 3.93 (dt, 2H,  $J = 4.3$  Hz and  $J = 11.1$  Hz,  $\text{H}_\text{H}$ ), 3.81-3.45 (m, 40H,  $\text{H}_\text{3}$ ,  $\text{H}_\text{4}$ ,  $\text{H}_\text{H}$ ,  $\text{H}_\text{I}$ ,  $\text{H}_\text{J}$ ,  $\text{H}_\text{K}$ ,  $\text{H}_\text{L}$ ,  $\text{H}_\text{M}$ ,  $\text{H}_\text{N}$  and  $\text{H}_\text{O}$ ), 3.20-2.97 (m, 4H,  $\text{H}_\text{8}$ ), 2.07, 2.04, 2.01, 1.99 (4s, 24H,  $\text{H-Ac}$ ), 1.51-1.17 (m, 8H,  $\text{H}_\text{5}$  and  $\text{H}_\text{7}$ ), 1.17-1.00 (m, 4H,  $\text{H}_\text{6}$ )  **$^{13}\text{C}$  NMR (100 MHz,  $\text{CDCl}_3$ ):**  $\delta$  170.7, 170.2, 169.4, 165.6, 165.5, 165.1, 144.0, 132.5, 130.2, 128.9, 128.1, 122.3, 100.8, 72.8, 71.7, 71.2, 70.6, 70.5, 70.5, 70.2, 70.0, 69.0, 68.3, 64.5, 64.1, 61.9, 55.4, 54.5, 45.9, 44.2, 44.2, 39.6, 29.6, 28.7, 27.8, 20.7, 20.6, 20.6, 20.5 **LRMALDI-MS:**  $m/z$  2824  $[\text{M}+\text{Na}]^+$ , isotopic pattern matches that calculated for  $\text{C}_{138}\text{H}_{154}\text{Cl}_{16}\text{N}_{12}\text{O}_{38}\text{Na}$  **m.p.** 96-98°C



Rotaxane **2.51** (40 mg, 0.018 mmol) was stirred for 4 days at room temperature in a 1M solution of NaOH in THF/H<sub>2</sub>O/EtOH (3/2/5) (10 mL). A 1M aqueous solution of HCl was added drop wise until pH equalled 7. The whole solution was loaded on a preparative silica TLC plate that was eluted with CH<sub>2</sub>Cl<sub>2</sub>/MeOH (15:85) to give macrocycle **2.53** as white waxy solid (18 mg, 0.016 mmol, **90%**).

**<sup>1</sup>H-NMR (400 MHz, CD<sub>3</sub>OD/CDCl<sub>3</sub> : 1/1):**  $\delta$  8.41 (2s, 4H, H<sub>A</sub>), 8.35 (bs, 2H, H<sub>B</sub>), 8.11 (t, 2H,  $J = 1.4$  Hz, H<sub>F</sub>), 7.28 (s, 8H, H<sub>E</sub>), 4.53 (s, 8H, H<sub>D</sub>), 4.70 (s, 2H, H<sub>G</sub>), 3.72-3.49 (m, 32H, H<sub>H+I+J+K+L+M+N+O</sub>) **<sup>13</sup>C-NMR (100 MHz, CD<sub>3</sub>OD/CDCl<sub>3</sub> : 1/1):**  $\delta$  166.4, 137.8, 137.7, 136.9, 128.9, 125.3, 122.7, 122.1, 72.8, 70.8, 70.7, 70.6, 70.5, 70.3, 70.1, 64.4, 61.4, 44.3 (x2) **LRESI-MS:  $m/z$  1101 [M+Na]<sup>+</sup> HRESI-MS:  $m/z$  1101.4651 (calcd. for C<sub>54</sub>H<sub>66</sub>N<sub>10</sub>O<sub>14</sub>Na 1101.4652 [M+Na]<sup>+</sup>)**



Rotaxane **2.52** (122 mg, 0.050 mmol) was stirred for 48 hours at room temperature in a 10M solution of NaOH in THF/H<sub>2</sub>O/EtOH (1/1/1) (10 mL). A 1M aqueous solution of HCl was added drop wise until pH equalled 7. Solvents were removed under vacuum. The resulting solid was re-dissolved in a 1/1 mixture of MeCN/H<sub>2</sub>O (10 mL), filtered by gravity and the filtrate used for purification by preparative RP-HPLC using a linear gradient of MeCN (25 to 40% in 20 min) in H<sub>2</sub>O to give macrocycle **2.54** as a white solid (18 mg, 0.012 mmol, **25%**).

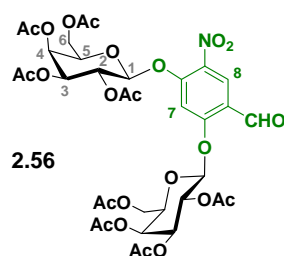
**<sup>1</sup>H-NMR (400 MHz, CD<sub>3</sub>OD/CDCl<sub>3</sub>: 1/1):**  $\delta$  8.41, 8.40 (2s, 6H, H<sub>A+B</sub>), 8.09 (s, 2H, H<sub>F</sub>), 7.23 (s, 8H, H<sub>E</sub>), 4.70 (s, 4H, H<sub>G</sub>), 4.55-4.42 (m, 8H, H<sub>D</sub>), 4.16 (d,  $J = 7.8$  Hz, 2H, H<sub>P</sub>), 3.95 to 3.83 (m, 2H, H<sub>O</sub>), 3.74 (dd, 2H,  $J = 2.7$  Hz,  $J = 12.1$  Hz, H<sub>U</sub>) 3.73-3.49 (m, 32H, H<sub>H+I+J+K+L+M+N+O'+U'</sub>) 3.26 to 3.00 (m, 8H, H<sub>Q+R+S+T</sub>) **<sup>13</sup>C-NMR (100 MHz, CD<sub>3</sub>OD/CDCl<sub>3</sub>: 1/1):**  $\delta$  166.5, 146.3, 137.8, 137.7, 136.8, 128.9, 125.4, 122.7, 122.2, 103.1, 76.6, 76.5, 73.8, 70.8 (x 2), 70.7, 70.6, 70.5, 70.4, 70.3, 70.0, 68.7, 64.4, 61.9, 44.3 **LRESI-MS:  $m/z$  1425 [M+H]<sup>+</sup> HRESI-MS:  $m/z$  1425.5709 (calcd. for C<sub>66</sub>H<sub>87</sub>N<sub>10</sub>O<sub>24</sub> 1425.5709 [M+H]<sup>+</sup>) mp. 205-207°C**

### V.3. *bis*-Galactosyl-based delivery system



2,4-Dihydroxybenzaldehyde (2.00 g, 14.49 mmol) was slowly added to a mixture of HNO<sub>3</sub>/AcOH (20 mL/8 mL). The solution was stirred overnight at room temperature and poured into water. Extraction with CH<sub>2</sub>Cl<sub>2</sub>, MgSO<sub>4</sub> drying and evaporation afforded a yellow powder which was co-evaporated with toluene several times to remove AcOH. Purification by column chromatography over silica gel (petroleum ether/ethyl acetate: 8/2 then 7/3) afforded **2.55** (1.3 g, 7.10 mmol, **48%**) as a yellow powder.

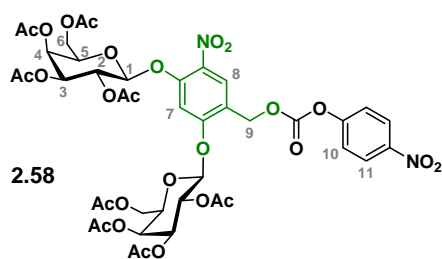
<sup>1</sup>H NMR (300 MHz, CDCl<sub>3</sub>): δ 11.64 (s, 1H, OH), 11.21 (s, 1H, OH), 9.83 (s, 1H, CHO), 8.49 (s, 1H, H<sub>2</sub>), 6.63 (s, 1H, H<sub>1</sub>) <sup>13</sup>C NMR (75 MHz, CDCl<sub>3</sub>): δ 194.0, 168.0, 161.4, 133.6, 125.9, 115.2, 106.1 LRESI-MS (negative mode): *m/z* 182 [M-H]<sup>-</sup> m.p. 144-146°C (litt. 146-147°C)



To a solution of α-D-galactopyranosyl bromide-2,3,4,6-tetraacetate (3.30 g, 2.1 equiv.) in CH<sub>3</sub>CN (30 mL) cooled in an ice-water bath was added **2.55** (730 mg, 3.99 mmol) and Ag<sub>2</sub>O (2.30 g, 2.5 equiv.). After overnight stirring at room temperature, the solution was filtered through silica, washed with ethyl acetate and concentrated under reduced pressure. Purification by column chromatography over silica gel (petroleum ether/ethyl acetate: 1/1 to 10/11) afforded **2.56** as a white powder (2.20 g, 2.61 mmol, **65%**).

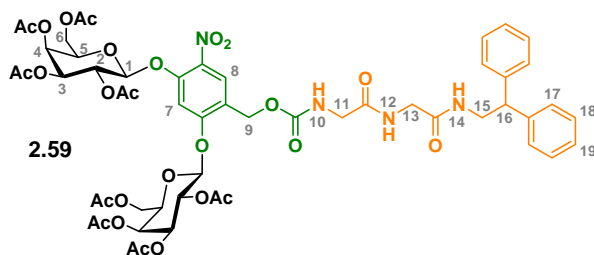
<sup>1</sup>H NMR (300 MHz, CDCl<sub>3</sub>): δ 10.22 (s, 1H, CHO), 8.43 (s, 1H, H<sub>8</sub>), 6.91 (s, 1H, H<sub>7</sub>), 5.44 (d, 1H, *J* = 7.9 Hz, H<sub>1</sub>), 5.65 to 5.28 (m, 6H, H<sub>2+3+4</sub>), 5.35 (d, 1H, *J* = 8.2 Hz, H<sub>1</sub>), 4.41 to 4.26





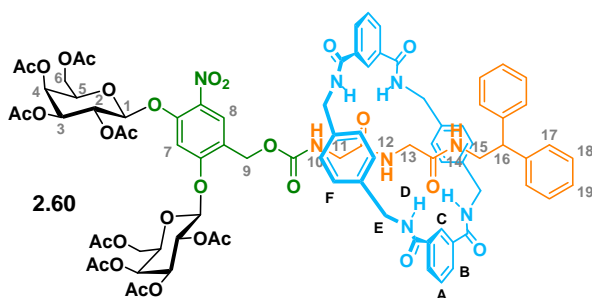
To a solution of **2.57** (700 mg, 0.83 mmol) in  $\text{CH}_2\text{Cl}_2$  (15 mL) was added *para*-nitrophenyl chloroformate (370 mg, 2.2 equiv.) and pyridine (170  $\mu\text{L}$ , 2.5 equiv.). After one day at room temperature, the solution was diluted with water and extracted with  $\text{CH}_2\text{Cl}_2$ . The combined organic layers were washed with water, dried over  $\text{MgSO}_4$  and concentrated *in vacuo*. Purification by column chromatography over silica gel (petroleum ether/ethyl acetate: 7/3-65/35 and 1/1) afforded **2.58** (803 mg, 0.80 mmol, **96%**) as a white powder.

**$^1\text{H}$  NMR (300 MHz,  $\text{CDCl}_3$ ):**  $\delta$  8.29 (d, 2H,  $J = 9.2$  Hz,  $\text{H}_{11}$ ), 8.07 (s, 1H,  $\text{H}_8$ ), 7.43 (d, 2H,  $J = 9.2$  Hz,  $\text{H}_{10}$ ), 6.94 (s, 1H,  $\text{H}_7$ ), 5.63 to 5.50 (m, 4H,  $\text{H}_{2+4}$ ), 5.36 to 5.14 (m, 6H,  $\text{H}_{1+3+9}$ ), 4.38 to 4.22 (m, 4H,  $\text{H}_{5+6b}$ ), 4.07 to 3.98 (m, 2H,  $\text{H}_{6a}$ ), 2.23 to 2.02 (m, 24H,  $\text{H-Ac}$ )  **$^{13}\text{C}$  NMR (75 MHz,  $\text{CDCl}_3$ ):**  $\delta$  171.1, 170.4, 170.3, 170.2, 170.1, 169.7, 169.5, 158.3, 155.5, 152.4, 151.8, 145.7, 135.0, 128.5, 125.5, 122.0, 118.8, 104.3, 99.5, 98.1, 71.1, 71.0, 70.5, 70.4, 68.0, 67.7, 67.0, 66.9, 64.6, 61.2, 61.1, 21.0 (x2), 20.8 (x3), 20.7 **LRESI-MS:**  $m/z$  1033, 1034, 1035  $[\text{M}+\text{Na}]^+$  **m.p.** 106-108°C



To a solution of **2.58** (780 mg, 0.77 mmol) in  $\text{CH}_3\text{CN}$  (40 mL) was added peptide **2.2** (286 mg, 1.2 equiv.) and  $\text{Et}_3\text{N}$  (0.3 mL, 2.5 equiv.). Stirring was continued at room temperature during a period of 19 hours then the solution was diluted with water and extracted with ethyl acetate. The combined extracts were washed with water, dried over  $\text{MgSO}_4$  and concentrated under reduced pressure. Purification by column chromatography over silica gel (petroleum ether/ethyl acetate: 4/6 to 2/8 then  $\text{CH}_2\text{Cl}_2/\text{MeOH}$ : 9/1) yielded **2.59** as a white powder (699 mg, 0.59 mmol, **77%**).

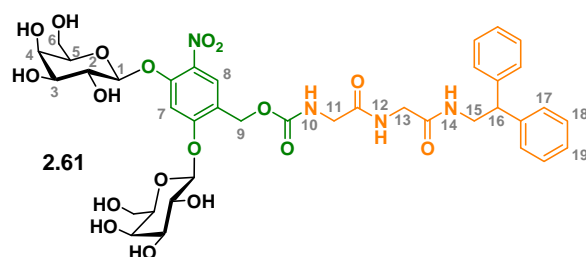
**$^1\text{H}$  NMR (400 MHz,  $\text{CDCl}_3$ ):**  $\delta$  7.89 (s, 1H,  $\text{H}_8$ ), 7.31 to 7.18 (m, 10H,  $\text{H}_{17+18+19}$ ), 7.07 (bt, 1H,  $J = 4.8$  Hz,  $\text{NH}_{14}$ ), 6.94 (s, 1H,  $\text{H}_7$ ), 6.32 (bt, 1H,  $J = 5.6$  Hz,  $\text{NH}_{12}$ ), 5.75 (bt, 1H,  $J = 5.2$  Hz,  $\text{NH}_{10}$ ), 5.57 (dd, 1H,  $J = 8.0$  Hz,  $J = 10.4$  Hz,  $\text{H}_2$ ), 5.51 to 5.49 (m, 3H,  $\text{H}_{2+4}$ ), 5.32 to 5.30 (m, 3H,  $\text{H}_{1+3}$ ), 5.23 (dd, 1H,  $J = 3.2$  Hz,  $J = 10.4$  Hz,  $\text{H}_3$ ), 5.19 (d, 1H,  $J = 8.0$  Hz,  $\text{H}_1$ ), 5.06 and 4.98 (d, AB system, 2H,  $J = 13.9$  Hz,  $\text{H}_9$ ), 4.37 to 4.26 (m, 3H,  $\text{H}_{5+6b}$ ), 4.20 to 4.16 (m, 2H,  $\text{H}_{5+16}$ ), 4.09 to 4.00 (m, 2H,  $\text{H}_{6a}$ ), 3.88 (t, 2H,  $J = 6.4$  Hz,  $\text{H}_{15}$ ), 3.81 to 3.78 (m, 4H,  $\text{H}_{11+13}$ ), 2.22 to 2.02 (m, 24H,  $\text{H-Ac}$ )  **$^{13}\text{C}$  NMR (100 MHz,  $\text{CDCl}_3$ ):**  $\delta$  170.9, 170.7, 170.2, 170.1, 170.0, 169.9, 169.7, 169.3 (x2), 168.6, 157.2, 156.1, 150.6, 141.7, 141.6, 135.0, 128.7, 127.9, 126.8, 126.3, 121.2, 104.9, 99.6, 98.0, 70.9, 70.4, 70.2, 68.1, 67.5, 66.8, 66.7, 61.0 (x2), 60.7, 50.3, 44.3, 43.7, 43.0, 20.8 (x2), 20.7 (x3), 20.6 **LRFAB-MS (3-NOBA matrix):**  $m/z$  1184  $[\text{M}+\text{H}]^+$ , 1206  $[\text{M}+\text{Na}]^+$  **HRFAB-MS (3-NOBA matrix):**  $m/z$  1183.3765 (calcd. for  $\text{C}_{54}\text{H}_{63}\text{N}_4\text{O}_{26}$  1183.3731  $[\text{M}+\text{H}]^+$ ) **m.p.** 128-130°C



Thread **2.59** (200 mg, 0.17 mmol) and triethylamine (0.9 mL, 35.0 equiv.) were dissolved in anhydrous chloroform (40 mL) and stirred vigorously whilst solutions of *p*-xylylene diamine (377 mg, 16.0 equiv.) in anhydrous chloroform (40 mL) and isophthaloyl dichloride (563 mg, 16.0 equiv.) in anhydrous chloroform (40 mL) were simultaneously added over a period of 3 hours using motor-driven syringe pumps. After overnight stirring, 1 mL of MeOH was added and the resulting suspension filtered through Celite<sup>®</sup>. The solid was washed with  $\text{CHCl}_3/\text{MeOH}$  2% (3 x 100 mL) and the combined filtrates were concentrated under reduced pressure. The residue was purified by column chromatography on silica gel using  $\text{CHCl}_3/\text{MeOH}$  (1 to 7% MeOH) as eluent to give a mixture of thread and rotaxane. This mixture was resolved by size exclusion chromatography using  $\text{CHCl}_3/\text{MeOH}$  (50/50: v/v) as eluent to give rotaxane **2.60** as a white powder (93 mg, 0.05 mmol, **31%**).

**$^1\text{H}$  NMR (400 MHz,  $\text{CDCl}_3$ ):**  $\delta$  8.15 (s, 2H,  $\text{H}_C$ ), 7.98 (t, 4H,  $J = 7.6$  Hz,  $\text{H}_B$ ), 7.64 (t, 2H,  $J = 4.4$  Hz,  $\text{H}_D$ ), 7.55 (bs, 3H,  $\text{H}_{8+D}$ ), 7.46 (t, 2H,  $J = 8.0$  Hz,  $\text{H}_A$ ), 7.32 (ls, 1H,  $\text{NH}_{14}$ ), 7.23 to

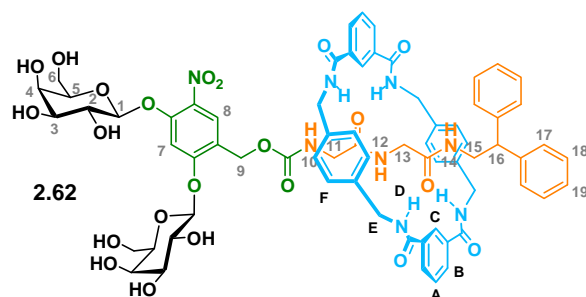
7.06 (m, 18H, H<sub>17+18+19+F</sub>), 6.91 (s, 1H, H<sub>7</sub>), 6.49 (bs, 1H, NH<sub>12</sub>), 5.64 (bs, 1H, NH<sub>10</sub>), 5.56 (dd, 1H, *J* = 8.0 Hz, *J* = 10.4 Hz, H<sub>2</sub>), 5.49 (d, 2H, *J* = 3.2 Hz, H<sub>4</sub>), 5.46 (dd, 1H, *J* = 8.0 Hz, *J* = 10.4 Hz, H<sub>2</sub>), 5.31 (dd, 1H, *J* = 3.6 Hz, *J* = 10.4 Hz, H<sub>3</sub>), 5.23 (dd, 1H, *J* = 10.4 Hz, *J* = 3.2 Hz, H<sub>3</sub>), 5.21 (t, 2H, *J* = 8.0 Hz, H<sub>1</sub>), 4.64 (bs, 2H, H<sub>9</sub>), 4.54 to 4.49 (m, 8H, H<sub>E</sub>), 4.45 to 4.27 (m, 3H, H<sub>5+6b</sub>), 4.19 (t, 1H, *J* = 6.4 Hz, H<sub>5</sub>), 4.10 to 4.00 (m, 3H, H<sub>6a+16</sub>), 3.71 (t, 2H, *J* = 6.0 Hz, H<sub>15</sub>), 3.34 (d, 2H, *J* = 5.2 Hz, H<sub>11</sub>), 2.80 (bdd, 2H, *J* = 22.4 Hz, *J* = 17.2 Hz, H<sub>13</sub>), 2.14 to 2.02 (m, 24H, *H*-Ac) <sup>13</sup>C NMR (100 MHz, CDCl<sub>3</sub>): δ 170.9, 170.8, 170.1 (x2), 170.0, 169.9, 169.5, 169.5, 169.4, 168.4, 166.9, 166.8, 157.2, 156.2, 156.1, 150.6, 141.4, 137.3, 137.2, 134.8, 134.0, 133.9, 131.0, 130.8, 128.9, 128.7, 127.8, 126.9, 126.3, 124.8, 120.8, 105.6, 99.5, 98.2, 77.2, 70.9, 70.3, 70.1, 68.1, 67.6, 66.8, 61.0, 60.4, 44.3, 44.1, 41.8, 29.6, 20.8 (x2), 20.7, 20.6, 20.5 LRESI-MS: *m/z* 1716 [M+H]<sup>+</sup> LRFAB-MS (3-NOBA matrix): *m/z* 1717 [M+H]<sup>+</sup> HRFAB-MS (3-NOBA matrix): *m/z* 1715.5789 (calcd. for C<sub>86</sub>H<sub>91</sub>N<sub>8</sub>O<sub>30</sub> 1715.5841 [M+H]<sup>+</sup>) m.p. 164-166°C



To a solution of **2.59** (250 mg, 0.21 mmol) in MeOH (40 mL) cooled in an ice-water bath was added dropwise at 0°C solution of MeONa (228 mg, 20.0 equiv.) in MeOH (12 mL). Stirring was continued for one hour at 0°C and the solution was neutralised with IRC-50 resin and filtered. MeOH was then evaporated and the resulting mixture was purified by column chromatography over silica gel (CH<sub>2</sub>Cl<sub>2</sub>/MeOH: 20 to 50% MeOH) to afford **2.61** (144 mg, 0.17 mmol, **81%**) as a yellow powder.

<sup>1</sup>H NMR (400 MHz, CDCl<sub>3</sub>): δ 7.98 (s, 1H, H<sub>8</sub>), 7.30 to 7.15 (m, 11H, H<sub>7+17+18+19</sub>), 5.18 (m, 2H, H<sub>9</sub>), 5.14 (d, 1H, *J* = 8.0 Hz, H<sub>1</sub>), 5.09 (d, 1H, *J* = 8.0 Hz, H<sub>1</sub>), 4.27 (t, 1H, *J* = 8.0 Hz, H<sub>16</sub>), 4.03 (dd, 2H, *J* = 4.0 Hz, *J* = 8.0 Hz, H<sub>5</sub>), 3.91 to 3.72 (m, 16H, H<sub>2+4+6+11+13+15</sub>) <sup>13</sup>C NMR (100 MHz, CD<sub>3</sub>OD): δ 172.8, 171.6, 170.4, 160.7, 153.7, 143.8, 134.7, 129.6, 129.2, 127.7, 127.6, 120.4, 104.7, 102.3, 102.1, 77.7, 74.9, 74.8, 71.9 (x2), 70.6, 63.1 (x2), 62.2, 51.7, 49.9, 45.1, 43.4 LRFAB-MS (3-NOBA matrix): *m/z* 847 [M+H]<sup>+</sup>, 869 [M+Na]<sup>+</sup>

**HRFAB-MS (3-NOBA matrix):**  $m/z$  869.2698 (calcd. for  $C_{38}H_{46}N_4O_{18}Na$  869.2699  $[M+Na]^+$ ) **m.p.** 135-137°C



To a solution of **2.60** (43 mg, 0.025 mmol) in MeOH (5 mL) cooled in an ice-water bath was added dropwise at 0°C solution of MeONa (27 mg, 20.0 equiv.) in MeOH (1.5 mL). Stirring was continued for one hour at 0°C and the solution was neutralised with IRC-50 resin and filtered. MeOH was then evaporated and the resulting mixture was purified by column chromatography over silica gel ( $CH_2Cl_2/MeOH$ : 10 to 50% MeOH) to afford **2.62** (30 mg, 0.022 mmol, **88%**) as a yellow powder.

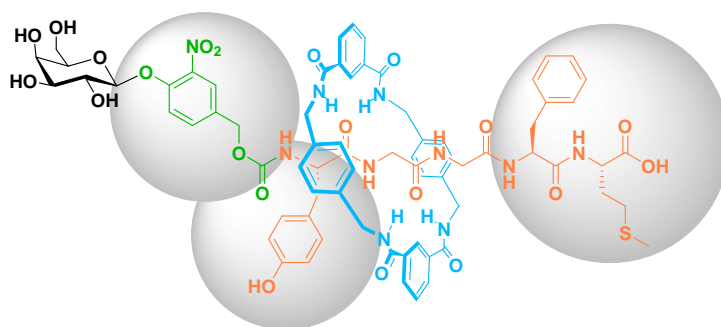
**$^1H$  NMR (400 MHz,  $CD_3OD$ ):**  $\delta$  8.27 (bs, 2H,  $H_C$ ), 8.01 (dd, 4H,  $J = 7.6$  Hz,  $J = 1.6$  Hz,  $H_B$ ), 7.62 to 7.58 (m, 3H,  $H_{8+A}$ ), 7.21 to 7.12 (m, 15H,  $H_{7+17+18+19+F}$ ), 6.99 to 6.97 (m, 4H,  $H_F$ ), 5.10 (d, 1H,  $J = 7.6$  Hz,  $H_I$ ), 4.98 (d, 1H,  $J = 8.0$  Hz,  $H_I$ ), 4.78 and 4.68 (d, AB system, 2H,  $J = 13.2$  Hz,  $H_9$ ), 4.33 (bs, 8H,  $H_E$ ), 4.06 to 3.80 (m, 11H,  $H_{2+4+5+6+15+16}$ ), 3.63 (dd, 1H,  $J = 9.6$  Hz,  $J = 3.2$  Hz,  $H_3$ ), 3.57 (dd, 1H,  $J = 9.6$  Hz,  $J = 3.2$  Hz,  $H_3$ ), 3.49 to 3.38 (m, 4H,  $H_{6+13}$ ), 2.78 and 2.65 (d, AB system, 2H,  $J = 16.4$  Hz,  $H_{11}$ )  **$^{13}C$  NMR (100 MHz,  $CD_3OD$ ):**  $\delta$  171.9, 170.3, 169.3, 160.4, 158.3, 153.6, 143.6, 138.6, 135.6, 135.5, 134.0, 131.8, 131.7, 130.1, 129.9, 129.8, 129.6, 129.0, 127.8, 127.7, 119.6, 104.3, 102.2, 102.1, 77.7, 77.6, 74.9, 74.8, 71.8, 71.7, 70.6, 70.5, 63.2, 63.1, 61.8, 49.9, 45.3, 45.2, 44.9, 44.8, 42.3 **LRESI-MS:**  $m/z$  1401.8, 1402.8, 1403.8  $[M+Na]^+$  **LRFAB-MS (3-NOBA matrix):**  $m/z$  1403  $[M+Na]^+$  **HRFAB-MS (3-NOBA matrix):**  $m/z$  1379.5001 (calcd. for  $C_{70}H_{75}N_8O_{22}$  1379.4996  $[M+H]^+$ ) **m.p.** decomposition

# **CHAPT. 3 | ROTAXANE-BASED DELIVERY SYSTEMS: PROTECTION AND ENZYMATIC RELEASE OF A BIOACTIVE PENTAPEPTIDE**

*Prepared as a paper for Angewandte Chemie*

The work presented in this chapter was done in collaboration with Aurélien Viterisi who carried out the HPLC purifications of the final prodrugs **1** and **7** and monitored their enzymatic hydrolysis and plasma stability.

In the light of the encouraging results obtained in the model studies presented in Chapter 2, we decided to apply our concept to a biologically active peptide, Met-enkephalin (H-Tyr-Gly-Gly-Phe-Met-OH). The anticancer potential of Met-enkephalin and the presence of the Gly-Gly motif in its primary structure prompted us to choose this opioid peptide. Moreover, the CPK models demonstrated on the one hand that the PheMet motif acts as a natural C-terminal stopper, on the other hand the consecutive HMR 1826 spacer and the first amino acid tyrosine also provide a natural stopper for the macrocycle (**Scheme 3.1**).



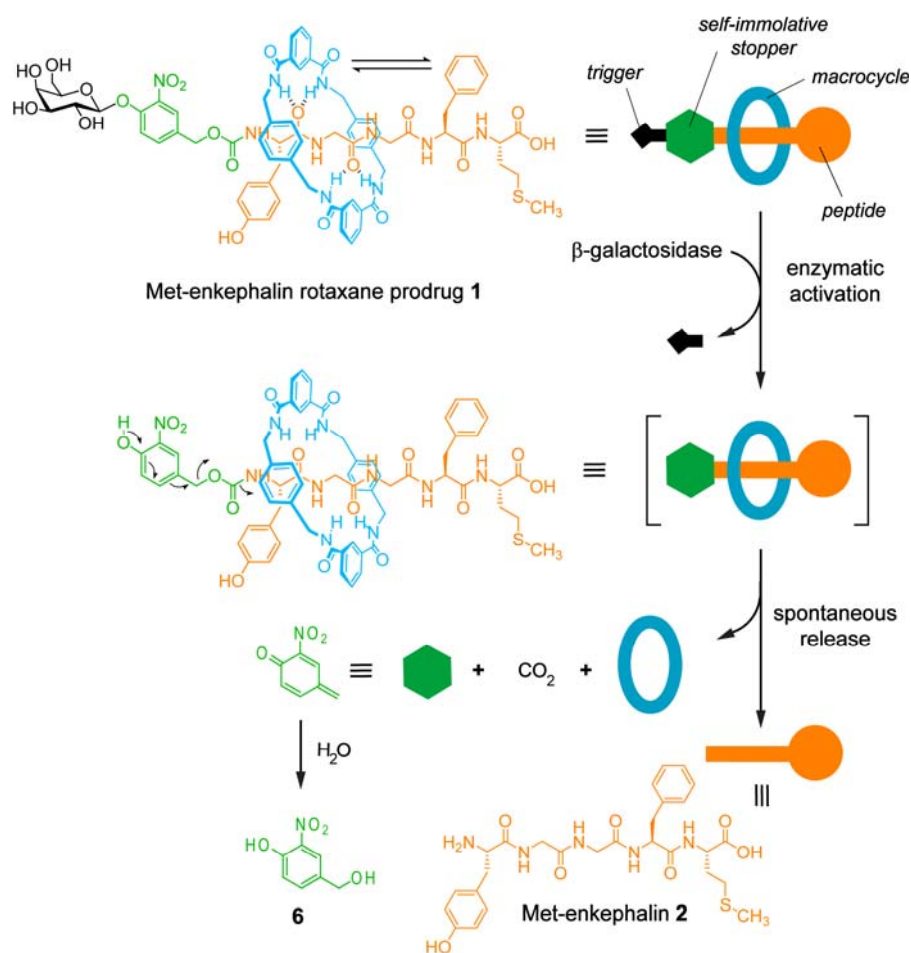
**Scheme 3.1** | The Met-enkephalin rotaxane prodrug

Accordingly, it is not necessary in this system to add a supplementary group to the self-immolative spacer (as we have tried to do in Chapter 2) to transform it into a stopper. As a result this system seems quite interesting since the spacer moiety is not modified and the macrocycle is held away from the trigger and the glycosidic bond. Additionally, the free C-terminus group also bodes well for good water solubility and persuaded us to use the easily synthesisable galactosyl derivative along with the classical non-functionalised amide-based macrocycle.

We designed the galactosylated Met-enkephalin rotaxane **1** associating the conventional enzyme-activated constructions with the hydrogen bond-directed assembly of peptide rotaxanes. Met-enkephalin **2** (H-Tyr-Gly-Gly-Phe-Met-OH), also termed the opioid growth factor (OGF), has unambiguously been identified as a potential antitumour peptide controlling cell growth activity.<sup>114</sup> The receptor-mediated antiproliferative effect of the opioid peptide was recently reported on human head and neck squamous cell carcinoma (HNSCC) and

<sup>114</sup> a) Fichna, J.; Janecka, A. *Cancer and Metastasis Rev.* **2004**, *23*, 351-366; b) Zagon, I. S.; Rahn, K. A.; McLaughlin, P. J. *Neuropeptides* **2007**, *41*, 441-452; c) Zagon, I. S.; McLaughlin, P. J. *Neuropeptides* **2005**, *39*, 495-5005; d) Zagon, I. S.; McLaughlin, P. J. *Neuropeptides* **2003**, *37*, 79-88.

pancreatic tumour xenografts in nude mice.<sup>115</sup> Consequently the attractive inhibitory system formed by OGF and its receptor (OGFr) has obviously gained attention in anticancer chemotherapy. Nevertheless the poor bioavailability of Met-enkephalin remains a serious restriction for further development.<sup>116</sup> Thus the three-part prodrug thread (comprising trigger, self-immolative linker and peptide) is trapped within a benzylic amide-based macrocycle (Scheme 3.2).



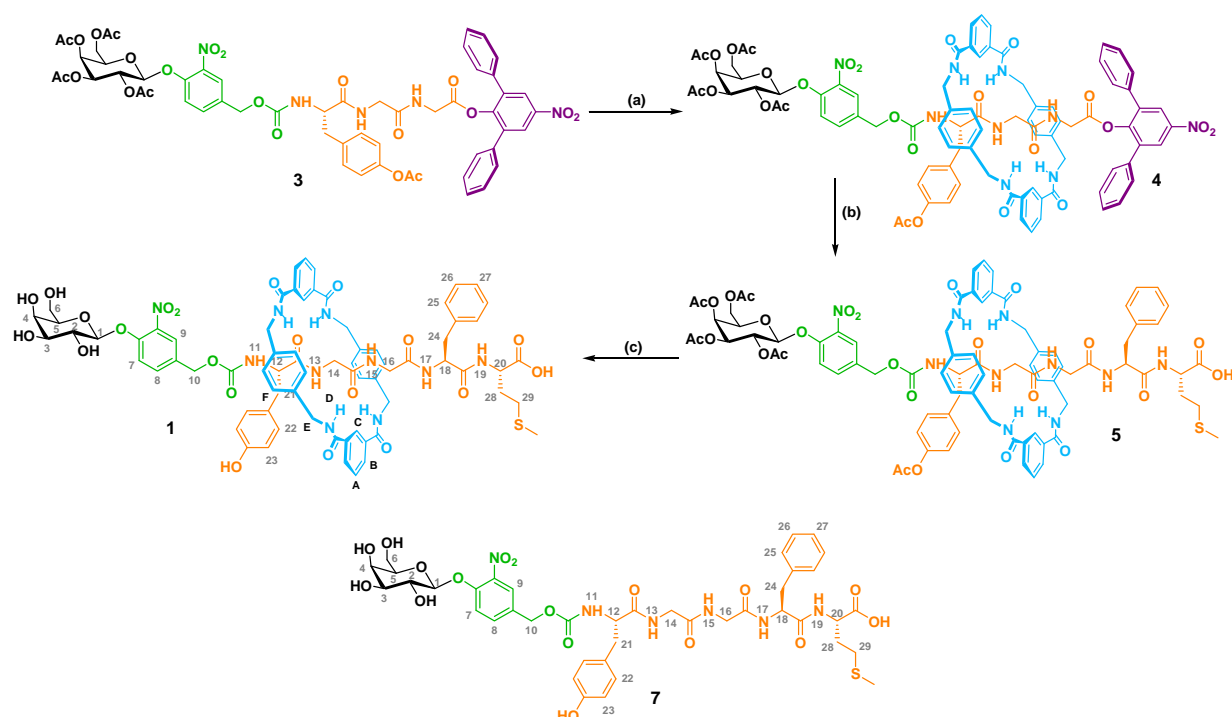
**Scheme 3.2.** Enzymatic release of Met-enkephalin by rotaxane prodrug 1.

<sup>115</sup> a) Cheng, F.; Zagon, I. S.; Verderame, M. F.; McLaughlin, P. J. *Cancer Res.* **2007**, *67*, 10511-10518; b) Zagon, I. S.; Smith, J. P.; McLaughlin, P. J. *Int. J. Oncol.* **1999**, *14*, 577-584; c) Zagon, I. S.; Hytrek, S. D.; Smith, J. P.; McLaughlin, P. J. *Cancer Lett.* **1997**, *112*, 167-175.

<sup>116</sup> Boarder, M. R.; McArdle, W. *Biochem. Pharmacol.* **1986**, *35*, 1043-1047.

The carbohydrate trigger designed to target cancer cells and hence to activate the prodrug molecule, is attached to the peptide drug through a benzyloxycarbonyl linker unit. Therefore following enzymatic activation, self-immolation of the sugar-free spacer results in the release of the parent Met-enkephalin **2** along with the mechanical disassembly of the rotaxane architecture.

Rotaxane **1** was prepared using the elongation strategy recently developed in our group which consists in a nucleophilic displacement of an activated ester stopper (**Scheme 3.3**).<sup>117</sup>

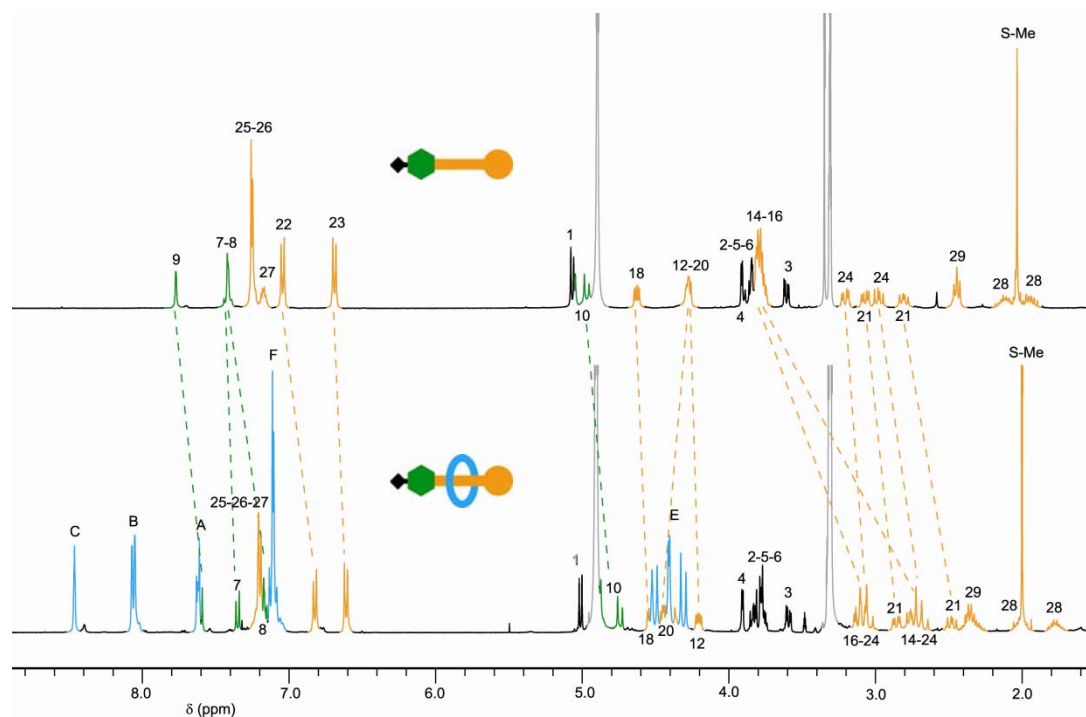


**Scheme 3.3.** Synthesis of rotaxane **1**. Reagents: a) isophthaloyl chloride, *p*-xylylenediamine,  $\text{CHCl}_3$ ,  $\text{Et}_3\text{N}$ ; b) H-Phe-Met-OH,  $\text{CHCl}_3$ , reflux; c)  $\text{MeONa}$ ,  $\text{MeOH}$ ,  $0^\circ\text{C}$ .

Thus glycorotaxane **4** was synthesised from galactosylated thread **3** bearing the temporary 2,6-diphenyl-4-nitrophenyl ester stopper. Treatment of **4** with H-Phe-Met-OH in  $\text{CHCl}_3$  afforded the elongated rotaxane **5** which was further deprotected to furnish final Met-enkephalin rotaxane prodrug **1**. The corresponding galactosylated prodrug of Met-enkephalin **7** was also prepared (*See Supporting Information*).

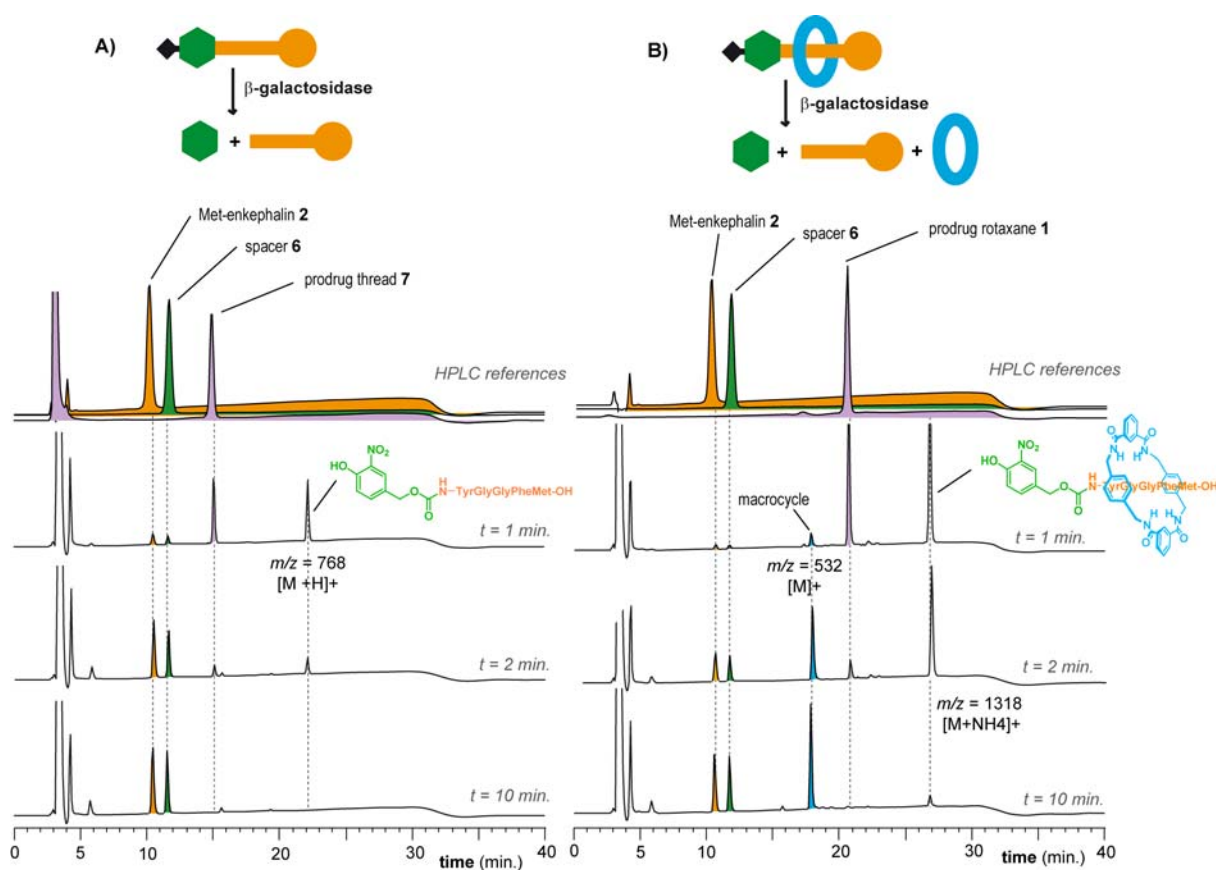
<sup>117</sup> Coutrot, F.; Leigh, D. A.; Potok, S.; Wong, J. K. Y. *to be submitted*

The  $^1\text{H}$  NMR spectra of **7** and **1** in  $\text{CD}_3\text{OD}$  are shown in **Figure 3.1**. Apart from the signals corresponding to the carbohydrate protons, most of the resonances in the thread are shifted in the rotaxane. Peptidic protons (shown in orange) along with spacer protons (shown in green) experience the shielding effect of the aromatic rings of the macrocycle. This effect is particularly observed for protons  $\text{H}_{14}$  and  $\text{H}_{16}$  thus indicating that the glycylic residues are directly located within the cavity of the macrocycle in the predominant structure of **4** in  $\text{CD}_3\text{OD}$ .



**Figure 3.1.**  $^1\text{H}$  NMR spectra of galactosylated prodrug **7** and rotaxane **1** (400 MHz, 298 K,  $\text{CD}_3\text{OD}$ ).

Accordingly we investigated the enzymatic activation of rotaxane **1** by HPLC since, contrary to the previous model rotaxane prodrugs, this rotaxane is soluble in water. Incubation of **1** with excess *E. coli*  $\beta$ -galactosidase in phosphate buffer (0.02 M, pH 7.2) at  $37^\circ\text{C}$  resulted in the simultaneous release of Met-enkephalin **2** together with a quinone methide intermediate which spontaneously reacts with water to form benzylic alcohol **6** (**Scheme 3.4**). A comparison with the non-interlocked galactosylated prodrug **7** was also conducted.

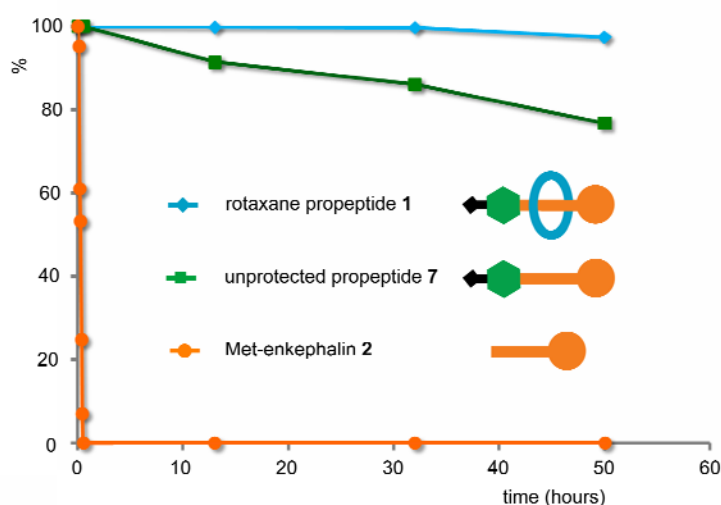


**Scheme 3.4.** Enzymatic hydrolysis of A) prodrug thread **7** and B) rotaxane **1** with *E. coli*  $\beta$ -galactosidase in phosphate buffer (0.02 M, pH 7.2) at 37°C using 10 U/ $\mu$ mol of substrate.

Therefore HPLC results obtained with non-interlocked prodrug **7** confirmed the release of Met-enkephalin **2** along with nitrophenol **6**. Concerning rotaxane **1**, HPLC also established the efficiency of our machine. Indeed, after treatment of the aliquots, chromatograms demonstrated the rapid delivery of the free peptide drug following the addition of *E. coli*  $\beta$ -galactosidase. After 10 minutes no starting rotaxane could be observed but the macrocycle along with free peptide and spacer **6**. It should also be noticed that for both prodrugs **1** and **7** the phenolic intermediates could be observed on LCMS.

In comparison with the models constructed in chapter 2, the fast kinetics of hydrolysis and release observed for these prodrug systems are explained by the absence of additional groups on the spacer moiety which hinder the recognition of the carbohydrate and the self-immolation step as discussed previously.

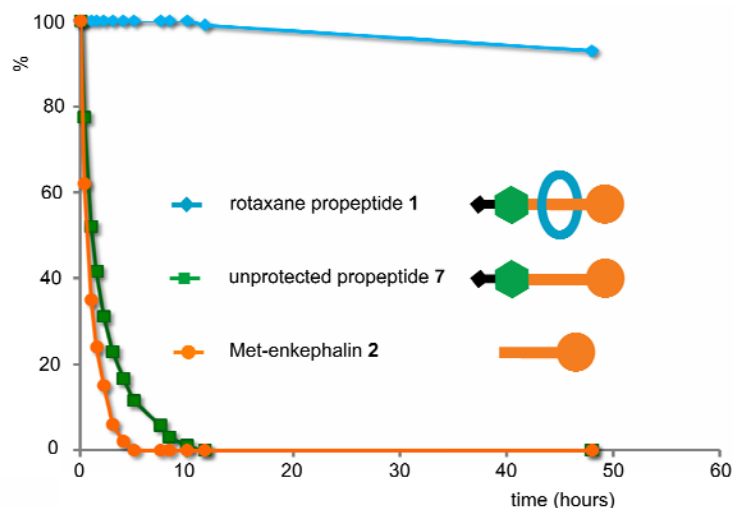
In the light of these results we first tried to ascertain the stability of Met-enkephalin rotaxane **1** in phosphate buffer at 37°C. After 48 hours no decomposition was observed by HPLC. Moreover, to assess the protease stability of our rotaxane prodrug we investigated and compared the behaviour of both Met-enkephalin **2**, rotaxane **1** and its non-interlocked derivative **7** under the action of peptidases. Initially, enzymatic digestion with Aminopeptidase M (which hydrolyses the *N*-terminal amide bond of Met-enkephalin) was conducted and monitored by HPLC (**Figure 3.2**).



**Figure 3.2.** Enzymatic digestion of rotaxane **1**, prodrug **7** and Met-enkephalin **2** with Aminopeptidase M. Reactions were carried out at 25°C in pH 7.2 phosphate buffer 0.05 M using 0.5 U/ $\mu$ mol of substrate. 0.25 U/ $\mu$ mol of enzyme was added every 12 hours.

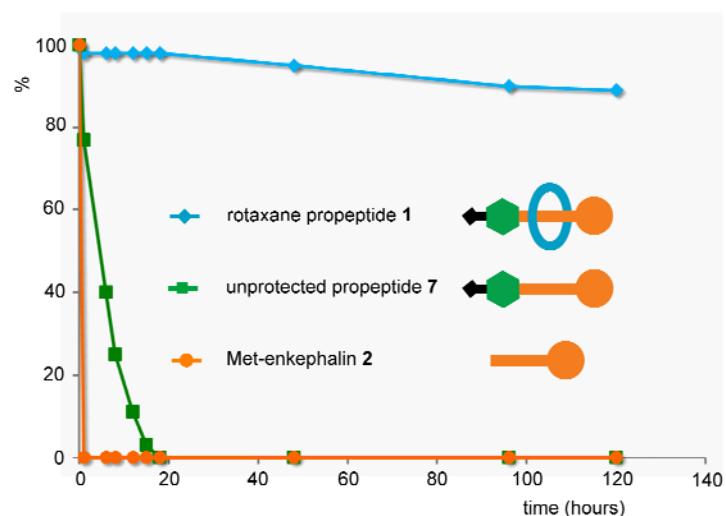
While Met-enkephalin is rapidly degraded (< 30 min.) prodrug **7** and rotaxane **1** displayed extremely enhanced stability. Accordingly such prolonged stability is easily explained by the fact that the *N*-terminus is masked in both interlocked and non-interlocked prodrugs.

Consequently we explored the enzymatic hydrolysis of **1**, **2** and **7** with Angiotensin Converting Enzyme (ACE) (**Figure 3.3**). ACE is a dipeptidyl exopeptidase which hydrolyses Met-enkephalin between Gly and Phe residues. HPLC monitoring allowed confirmation of the protective effect of encapsulating peptides within rotaxane architectures. Indeed, although **2** and **7** are readily hydrolysed within hours, rotaxane **1** exhibits almost total unreactivity towards the action of ACE.



**Figure 3.3.** Enzymatic digestion of rotaxane **1**, prodrug **7** and Met-enkephalin **2** with Angiotensin Converting Enzyme (ACE). Reactions were carried out at 25°C in pH 8.3 HEPES buffer 0.05 M, NaCl 0.3 M using 0.8 U/ $\mu\text{mol}$  of substrate. 0.4 U/ $\mu\text{mol}$  of enzyme was added every 12 hours.

Finally the stability of both compounds **1**, **2** and **7** was evaluated in human plasma (**Figure 3.4**). The results confirmed the poor bioavailability of Met-enkephalin **2** which is totally degraded in less than 5 min in human plasma. Under identical conditions prodrug thread **7** was degraded with a half-life of approximately 5 hours while only 10% degradation of the rotaxane **1** could be observed on HPLC after 120 hours incubation.



**Figure 3.4.** Stability of **1**, **2** and **7** in human plasma.

In conclusion, we have developed the first rotaxane-based delivery device designed to simultaneously protect and target bioactive peptides to tumour cells. In this study we have demonstrated that a rotaxane prodrug of the anticancerous peptide Met-enkephalin is efficiently and selectively activated by the action of  $\beta$ -galactosidase, an enzyme that can be targeted to cancer cells *via* an ADEPT protocol. Moreover the protective effect of the macrocycle was evidenced with two proteases which are largely responsible for the poor bioavailability of the OGF.<sup>118</sup> Thus until the trigger is selectively recognised at the tumour site, the peptide drug stays entirely protected within the cavity of the macrocycle. Therefore associating the hydrogen bond-directed assembly of peptide rotaxanes with the enzyme-responsive prodrugs has allowed the construction of versatile nanosystems to overcome the limited stability of peptides while selectively targeting their active release to malignant tissues. The concept presented here might find interesting development since the modularity of our construction allows the fine tuning of both trigger, spacer and macrocycle units.

---

<sup>118</sup> a) Marini, M.; Urbani, A.; Trani, E.; Bongiorno, L.; Roda, L. G. *Peptides* **1997**, *18*, 741-748; b) Marini, M.; Roscetti, G.; Bongiorno, L.; Urbani, A.; Roda, L. G. *Neurochem. Res.* **1990**, *15*, 61-67; c) Shibanoki, S.; Weinberger, S. B.; Ishikawa, K.; Martinez Jr, J. L. *Regul. Pept.* **1991**, *32*, 267-278; d) Shibanoki, S.; Weinberger, S. B.; Ishikawa, K.; Martinez Jr, J. L. *Prog. Clin. Biol. Res.* **1990**, *328*, 253-256.

## Supporting information

### Table of Contents

#### 1. General Experimental Section

#### 2. Synthetic Routes to Met-enkephalin Rotaxane Prodrug 1 and Prodrug 7

**Scheme 1** - Synthesis of H-Tyr(Ac)-Gly-Gly-OAll

**Scheme 2** - Synthesis of H-Phe-Met-OAll and H-Phe-Met-OH

**Scheme 3** - Synthesis of Met-enkephalin Rotaxane Prodrug

**Scheme 4** - Synthesis of Met-enkephalin Prodrug

#### 3. Experimental Procedures

#### 4. Representative Stacked $^1\text{H}$ NMR Plots

## 1. General Experimental Section

Unless otherwise stated, all reactions were run under an atmosphere of N<sub>2</sub>. Prior to use, isophthaloyl dichloride was purified by recrystallization from hexane; *p*-xylylenediamine was purified by distillation under reduced pressure. Met-enkephalin was purchased from Sigma-Aldrich. Dry acetonitrile, chloroform, dichloromethane, *N,N*-dimethylformamide, methanol, tetrahydrofuran and toluene were obtained by passing these solvents through activated alumina columns on a PureSolv™ solvent purification system (Innovative Technologies, Inc., MA). Unless otherwise stated, all other reagents were purchased from commercial sources and used without further purification. Flash column chromatography was carried out using Kiesegel C60 (Fisher Scientific) as the stationary phase. Analytical TLC was performed on aluminium-backed sheets pre-coated with silica 60 F254 adsorbent (0.25 mm thick, Merck, Germany) and visualized under UV light. Size exclusion chromatography was performed using Toyopearl HW-405 (Tosoh, Japan) with methanol/chloroform in a 1:1 v/v ratio as the eluent. <sup>1</sup>H and <sup>13</sup>C NMR spectra were recorded at 400 MHz on a Bruker AV 400 instrument. Chemical shifts (δ) are reported in parts per million from low to high field and referenced to residual solvent. Coupling constants (*J*) are reported in hertz (Hz). Standard abbreviations indicating multiplicity are used as follows: b = broad, s = singlet, d = doublet, t = triplet, q = quartet, quint. = quintet, m = multiplet. All melting points were determined using a Sanyo Gallenkamp apparatus and are uncorrected. FAB and ESI mass spectrometry was carried out by the mass spectrometry services at the University of Edinburgh and at the EPSRC National Centre, Swansea. Analytical RP-HPLC was carried out on a Gilson instrument composed of 306 pumps, 811C dynamic mixer (100 μL), 806 manometric module and an Applied Biosciences 759A UV detector with a Phenomenex C18 (2) Luna column (2 x 250 mm, 5 μm, 100A). Preparative RP-HPLC was carried out on a Gilson instrument composed of 306 pumps, 811C dynamic mixer (1.5 ml), 806 manometric module and a 118 UV detector with a Spherisorb ODS2 column (21.2 x 250 mm, 5 μm, 100A). LCMS was carried out on a Finnigan Mat system composed of an LCQ mass spectrometer, P4000 pumps, and a UV2000 UV detector with a Phenomenex C18 (2) Luna column (2 x 250 mm, 5μ, 100A). Chromatograms were recorded at 220 nm unless stated otherwise.

***E. coli*  $\beta$ -galactosidase enzymatic cleavage**

Enzymatic hydrolysis was carried out with commercial  $\beta$ -galactosidase from *Escherichia coli* E.C. 3.2.1.23 (1000 units/mg protein (biuret), aqueous glycerol suspension (1:1), 10 mM Tris buffer salts and 10 mM magnesium chloride, pH 7.3). Prodrugs were incubated at 37°C with the enzyme (1-100 Units/0.1  $\mu$ mol of substrate) in 20 mM Phosphate buffer at pH 7.0 containing 2.5-10% DMSO (0.2-0.33  $\mu$ mol of substrate/ml). Aliquots (20  $\mu$ L) were periodically withdrawn from the medium and diluted into a solution of TFA (0.1%) in H<sub>2</sub>O (40  $\mu$ L). Rate of hydrolysis was monitored by analytical HPLC and LCMS.

**Enzymatic stability toward Aminopeptidase M**

Peptidase degradation was carried out with commercial microsomal Leucine Aminopeptidase (Aminopeptidase M), from porcine kidney, type IV-S, E.C. 3.4.11.2 (24 units/mg protein (Bradford), suspension in 3.5 M (NH<sub>4</sub>)<sub>2</sub>SO<sub>4</sub> solution, pH 7.7, containing 10 mM MgCl<sub>2</sub>). Peptide and prodrugs were incubated at 25°C (to minimize loss of activity) with the enzyme (5.10<sup>-4</sup> Units/0.1  $\mu$ mol of substrate) in 50 mM Phosphate buffer at pH 7.2 containing 5% DMSO (C 0.25  $\mu$ mol of substrate/ml). Enzyme was added to the medium every 12 hours to compensate for loss of activity (2.5.10<sup>-4</sup> Units). Aliquots (5  $\mu$ L) were periodically withdrawn from the medium and directly used for analytical HPLC monitoring. Rate of decomposition was measured by plotting the absolute area of the peak of interest against time.

**Enzymatic stability toward Angiotensin Converting Enzyme**

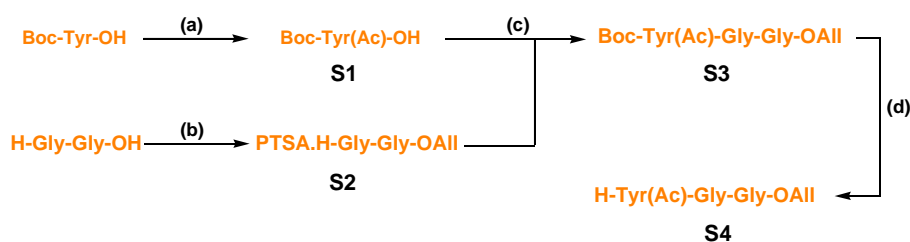
Peptidase degradation was carried out with commercial Angiotensin Converting Enzyme from rabbit lung (3.92 units/mg protein (modified Warburg-Christian), lyophilized powder). The enzyme was kept in a solution of in 10 mM potassium phosphate buffer, pH 7.0, containing 0.5 M NaCl (1 mg of enzyme/mL) and stored at -20°C. Peptide and prodrugs were incubated at 25°C (to minimize loss of activity) with the enzyme (0.02 Units/0.025  $\mu$ mol of substrate) in 50 mM HEPES buffer at pH 8.3 containing 0.3 M NaCl and 5% DMSO (C 0.125  $\mu$ mol of substrate/ml). Enzyme was added to the medium every 12 hours to compensate for loss of activity (0.01 Units). Aliquots (5  $\mu$ L) were periodically withdrawn from the medium and directly used for analytical HPLC monitoring. The rate of decomposition was measured by plotting the absolute area of the peak of interest against time.

### Stability in human plasma

Stability in human plasma was carried out with commercial lyophilized human plasma reconstituted by dissolving the solid in the appropriate volume of 0.01M Tris buffer at pH 7.4. Peptide and prodrugs were incubated at 37°C in the freshly prepared solution (0.150  $\mu\text{mol}$  of substrate/ml). Aliquots (50  $\mu\text{L}$ ) were periodically withdrawn from the medium, poured into cold MeOH (50  $\mu\text{L}$ ) to precipitate the proteins and cooled on ice. After 30 min., the sample was centrifuged (17 000 g, 2 min) and the supernatant analyzed by analytical HPLC. The rate of decomposition was measured by plotting the absolute area of the peak of interest against time.

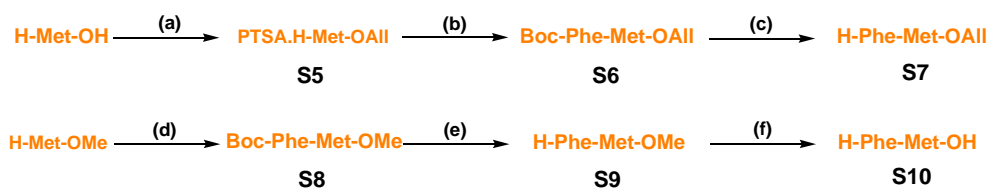
## 2. Synthetic Routes to Met-enkephalin Rotaxane Prodrug 1 and Prodrug 7

### Scheme 1 - Synthesis of H-Tyr(Ac)-Gly-Gly-OAll

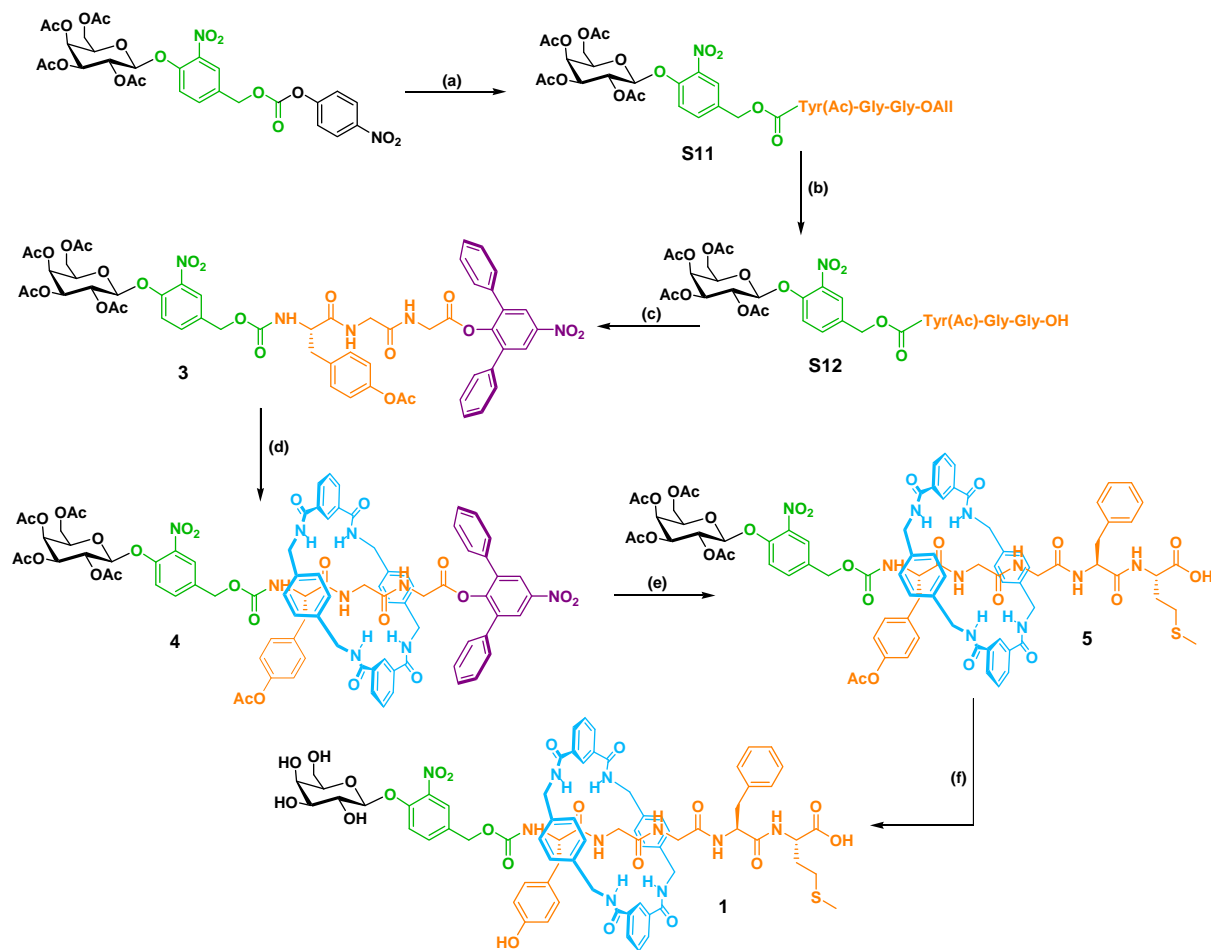


(a)  $\text{Ac}_2\text{O}$ , NaOH,  $\text{H}_2\text{O}$ , 91% (b) All-OH, PTSA, toluene, reflux, quant. (c) EDC.HCl, HOBT, DIPEA,  $\text{CH}_2\text{Cl}_2$ , 45% (d) TFA,  $\text{CH}_2\text{Cl}_2$ , 92%.

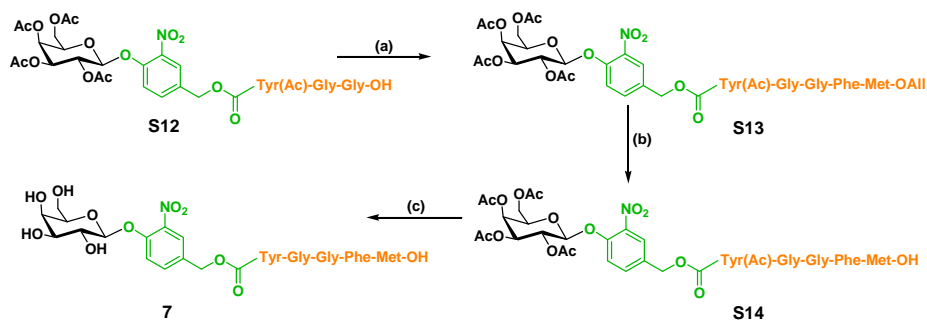
### Scheme 2 - Synthesis of H-Phe-Met-OAll and H-Phe-Met-OH



(a) All-OH, PTSA, toluene, reflux, 82% (b) Boc-Phe-OH, EDC.HCl, HOBT, DIPEA,  $\text{CH}_2\text{Cl}_2$ , 43% (c) TFA,  $\text{CH}_2\text{Cl}_2$ , 92% (d) Boc-Phe-OH, EDC.HCl, HOBT, DIPEA,  $\text{CH}_2\text{Cl}_2$ , 42% (e) TFA,  $\text{CH}_2\text{Cl}_2$ , 97% (f) NaOH,  $\text{H}_2\text{O}$ , THF, 0°C, 93%.

**Scheme 3 - Synthesis of Met-enkephalin Rotaxane Prodrug 1**


(a) H-Tyr(Ac)-Gly-Gly-OAll, pyridine, DMF, 97% (b) Pd(PPh<sub>3</sub>)<sub>4</sub>, PhSiH<sub>3</sub>, CH<sub>2</sub>Cl<sub>2</sub>, 85% (c) 2,6-diphenyl-4-nitrophenol, BOP, Et<sub>3</sub>N, CHCl<sub>3</sub>, 67% (d) *p*-xylylenediamine, isophthaloyl dichloride, Et<sub>3</sub>N, CHCl<sub>3</sub>, 26% (e) H-Phe-Met-OH, CHCl<sub>3</sub>, reflux, 40% (f) MeONa, MeOH, 0°C, quant.

**Scheme 4 - Synthesis of Met-enkephalin Prodrug 7**


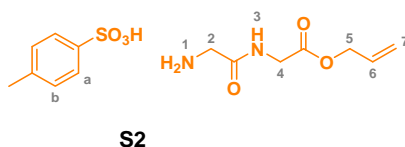
(a) H-Phe-Met-OAll, EDC.HCl, DIPEA, CH<sub>2</sub>Cl<sub>2</sub>, 37% (b) Pd(PPh<sub>3</sub>)<sub>4</sub>, PhSiH<sub>3</sub>, CH<sub>2</sub>Cl<sub>2</sub>, 67% (c) MeONa, MeOH, 0°C, 87%.

### 3. Experimental Procedures



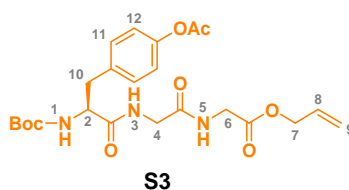
Compound **S1** was prepared according to the procedure described in Braun, N. A.; Ousmer, M.; Bray, J. D.; Bouchu, D.; Peters, K.; Peters, E-M; Ciufolini, M. A. *J. Org. Chem.* **2000**, *65*, 4397-4408. Boc-L-Tyrosine (7.00 g, 24.91 mmol) was dissolved in a 15% aqueous NaOH solution (25 mL) and a few chips of ice were added. Acetic anhydride (8.8 mL, 3.75 equiv.) was added and the solution stirred for 25 minutes. The mixture was then cooled to 0°C, acidified with 3N HCl and extracted with ethyl acetate. The combined organic layers were dried over MgSO<sub>4</sub>, filtered and concentrated *in vacuo*. The resulting oil was co-evaporated several times with toluene to obtain **S1** as clear yellow oil (7.35 g, 22.75 mmol, **91%**). (**S1** Registry Number: 80971-82-0)

**<sup>1</sup>H NMR (400 MHz, DMSO-*d*<sub>6</sub>):**  $\delta$  7.28 (d, 2H,  $J = 8.0$  Hz, H<sub>4</sub>), 7.10 (d, 1H,  $J = 8.4$  Hz, NH), 7.02 (d, 2H,  $J = 8.0$  Hz, H<sub>5</sub>), 4.17 to 4.11 (m, 1H, H<sub>2</sub>), 3.05 (dd, 1H,  $J = 14.0$  Hz,  $J = 4.0$  Hz, H<sub>3</sub>), 2.86 (dd, 1H,  $J = 13.2$  Hz,  $J = 11.2$  Hz, H<sub>3</sub>), 2.23 (s, 3H, *H*-Ac), 1.33 (s, 9H, *H*-*t*Bu) **<sup>13</sup>C NMR (100 MHz, DMSO-*d*<sub>6</sub>):**  $\delta$  173.7, 169.3, 155.6, 149.2, 135.6, 130.2, 121.5, 78.2, 59.9, 55.2, 35.9, 28.2, 20.9 **LRFAB-MS (3-NOBA matrix):**  $m/z$  346 [M+Na]<sup>+</sup> **HRFAB-MS (3-NOBA matrix):**  $m/z$  346.1260 (calcd. for C<sub>16</sub>H<sub>21</sub>NO<sub>6</sub>Na 346.1261 [M+H]<sup>+</sup>)



To a solution of glycylglycine (7.00 g, 53.03 mmol) in toluene (20 mL) was added allyl alcohol (21.7 mL, 6.0 equiv.) and PTSA (11.00 g, 1.2 equiv.). The mixture was refluxed in a Dean-Stark apparatus until no water was recovered and the solvent was removed under reduced pressure. The residue was crystallized from diethylether to give **S2** as a yellowish solid (18.10 g, 52.62 mmol, **quant.**).

**<sup>1</sup>H NMR (400 MHz, CDCl<sub>3</sub>):**  $\delta$  8.15 (t, 1H,  $J = 5.6$  Hz, NH<sub>3</sub>), 7.63 (m, 3H, <sup>+</sup>NH<sub>3</sub>), 7.61 (d, 2H,  $J = 8.0$  Hz, H<sub>a</sub>), 6.95 (d, 2H,  $J = 8.0$  Hz, H<sub>b</sub>), 5.80 to 5.71 (m, 1H, H<sub>6</sub>), 5.20 (dd, 1H,  $J = 17.2$  Hz,  $J = 1.6$  Hz, H<sub>7</sub>), 5.14 (dd, 1H,  $J = 10.4$  Hz,  $J = 1.2$  Hz, H<sub>7</sub>), 4.43 (d, 2H,  $J = 5.6$  Hz, H<sub>5</sub>), 3.94 (bd, 2H,  $J = 4.8$  Hz, H<sub>2</sub>), 3.74 (d, 2H,  $J = 5.2$  Hz, H<sub>4</sub>), 2.25 (s, 3H, CH<sub>3</sub>) **<sup>13</sup>C NMR (100 MHz, CDCl<sub>3</sub>):**  $\delta$  169.7, 167.3, 141.2, 140.4, 131.8, 129.1, 126.1, 118.7, 66.0, 41.4, 41.2, 21.4 **LRFAB-MS (3-NOBA matrix):**  $m/z$  345 [M+H]<sup>+</sup> **HRFAB-MS (3-NOBA matrix):**  $m/z$  173.0920 (calcd. for C<sub>7</sub>H<sub>13</sub>N<sub>2</sub>O<sub>3</sub> 173.0921 [M-PTSA+H]<sup>+</sup>) **m.p.** 78-80°C



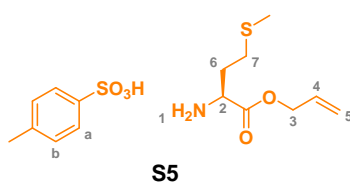
To a solution of Boc-Tyr(Ac)-OH **S1** (1.00 g, 3.10 mmol) and glycylglycine salt **S2** (1.28 g, 1.2 equiv.) in CH<sub>2</sub>Cl<sub>2</sub> (10 mL) was added EDC.HCl (713 mg, 1.2 equiv.), HOBT (167 mg, 0.4 equiv.) and DIPEA (1.35 mL, 2.5 equiv.). The mixture was stirred for 64 hours at room temperature, hydrolyzed and extracted with CH<sub>2</sub>Cl<sub>2</sub>. The combined organic layers were washed with water, brine, dried and concentrated *in vacuo*. Purification by column chromatography over silica gel (petroleum ether/ethyl acetate: 6/4 then CH<sub>2</sub>Cl<sub>2</sub>/MeOH: 2.5 to 5% MeOH) afforded **S3** (665 mg, 1.39 mmol, **45%**) as a white solid.

**<sup>1</sup>H NMR (400 MHz, CDCl<sub>3</sub>):**  $\delta$  7.46 (bs, 1H, NH), 7.32 (bs, 1H, NH), 7.17 (d, 2H,  $J = 8.0$  Hz, H<sub>11</sub>), 6.95 (d, 2H,  $J = 8.0$  Hz, H<sub>12</sub>), 5.89 to 5.79 (m, 1H, H<sub>8</sub>), 5.57 (d, 1H,  $J = 6.8$  Hz, NH<sub>1</sub>), 5.27 (d, 1H,  $J = 18.4$  Hz, H<sub>9</sub>), 5.19 (d, 1H,  $J = 10.4$  Hz, H<sub>9</sub>), 4.52 (d, 2H,  $J = 6.0$  Hz, H<sub>7</sub>), 4.37 (bd, 1H,  $J = 6.4$  Hz, H<sub>2</sub>), 3.84 to 4.03 (m, 4H, H<sub>4+6</sub>), 3.09 (dd, 1H,  $J = 13.6$  Hz,  $J = 5.6$  Hz, H<sub>10</sub>), 2.91 (dd, 1H,  $J = 13.6$  Hz,  $J = 8.0$  Hz, H<sub>10</sub>), 2.23 (s, 3H, H-Ac), 1.32 (s, 9H, H-*t*Bu) **<sup>13</sup>C NMR (100 MHz, CDCl<sub>3</sub>):**  $\delta$  172.4, 169.6, 169.5, 155.9, 149.5, 134.3, 131.5, 130.3, 121.6, 118.8, 80.2, 65.9, 55.9, 42.8, 41.1, 37.4, 28.2, 21.1 **LRFAB-MS (3-NOBA matrix):**  $m/z$  479 [M+H]<sup>+</sup> **HRFAB-MS (3-NOBA matrix):**  $m/z$  478.2180 (calcd. for C<sub>23</sub>H<sub>32</sub>N<sub>3</sub>O<sub>8</sub> 478.2184 [M+H]<sup>+</sup>) **m.p.** 112-114°C



Trifluoroacetic acid (27 mL, 45.0 equiv.) was added dropwise to a solution of Boc-Tyr(Ac)-Gly-Gly-OAll **S3** (3.80 g, 7.97 mmol) in CH<sub>2</sub>Cl<sub>2</sub> (200 mL) at 0°C. After 30 minutes at 0°C, the solution was stirred a further 2 hours at room temperature and then cooled to 0°C. After neutralisation with a saturated solution of NaHCO<sub>3</sub>, the mixture was extracted with a CHCl<sub>3</sub>/*i*PrOH (3/1, v/v) mixture, dried and evaporated to give **S4** (2.77 g, 7.35 mmol, **92%**) as a white solid.

**<sup>1</sup>H NMR (400 MHz, CDCl<sub>3</sub>):**  $\delta$  7.99 (t, 1H,  $J = 5.2$  Hz, NH), 7.20 (d, 2H,  $J = 8.4$  Hz, H<sub>11</sub>), 7.07 (t, 1H,  $J = 5.6$  Hz, NH), 7.00 (d, 2H,  $J = 8.4$  Hz, H<sub>12</sub>), 5.92 to 5.82 (m, 1H, H<sub>8</sub>), 5.30 (dd, 1H,  $J = 17.2$  Hz,  $J = 1.6$  Hz, H<sub>9</sub>), 5.23 (dd, 1H,  $J = 10.4$  Hz,  $J = 1.2$  Hz, H<sub>9</sub>), 4.60 (d, 2H,  $J = 5.6$  Hz, H<sub>7</sub>), 3.99 (dd, 4H,  $J = 16.8$  Hz,  $J = 5.6$  Hz, H<sub>4+6</sub>), 3.61 (dd, 1H,  $J = 9.2$  Hz,  $J = 4.0$  Hz, H<sub>2</sub>), 3.20 (dd, 1H,  $J = 14.0$  Hz,  $J = 4.0$  Hz, H<sub>10</sub>), 2.69 (dd, 1H,  $J = 13.6$  Hz,  $J = 9.2$  Hz, H<sub>10</sub>), 2.26 (s, 3H, *H*-Ac), 1.64 (bs, 2H, NH<sub>2</sub>) **<sup>13</sup>C NMR (100 MHz, CDCl<sub>3</sub>):**  $\delta$  175.3, 169.7, 169.5, 149.6, 135.4, 131.5, 130.3, 121.9, 119.0, 66.1, 56.4, 42.9, 41.3, 40.4, 21.2 **LRFAB-MS (3-NOBA matrix):**  $m/z$  378 [M+H]<sup>+</sup> **HRFAB-MS (3-NOBA matrix):**  $m/z$  378.1664 (calcd. for C<sub>18</sub>H<sub>24</sub>N<sub>3</sub>O<sub>6</sub> 378.1660 [M+H]<sup>+</sup>) **m.p.** 116-118°C



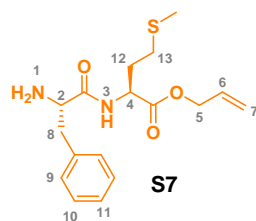
To a solution of L-methionine (7.00 g, 46.98 mmol) in toluene (20 mL) was added allyl alcohol (19.3 mL, 6.0 equiv.) and PTSA (10.70 g, 1.2 equiv.). The mixture was refluxed in a Dean-Stark apparatus until no water was recovered and the solvent was removed under pressure. The residue was co-evaporated several times with toluene and precipitated with diethylether to give a white solid. Purification by column chromatography over silica gel (CH<sub>2</sub>Cl<sub>2</sub>/MeOH: 5 to 10% MeOH) afforded **S5** as a white solid (11.00 g, 53.49 mmol, **82%**). (**S5** Registry Number: 142601-87-4)

$^1\text{H NMR}$  (400 MHz,  $\text{CDCl}_3$ ):  $\delta$  8.22 (s, 3H,  $^+\text{NH}_3$ ), 7.74 (d, 2H,  $J = 8.0$  Hz,  $\text{H}_a$ ), 7.15 (d, 2H,  $J = 8.0$  Hz,  $\text{H}_b$ ), 5.83 to 5.73 (m, 1H,  $\text{H}_4$ ), 5.25 (dd, 1H,  $J = 17.2$  Hz,  $J = 1.6$  Hz,  $\text{H}_5$ ), 5.17 (dd, 1H,  $J = 10.4$  Hz,  $J = 1.2$  Hz,  $\text{H}_5$ ), 4.55 and 4.47 (dd, AB system, 2H,  $J = 12.8$  Hz,  $J = 6.0$  Hz,  $\text{H}_3$ ), 4.14 (bs, 1H,  $\text{H}_2$ ), 2.59 to 2.43 (m, 2H,  $\text{H}_7$ ), 2.35 (s, 3H,  $\text{CH}_3\text{-PTSA}$ ), 2.02 to 2.19 (m, 2H,  $\text{H}_6$ ), 1.90 (s, 3H,  $\text{S-CH}_3$ )  $^{13}\text{C NMR}$  (100 MHz,  $\text{CDCl}_3$ ):  $\delta$  168.8, 141.2, 140.8, 131.2, 129.1, 126.2, 119.4, 67.0, 52.3, 29.5, 29.2, 21.5, 15.0 **LRFAB-MS** (3-NOBA matrix):  $m/z$  191  $[\text{M-PTSA+H}]^+$  **HRFAB-MS** (3-NOBA matrix):  $m/z$  190.0899 (calcd. for  $\text{C}_8\text{H}_{16}\text{NO}_2\text{S}$  190.0896  $[\text{M-PTSA+H}]^+$ ) **m.p.** 98-100°C (litt. 114-116°C)



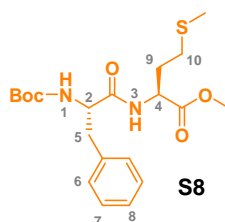
To a solution of Boc-Phe-OH (3.40 g, 12.83 mmol) and L-methionine salt **S5** (7.00 g, 1.5 equiv.) in  $\text{CH}_2\text{Cl}_2$  (50 mL) was added EDC.HCl (3.70 g, 1.5 equiv.), HOBt (693 mg, 0.4 equiv.) and DIPEA (6.7 mL, 3.0 equiv.). The mixture was stirred for 24 hours at room temperature, hydrolyzed and extracted with  $\text{CH}_2\text{Cl}_2$ . The combined organic layers were washed with water, brine, dried and concentrated *in vacuo*. Purification by column chromatography over silica gel (petroleum ether/ethyl acetate: 6/4 then  $\text{CH}_2\text{Cl}_2/\text{MeOH}$ : 2.5 to 5% MeOH) afforded **S6** (2.38 g, 1.39 mmol, **43%**) as a white solid.

$^1\text{H NMR}$  (400 MHz,  $\text{CDCl}_3$ ):  $\delta$  7.32 to 7.19 (m, 5H,  $\text{H}_{9+10+11}$ ), 6.55 (d, 1H,  $J = 7.6$  Hz,  $\text{NH}_3$ ), 5.93 to 5.84 (m, 1H,  $\text{H}_6$ ), 5.32 (dd, 1H,  $J = 17.2$  Hz,  $J = 1.2$  Hz,  $\text{H}_7$ ), 5.27 (dd, 1H,  $J = 10.4$  Hz,  $J = 1.2$  Hz,  $\text{H}_7$ ), 4.97 (bs, 1H,  $\text{NH}_1$ ), 4.65 (dd, 1H,  $J = 12.4$  Hz,  $J = 7.2$  Hz,  $\text{H}_4$ ), 4.61 (dd, 2H,  $J = 5.6$  Hz,  $J = 1.2$  Hz,  $\text{H}_5$ ), 4.36 (bd, 1H,  $J = 7.2$  Hz,  $\text{H}_2$ ), 3.10 and 3.05 (dd, AB system, 2H,  $J = 14.0$  Hz,  $J = 6.8$  Hz,  $\text{H}_8$ ), 2.46 to 2.35 (m, 2H,  $\text{H}_{13}$ ), 2.17 to 2.09 (m, 1H,  $\text{H}_{12}$ ), 2.05 (s, 3H,  $\text{S-CH}_3$ ), 1.99 to 1.88 (m, 1H,  $\text{H}_{12}$ ), 1.41 (s, 9H,  $\text{H-}t\text{Bu}$ )  $^{13}\text{C NMR}$  (100 MHz,  $\text{CDCl}_3$ ):  $\delta$  171.1, 131.5, 129.5, 128.9, 127.2, 119.3, 66.3, 55.9, 51.8, 38.1, 31.8, 29.8, 28.4, 15.5 **LRFAB-MS** (3-NOBA matrix):  $m/z$  438  $[\text{M+H}]^+$  **HRFAB-MS** (3-NOBA matrix):  $m/z$  437.2104 (calcd. for  $\text{C}_{22}\text{H}_{33}\text{N}_2\text{O}_5\text{S}$  437.2105  $[\text{M+H}]^+$ ) **m.p.** 106-108°C



Trifluoroacetic acid (16 mL, 45.0 equiv.) was added dropwise to a solution of Boc-Phe-Met-OAll **S6** (2.13 g, 4.89 mmol) in  $\text{CH}_2\text{Cl}_2$  (100 mL) at  $0^\circ\text{C}$ . After 30 minutes at  $0^\circ\text{C}$ , the solution was stirred a further 1.5 hours at room temperature and then cooled to  $0^\circ\text{C}$ . After neutralisation with a saturated solution of  $\text{NaHCO}_3$ , the mixture was extracted with a  $\text{CHCl}_3/i\text{PrOH}$  (3/1, v/v) mixture, dried and evaporated to give **S7** (1.51 g, 4.49 mmol, **92%**) as a white solid.

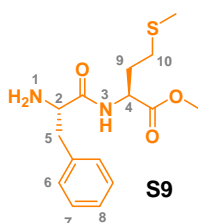
**$^1\text{H}$  NMR (400 MHz,  $\text{CDCl}_3$ ):**  $\delta$  7.92 (d, 1H,  $J = 6.4$  Hz,  $\text{H}_3$ ), 7.31 to 7.18 (m, 5H,  $\text{H}_{9+10+11}$ ), 5.93 to 5.83 (m, 1H,  $\text{H}_6$ ), 5.31 (dd, 1H,  $J = 17.2$  Hz,  $J = 1.2$  Hz,  $\text{H}_7$ ), 5.23 (dd, 1H,  $J = 10.4$  Hz,  $J = 1.2$  Hz,  $\text{H}_7$ ), 4.71 to 4.66 (m, 1H,  $\text{H}_4$ ), 4.60 (d, 2H,  $J = 6.0$  Hz,  $\text{H}_5$ ), 3.67 (bs, 1H,  $\text{H}_2$ ), 3.18 (dd, 1H,  $J = 13.6$  Hz,  $J = 3.6$  Hz,  $\text{H}_8$ ), 2.79 (dd, 1H,  $J = 13.6$  Hz,  $J = 8.4$  Hz,  $\text{H}_8$ ), 2.46 to 2.35 (m, 2H,  $\text{H}_{13}$ ), 2.18 to 2.09 (m, 1H,  $\text{H}_{12}$ ), 2.05 (s, 3H, S- $\text{CH}_3$ ), 2.00 to 1.91 (m, 3H,  $\text{H}_{12}+\text{NH}_2$ )  **$^{13}\text{C}$  NMR (100 MHz,  $\text{CDCl}_3$ ):**  $\delta$  174.0, 171.6, 137.3, 131.5, 129.4, 128.7, 127.0, 119.0, 66.1, 56.1, 51.2, 40.6, 31.7, 29.9, 15.4 **LRFAB-MS (3-NOBA matrix):**  $m/z$  338  **$[\text{M}+\text{H}]^+$  HRFAB-MS (3-NOBA matrix):**  $m/z$  337.1575 (calcd. for  $\text{C}_{17}\text{H}_{25}\text{N}_2\text{O}_3\text{S}$  337.1580  $[\text{M}+\text{H}]^+$ ) **m.p.** decomposition



To a solution of Boc-Phe-OH (9.00 g, 33.96 mmol) and L-methionine methyl ester hydrochloride salt (8.13 g, 1.2 equiv.) in  $\text{CH}_2\text{Cl}_2$  (150 mL) was added EDC.HCl (7.82 g, 1.2 equiv.), HOBt (1.83 g, 0.4 equiv.) and DIPEA (14.8 mL, 2.5 equiv.). The mixture was stirred overnight at room temperature, hydrolyzed and extracted with  $\text{CH}_2\text{Cl}_2$ . The combined organic layers were washed with water, brine, dried and concentrated *in vacuo*. Purification by

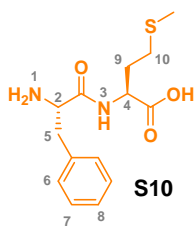
column chromatography over silica gel (petroleum ether/ethyl acetate: 9/1 to 3/7) afforded **S8** (6.68 g, 16.30 mmol, **42%**) as a white solid. (**S8** Registry Number: 40290-63-9)

**<sup>1</sup>H NMR (400 MHz, CDCl<sub>3</sub>):**  $\delta$  7.34 to 7.21 (m, 5H, H<sub>6+7+8</sub>), 6.57 (d, 1H,  $J = 7.2$  Hz, NH<sub>3</sub>), 5.01 (bs, 1H, NH<sub>1</sub>), 4.66 (dd, 1H,  $J = 12.0$  Hz,  $J = 6.8$  Hz, H<sub>4</sub>), 4.37 (bd, 1H,  $J = 6.4$  Hz, H<sub>2</sub>), 3.73 (s, 3H, COOCH<sub>3</sub>), 3.15 to 3.04 (m, 2H, H<sub>5</sub>), 2.45 to 2.36 (m, 2H, H<sub>10</sub>), 2.18 to 2.09 (m, 1H, H<sub>9</sub>), 2.07 (s, 3H, S-CH<sub>3</sub>), 1.99 to 1.90 (m, 1H, H<sub>9</sub>), 1.43 (s, 9H, *H-t*Bu) **<sup>13</sup>C NMR (100 MHz, CDCl<sub>3</sub>):**  $\delta$  171.9, 171.2, 155.5, 136.5, 129.5, 128.8, 127.1, 80.5, 55.9, 52.6, 51.6, 38.1, 31.7, 29.8, 28.4, 15.5 **LRFAB-MS (3-NOBA matrix):**  $m/z$  411 [M+H]<sup>+</sup> **HRFAB-MS (3-NOBA matrix):**  $m/z$  411.1947 (calcd. for C<sub>20</sub>H<sub>31</sub>N<sub>2</sub>O<sub>5</sub>S 411.1948 [M+H]<sup>+</sup>) **m.p.** 68-70°C



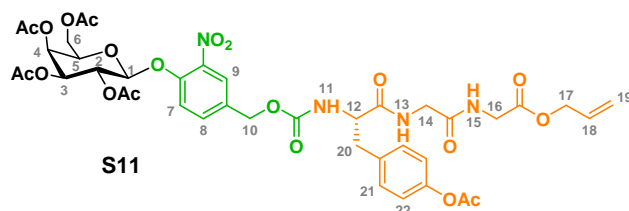
Trifluoroacetic acid (12.2 mL, 45.0 equiv.) was added dropwise to a solution of Boc-Phe-Met-OMe **S8** (1.60 g, 3.90 mmol) in CH<sub>2</sub>Cl<sub>2</sub> (70 mL) at 0°C. After 30 minutes at 0°C, the solution was stirred a further 1.5 hours at room temperature and then cooled to 0°C. After neutralisation with a saturated solution of NaHCO<sub>3</sub>, the mixture was extracted with a CHCl<sub>3</sub>/*i*PrOH (3/1, v/v) mixture, dried and evaporated to give **S9** (1.17 g, 3.77 mmol, **97%**) as a yellow oil.

**<sup>1</sup>H NMR (400 MHz, CDCl<sub>3</sub>):**  $\delta$  7.90 (bd, 1H,  $J = 6.0$  Hz, H<sub>3</sub>), 7.29 to 7.16 (m, 5H, H<sub>6+7+8</sub>), 4.65 (bd, 1H,  $J = 4.8$  Hz, H<sub>4</sub>), 3.68 (m, 4H, H<sub>2</sub> + COOCH<sub>3</sub>), 3.14 (d, 1H,  $J = 12.4$  Hz, H<sub>5</sub>), 2.80 to 2.75 (m, 1H, H<sub>5</sub>), 2.39 to 2.35 (m, 2H, H<sub>10</sub>), 2.14 to 2.05 (m, 1H, H<sub>9</sub>), 2.02 (s, 3H, S-CH<sub>3</sub>), 1.96 to 1.87 (m, 1H, H<sub>9</sub>), 1.77 (bs, 2H, NH<sub>2</sub>) **<sup>13</sup>C NMR (100 MHz, CDCl<sub>3</sub>):**  $\delta$  174.0, 172.1, 137.2, 129.2, 128.5, 126.7, 55.9, 52.3, 50.9, 40.5, 31.4, 29.7, 15.2 **LRFAB-MS (3-NOBA matrix):**  $m/z$  311 [M+H]<sup>+</sup> **HRFAB-MS (3-NOBA matrix):**  $m/z$  311.1420 (calcd. for C<sub>15</sub>H<sub>23</sub>N<sub>2</sub>O<sub>3</sub>S 311.1424 [M+H]<sup>+</sup>)



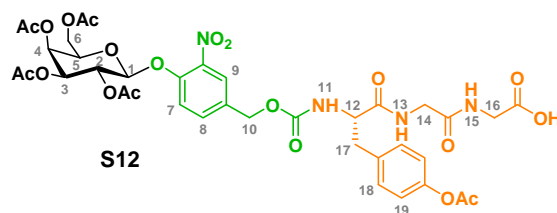
To a solution of H-Phe-Met-OMe **S9** (155 mg, 0.5 mmol) in H<sub>2</sub>O/THF (4.8 mL / 2.4 mL) cooled in an ice-water bath was added dropwise a 0°C solution of NaOH (100 mg, 5.0 equiv.) in H<sub>2</sub>O (5 mL). Stirring was continued for 2.5 h at 0°C and the solution was neutralized with Amberlite IR-120, filtered and washed with MeOH. MeOH was then evaporated to afford **S10** (137 mg, mmol, **93%**) as a white oily solid. (**S10** Registry Number: 15080-84-9)

**<sup>1</sup>H NMR (400 MHz, CD<sub>3</sub>OD):**  $\delta$  7.33 to 7.20 (m, 5H, H<sub>6+7+8</sub>), 4.30 (dd, 1H,  $J = 7.6$  Hz,  $J = 4.8$  Hz, H<sub>4</sub>), 3.88 (dd, 1H,  $J = 7.6$  Hz,  $J = 5.6$  Hz, H<sub>2</sub>), 3.18 (dd, 1H,  $J = 14.0$  Hz,  $J = 5.2$  Hz, H<sub>5</sub>), 2.94 (dd, 1H,  $J = 14.0$  Hz,  $J = 8.0$  Hz, H<sub>5</sub>), 2.46 to 2.42 (m, 2H, H<sub>10</sub>), 2.17 to 2.09 (m, 1H, H<sub>9</sub>), 2.06 (s, 3H, S-CH<sub>3</sub>), 2.01 to 1.95 (m, 1H, H<sub>9</sub>) **<sup>13</sup>C NMR (100 MHz, CD<sub>3</sub>OD):**  $\delta$  178.1, 173.0, 137.5, 130.6, 129.8, 128.2, 56.7, 55.8, 40.3, 33.7, 31.3, 15.3 **LRFAB-MS (3-NOBA matrix):**  $m/z$  297 [M+H]<sup>+</sup> **HRFAB-MS (3-NOBA matrix):**  $m/z$  297.1267 (calcd. for C<sub>14</sub>H<sub>21</sub>N<sub>2</sub>O<sub>3</sub>S 297.1267 [M+H]<sup>+</sup>)



To a solution of activated galactoside (1.32 g, 1.99 mmol) in DMF (50 mL) was added H-Tyr(Ac)-Gly-Gly-OAll **S4** (1.50 g, 2.0 equiv.) and pyridine (400  $\mu$ L, 2.5 equiv.). Stirring was continued at room temperature during one day then the solution was diluted with 1N HCl and extracted with ethyl acetate. The combined extracts were washed with 1N HCl, dried with MgSO<sub>4</sub>, filtered and concentrated under reduced pressure. Purification by column chromatography over silica gel (petroleum ether/ethyl acetate: 4/6 to 2/8 then CH<sub>2</sub>Cl<sub>2</sub>/MeOH: 2.5 to 7% MeOH) yielded **S11** as a white yellow powder (1.74 g, 1.93 mmol, **97%**).

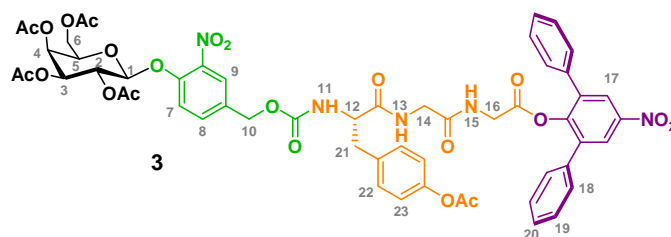
**<sup>1</sup>H NMR (400 MHz, CDCl<sub>3</sub>):**  $\delta$  7.72 (s, 1H, H<sub>9</sub>), 7.43 (d, 1H,  $J$  = 8.0 Hz, NH), 7.30 (d, 1H,  $J$  = 8.4 Hz, NH), 7.19 to 7.14 (m, 3H, H<sub>8+21</sub>), 6.96 (d, 3H,  $J$  = 8.0 Hz, H<sub>7+22</sub>), 5.91 to 5.81 (m, 2H, NH+H<sub>18</sub>), 5.51 (dd, 1H,  $J$  = 10.8 Hz,  $J$  = 8.0 Hz, H<sub>2</sub>), 5.45 (d, 1H,  $J$  = 3.2 Hz, H<sub>4</sub>), 5.30 (dd, 1H,  $J$  = 13.2 Hz,  $J$  = 1.2 Hz, H<sub>19</sub>), 5.22 (d, 1H,  $J$  = 10.4 Hz, H<sub>19</sub>), 5.10 (dd, 1H,  $J$  = 10.4 Hz,  $J$  = 3.2 Hz, H<sub>3</sub>), 5.07 (d, 1H,  $J$  = 8.0 Hz, H<sub>1</sub>), 4.99 (bs, 2H, H<sub>10</sub>), 4.59 (d, 2H,  $J$  = 6.0 Hz, H<sub>17</sub>), 4.44 (dd, 1H,  $J$  = 13.6 Hz,  $J$  = 6.8 Hz, H<sub>12</sub>), 4.25 to 4.08 (m, 3H, H<sub>5+6</sub>), 4.01 to 3.83 (m, 4H, H<sub>14+16</sub>), 3.09 (dd, 1H,  $J$  = 14.0 Hz,  $J$  = 6.0 Hz, H<sub>20</sub>), 2.97 (dd, 1H,  $J$  = 13.2 Hz,  $J$  = 7.2 Hz, H<sub>20</sub>), 2.26 (s, 3H, *H*-Ac-Tyr), 2.17 (s, 3H, *H*-Ac), 2.10 (s, 3H, *H*-Ac), 2.05 (s, 3H, *H*-Ac), 2.00 (s, 3H, *H*-Ac) **<sup>13</sup>C NMR (100 MHz, CDCl<sub>3</sub>):**  $\delta$  171.7, 170.5, 170.3, 170.2, 169.8, 169.7, 169.5, 169.1, 155.9, 149.8, 149.1, 141.1, 134.0, 133.4, 132.3, 131.5, 130.4, 124.8, 121.9, 119.6, 119.1, 100.6, 71.4, 70.6, 67.9, 66.8, 66.2, 65.3, 61.4, 56.3, 42.9, 41.3, 37.7, 21.2, 20.8, 20.7 (x2) **LRFAB-MS (3-NOBA matrix):**  $m/z$  904 [M+H]<sup>+</sup> **HRFAB-MS (3-NOBA matrix):**  $m/z$  903.2779 (calcd. for C<sub>40</sub>H<sub>47</sub>N<sub>4</sub>O<sub>20</sub> 903.2778 [M+H]<sup>+</sup>) **m.p.** 96-98°C



To a solution of **S11** (1.74 g, 1.93 mmol) in degassed CH<sub>2</sub>Cl<sub>2</sub> (150 mL) were added phenylsilane (480  $\mu$ L, 2.0 equiv.) and Pd(PPh<sub>3</sub>)<sub>4</sub> (223 mg, 0.1 equiv.). The mixture was stirred during 2.5 hours at room temperature and the solvent evaporated under reduced pressure. The crude mixture was purified by column chromatography over silica gel (CH<sub>2</sub>Cl<sub>2</sub>/MeOH/AcOH: 0.5 to 7% MeOH, 1% AcOH) to afford **S12** (1.42 g, 1.65 mmol, **85%**) as a white brown solid.

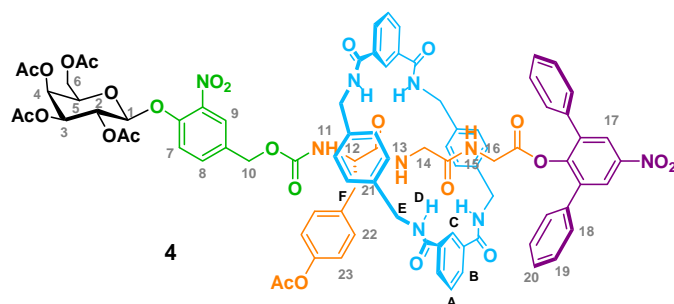
**<sup>1</sup>H NMR (400 MHz, CDCl<sub>3</sub>/CD<sub>3</sub>OD: 9/1):**  $\delta$  7.65 (s, 1H, H<sub>9</sub>), 7.36 (d, 1H,  $J$  = 8.4 Hz, NH), 7.22 (d, 1H,  $J$  = 8.8 Hz, NH), 7.14 to 7.02 (m, 4H, H<sub>7+8+18</sub>), 6.87 (d, 2H,  $J$  = 8.4 Hz, H<sub>19</sub>), 5.39 (dd, 1H,  $J$  = 10.4 Hz,  $J$  = 8.0 Hz, H<sub>2</sub>), 5.35 (d, 1H,  $J$  = 3.2 Hz, H<sub>4</sub>), 5.04 to 4.99 (m, 2H, H<sub>1+3</sub>), 4.93 and 4.89 (d, AB system, 2H,  $J$  = 13.2 Hz, H<sub>10</sub>), 4.23 (t, 1H,  $J$  = 6.0 Hz, H<sub>12</sub>), 4.13 to 4.02 (m, 3H, H<sub>5+6</sub>), 3.88 to 3.67 (m, 4H, H<sub>14+16</sub>), 3.01 (dd, 1H,  $J$  = 13.6 Hz,  $J$  = 6.0 Hz, H<sub>17</sub>), 2.84 (dd, 1H,  $J$  = 13.2 Hz,  $J$  = 7.6 Hz, H<sub>17</sub>), 2.17 (s, 3H, *H*-Ac-Tyr), 2.08 (s, 3H, *H*-Ac), 2.01 (s, 3H, *H*-Ac), 1.95 (s, 3H, *H*-Ac), 1.90 (s, 3H, *H*-Ac) **<sup>13</sup>C NMR (100 MHz, CDCl<sub>3</sub>/CD<sub>3</sub>OD: 9/1):**  $\delta$  172.2, 171.7, 170.7, 170.5, 170.4, 170.1, 169.8, 169.7, 156.2, 149.5, 148.9, 134.1,

133.1, 132.3, 130.2, 128.9, 128.1, 125.2, 124.4, 121.6, 119.1, 100.2, 71.2, 70.5, 67.9, 66.8, 65.0, 61.3, 56.4, 42.4, 40.7, 37.0, 20.9, 20.5 (x2), 20.4, 20.3 **LRFAB-MS (3-NOBA matrix):**  $m/z$  864  $[M+H]^+$  **HRFAB-MS (3-NOBA matrix):**  $m/z$  863.2464 (calcd. for  $C_{37}H_{43}N_4O_{20}$  863.2465  $[M+H]^+$ ) **m.p.** 138-140°C



To a solution of **S12** (985 mg, 1.14 mmol) in  $CHCl_3$  (50 mL) were added 2,6-diphenyl-4-nitrophenol (1.33 g, 4.0 equiv.),  $Et_3N$  (2.4 mL, 15.0 equiv.) and BOP (758 mg, 1.5 equiv.). The reaction mixture was stirred 3 hours at room temperature and then evaporated under reduced pressure. The crude mixture was purified by column chromatography over silica gel ( $CH_2Cl_2$ /acetone: 5 to 30% acetone) to afford **3** (867 mg, 0.35 mmol, **67%**) as a white solid.

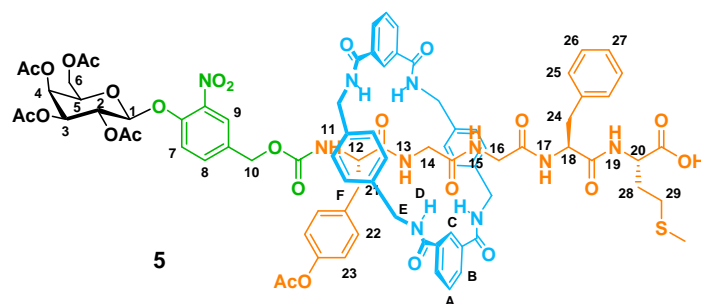
**$^1H$  NMR (400 MHz,  $CDCl_3$ ):**  $\delta$  8.28 (s, 2H,  $H_{17}$ ), 7.70 (d, 1H,  $J = 1.2$  Hz,  $H_9$ ), 7.48 to 7.39 (m, 7H,  $H_{8+18+19+20}$ ), 7.31 (d, 1H,  $J = 8.8$  Hz,  $H_7$ ), 7.12 (d, 2H,  $J = 8.4$  Hz,  $H_{22}$ ), 6.96 (d, 2H,  $J = 8.4$  Hz,  $H_{23}$ ), 6.54 (t, 1H,  $J = 4.8$  Hz,  $NH_{13}$ ), 6.34 (bs, 1H,  $NH_{15}$ ), 5.54 (dd, 1H,  $J = 10.8$  Hz,  $J = 8.0$  Hz,  $H_2$ ), 5.47 (d, 1H,  $J = 3.6$  Hz,  $H_4$ ), 5.42 (d, 1H,  $J = 7.2$  Hz,  $NH_{11}$ ), 5.11 (dd, 1H,  $J = 10.4$  Hz,  $J = 3.2$  Hz,  $H_3$ ), 5.07 (d, 1H,  $J = 8.0$  Hz,  $H_1$ ), 4.94 (bs, 2H,  $H_{10}$ ), 4.31 (dd, 1H,  $J = 13.6$  Hz,  $J = 6.8$  Hz,  $H_{12}$ ), 4.24 (dd, 1H,  $J = 11.2$  Hz,  $J = 6.8$  Hz,  $H_6$ ), 4.16 (dd, 1H,  $J = 11.2$  Hz,  $J = 6.4$  Hz,  $H_6$ ), 4.08 (t, 1H,  $J = 6.8$  Hz,  $H_5$ ), 3.83 to 3.69 (m, 4H,  $H_{14+16}$ ), 3.05 (dd, 1H,  $J = 14.0$  Hz,  $J = 6.4$  Hz,  $H_{21}$ ), 2.96 (dd, 1H,  $J = 13.6$  Hz,  $J = 7.2$  Hz,  $H_{21}$ ), 2.28 (s, 3H,  $H$ -Ac-Tyr), 2.19 (s, 3H,  $H$ -Ac), 2.13 (s, 3H,  $H$ -Ac), 2.06 (s, 3H,  $H$ -Ac), 2.02 (s, 3H,  $H$ -Ac)  **$^{13}C$  NMR (100 MHz,  $CDCl_3$ ):**  $\delta$  171.2, 170.5, 170.3, 170.2, 169.7, 169.5, 168.4, 167.3, 155.8, 149.9, 149.3, 149.2, 146.2, 141.3, 137.5, 135.4, 133.6, 133.4, 132.1, 130.3, 129.1, 129.0, 128.9, 125.1, 124.9, 122.1, 119.8, 100.8, 77.4, 71.5, 70.6, 67.9, 66.8, 65.4, 61.4, 56.5, 42.8, 41.1, 37.6, 29.4, 21.2, 20.9, 20.8 (x2), 20.7 **LRFAB-MS (3-NOBA matrix):**  $m/z$  1137  $[M+H]^+$  **HRFAB-MS (3-NOBA matrix):**  $m/z$  1136.3286 (calcd. for  $C_{55}H_{54}N_5O_{22}$  1136.3260  $[M+H]^+$ ) **m.p.** 122-126°C



Thread **3** (390 mg, 0.34 mmol) was dissolved in anhydrous chloroform (80 mL) and stirred vigorously whilst solutions of *p*-xylylene diamine (766 mg, 16.0 equiv.) and Et<sub>3</sub>N (1.71 mL, 35.0 equiv.) in anhydrous chloroform (60 mL) and isophthaloyl dichloride (1.14 g, 16.0 equiv.) in anhydrous chloroform (60 mL) were simultaneously added over a period of 3 hours using motor-driven syringe pumps. After overnight stirring, 2 mL of MeOH were added and the resulting suspension filtered through Celite®. The pad was washed with CHCl<sub>3</sub>/MeOH 2% (3 x 200 mL) and the combined filtrates were concentrated under reduced pressure. The residue was purified by column chromatography on silica gel using CHCl<sub>3</sub>/acetone (5 to 35% acetone) as eluent to give a mixture of thread **3** and rotaxane **4**. This mixture was resolved by size exclusion chromatography using CHCl<sub>3</sub>/MeOH (50/50: v/v) as eluent to give rotaxane **4** as a white powder (143 mg, 0.09 mmol, **26%**).

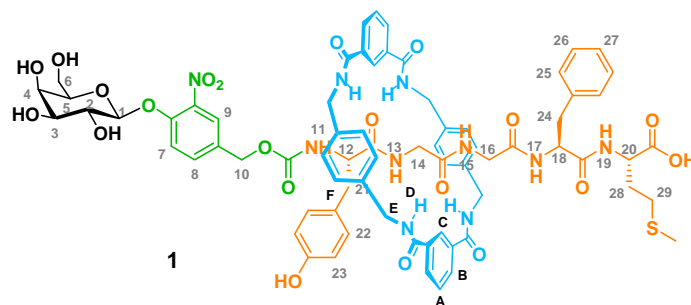
**<sup>1</sup>H NMR (400 MHz, CDCl<sub>3</sub>):**  $\delta$  8.18 (s, 2H, H<sub>17</sub>), 8.00 to 7.94 (m, 6H, H<sub>B+C</sub>), 7.68 to 7.63 (m, 4H, H<sub>D</sub>), 7.50 to 7.47 (m, 3H, H<sub>9+A</sub>), 7.38 (bs, 1H, NH<sub>15</sub>), 7.36 to 7.34 (m, 3H, H<sub>7+8+NH15</sub>), 7.27 to 7.18 (m, 10H, H<sub>18+19+20</sub>), 6.94 (d, 4H, *J* = 8.0 Hz, H<sub>F</sub>), 6.79 (d, 4H, *J* = 8.0 Hz, H<sub>F</sub>), 6.70 and 6.66 (d, AB system, 4H, *J* = 8.8 Hz, H<sub>22+23</sub>), 6.34 (bs, 1H, NH<sub>13</sub>), 5.49 (dd, 1H, *J* = 10.4 Hz, *J* = 8.0 Hz, H<sub>2</sub>), 5.43 (d, 1H, *J* = 3.2 Hz, H<sub>4</sub>), 5.20 (d, 1H, *J* = 8.4 Hz, NH<sub>11</sub>), 5.08 (dd, 1H, *J* = 10.4 Hz, *J* = 3.2 Hz, H<sub>3</sub>), 5.04 (d, 1H, *J* = 8.0 Hz, H<sub>1</sub>), 4.70 and 4.55 (d, AB system, 2H, *J* = 12.4 Hz, H<sub>10</sub>), 4.46 to 4.37 (m, 4H, H<sub>E</sub>), 4.30 to 4.20 (m, 4H, H<sub>E</sub>), 4.17 to 4.07 (m, 3H, H<sub>5+6</sub>), 4.00 (dd, 1H, *J* = 14.8 Hz, *J* = 7.6 Hz, H<sub>12</sub>), 3.58 and 3.50 (dd, AB system, 2H, *J* = 18.8 Hz, *J* = 5.6 Hz, H<sub>16</sub>), 2.70 (dd, 1H, *J* = 13.2 Hz, *J* = 8.0 Hz, H<sub>21</sub>), 2.55 (dd, 1H, *J* = 13.6 Hz, *J* = 6.0 Hz, H<sub>21</sub>), 2.25 (s, 3H, *H*-Ac-Tyr), 2.19 to 2.25 (m, 2H, H<sub>14</sub>), 2.13 (s, 3H, *H*-Ac), 2.06 (s, 3H, *H*-Ac), 2.02 (s, 3H, *H*-Ac), 1.97 (s, 3H, *H*-Ac) **<sup>13</sup>C NMR (100 MHz, CDCl<sub>3</sub>):**  $\delta$  170.5, 170.3 (x3), 169.6, 169.5, 169.0, 167.4 (x2), 166.3, 155.6, 149.3, 149.1, 146.2, 141.0, 137.8, 137.5, 137.2, 135.4, 134.9, 134.4, 133.8, 133.7, 131.8, 130.9, 130.5, 130.4, 129.2, 128.9 (x2), 128.8, 128.4, 126.2, 125.1, 124.9, 121.3, 119.5, 100.6, 71.5, 70.6, 67.9, 66.8, 65.4, 61.3, 55.3, 44.6, 44.2, 41.4, 40.8, 36.5, 29.8, 29.2, 22.7, 21.4, 20.8 (x3), 20.7

**LRFAB-MS (3-NOBA matrix):**  $m/z$  1668  $[M+H]^+$  **HRFAB-MS (3-NOBA matrix):**  $m/z$  1668.5323 (calcd. for  $C_{87}H_{82}N_9O_{26}$  1668.5371  $[M+H]^+$ ) **m.p.** 164-166°C



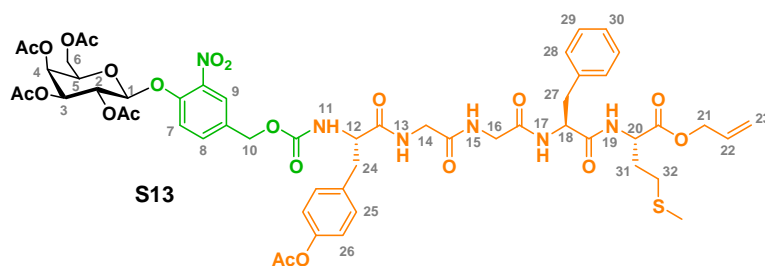
Rotaxane **4** (63 mg, 0.038 mmol) and H-Phe-Met-OH **S10** (56 mg, 5.0 equiv.) were dissolved in  $CHCl_3$  (10 mL). The reaction mixture was then heated at reflux during 4 days. The solvent was removed under reduced pressure and the crude material purified by column chromatography on silica gel ( $CHCl_3/MeOH$ : 2 to 30% MeOH) to give elongated rotaxane **5** as a white powder (25 mg, 0.015 mmol, **40%**) and starting rotaxane **4** (37 mg, **59%**)

**$^1H$  NMR (400 MHz,  $CDCl_3/CD_3OD$ : 5/3):**  $\delta$  8.26 (bs, 2H,  $H_C$ ), 7.97 (d, 4H,  $J = 7.2$  Hz,  $H_B$ ), 7.52 to 7.48 (m, 3H,  $H_{9+A}$ ), 7.28 to 7.15 (m, 3H,  $H_{7+8+D}$ ), 7.10 to 6.99 (m, 13H,  $H_{25+26+27+F}$ ), 6.92 (d, 2H,  $J = 8.4$  Hz,  $H_{22}$ ), 6.80 (d, 2H,  $J = 8.4$  Hz,  $H_{23}$ ), 5.43 to 5.39 (m, 2H,  $H_{2+4}$ ), 5.13 (d, 1H,  $J = 8.0$  Hz,  $H_1$ ), 5.10 (dd, 1H,  $J = 10.4$  Hz,  $J = 3.6$  Hz,  $H_3$ ), 4.79 and 4.64 (d, AB system, 2H,  $J = 12.8$  Hz,  $H_{10}$ ), 4.46 to 4.26 (m, 10H,  $H_{18+20+E}$ ), 4.20 to 4.11 (m, 4H,  $H_{5+6+12}$ ), 2.99 to 2.95 (m, 1H,  $H_{24}$ ), 2.90 to 2.80 (m, 5H,  $H_{14+16+21}$ ), 2.76 to 2.71 (m, 1H,  $H_{24}$ ), 2.58 (dd, 1H,  $J = 14.0$  Hz,  $J = 8.8$  Hz,  $H_{21}$ ), 2.27 (m, 2H,  $H_{29}$ ), 2.22 (s, 3H,  $H$ -Ac-Tyr), 2.12 (s, 3H,  $H$ -Ac), 2.05 (s, 3H,  $H$ -Ac), 2.00 (s, 3H,  $H$ -Ac), 1.94 (s, 3H,  $H$ -Ac), 1.93 (s, 3H, S- $CH_3$ ), 1.99 to 1.93 (m, 2H,  $H_{28}$ ),  **$^{13}C$  NMR (100 MHz,  $CDCl_3/CD_3OD$ : 5/3):**  $\delta$  174.1, 173.0, 171.7, 171.0, 170.8, 170.7, 170.6, 170.4, 170.2, 169.9, 156.7, 149.7, 149.2, 141.1, 136.9, 134.5, 133.6, 132.6, 130.4, 129.4, 128.7, 127.1, 124.8, 121.8, 119.3, 100.4, 71.4, 70.9, 68.2, 67.1, 65.3, 61.6, 56.7, 54.9, 52.1, 43.1, 42.8, 37.8, 37.3, 31.4, 30.1, 29.8, 21.1, 20.7 (x2), 20.6 (x2) **LRFAB-MS (3-NOBA matrix):**  $m/z$  1674  $[M+H]^+$ , 1679  $[M+Li]^+$  **LRESI-MS:**  $m/z$  838  $[M+2H]^{2+}$ , 1674  $[M+H]^+$ , 1697  $[M+Na]^+$  **LRESI-MS (negative mode):**  $m/z$  1672  $[M-H]^-$  **HRFAB-MS (3-NOBA matrix):**  $m/z$  1673.5680 (calcd. for  $C_{83}H_{89}N_{10}O_{26}S$  1673.5670  $[M+H]^+$ ) **m.p.** decomposition



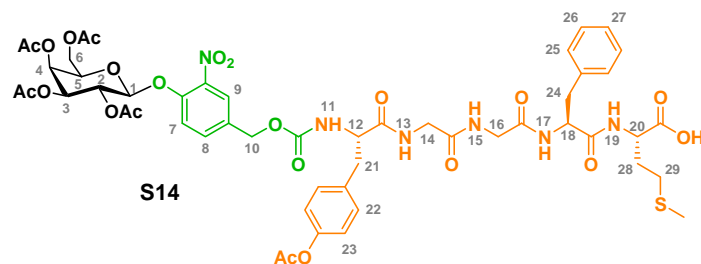
To a solution of **5** (31 mg, 0.019 mmol) in MeOH (5 mL) cooled in an ice-water bath was added dropwise a 0°C solution of MeONa (10 mg, 10.0 equiv.) in MeOH (3 mL). Stirring was continued for 1 hour at 0°C and the solution was neutralized with Amberlite IR-120 and filtered. MeOH was then evaporated to afford **1** (29 mg, 0.019 mmol, **quant.**) as a white brown solid which was then purified by preparative RP-HPLC using a linear gradient (58 to 80% in 20 min) of MeCN (containing 6.6 mM of HCOOH) in H<sub>2</sub>O (containing 6.6 mM of HCOOH) at a flow rate of 10 ml/min to give rotaxane **1** as a light yellow solid. Purity (HPLC): >95%.

**<sup>1</sup>H NMR (400 MHz, CD<sub>3</sub>OD):**  $\delta$  8.46 (s, 2H, H<sub>C</sub>), 8.06 (d, 4H,  $J = 8.0$  Hz, H<sub>B</sub>), 7.63 to 7.59 (m, 3H, H<sub>9+A</sub>), 7.35 (d, 1H,  $J = 8.8$  Hz, H<sub>7</sub>), 7.23 to 7.08 (m, 16H, H<sub>8+25+26+27+F</sub>), 6.82 (d, 2H,  $J = 8.4$  Hz, H<sub>22</sub>), 6.61 (d, 2H,  $J = 8.4$  Hz, H<sub>23</sub>), 5.01 (d, 1H,  $J = 8.0$  Hz, H<sub>1</sub>), 4.95 to 4.73 (m, 2H, H<sub>10</sub>), 4.56 to 4.29 (m, 10H, H<sub>18+20+E</sub>), 4.21 (dd, 1H,  $J = 9.6$  Hz,  $J = 4.8$  Hz, H<sub>12</sub>), 3.91 (d, 1H,  $J = 3.2$  Hz, H<sub>4</sub>), 3.85 to 3.74 (m, 4H, H<sub>2+5+6</sub>), 3.59 (dd, 1H,  $J = 9.6$  Hz,  $J = 3.2$  Hz, H<sub>3</sub>), 3.15 to 3.02 (m, 3H, H<sub>16+24</sub>), 2.86 (dd, 1H,  $J = 14.0$  Hz,  $J = 5.2$  Hz, H<sub>21</sub>), 2.78 to 2.64 (m, 3H, H<sub>14+24</sub>), 2.48 (dd, 1H,  $J = 14.0$  Hz,  $J = 10$  Hz, H<sub>21</sub>), 2.39 to 2.28 (m, 2H, H<sub>29</sub>), 2.06 to 1.97 (m, 1H, H<sub>28</sub>), 2.00 (s, 3H, S-CH<sub>3</sub>), 1.83 to 1.72 (m, 1H, H<sub>28</sub>) **<sup>13</sup>C NMR (100 MHz, CD<sub>3</sub>OD):**  $\delta$  174.8, 174.2, 173.9, 170.7, 170.0, 169.2, 169.1, 157.8, 157.1, 156.7, 151.0, 141.5, 138.6, 138.5, 138.4, 135.6 (x2), 134.1, 132.4, 132.0, 131.4, 130.4, 130.2 (x2), 130.0, 129.6, 129.2, 128.0, 127.9, 125.3, 125.2, 118.7, 116.2, 102.9, 77.4, 74.9, 72.0, 70.2, 65.8, 62.5, 57.6, 56.2, 52.8, 45.4, 45.3, 43.2, 42.4, 39.2, 37.9, 31.9, 31.2, 30.8, 15.2 **LRFAB-MS (3-NOBA matrix):**  $m/z$  1463 [M+H]<sup>+</sup>, 1485 [M+Na]<sup>+</sup> **LRESI-MS:**  $m/z$  1463 [M+H]<sup>+</sup> **HRESI-MS:**  $m/z$  1463.5122 (calcd. for C<sub>73</sub>H<sub>79</sub>N<sub>10</sub>O<sub>21</sub>S 1463.5136 [M+H]<sup>+</sup>) **m.p.** 172-174°C



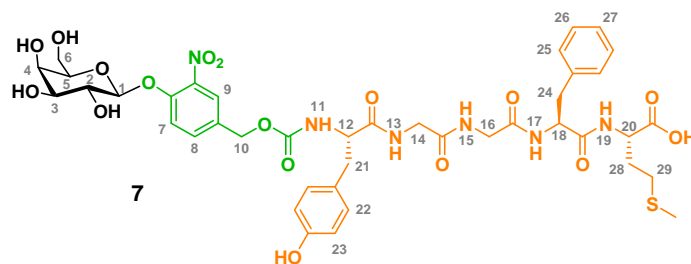
To a solution of **S12** (500 mg, 0.58 mmol) in  $\text{CH}_2\text{Cl}_2$  was added H-Phe-Met-OAll **S7** (292 mg, 1.5 equiv.) and DIPEA (0.2 mL, 2.0 equiv.). The mixture was then cooled to  $0^\circ\text{C}$  and EDC.HCl (167 mg, 1.5 equiv.) was added. After 30 minutes at  $0^\circ\text{C}$ , the reaction was allowed to reach room temperature and stirred overnight. The crude mixture was then extracted with 1N NaOH, 1N HCl and brine. The organic phase was dried over  $\text{MgSO}_4$  and evaporated under reduced pressure. Purification by column chromatography over silica gel ( $\text{CH}_2\text{Cl}_2/\text{MeOH}$ : 2 to 8% MeOH) afforded **S13** (255 mg, 0.22 mmol, **37%**) as a white yellow powder.

**$^1\text{H}$  NMR (400 MHz,  $\text{CDCl}_3/\text{CD}_3\text{OD}$ : 7/3):**  $\delta$  7.71 (d, 1H,  $J = 1.6$  Hz,  $\text{H}_9$ ), 7.42 (dd, 1H,  $J = 8.4$  Hz,  $J = 1.6$  Hz,  $\text{H}_8$ ), 7.28 (d, 1H,  $J = 8.4$  Hz,  $\text{H}_7$ ), 7.26 to 7.12 (m, 7H,  $\text{H}_{25+28+29+30}$ ), 6.91 (d, 2H,  $J = 8.4$  Hz,  $\text{H}_{26}$ ), 5.86 to 5.76 (m, 1H,  $\text{H}_{22}$ ), 5.43 (dd, 1H,  $J = 10.4$  Hz,  $J = 8$  Hz,  $\text{H}_2$ ), 5.40 (d, 1H,  $J = 3.6$  Hz,  $\text{H}_4$ ), 5.24 (dd, 1H,  $J = 17.2$  Hz,  $J = 1.6$  Hz,  $\text{H}_{23}$ ), 5.17 (dd, 1H,  $J = 10.4$  Hz,  $J = 1.2$  Hz,  $\text{H}_{23}$ ), 5.12 (d, 1H,  $J = 8.0$  Hz,  $\text{H}_1$ ), 5.08 (dd, 1H,  $J = 10.4$  Hz,  $J = 3.2$  Hz,  $\text{H}_3$ ), 4.98 and 4.92 (d, AB system, 2H,  $J = 12.8$  Hz,  $\text{H}_{10}$ ), 4.56 (dd, 1H,  $J = 8.4$  Hz,  $J = 5.6$  Hz,  $\text{H}_{18}$ ), 4.52 (d, 2H,  $J = 6.0$  Hz,  $\text{H}_{21}$ ), 4.52 to 4.48 (m, 1H,  $\text{H}_{20}$ ), 4.27 (dd, 1H,  $J = 8.0$  Hz,  $J = 6.4$  Hz,  $\text{H}_{12}$ ), 4.17 to 4.11 (m, 3H,  $\text{H}_{5+6}$ ), 3.84 to 3.77 (m, 2H,  $\text{H}_{14/16}$ ), 3.72 to 3.65 (m, 2H,  $\text{H}_{14/16}$ ), 3.12 to 3.03 (m, 2H,  $\text{H}_{24+27}$ ), 2.95 to 2.84 (m, 2H,  $\text{H}_{24+27}$ ), 2.46 to 2.32 (m, 2H,  $\text{H}_{32}$ ), 2.22 (s, 3H, *H*-Ac-Tyr), 2.12 (s, 3H, *H*-Ac), 2.07 to 2.03 (m, 4H,  $\text{H}_{31+}$  *H*-Ac), 2.00 (s, 3H, *H*-Ac), 1.98 (s, 3H, S- $\text{CH}_3$ ), 1.96 to 1.93 (m, 4H,  $\text{H}_{31+}$  *H*-Ac)  **$^{13}\text{C}$  NMR (100 MHz,  $\text{CDCl}_3/\text{CD}_3\text{OD}$ : 7/3):**  $\delta$  173.3, 172.1, 171.8, 171.2, 171.1, 170.9, 170.8, 170.7, 170.4, 170.1, 168.5, 167.8, 156.9, 150.0, 149.4, 141.3, 137.1, 135.4, 134.7, 133.7, 132.8, 131.9, 130.8, 130.6, 129.6, 129.0, 128.8, 127.9, 127.2, 124.9, 122.0, 119.4, 119.1, 100.6, 71.7, 71.1, 68.5, 67.4, 66.4, 65.5, 61.8, 56.9, 56.5, 54.9, 53.9, 52.0, 43.4, 42.9, 39.8, 37.9, 37.4, 33.3, 31.3, 30.2, 29.5, 21.2, 20.9, 20.8 (x2), 20.7, 15.3, 15.0 **LRFAB-MS (3-NOBA matrix):**  $m/z$  1181  $[\text{M}+\text{H}]^+$  **HRFAB-MS (3-NOBA matrix):**  $m/z$  1181.3897 (calcd. for  $\text{C}_{54}\text{H}_{65}\text{N}_6\text{O}_{22}\text{S}$  1181.3873  $[\text{M}+\text{H}]^+$ ) **m.p.** 196-198 $^\circ\text{C}$



To a solution of **S13** (210 mg, 0.18 mmol) in degassed  $\text{CH}_2\text{Cl}_2$  (15 mL) were added phenylsilane (40  $\mu\text{L}$ , 2.0 equiv.) and  $\text{Pd}(\text{PPh}_3)_4$  (21 mg, 0.1 equiv.). The mixture was stirred overnight at room temperature and the solvent was evaporated *in vacuo*. The crude mixture was purified by column chromatography over silica gel ( $\text{CHCl}_3/\text{MeOH}/\text{AcOH}$ : 1 to 8% MeOH, 1% AcOH) to afford **S14** (139 mg, 0.12 mmol, **67%**) as a white brown solid.

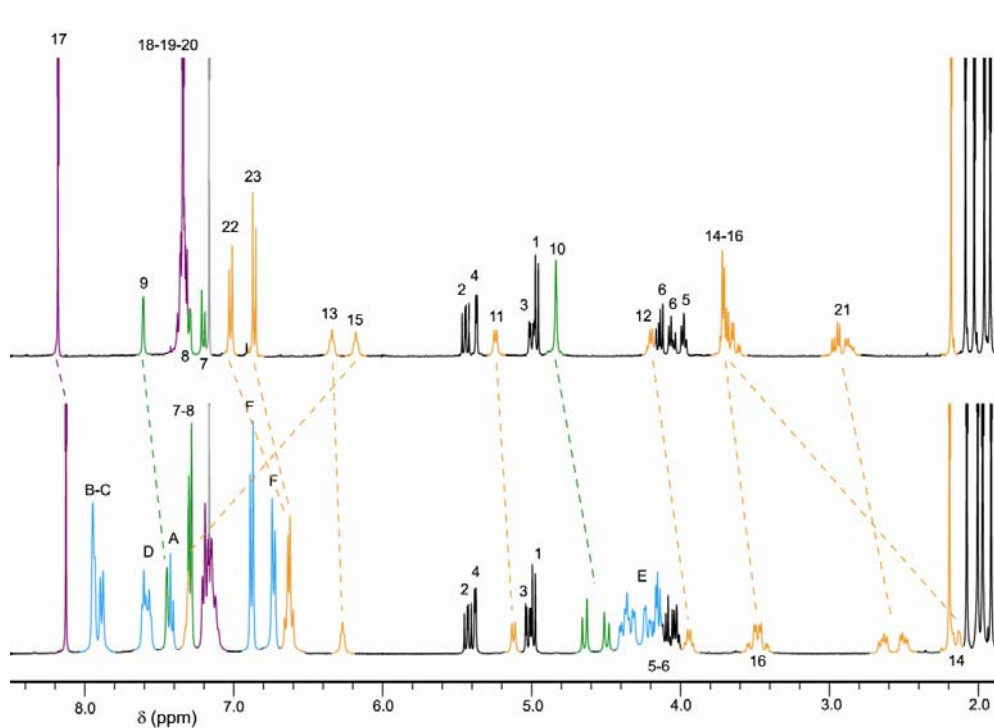
**$^1\text{H}$  NMR (400 MHz,  $\text{CDCl}_3/\text{CD}_3\text{OD}$ : 8/2):**  $\delta$  7.69 (s, 1H,  $\text{H}_9$ ), 7.40 (d, 1H,  $J = 8.4$  Hz,  $\text{H}_8$ ), 7.26 (d, 1H,  $J = 8.8$  Hz,  $\text{H}_7$ ), 7.19 to 7.11 (m, 7H,  $\text{H}_{22+25+26+27}$ ), 6.90 (d, 2H,  $J = 8.0$  Hz,  $\text{H}_{23}$ ), 5.43 (dd, 1H,  $J = 10.4$  Hz,  $J = 8.0$  Hz,  $\text{H}_2$ ), 5.39 (d, 1H,  $J = 3.2$  Hz,  $\text{H}_4$ ), 5.11 to 5.05 (m, 2H,  $\text{H}_{1+3}$ ), 4.97 and 4.89 (d, AB system, 2H,  $J = 12.8$  Hz,  $\text{H}_{10}$ ), 4.57 (t, 1H,  $J = 6.8$  Hz,  $\text{H}_{12/18}$ ), 4.41 (bs, 1H,  $\text{H}_{20}$ ), 4.29 (t, 1H,  $J = 7.6$  Hz,  $\text{H}_{12/18}$ ), 4.18 to 4.10 (m, 3H,  $\text{H}_{5+6}$ ), 3.83 to 3.65 (m, 4H,  $\text{H}_{14+16}$ ), 3.11 to 3.04 (m, 2H,  $\text{H}_{21+24}$ ), 2.93 to 2.83 (m, 2H,  $\text{H}_{21+24}$ ), 2.38 to 2.37 (m, 2H,  $\text{H}_{29}$ ), 2.21 (s, 3H, *H*-Ac), 2.11 (s, 3H, *H*-Ac-Tyr), 2.05 (s, 3H, *H*-Ac), 1.99 to 1.94 (m, 11H, S-*CH*<sub>3</sub>, *H*-Ac (x2),  $\text{H}_{28}$ )  **$^{13}\text{C}$  NMR (100 MHz,  $\text{CDCl}_3/\text{CD}_3\text{OD}$ : 8/2):**  $\delta$  174.1, 173.0, 171.7, 171.0, 170.8, 170.7, 170.6, 170.4, 170.2, 169.9, 156.7, 149.7, 149.2, 141.1, 136.9, 134.5, 133.6, 132.6, 130.4, 129.4, 128.7, 127.1, 124.8, 121.8, 119.3, 100.4, 71.4, 70.9, 68.2, 67.1, 65.3, 61.6, 56.7, 54.9, 52.1, 43.1, 42.8, 37.8, 37.3, 31.4, 30.1, 29.8, 21.1, 20.7 (x2), 20.6 (x2), 15.2 **LRFAB-MS (3-NOBA matrix):**  $m/z$  1143  $[\text{M}+\text{H}]^+$ , 1165  $[\text{M}+\text{Na}]^+$  **HRFAB-MS (3-NOBA matrix):**  $m/z$  1141.3584 (calcd. for  $\text{C}_{51}\text{H}_{61}\text{N}_6\text{O}_{22}\text{S}$  1141.3560  $[\text{M}+\text{H}]^+$ ) **m.p.** 170-172°C



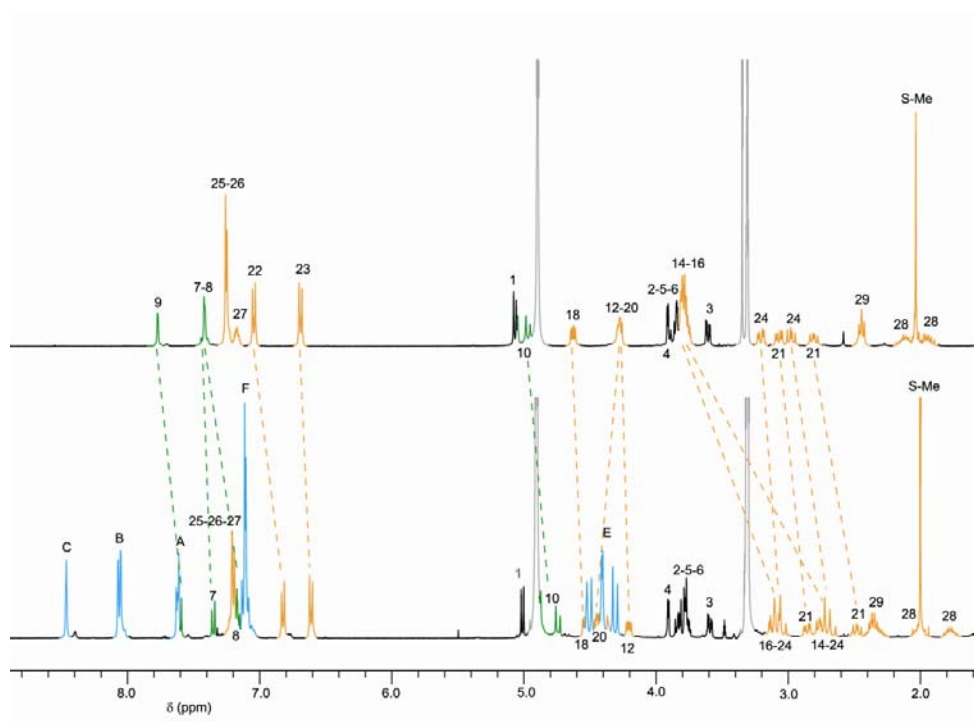
To a solution of **S14** (54 mg, 0.047 mmol) in MeOH (7 mL) cooled in an ice-water bath was added dropwise a 0°C solution of MeONa (26 mg, 10.0 equiv.) in MeOH (4 mL). Stirring was continued for one hour at 0°C and the solution was neutralized with Amberlite IR-120 and filtered. MeOH was then evaporated and the resulting mixture was purified by column chromatography over silica gel (CH<sub>2</sub>Cl<sub>2</sub>/MeOH: 10 to 50% MeOH) to afford **7** (38 mg, 0.041 mmol, **87%**) as a white brown solid which was then purified by preparative RP-HPLC using a linear gradient (27 to 45% in 15 min) of MeCN (containing 6.6 mM of HCOOH) in H<sub>2</sub>O (containing 6.6 mM of HCOOH) at a flow rate of 10 ml/min to give rotaxane **7** as a white solid. Purity (HPLC): >98%.

**<sup>1</sup>H NMR (400 MHz, CD<sub>3</sub>OD):**  $\delta$  7.76 (bs, 1H, H<sub>9</sub>), 7.41 (bs, 2H, H<sub>7+8</sub>), 7.26 to 7.24 (m, 4H, H<sub>25+26</sub>), 7.19 to 7.16 (m, 1H, H<sub>27</sub>), 7.04 (d, 2H,  $J = 8.0$  Hz, H<sub>22</sub>), 6.69 (d, 2H,  $J = 8.0$  Hz, H<sub>23</sub>), 5.08 (d, 1H,  $J = 7.6$  Hz, H<sub>1</sub>), 5.09 to 4.94 (m, 2H, H<sub>10</sub>), 4.63 (dd, 1H,  $J = 9.2$  Hz,  $J = 4.4$  Hz, H<sub>18</sub>), 4.30 (m, 2H, H<sub>12+20</sub>), 3.93 (d, 1H,  $J = 3.2$  Hz, H<sub>4</sub>), 3.89 to 3.75 (m, 8H, H<sub>2+5+6+14+16</sub>), 3.63 (dd, 1H,  $J = 9.6$  Hz,  $J = 3.2$  Hz, H<sub>3</sub>), 3.21 (dd, 1H,  $J = 14.4$  Hz,  $J = 4.4$  Hz, H<sub>24</sub>), 3.07 (dd, 1H,  $J = 13.6$  Hz,  $J = 5.6$  Hz, H<sub>21</sub>), 2.98 (dd, 1H,  $J = 14.0$  Hz,  $J = 9.6$  Hz, H<sub>24</sub>), 2.81 (dd, 1H,  $J = 13.6$  Hz,  $J = 9.2$  Hz, H<sub>21</sub>), 2.46 (t, 2H,  $J = 8.0$  Hz, H<sub>29</sub>), 2.13 to 2.10 (m, 1H, H<sub>28</sub>), 2.03 (s, 3H, S-CH<sub>3</sub>), 2.00 to 1.93 (m, 1H, H<sub>28</sub>) **<sup>13</sup>C NMR (100 MHz, CD<sub>3</sub>OD):**  $\delta$  177.6, 175.2, 172.8, 172.2, 171.6, 170.0, 158.4, 157.3, 151.0, 141.7, 138.7, 134.3, 132.6, 131.4, 130.4, 129.5, 129.1, 127.8, 125.3, 118.8, 116.3, 102.9, 77.2, 74.8, 72.0, 70.2, 66.1, 62.4, 58.6, 56.5, 55.4, 43.9, 43.4, 38.4, 37.9, 33.6, 31.2, 15.3 **LRESI-MS:  $m/z$  953 [M+Na]<sup>+</sup>** **LRESI-MS (negative mode):  $m/z$  929 [M-H]<sup>-</sup>** **HRESI-MS  $m/z$  948.3287 (calcd. for C<sub>41</sub>H<sub>54</sub>N<sub>7</sub>O<sub>17</sub>S 948.3297 [M+NH<sub>4</sub>]<sup>+</sup>)** **m.p.** 158-160°C

#### 4. Representative Stacked $^1\text{H}$ NMR Plots



$^1\text{H}$  NMR spectra of thread **3** and rotaxane **4**,  
(400 MHz, 298 K,  $\text{CDCl}_3$ )



$^1\text{H}$  NMR spectra of Met-enkephalin prodrug **7** and rotaxane prodrug **1**,  
(400 MHz, 298 K,  $\text{CD}_3\text{OD}$ )

# CHAPT. 4 | TOWARDS A SYNTHETIC MOLECULAR PEPTIDE SYNTHESISER

During the final months of my PhD, I was involved together with Dr. Dominik Heckmann, Dr. Daniel D'Souza and Dr. Stephen Goldup in the construction of a novel rotaxane-based molecular machine designed to sequentially synthesise an oligopeptide unit. In this project, I prepared macrocycle **4.C**, hydroxylamine **4.E** and re-synthesised unit **4.B**.

|   |            |
|---|------------|
| <b>I. Introduction.....</b>                                   | <b>139</b> |
| I.1. Preliminary study .....                                  | 141        |
| <b>II. Synthesis.....</b>                                     | <b>142</b> |
| II.1. Synthesis of aldehyde macrocycle 4.C .....              | 144        |
| II.2. Synthesis of alkyne thread 4.B .....                    | 146        |
| II.3. Synthesis of pyrrolidinopyridine hydroxylamine 4.E..... | 148        |
| <b>III. Discussion and outlook.....</b>                       | <b>148</b> |
| <b>IV. Supporting information.....</b>                        | <b>150</b> |

## I. Introduction

Rotaxanes constitute interesting molecular architectures for the construction of nanoscale devices and have inspired numerous attempts to create artificial machines.<sup>119</sup> In nature, the accurate synthesis of biopolymers such as nucleic acids or proteins relies primarily on complex macromolecular machines. The ribosome, for instance, is used in cells to catalyse the assembly of individual amino acids into polypeptides. The ribosome translates each codon expressed in the mRNA strand into a peptide chain using the appropriate amino acids provided by tRNA. The high level of processivity and accuracy displayed by the transcription machinery is the consequence of its unusual arrangement with the mRNA template.<sup>120</sup> The ribosome forms a sort of dynamic clamp which holds the mRNA template, as in rotaxanes, and unidirectionally shuttles along it to read and translate the genetic information.

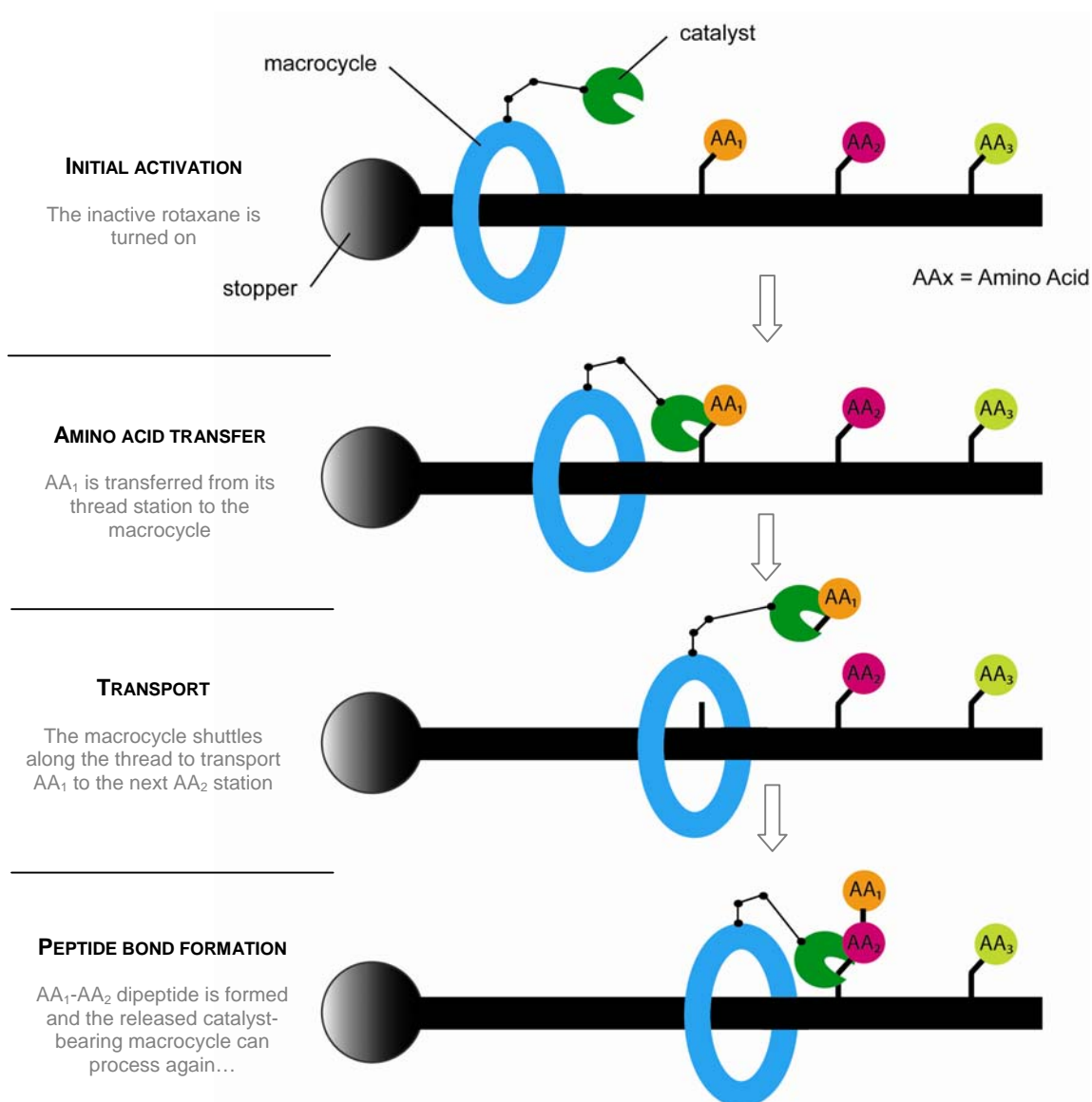
Therefore, encouraged by such a remarkable biological process we devised a rotaxane that might be capable of assembling a peptide from the amino acid information carried by the thread subunit. Thus our prototype rotaxane consists of a macrocycle, displaying catalyst and transporter properties, entrapped around a template thread possessing three distinctive amino acid stations (**Scheme 4.1**).

Accordingly, following activation of the rotaxane machine, the macrocycle unit shuttles and catalyses the undocking of the first amino acid (AA<sub>1</sub>). Transport of AA<sub>1</sub> along the thread and reaction with the second amino acid (AA<sub>2</sub>) simultaneously forms dipeptide AA<sub>1</sub>-AA<sub>2</sub> and releases the active catalyst, which can in turn uncouple the dipeptide cargo from the thread. Processively, the machine would prepare the tripeptide AA<sub>1</sub>-AA<sub>2</sub>-AA<sub>3</sub> in a sequence specific manner.

---

<sup>119</sup> a) Balzani, V.; Credi, A.; Raymo, E. M.; Stoddart, J. F. *Angew. Chem. Int. Ed.* **2000**, *39*, 3348-3491; b) Kay, E. R.; Leigh, D. A.; Zerbetto, F. *Angew. Chem. Int. Ed.* **2007**, *46*, 72-191.

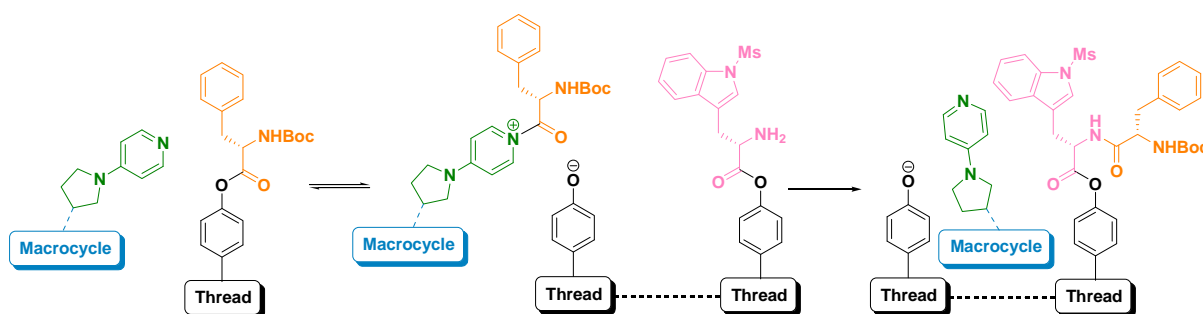
<sup>120</sup> Patrick, G. L. *An Introduction to Medicinal Chemistry (Fourth Edition)* **2009**, Oxford University Press.



**Scheme 4.1** | Operation of the rotaxane-based peptide synthesiser

The operation of our machine relies on acyl-transfer catalysis. Indeed the catalytic moiety carried by the macrocycle (a pyrrolidinopyridine, PPY) is designed to mediate the transfer of the amino acid building blocks to the adjacent station on the track. Each amino acid is anchored to the thread as a phenolic ester. Phenolic esters of the amino acids were chosen as acyl donors to maintain the balance between the stability needed for the synthesis of the target rotaxane and the lability towards nucleophilic attack of the catalyst.

Consecutively the macrocycle transports the peptide as an activated pyridinium species to react with the second *N*-free amino acid station (Scheme 4.2).

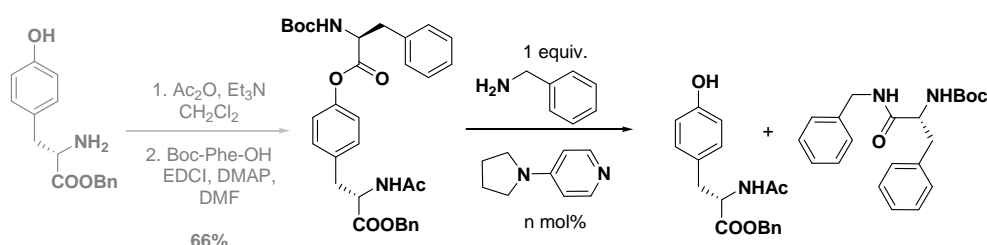


Scheme 4.2 | Acyl-transfer catalysis as a motor mechanism

Such construction implies that the successive phenolic amino acid esters efficiently act as stoppers for the macrocycle, until the latter properly deactivates each station one after the other. Accordingly the high local concentration of the catalyst in the rotaxane architecture should drive the formation of the *N*-acyl pyridinium species which irreversibly reacts to form the new peptide bond. Moreover, high dilution conditions should preclude intermolecular reactions that would lead to unexpected peptide sequences.

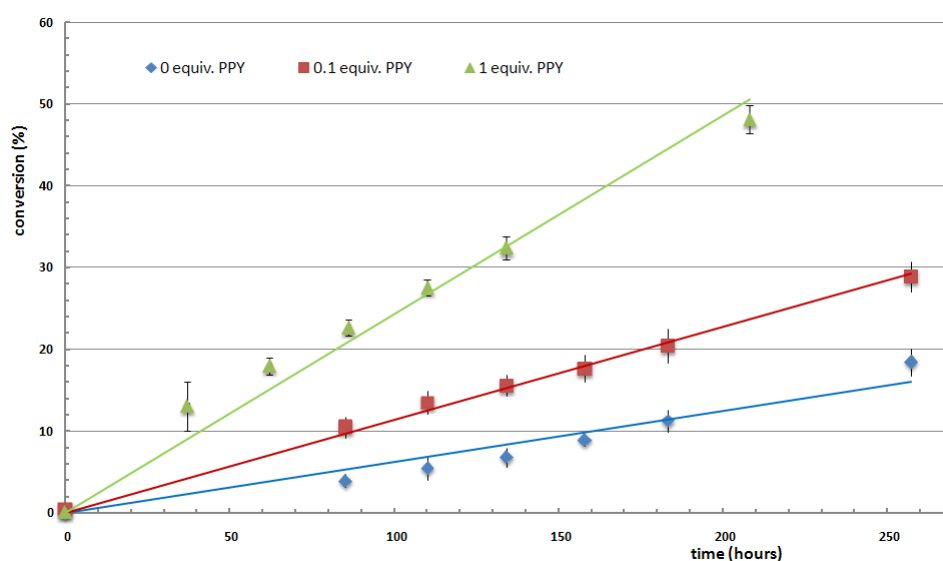
### I.1. Preliminary study

A model system was designed in order to study the kinetics of transacylation of a tyrosine ester using benzyl amine as a model nucleophile (Scheme 4.3).



Scheme 4.3 | Transacylation on a tyrosine ester model

We observed by NMR spectroscopy the reaction of the tyrosine ester ( $33 \mu\text{M}$  in  $\text{CDCl}_3$  – the high dilution in which the molecular machine should work best) with benzylamine (1 equiv.) under the action of different amounts of the PPY catalyst. Results showed that PPY significantly catalyses the transacylation of phenolic esters under high dilution conditions, with a conversion approximatively 4-times higher than without catalyst (**Figure 4.1**). Despite the slow kinetics of the reaction (half-life of 200 hours), further acceleration is expected in the rotaxane structure since the interlocked macrocycle would provide a high local concentration of the PPY catalyst.



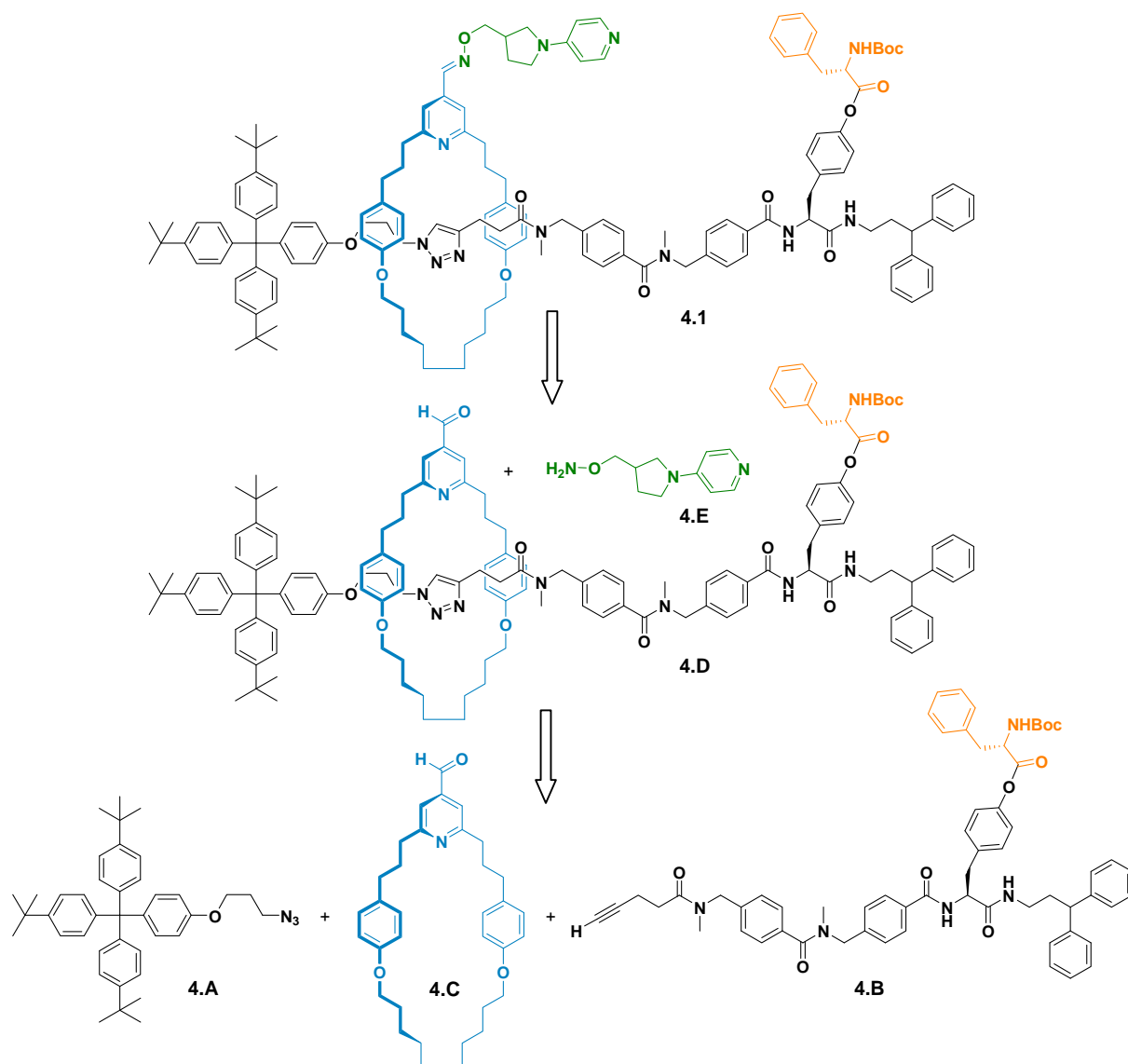
**Figure 4.1** | Transacylation on a tyrosine ester model observed by  $^1\text{H}$  NMR spectroscopy ( $33 \mu\text{M}$  in  $\text{CDCl}_3$ )

## II. Synthesis

Initially, we proposed the preparation of a rotaxane possessing the general structure depicted in **Figure 4.2** using the CuCAAC active-template methodology recently reported in our group.<sup>121</sup> Reaction of the alkyne thread with an azide stopper within the cavity of an endopyridine-bearing macrocycle should promote efficient access to the interlocked architecture. The alkyne thread was designed to consist of peptidic building blocks, each of them bearing two *N*-methyl(aminomethyl)benzoic acids and one tyrosine.

<sup>121</sup> Aucagne, V.; Hänni, K.; Leigh, D. A.; Lusby, P. J.; Walker, D. B. *J. Am. Chem. Soc.* **2006**, *128*, 2186-2187.

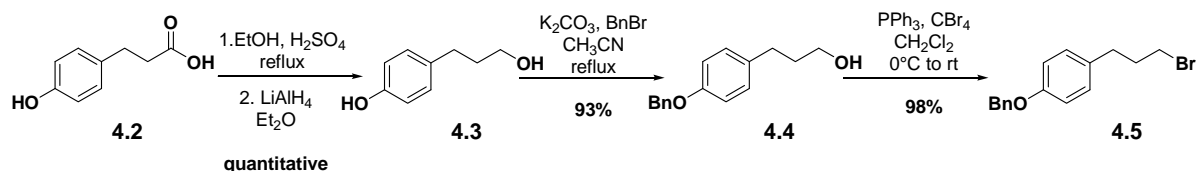




**Scheme 4.4** | Convergent approach to model rotaxane **4.1**

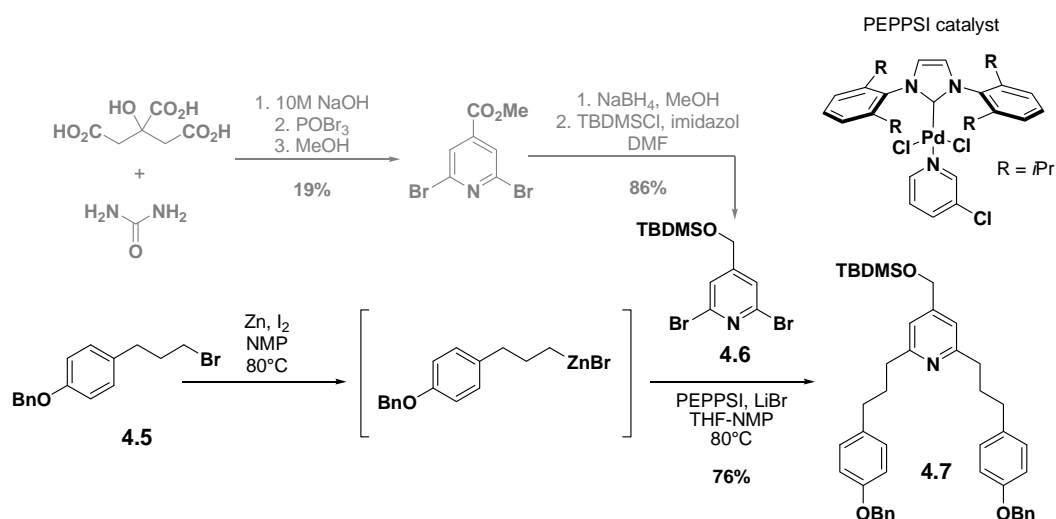
## II.1. Synthesis of aldehyde macrocycle **4.C**

Synthesis of macrocycle **4.C** started simply by preparation of building block **4.5**. Reduction of commercially available 3-(4-hydroxyphenyl)propionic acid **4.2** afforded hydroxy phenol **4.3**. Benzylation of the phenolic position followed by bromination of primary alcohol **4.4** afforded intermediate **4.5** in excellent yields (**Scheme 4.5**).



Scheme 4.5 | Synthesis of 4.5

An organozinc derivative was prepared from bromide **4.5** using the procedure described by Huo.<sup>122</sup> This was then subjected to a PEPPSI (Pyridine-Enhanced Precatalyst Preparation Stabilisation and Initiation)-catalysed Negishi coupling with dibromo pyridine **4.6** (prepared by Dr. Daniel D'Souza) (Scheme 4.6).<sup>123</sup>

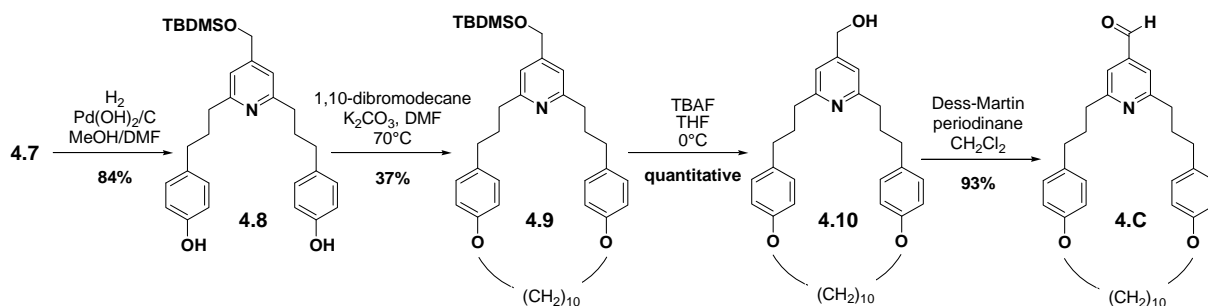


Scheme 4.6 | Synthesis of U-shape 4.7

The U-shape **4.7** was debenzylated by hydrogenolysis using Pearlman's catalyst ( $\text{Pd}(\text{OH})_2/\text{C}$ ). Double Williamson macrocyclisation of *bis*-phenol **4.8** with 1,10-dibromodecane at high dilution afforded pyridine macrocycle **4.9** in 37% yield, which after TBDMS deprotection and Dess-Martin oxidation yielded aldehyde macrocycle **4.C** (Scheme 4.7).

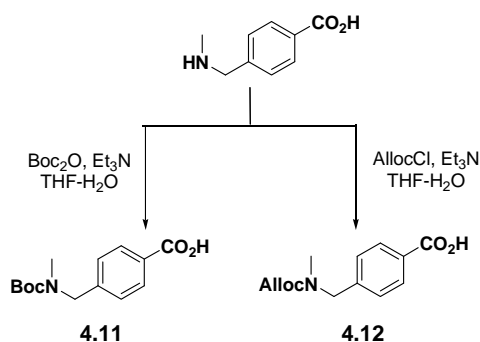
<sup>122</sup> Huo, S. *Org. Lett.* **2003**, *5*, 423-425.

<sup>123</sup> Organ, M. G.; Avola, S.; Dubovyk, I.; Hadei, N.; Kantchev, E. A. B.; O'Brien, C. J.; Valente, C. *Chem. Eur. J.* **2006**, *12*, 4749-4755.

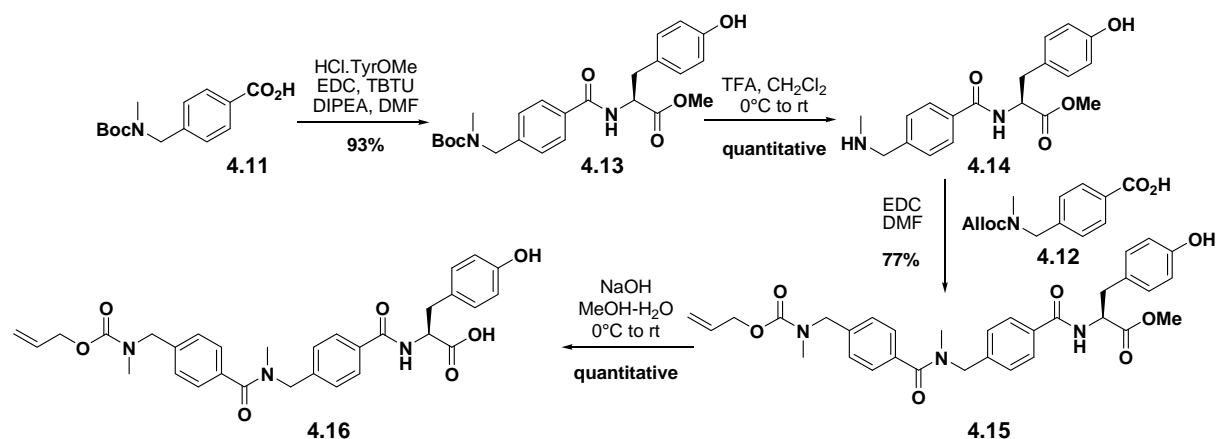

 Scheme 4.7 | Synthesis of aldehyde macrocycle **4.C**

## II.2. Synthesis of alkyne thread **4.B**

Thread building block **4.16** has been designed to serve as a monomer for the preparation of the multi-station rotaxane track. Boc- and Alloc-protected derivatives (**4.11** and **4.12** respectively) were prepared from *N*-methylated 4-aminomethylbenzoic acid (Scheme 4.8).

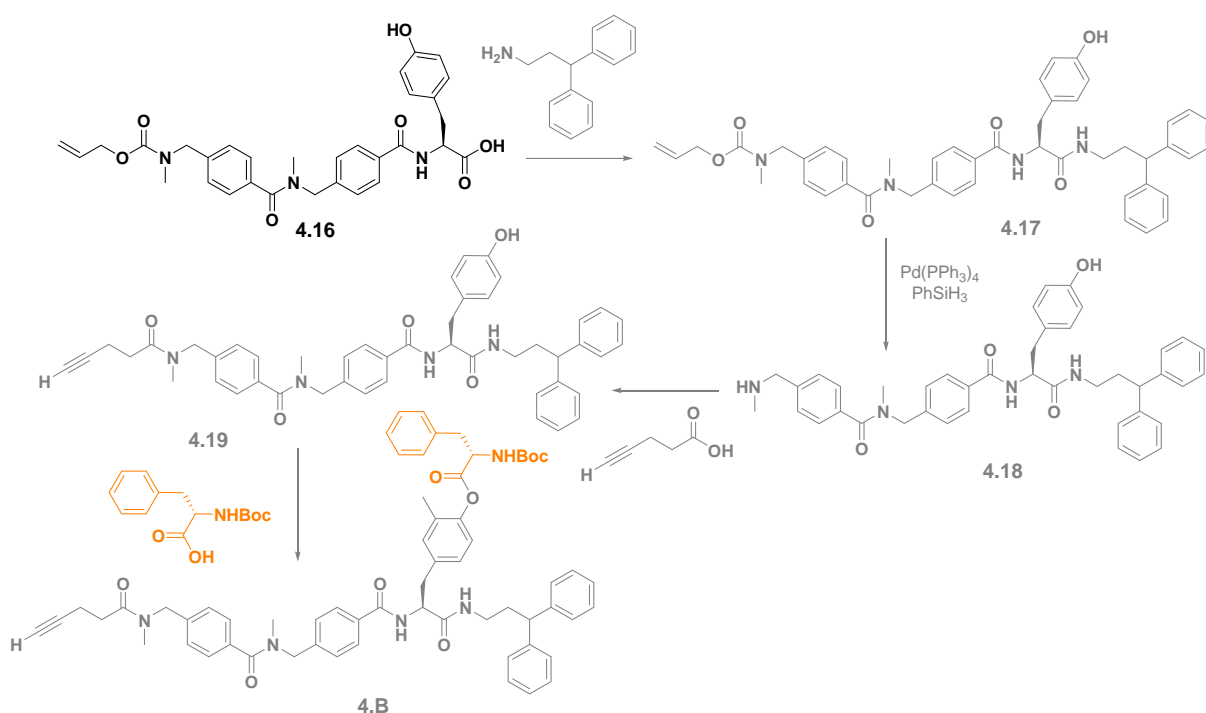

 Scheme 4.8 | Preparation of intermediates **4.11** and **4.12**

Boc-derivative **4.11** was coupled with tyrosine methyl ester hydrochloride to afford **4.13**. Boc-deprotection afforded *N*-methyl benzylamine **4.14** which was further reacted with the Alloc-protected benzoic acid **4.12**. Tyrosine methyl ester was hydrolysed to yield **4.16**, which was as far as I progressed with this synthesis (Scheme 4.9).



Scheme 4.9 | Synthesis of building block 4.16

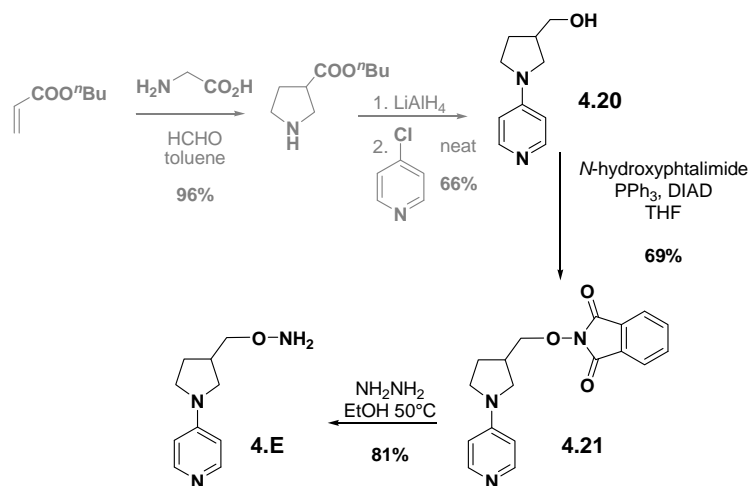
Coupling of the resulting carboxylic acid **4.16** with 3,3-diphenylpropylamine will give tyrosine derivative **4.17**. Subsequent palladium-mediated Alloc deprotection will afford intermediate **4.18**. Reaction of the resulting secondary amine **4.18** with 4-pentynoic acid will afford alkyne thread **4.19**. Finally, formation of phenolic ester with *N*-Boc phenylalanine will yield alkyne thread **4.B** (Scheme 4.10).



Scheme 4.10 | Access to alkyne thread 4.B

### II.3. Synthesis of pyrrolidinopyridine hydroxylamine 4.E

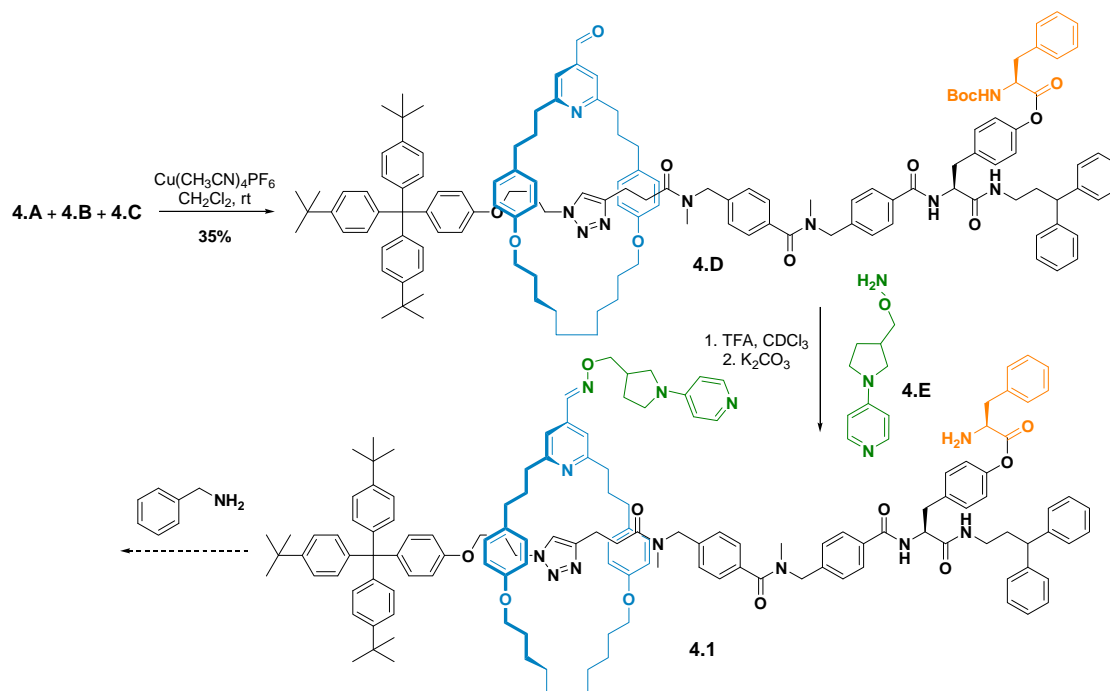
Hydroxylamine **4.E** was prepared starting with pyrrolidinopyridine **4.20** (prepared by Dr. Dominik Heckmann) (Scheme 4.11). The hydroxylamine moiety was introduced by Mitsunobu reaction of alcohol **4.20** with *N*-hydroxyphthalimide **4.21**. Hydrazinolysis of **4.21** finally gave hydroxylamine **4.E**.



Scheme 4.11 | Synthesis of fragment **4.E**

### III. Discussion and outlook

To date, aldehyde rotaxane **4.D** has been successfully synthesised and isolated in a reasonable 35% yield. Assembly of the final machine was monitored by NMR. Acid-catalysed oxime ligation of aldehyde rotaxane **4.D** with hydroxylamine **4.E** afforded the Boc-protected one-station rotaxane TFA salt in short reaction times and nearly quantitative conversion by NMR. The mixture was then passed through a pad of potassium carbonate to give the one-station rotaxane **4.1** (Scheme 4.12).

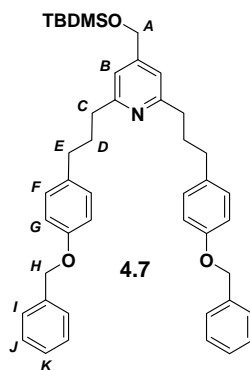

**Scheme 4.12** | Recent results

However, against all expectations, no evidence was found to demonstrate the function of our machine. The intramolecular catalyst did not react with the tyrosine ester and no reaction could be observed, even on addition of an external nucleophile. As initial model studies on the PPY-catalysed aminolysis of tyrosine esters displayed a reaction rate proportional to the catalyst concentration, this would mean that one premise – a high local concentration of catalyst – was not met by the system. Saponification ( $\text{MeOH}$ ,  $\text{K}_2\text{CO}_3$ ) resulted in cleavage of the ester and loss of the macrocycle for both rotaxanes **4.D** and **4.1**.

Accordingly, several factors can be considered. First of all, phenolic esters are too stable against the attack of the trans-acylation catalyst, that means the equilibrium between the acyl-pyridinium and the ester lies almost totally on the side of the ester. On the other hand, folding of the thread can prevent the shuttle of the macrocycle which then cannot reach the amino acid station. Our intention was that this would be prevented by the use of *N*-methylated peptide bonds in the thread as such bonds tend to decrease the energy barrier between *cis*- and *trans*-amide bonds thus favouring flexibility of the backbone. Indeed a general line broadening along with the presence of two sets of signals per *N*-methylated amide bond has been observed in NMR spectra, which means that the interconversion between *cis*- and *trans* peptide bonds occurs on the NMR-timescale.

Finally, it can be envisaged that the acyl-transfer catalyst grafted on the macrocycle is inappropriate. Different solutions are now being thought of to construct an improved 2<sup>nd</sup> generation design for the rotaxane-based peptide synthesiser (*e.g.* labile *o*-nitro-tyrosine esters on the thread, an additional thiol-based transporter on the macrocycle).

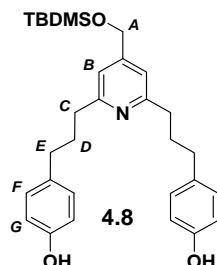
#### IV. Supporting information



To a solution of Zn dust (2.31 g, 1.5 equiv.) in NMP (24 mL, 1M) was added I<sub>2</sub> (299 mg, 0.05 equiv.). After the coloration vanished 3-[4-(benzyloxy)phenyl]propyl bromide (7.18 g, 23.50 mmol) was added and the mixture heated at 80°C for 7 hours. The mixture was then allowed to reach room temperature. In another flask, PEPPSI (Pyridine-Enhanced Precatalyst Preparation Stabilisation and Initiation) catalyst (160 mg, 0.01 equiv.) was dissolved in THF (24 mL) / NMP (24 mL) and LiBr (4.10 g, 2.0 equiv.) was added. When all solids had dissolved, the organozinc solution was added followed by the substituted 2,6-dibromopyridine (2.70 g, 0.3 equiv.). The resulting solution was then stirred overnight at room temperature and, after this time the mixture was diluted with diethyl ether and brine was added. The aqueous layer was extracted with diethyl ether and the combined organic layers washed several times with water. After drying (MgSO<sub>4</sub>), the solution was filtered and concentrated under reduced pressure. Purification by column chromatography over silica gel (petroleum ether/ethyl acetate: 5 then 15% ethyl acetate) yielded **4.7** as a yellowish oil (3.60 g, 5.36 mmol, **76%**).

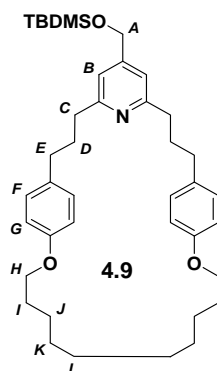
**<sup>1</sup>H NMR (400 MHz, CDCl<sub>3</sub>):**  $\delta$  7.50 to 7.35 (m, 10H, H<sub>I+J+K</sub>), 7.19 (d, 4H, *J* = 8.0 Hz, H<sub>F</sub>), 6.96 to 7.00 (m, 6H, H<sub>B+G</sub>), 5.09 (s, 4H, H<sub>H</sub>), 4.76 (s, 2H, H<sub>A</sub>), 2.89 (t, 4H, *J* = 7.6 Hz, H<sub>C</sub>), 2.71 (t, 4H, *J* = 7.6 Hz, H<sub>E</sub>), 2.07 to 2.15 (m, 4H, H<sub>D</sub>), 1.05 (s, 9H, *H*-Si-*t*Bu), 0.20 (s, 6H, *H*-

SiMe<sub>2</sub>) <sup>13</sup>C NMR (100 MHz, CDCl<sub>3</sub>): δ 161.4, 157.0, 151.0, 137.3, 134.7, 129.4, 128.6, 127.9, 127.5, 117.0, 114.7, 70.0, 63.8, 38.0, 34.7, 32.0, 26.0 LRESI-MS: *m/z* 672 [M+H]<sup>+</sup> HRESI-MS: *m/z* 672.3859 (calcd. for C<sub>44</sub>H<sub>54</sub>NO<sub>3</sub>Si 672.3868 [M+H]<sup>+</sup>)



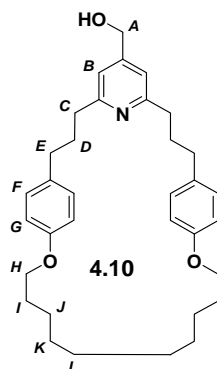
To a solution of **4.7** (1.09 g, 1.62 mmol) in MeOH (50 mL)/DMF (10 mL) was added Pd(OH)<sub>2</sub> on carbon (109 mg, 10% by weight). The solution was degassed under low pressure and H<sub>2</sub> was added. After two days stirring, the resulting mixture was filtered over celite and the pad washed with MeOH. The solution was then concentrated under reduced pressure and purified by column chromatography over silica gel (petroleum ether/ethyl acetate: 15 to 50% ethyl acetate then DCM/MeOH: 10% MeOH) to afford **4.8** as a yellowish oil (670 mg, 1.36 mmol, **84%**).

<sup>1</sup>H NMR (400 MHz, CDCl<sub>3</sub>): δ 7.23 (s, 2H, H<sub>B</sub>), 7.12 (d, 4H, *J* = 8.4 Hz, H<sub>F</sub>), 6.94 (d, 4H, *J* = 8.4 Hz, H<sub>G</sub>), 4.96 (s, 2H, H<sub>A</sub>), 3.05 (t, 4H, *J* = 7.6 Hz, H<sub>C</sub>), 2.76 (t, 4H, *J* = 7.6 Hz, H<sub>E</sub>), 2.15 to 2.23 (m, 4H, H<sub>D</sub>), 1.20 (s, 9H, *H*-Si-*t*Bu), 0.37 (s, 6H, *H*-SiMe<sub>2</sub>) <sup>13</sup>C NMR (100 MHz, CDCl<sub>3</sub>): δ 163.0, 161.4, 154.8, 152.5, 133.0, 129.4, 117.7, 115.4, 63.8, 37.1, 34.8, 32.2, 26.0 LRESI-MS: *m/z* 492 [M+H]<sup>+</sup> HRESI-MS: *m/z* 492.2937 (calcd. for C<sub>30</sub>H<sub>42</sub>NO<sub>3</sub>Si 492.2929 [M+H]<sup>+</sup>)



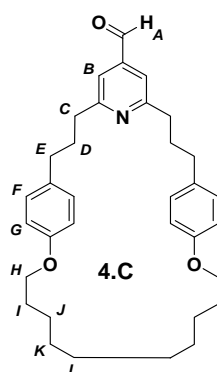
To a solution of **4.8** (670 mg, 1.36 mmol) in DMF (680 mL, 2 mM) was added  $K_2CO_3$  (3.76 g, 20.0 equiv.) and 1,10-dibromodecane (409 mg, 1.0 equiv.) and the resulting suspension stirred at 70°C for two days. The solvent was removed under reduced pressure and the residue dissolved in Ethyl acetate. This solution was washed with sat. aqueous  $NaHCO_3$  and the aqueous layer extracted with ethyl acetate. The resulting organic layers were washed with water, dried ( $MgSO_4$ ) and concentrated *in vacuo*. Purification by column chromatography over silica gel (petroleum ether then petroleum ether/ethyl acetate: 10% ethyl acetate) yielded **4.9** as a colourless oil that crystallised upon standing (314 mg, 0.50 mmol, **37%**).

**$^1H$  NMR (400 MHz,  $CDCl_3$ ):**  $\delta$  7.06 (d, 4H,  $J = 8.4$  Hz,  $H_F$ ), 6.93 (s, 2H,  $H_B$ ), 6.77 (d, 4H,  $J = 8.4$  Hz,  $H_G$ ), 4.70 (s, 2H,  $H_A$ ), 3.94 (t, 4H,  $J = 6.4$  Hz,  $H_H$ ), 2.79 (t, 4H,  $J = 7.6$  Hz,  $H_C$ ), 2.59 (t, 4H,  $J = 8.0$  Hz,  $H_E$ ), 1.95 to 2.03 (m, 4H,  $H_D$ ), 1.75 (qt, 4H,  $J = 6.8$  Hz,  $H_I$ ), 1.43 to 1.46 (m, 4H,  $H_J$ ), 1.31 (bs, 8H,  $H_{K+L}$ ), 0.97 (s, 9H,  $H-Si-tBu$ ), 0.13 (s, 6H,  $H-SiMe_2$ )  **$^{13}C$  NMR (100 MHz,  $CDCl_3$ ):**  $\delta$  161.5, 157.3, 134.5, 129.4, 117.2, 114.6, 67.6, 63.9, 38.2, 34.9, 32.6, 29.0, 28.8, 28.4, 26.1, 25.7 **LRESI-MS:**  $m/z$  630  $[M+H]^+$  **HRESI-MS:**  $m/z$  630.4328 (calcd. for  $C_{40}H_{60}NO_3Si$  630.4337  $[M+H]^+$ ) **m.p.** 71-73°C



To a solution of **4.9** (100 mg, 0.16 mmol) in THF (5 mL) cooled to 0°C was added TBAF (0.2 mL, 1M in THF) and the solution stirred for 30 minutes at 0°C. The resulting mixture was then concentrated under reduced pressure and purified by column chromatography over silica gel (petroleum ether then petroleum ether/ethyl acetate: 20 to 50% ethyl acetate) yielded **4.10** as a white solid (83 mg, 0.16 mmol, **quant.**).

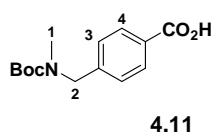
**<sup>1</sup>H NMR (400 MHz, CDCl<sub>3</sub>):**  $\delta$  7.05 (d, 4H,  $J$  = 8.4 Hz, H<sub>F</sub>), 6.95 (s, 2H, H<sub>B</sub>), 6.77 (d, 4H,  $J$  = 8.4 Hz, H<sub>G</sub>), 4.65 (s, 2H, H<sub>A</sub>), 3.94 (t, 4H,  $J$  = 6.4 Hz, H<sub>H</sub>), 2.79 (t, 4H,  $J$  = 7.6 Hz, H<sub>C</sub>), 2.58 (t, 4H,  $J$  = 8.0 Hz, H<sub>E</sub>), 1.95 to 2.03 (m, 4H, H<sub>D</sub>), 1.72 to 1.79 (m, 4H, H<sub>I</sub>), 1.45 (t, 4H,  $J$  = 6.4 Hz, H<sub>J</sub>), 1.31 (bs, 8H, H<sub>K+L</sub>) **<sup>13</sup>C NMR (100 MHz, CDCl<sub>3</sub>):**  $\delta$  161.7, 157.3, 150.6, 134.4, 129.4, 117.7, 114.6, 67.7, 63.7, 38.0, 34.9, 32.4, 28.9, 28.8, 28.4, 25.7 **LRESI-MS:**  $m/z$  517 [M+H]<sup>+</sup> **HRESI-MS:**  $m/z$  516.3477 (calcd. for C<sub>34</sub>H<sub>46</sub>NO<sub>3</sub> 516.3472 [M+H]<sup>+</sup>) **m.p.** 104-106°C



To a solution of macrocycle **4.10** (228 mg, 0.44 mmol) in CH<sub>2</sub>Cl<sub>2</sub> (20 mL) was added Dess-Martin periodinane (234 mg, 1.25 equiv.) at 0°C. The reaction was then allowed to reach room temperature and stirred for 4 hours. The resulting mixture was then concentrated under reduced pressure and purified by column chromatography over silica gel (petroleum

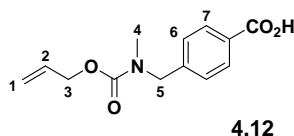
ether/ethyl acetate: 20% ethyl acetate) to yield **4.C** as a colourless oil that crystallised upon standing (210 mg, 0.41 mmol, **93%**).

**<sup>1</sup>H NMR (400 MHz, CDCl<sub>3</sub>):**  $\delta$  10.03 (s, 1H, H<sub>A</sub>), 7.38 (s, 2H, H<sub>B</sub>), 7.08 (d, 4H,  $J = 8.4$  Hz, H<sub>F</sub>), 6.80 (d, 4H,  $J = 8.4$  Hz, H<sub>G</sub>), 3.96 (t, 4H,  $J = 6.4$  Hz, H<sub>H</sub>), 2.91 (t, 4H,  $J = 7.6$  Hz, H<sub>C</sub>), 2.63 (t, 4H,  $J = 7.6$  Hz, H<sub>E</sub>), 2.09 to 2.02 (m, 4H, H<sub>D</sub>), 1.80 to 1.74 (m, 4H, H<sub>I</sub>), 1.48 to 1.45 (m, 4H, H<sub>J</sub>), 1.33 (bs, 8H, H<sub>K+L</sub>) **<sup>13</sup>C NMR (100 MHz, CDCl<sub>3</sub>):**  $\delta$  192.4, 163.4, 157.3, 142.4, 134.0, 129.4, 118.8, 114.5, 67.5, 37.9, 34.8, 32.1, 28.9, 28.7, 28.3, 25.6 **LRESI-MS:**  $m/z$  547 [M+Na]<sup>+</sup> **HRESI-MS:**  $m/z$  514.3318 (calcd. for C<sub>34</sub>H<sub>44</sub>NO<sub>3</sub> 514.3316 [M+H]<sup>+</sup>) **m.p.** 52-54°C



To a solution of *N*-methylated 4-aminomethylbenzoic acid (12.00 g, 26.80 mmol) in THF-H<sub>2</sub>O (200 mL-100 mL) cooled to 0°C was added Et<sub>3</sub>N (7.5 mL, 2.0 equiv.) and Boc<sub>2</sub>O (5.90 g, 1.0 equiv.). The resulting mixture was allowed to reach room temperature and then stirred overnight. After concentration under reduced pressure, the aqueous layer was extracted with Et<sub>2</sub>O and acidified with 1N HCl. The resulting acidic aqueous layer was then extracted with ethyl acetate, dried (MgSO<sub>4</sub>) and concentrated to give **4.11** as a white powder (7.50 g, 28.30 mmol). (**4.11** Registry Number: 210963-04-05)

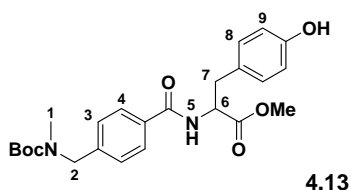
**<sup>1</sup>H NMR (400 MHz, CDCl<sub>3</sub>):**  $\delta$  8.08 (d, 2H,  $J = 8.0$  Hz, H<sub>4</sub>), 7.32 (d, 2H,  $J = 8.0$  Hz, H<sub>3</sub>), 4.49 (bs, 2H, H<sub>2</sub>), 2.90 and 2.82 (m, 3H, H<sub>1</sub>), 1.50 and 1.45 (m, 9H, *H-t*Bu) **<sup>13</sup>C NMR (100 MHz, CDCl<sub>3</sub>):**  $\delta$  171.8, 156.4, 155.9, 144.5, 130.6, 128.5, 127.6, 127.1, 80.3, 52.7, 52.0, 34.5, 34.4, 28.5 **LRESI-MS:**  $m/z$  266 [M+H]<sup>+</sup> **HRESI-MS:**  $m/z$  266.1382 (calcd. for C<sub>14</sub>H<sub>20</sub>NO<sub>4</sub> 166.1387 [M+H]<sup>+</sup>) **m.p.** 119-121°C



To a solution of *N*-methylated 4-aminomethylbenzoic acid (10.40 g, 23.30 mmol) in THF-H<sub>2</sub>O (100 mL-100 mL) cooled to 0°C was added Et<sub>3</sub>N (6.5 mL, 2.0 equiv.) and allyl

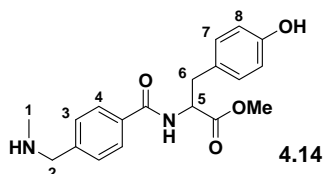
chloroformate (2.5 mL, 1.0 equiv.). The resulting mixture was then allowed to reach room temperature and stirred overnight. After concentration under reduced pressure, the aqueous layer was extracted with Et<sub>2</sub>O and acidified with 1N HCl. The resulting acid layer was then extracted with ethyl acetate, dried (MgSO<sub>4</sub>) and concentrated to give **4.12** as a white powder (3.90 g, 15.70 mmol).

**<sup>1</sup>H NMR (400 MHz, CDCl<sub>3</sub>):** δ 11.00 (bs, 1H, COOH), 8.08 (d, 2H, *J* = 8.0 Hz, H<sub>7</sub>), 7.31 to 7.36 (m, 2H, H<sub>6</sub>), 5.88 to 6.01 (m, 1H, H<sub>2</sub>), 5.18 to 5.36 (m, 2H, H<sub>1</sub>), 4.66 (bs, 2H, H<sub>3</sub>), 4.57 (bs, 2H, H<sub>5</sub>), 2.94 and 2.89 (m, 3H, H<sub>4</sub>) **<sup>13</sup>C NMR (100 MHz, CDCl<sub>3</sub>):** δ 171.7, 156.9, 156.3, 143.8, 133.0, 132.9, 130.7, 128.7, 127.8, 127.3, 117.8, 117.6, 66.5, 52.6, 52.3, 34.8, 34.0 **LRESI-MS:** *m/z* 250 [M+H]<sup>+</sup> **HRESI-MS:** *m/z* 250.1069 (calcd. for C<sub>13</sub>H<sub>16</sub>NO<sub>4</sub> 250.1074 [M+H]<sup>+</sup>) **m.p.** 59-61°C



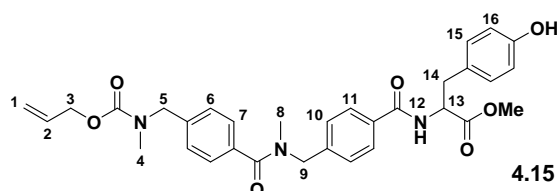
To a solution of **4.11** (2.45 g, 9.20 mmol) and HCl.TyrOMe (2.14 g, 1.0 equiv.) in DMF (50 mL) was added EDC (1.80 g, 1.0 equiv.), HOBT (1.40 g, 1.1 equiv.) and DIPEA (1.8 mL, 1.1 equiv.). After stirring overnight the solution was concentrated under reduced pressure. The resulting oil was diluted with ethyl acetate, washed with water, brine, dried (MgSO<sub>4</sub>) and concentrated. Purification by column chromatography over silica gel (petroleum ether/ethyl acetate: 50 to 65% ethyl acetate) yielded **4.13** as a white solid (3.10 g, 7.00 mmol, **76%**).

**<sup>1</sup>H NMR (400 MHz, CDCl<sub>3</sub>):** δ 7.59 (d, 2H, *J* = 7.6 Hz, H<sub>4</sub>), 7.26 (d, 2H, *J* = 7.6 Hz, H<sub>3</sub>), 6.97 (d, 2H, *J* = 8.4 Hz, H<sub>8</sub>), 6.75 (d, 2H, *J* = 8.4 Hz, H<sub>9</sub>), 6.58 (d, 2H, *J* = 7.6 Hz, H<sub>5</sub>), 5.04 (dd, 1H, *J* = 13.2 Hz, *J* = 5.6 Hz, H<sub>6</sub>), 4.45 (bs, 2H, H<sub>2</sub>), 3.77 (bs, 3H, OMe), 3.21 and 3.13 (dd, AB system, 2H, *J* = 14.0 Hz, *J* = 5.6 Hz, H<sub>7</sub>), 2.85 and 2.80 (m, 3H, H<sub>1</sub>), 1.49 and 1.45 (m, 9H, *H-t*Bu) **<sup>13</sup>C NMR (100 MHz, CDCl<sub>3</sub>):** δ 172.3, 155.3, 132.9, 130.6, 127.5 (x2), 115.7, 53.8, 52.6, 37.2, 34.4, 28.6 **LRESI-MS:** *m/z* 466 [M+Na]<sup>+</sup> **HRESI-MS:** *m/z* 465.1997 (calcd. for C<sub>24</sub>H<sub>30</sub>N<sub>2</sub>O<sub>6</sub>Na 465.1996 [M+Na]<sup>+</sup>) **m.p.** 48-50°C



Trifluoroacetic acid (19.5 mL, 40.0 equiv.) was added dropwise to a solution of **4.13** (2.90 g, 6.60 mmol) in CH<sub>2</sub>Cl<sub>2</sub> (70 mL) at 0°C. After 30 minutes at 0°C, the solution was stirred for a further 2 hours at room temperature and then cooled to 0°C. After neutralisation with a saturated solution of NaHCO<sub>3</sub>, the mixture was extracted with a CHCl<sub>3</sub>/*i*PrOH (3/1, v/v) mixture, dried (MgSO<sub>4</sub>) and evaporated to give **4.14** (2.26 g, 6.60 mmol, **quant.**) as a white solid.

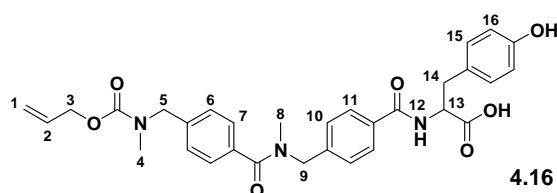
**<sup>1</sup>H NMR (400 MHz, CD<sub>3</sub>OD):** δ 7.69 (d, 2H, *J* = 8.0 Hz, H<sub>4</sub>), 7.37 (d, 2H, *J* = 8.0 Hz, H<sub>3</sub>), 7.02 (d, 2H, *J* = 8.4 Hz, H<sub>7</sub>), 6.65 (d, 2H, *J* = 8.4 Hz, H<sub>8</sub>), 4.73 (dd, 1H, *J* = 9.2 Hz, *J* = 6.0 Hz, H<sub>5</sub>), 3.76 (bs, 2H, H<sub>2</sub>), 3.67 (bs, 3H, OMe), 3.14 and 2.98 (dd, AB system, 2H, *J* = 14.0 Hz, *J* = 6.0 Hz, H<sub>6</sub>), 2.37 (s, 3H, H<sub>1</sub>) **<sup>13</sup>C NMR (100 MHz, CD<sub>3</sub>OD):** δ 173.8, 169.9, 157.4, 143.3, 134.4, 131.3, 129.8, 129.1, 128.8, 116.3, 56.2, 55.5, 52.8, 37.4, 35.2 **LRFAB-MS (3-NOBA matrix):** *m/z* 343 [M+H]<sup>+</sup> **HRFAB-MS (3-NOBA matrix):** *m/z* 343.1645 (calcd. for C<sub>19</sub>H<sub>23</sub>N<sub>2</sub>O<sub>4</sub> 343.1652 [M+H]<sup>+</sup>) **m.p.** 153-155°C



To a solution of **4.12** (2.00 g, 1.2 equiv.) and **4.14** (1.20 g, 4.80 mmol) in DMF (26 mL) was added EDC (1.20 g, 1.2 equiv.). After stirring overnight at room temperature the solution was concentrated under reduced pressure. The resulting oil was extracted with ethyl acetate, washed with water, brine, dried (MgSO<sub>4</sub>) and concentrated. Purification by column chromatography over silica gel (petroleum ether/ethyl acetate: 50 to 100% ethyl acetate) yielded **4.15** as a white solid (2.10 g, 3.70 mmol, **77%**).

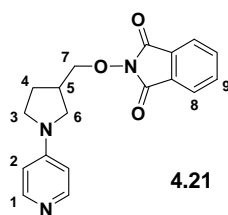
**<sup>1</sup>H NMR (400 MHz, CDCl<sub>3</sub>):** δ 7.71 (d, 2H, *J* = 8.0 Hz, H<sub>11</sub>), 7.39 to 7.20 (m, 6H, H<sub>6+7+10</sub>), 6.94 (d, 2H, *J* = 8.0 Hz, H<sub>15</sub>), 6.75 (d, 2H, *J* = 8.4 Hz, H<sub>16</sub>), 6.63 (bs, 1H, H<sub>12</sub>), 5.94 (bs, 1H,

H<sub>2</sub>), 5.33 to 5.21 (m, 2H, H<sub>3</sub>), 5.02 (dd, 1H,  $J = 13.2$  Hz,  $J = 5.6$  Hz, H<sub>13</sub>), 4.77 to 4.50 (m, 4H, H<sub>5+9</sub>), 4.63 (bs, 2H, H<sub>1</sub>), 3.76 (s, 3H, OMe), 3.20 and 3.12 (dd, AB system, 2H,  $J = 14.0$  Hz,  $J = 5.6$  Hz, H<sub>14</sub>), 3.06 to 2.88 (m, 6H, H<sub>4+8</sub>) **<sup>13</sup>C NMR (100 MHz, CDCl<sub>3</sub>):**  $\delta$  172.3, 166.8, 155.8, 141.0, 139.5, 134.9, 133.3, 132.9, 130.5, 128.4, 127.9, 127.7, 127.6, 127.5, 127.2, 126.9, 117.7, 117.6, 115.8, 66.5, 55.1, 53.8, 52.6, 52.4, 52.2, 50.9, 37.5, 37.1, 34.7, 33.9 **LRESI-MS:**  $m/z$  575 [M+H]<sup>+</sup> **HRESI-MS:**  $m/z$  574.2548 (calcd. for C<sub>32</sub>H<sub>36</sub>N<sub>3</sub>O<sub>7</sub> 574.2548 [M+H]<sup>+</sup>) **m.p.** 59-61°C



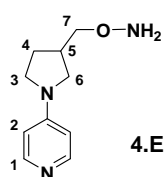
To a solution of **4.15** (3.10 g, 5.40 mmol) in MeOH (50 mL) - H<sub>2</sub>O (20 mL) cooled in an ice-water bath was added dropwise a 0°C solution of NaOH (1.10 g, 5.0 equiv.) in MeOH (15 mL). Stirring was continued for 30 minutes at 0°C then the solution was allowed to reach room temperature and stirred for 4 hours. MeOH was then evaporated under reduced pressure and the resulting mixture extracted with CHCl<sub>3</sub>. The aqueous layer was acidified with 1N HCl and then extracted with a CHCl<sub>3</sub>/*i*PrOH (3/1, v/v) mixture, dried (MgSO<sub>4</sub>) and evaporated to give **4.16** (3.00 g, 5.40 mmol, **quant.**) as a white solid.

**<sup>1</sup>H NMR (400 MHz, CD<sub>3</sub>OD):**  $\delta$  8.41 (d, 0.5H,  $J = 8.0$  Hz, H<sub>12</sub>), 7.76 to 7.23 (m, 8H, H<sub>6+7+10+11</sub>), 7.09 (d, 2H,  $J = 8.4$  Hz, H<sub>15</sub>), 6.69 (d, 2H,  $J = 8.4$  Hz, H<sub>16</sub>), 5.96 (bs, 1H, H<sub>2</sub>), 5.34 to 5.14 (m, 2H, H<sub>3</sub>), 4.79 to 4.52 (m, 7H, H<sub>1+5+9+13</sub>), 3.24 (dd, 1H,  $J = 14.0$  Hz,  $J = 4.8$  Hz, H<sub>14</sub>), 3.05 to 2.88 (m, 7H, H<sub>4+8+14</sub>) **<sup>13</sup>C NMR (100 MHz, CD<sub>3</sub>OD):**  $\delta$  174.2, 173.7, 173.5, 169.6, 169.5, 158.2, 157.7, 157.3, 142.2, 141.8, 141.1, 136.0, 134.5, 134.3, 134.2, 134.1, 131.2, 129.1, 129.0 (x2), 128.8, 128.5, 128.2, 127.9, 117.9, 117.8, 116.3, 67.4, 56.1, 55.8, 53.0, 52.8, 51.6, 49.9, 38.0, 37.3, 35.1, 34.3, 34.0 **LRFAB-MS (3-NOBA matrix):**  $m/z$  560 [M+H]<sup>+</sup> **HRFAB-MS (3-NOBA matrix):**  $m/z$  560.2391 (calcd. for C<sub>31</sub>H<sub>34</sub>N<sub>3</sub>O<sub>7</sub> 560.2391 [M+H]<sup>+</sup>) **m.p.** 76-78°C



Compound **4.20** (585 mg, 3.30 mmol), *N*-hydroxyphthalimide (589 mg, 1.1 equiv.) and  $\text{PPh}_3$  (1.10 g, 1.3 equiv.) were dissolved in THF (30 mL) and cooled to  $0^\circ\text{C}$ . DIAD (0.84 mL, 1.3 equiv.) was then slowly added and then the reaction mixture was allowed to reach temperature. After overnight stirring, the solution was concentrated and purified by column chromatography over silica gel twice (first: DCM/MeOH: 2% to 20% MeOH, second: DCM/MeOH/ $\text{Et}_3\text{N}$ : 2% to 3% MeOH, 0.5%  $\text{Et}_3\text{N}$ ) yielding **4.21** as a white solid (735 mg, 2.28 mmol, **69%**).

**$^1\text{H}$  NMR (400 MHz,  $\text{CDCl}_3$ ):**  $\delta$  8.15 (d, 2H,  $J = 6.4$  Hz,  $\text{H}_1$ ), 7.82 to 7.70 (m, 4H,  $\text{H}_{8+9}$ ), 6.36 (d, 2H,  $J = 6.4$  Hz,  $\text{H}_2$ ), 4.25 (dd, 1H,  $J = 9.2$  Hz,  $J = 6.4$  Hz,  $\text{H}_7$ ), 4.15 (dd, 1H,  $J = 8.8$  Hz,  $J = 7.6$  Hz,  $\text{H}_7$ ), 3.58 (dd, 1H,  $J = 10.0$  Hz,  $J = 7.6$  Hz,  $\text{H}_6$ ), 3.43 to 3.35 (m, 1H,  $\text{H}_3$ ), 3.31 (dd, 2H,  $J = 10.0$ ,  $J = 6.8$  Hz,  $\text{H}_{3+6}$ ), 2.88 to 2.77 (m, 1H,  $\text{H}_5$ ), 2.28 to 2.20 (m, 1H,  $\text{H}_4$ ), 2.00 to 1.91 (m, 1H,  $\text{H}_4$ )  **$^{13}\text{C}$  NMR (100 MHz,  $\text{CDCl}_3$ ):**  $\delta$  163.5, 151.7, 149.1, 134.7, 128.8, 123.6, 107.1, 79.8, 49.8, 46.3, 37.3, 27.6 **LRESI-MS:**  $m/z$  324  $[\text{M}+\text{H}]^+$ , 356  $[\text{M}+\text{Na}]^+$  **HRESI-MS:**  $m/z$  324.1343 (calcd. for  $\text{C}_{18}\text{H}_{18}\text{N}_3\text{O}_3$  324.1343  $[\text{M}+\text{H}]^+$ ) **m.p.** 149-151 $^\circ\text{C}$



Compound **4.21** (155 mg, 0.48 mmol) was dissolved in EtOH (4 mL) and hydrazine hydrate (0.026 mL, 1.1 equiv.) was added. The mixture was heated at  $50^\circ\text{C}$  for 4 hours and then filtered through cotton wool. The filtrate was then concentrated under reduced pressure and the resulting mixture purified by column chromatography over silica gel (DCM/MeOH: 5 to 15% MeOH then DCM/MeOH/ $\text{Et}_3\text{N}$ : 5 to 15% MeOH, 1%  $\text{Et}_3\text{N}$ ) yielding **4.E** as a colourless oil (76 mg, 0.39 mmol, **81%**).

**<sup>1</sup>H NMR (400 MHz, CDCl<sub>3</sub>):**  $\delta$  8.10 (d, 2H,  $J = 6.4$  Hz, H<sub>1</sub>), 6.29 (d, 2H,  $J = 6.4$  Hz, H<sub>2</sub>), 5.38 (bs, 2H, NH<sub>2</sub>), 3.67 (dd, 1H,  $J = 10.0$  Hz,  $J = 6.4$  Hz, H<sub>7</sub>), 3.58 (dd, 1H,  $J = 9.6$  Hz,  $J = 7.6$  Hz, H<sub>7</sub>), 3.38 (dd, 1H,  $J = 9.6$  Hz,  $J = 7.6$  Hz, H<sub>6</sub>), 3.34 to 3.20 (m, 2H, H<sub>3</sub>), 3.03 (dd, 1H,  $J = 9.6$  Hz,  $J = 6.8$  Hz, H<sub>6</sub>), 2.68 to 2.58 (m, 1H, H<sub>5</sub>), 2.12 to 2.04 (m, 1H, H<sub>4</sub>), 1.81 to 1.68 (m, 1H, H<sub>4</sub>) **<sup>13</sup>C NMR (100 MHz, CDCl<sub>3</sub>):**  $\delta$  151.7, 149.1, 106.9, 77.5, 50.0, 46.3, 37.4, 27.9 **LRESI-MS:**  $m/z$  194 [M+H]<sup>+</sup> **HRESI-MS:**  $m/z$  194.1285 (calcd. for C<sub>10</sub>H<sub>16</sub>N<sub>3</sub>O 194.1288 [M+H]<sup>+</sup>)

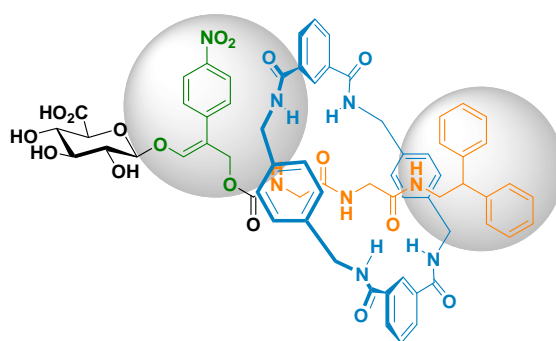
# CONCLUSION

Peptides unambiguously represent expanding therapeutic targets and are likely prone to become the drugs of choice for the treatment of many important diseases such as cancer. Most of the biological processes in life are tightly controlled by peptides in an extraordinarily selective fashion. Therefore molecular diversity along with high selectivity constitute the cornerstone of peptide drug development. Despite such potential, a limited number of peptides are currently approved because pre-systemic degradation and poor membrane penetration restrict their use. In spite of the many advances reached in improving peptide oral administration, few approaches retain the integrity of the peptide molecular structure. The peptidomimetic approach rationally imitates bioactive peptides and integrates their pharmacophoric elements into rigid structures, the final resemblance of which to the original peptide is hardly distinguishable. The prodrug approach represents a more versatile strategy since the peptide is only temporarily modified to enhance its pharmaceutical profile. The more promising targeted prodrugs additionally allow the controlled and selective delivery of drugs to specific organs, which is essential in the case of anticancer chemotherapy. Another encouraging alternative is the derivatisation of peptides into rotaxane architectures. In this approach the physicochemical properties of a peptide thread are remarkably modified by its encapsulation within a macrocycle.

During this PhD thesis we tried to design, synthesise and study some novel innovative devices aiming at protecting, targeting and delivering peptides to tumour cells. This project has been conducted as a collaboration between the Gesson group (Poitiers, France) and the Leigh group (Edinburgh, Scotland) specialised in glycosylated prodrugs for anticancer chemotherapy and peptide rotaxane assembly respectively. Therefore based on the knowledge acquired by the two universities we attempted to construct some enzyme-activated peptide rotaxanes to develop a new advanced concept in peptide delivery.

### *Towards a model rotaxane-based peptide prodrug*

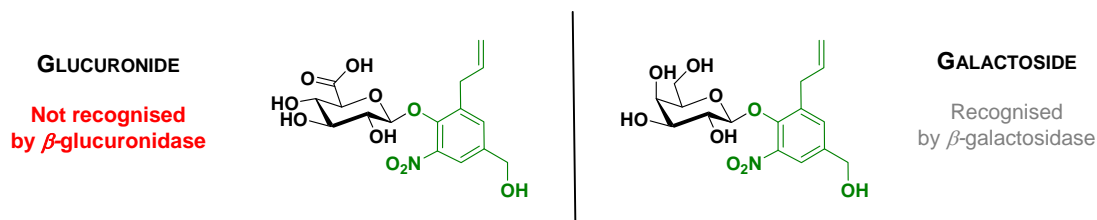
First of all we focused on the preparation of a simple model rotaxane-based prodrug. We constructed threads consisting of a trigger, a self-immolative spacer and a model stoppered glycine-based peptide which has commonly been used for the templated assembly of peptide rotaxanes. However the construction of such threads has to provide the essential features required for rotaxane synthesis. Indeed in the clipping approach the thread has to present final bulky stoppers indispensable for the mechanical lock of the macrocycle unit. As a consequence, modification of the classic prodrug design was necessary to access the interlocked device. Therefore we examined some of the spacers developed by Gesson *et al.* and found that the nitro-arylmalonaldehyde was a good candidate. Thus associating this spacer with the stoppered glycylglycine model peptide furnished the crucial elements to assemble the first model rotaxane (**Scheme 1**). Unfortunately we found difficulty in isolating the pure rotaxane prodrug and decided to design a new model system.



**Scheme 1** | The first model rotaxane prodrug incorporating the arylmalonaldehyde spacer

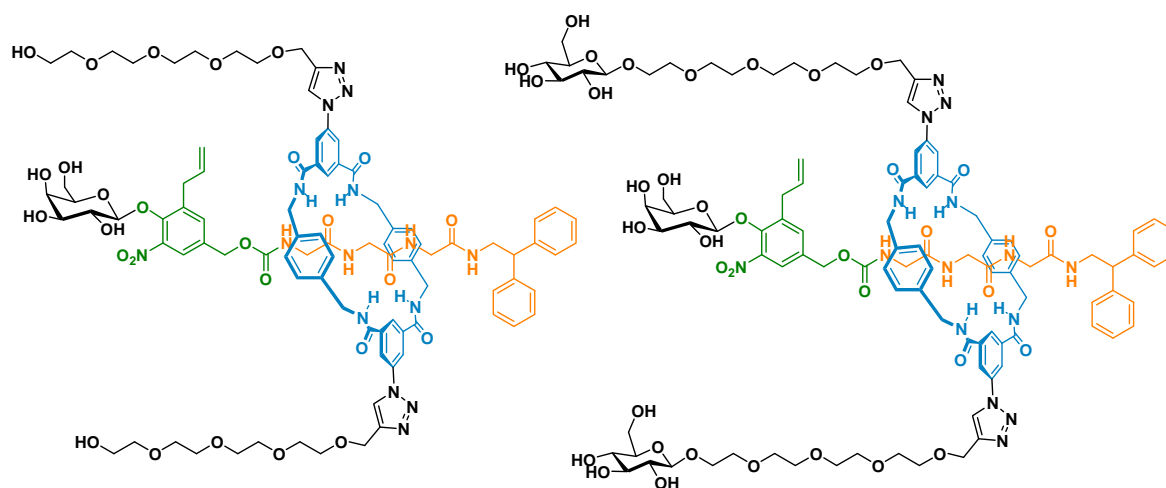
Among the self-immolative spacers developed within Gesson group, the benzyloxycarbonyl one is quite attractive. Indeed a glucuronylated prodrug incorporating this motif (HMR 1826) has demonstrated valuable results *in vivo*. Accordingly, we concentrated our efforts on derivatising this spacer to obtain an effective stopper for this side of the molecule. Spacers are crucial units in prodrugs: they move the drug away from the trigger for efficient enzymatic recognition and release the drug after activation of the prodrug. Therefore careful modification should be accomplished without depleting the essential function of the spacer.

The “allyl spacer” was the first solution we explored. Simply derived from HMR 1826, this new spacer appeared to completely inhibit the recognition of the glucuronide motif (**Scheme 2**). Therefore a galactoside derivative was synthesised and proved to be hydrolysed by *E. coli*  $\beta$ -galactosidase, albeit with prolonged reaction time. This provided the starting point of our model study.



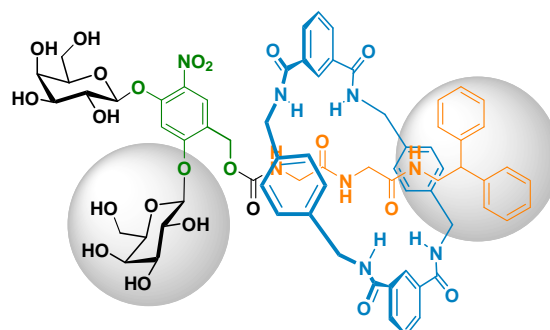
**Scheme 2** | Preliminary evaluation of the “allyl spacer”

Accordingly we prepared the galactosylated prodrug thread and its corresponding rotaxane for use in an ADEPT protocol. However while the prodrug thread released the model peptide, the rotaxane proved to be insoluble in water thus preventing its enzymatic activation. As a result we explored the functionalisation of the macrocycle unit in order to tune the solubility of the model rotaxane prodrug. In this direction, two PEG-grafted rotaxanes were successfully synthesised and evaluated (**Scheme 3**). Enzymatic studies with *E. coli*  $\beta$ -galactosidase revealed that while the machine liberates the peptide, the release is significantly slowed down in comparison with the non-interlocked prodrug. This can be explained by the fact that the supplementary allyl group still hinders the glycosidic bond. Moreover its position on the spacer allows the macrocycle to shuttle close to the carbohydrate moiety resulting in a supplementary steric effect deterring enzymatic approach.



**Scheme 3** | The water-soluble PEG-grafted rotaxane

In the light of these results we decided to construct a new model rotaxane. The *bis*-galactosylated system appeared quite interesting in two respects. Indeed the supplementary galactose unit is placed one position away from the *o*-nitro galactose and the presence of two carbohydrates should significantly improve the water solubility of the rotaxane (**Scheme 4**).

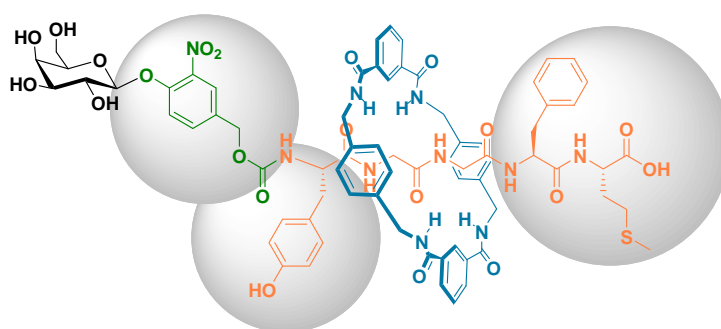


**Scheme 4** | The *bis*-galactosylated model rotaxane prodrug

Nevertheless it appeared that such modifications tend to complicate the enzymatic release of the model peptide where compared with the non-interlocked prodrug. Unfortunately the rotaxane, even though flanked with two galactose units, is once again insoluble in water. However this model still remains promising since the use of glucuronic acid triggers seems viable.

### ***Protection and targeted delivery of Met-enkephalin***

On the other hand, we concentrated our efforts on applying our concept to the anticancerous Met-enkephalin pentapeptide (H-TyrGlyGlyPheMet-OH). Indeed the opioid peptide displays the essential glycyl residue for templating the assembly of peptide rotaxane and CPK models demonstrated that its C-terminal amino acids (PheMet) constitute a natural stopper for the amide-based macrocycle. In addition the models also showed that the simplest non-modified HMR 1826 spacer along with the adjacent tyrosine residue effectively block the macrocycle (**Scheme 5**).

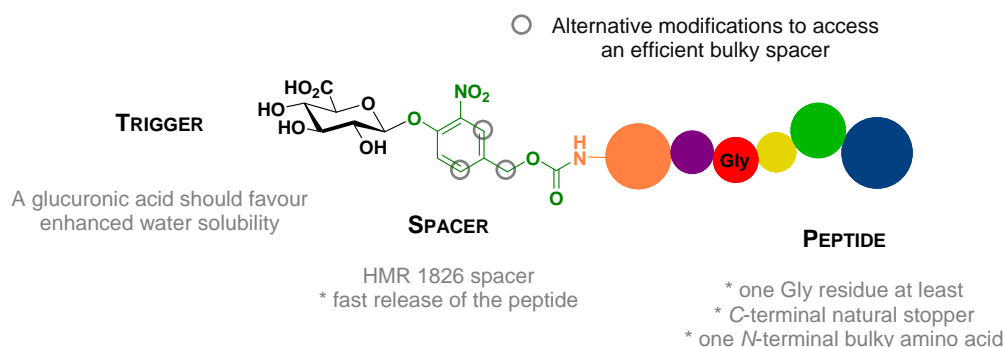


**Scheme 5** | The galactosylated Met-enkephalin rotaxane prodrug

Hence we prepared the Met-enkephalin rotaxane prodrug along with its non-interlocked derivative. Enzymatic studies revealed that the rotaxane efficiently and rapidly releases the peptide after the action of *E. coli*  $\beta$ -galactosidase. This finding reinforces the idea that confining the macrocycle far away from the trigger results in enhanced recognition and delivery kinetics of the encapsulated peptide. Moreover the solubility of the rotaxane was assured by the presence of the C-terminal carboxylic acid, suggesting that glucuronylated rotaxane should present satisfying water solubility. The protective effect of the macrocycle was also demonstrated with two different proteases which are largely responsible for the poor bioavailability of Met-enkephalin. Moreover, experiments conducted in human plasma provided evidence for the high stability of the rotaxane in comparison with Met-enkephalin and its galactosylated prodrug thread.

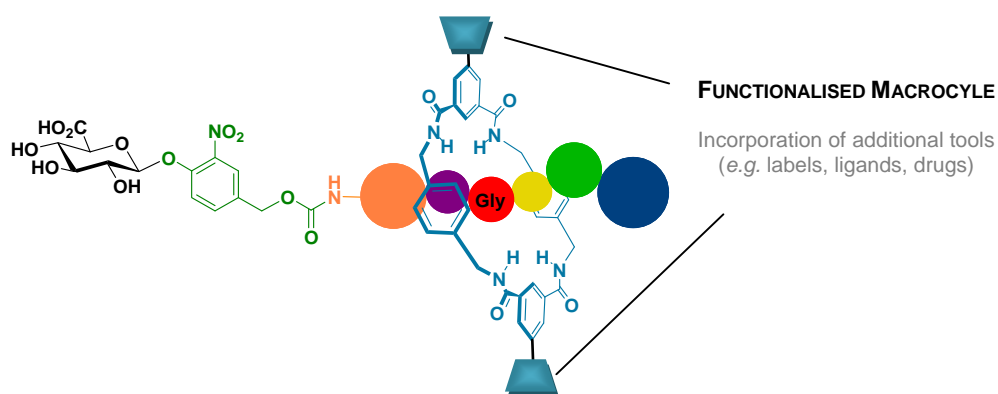
Overall, these studies evidenced that rotaxane-based peptide prodrugs represent a valuable innovative concept for the delivery of bioactive peptides. We demonstrated that, in a simple rotaxane system, the device efficiently protects and delivers a peptide following specific enzyme-mediated activation. However to reach a generally applicable device, several points have to be considered. On one hand, a crucial prerequisite is that the peptide has to possess at least one glycine residue and present a natural C-terminal stopper. Furthermore another stopper has to be constructed on the prodrug thread. While we focused in the model study on adding a hindering component on the spacer unit, the Met-enkephalin rotaxane demonstrated that locking the macrocycle away from the trigger-spacer conjugate results in increased performance of the rotaxane. Over and above the considerations above, the hydrophilic character of the rotaxane has to be finely tuned since good water solubility is essential for enzymatic activation.

Consequently an efficient prodrug thread can be rationally devised considering the preliminary results presented in this thesis to efficiently reach a rotaxane-based delivery device (**Scheme 6**).



**Scheme 6** | Enhanced design of the prodrug thread

Alternatively (if the N-terminal amino acid is not as bulky as necessary), modification of HMR 1826 spacer in the *m*-positions or in the benzylic position should contain the macrocycle away from the glycosidic bond. Furthermore, 2<sup>nd</sup> generation rotaxanes can be devised from that point. Indeed we demonstrated with the “allyl based” models that the macrocycle can be easily functionalised. As a consequence supplementary tools can be grafted on the rotaxane to reach multifunctional advanced materials (e.g. labels, ligands, drugs etc.) (**Scheme 7**).

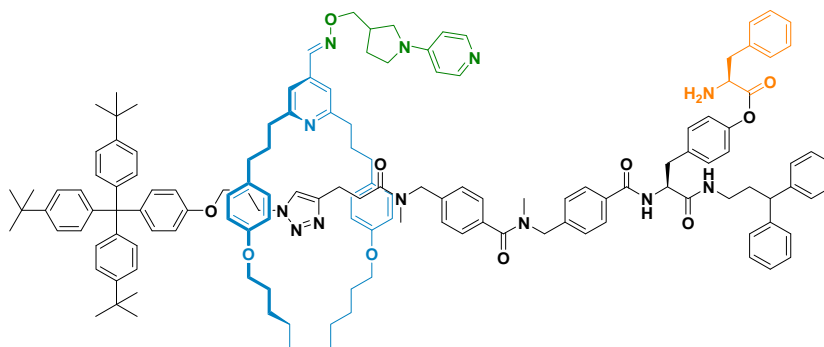


**Scheme 7** | 2<sup>nd</sup> generation rotaxane-based delivery devices

The toxicity of the macrocycles (functionalised or not) must also be evaluated. If their toxicity is proved against cancer then our devices can present combined toxicity or simply be used to target and deliver a cytotoxic macrocycle to tumour cells. Therefore in this case the thread could be easily devised and incorporate additional functions.

### *Toward a molecular peptide synthesiser*

In the final part of this PhD thesis we described the design of a rotaxane-based machine that, following the information carried on its thread, would in principle be able to processively assemble a sequence-specific peptide oligomer. While we successfully synthesised a one-station model rotaxane (**Scheme 8**), the first experiments we conducted did not result in the expected outcomes. However the study is only at an early stage and many parameters remain to be investigated and optimised before reaching such processive task performance.



**Scheme 8** | The one-station model rotaxane